

Praxis und Theorie der gaschromatographischen
Enantiomerentrennung an chiralen
Stationärphasen mit einfachen
und binären Selektoren

Practice and theory of gas chromatographic
enantioseparation on single- and binary-
selector chiral stationary phases

DISSERTATION

der Fakultät für Chemie und Pharmazie
der Eberhard-Karls-Universität Tübingen

zur Erlangung des Grades eines Doktors
der Naturwissenschaften

2007

vorgelegt von
PAVEL LEVKIN

Praxis und Theorie der gaschromatographischen
Enantiomerentrennung an chiralen
Stationärphasen mit einfachen
und binären Selektoren

Practice and theory of gas chromatographic
enantioseparation on single- and binary-
selector chiral stationary phases

DISSERTATION

der Fakultät für Chemie und Pharmazie
der Eberhard-Karls-Universität Tübingen

zur Erlangung des Grades eines Doktors
der Naturwissenschaften

2007

vorgelegt von
PAVEL LEVKIN

Tag der mündlichen Prüfung:

20. April 2007

Dekan:

Prof. Dr. Lars Wesemann

1. Berichterstatter:

Prof. Dr. V. Schurig

2. Berichterstatter:

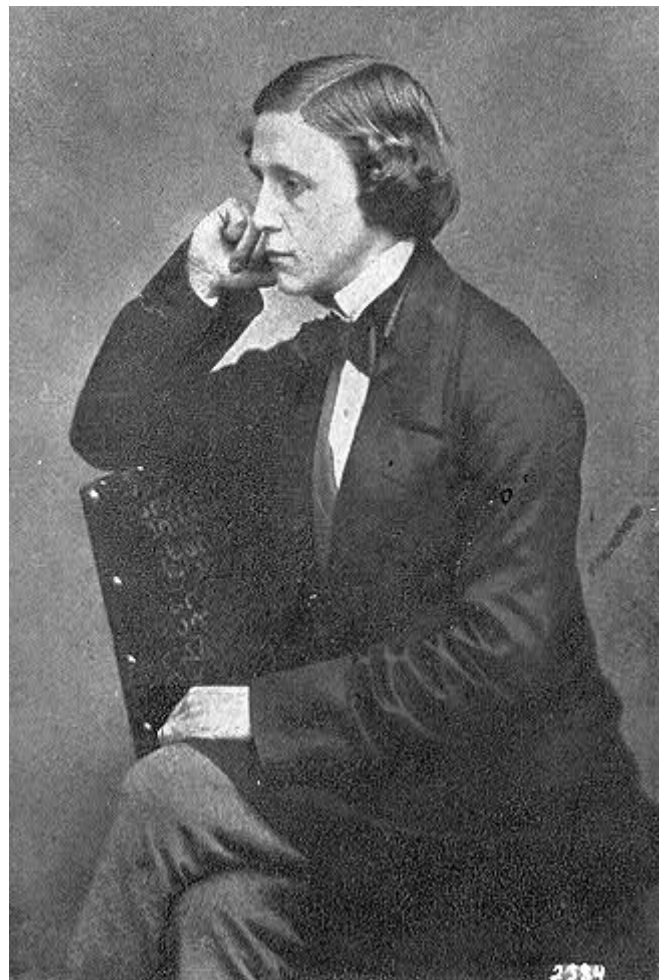
Prof. Dr. K. Albert

3. Berichterstatter:

Prof. Dr. H. Frank

“...Oh, how nice it would be if we could only get through into Looking-glass House! I’m sure it’s got, oh! Such beautiful things in it! Let’s pretend there’s a way of getting through into it, somehow...”

In another moment Alice was through the glass, and had jumped lightly down into the Looking-glass room...”



Charles Lutwidge Dodgson (Lewis Carroll) (1832-1898)

Die vorliegende Arbeit wurde unter der Leitung von Prof. Dr. V. Schurig in der Zeit von September 2003 bis Oktober 2006 am Institut für Organische Chemie der Eberhard-Karls-Universität Tübingen durchgeführt.

Ich danke Herrn Prof. Dr. Volker Schurig für die Themenstellung, sein stetiges Interesse am Fortgang, die großzügige Unterstützung bei der Durchführung dieser Arbeit und die wertvollen Anregungen und Diskussionen.

Den Mitgliedern des Arbeitskreises (Dorothee Wistuba, Harri Czesla, Giuseppe Sicoli, Z.J. Jiang, Alexander Ruderisch, Leena Banspach, Anja Bogdansky, Clarissa Reiner, Diana Kreidler) danke ich für die gute Zusammenarbeit und vielen wertvollen Diskussionen. Ich danke auch Dr. Oliver Trapp, Dr. Ashraf Ghanem, Nikolas Plumeré, Anton Khartulyari für viele und wertvolle Diskussionen.

Meinen vorigen Betreuer Herrn Prof. Dr. R. Kostyanovsky und Kollegen Dr. G.K. Kadorkina, Dr. O.N. Krutius, Dr. D. Lenev, V. Yu. Torbeev (N.N. Semenov Institute of Chemical Physics, Moskau, Russische Föderation) danke ich für die fortwährende wertvolle Kooperation und für viele nützliche Diskussionen.

Herrn G. Nicholson (FT-ICR-MS, GC/MS), Herrn H.-J. Kolb (DSC, X-ray), Herrn P. Schuler (EPR, NMR) danke ich für die jeweiligen Messungen und nützliche Diskussionen.

Dem Graduiertenkolleg „Chemie in Interphasen“ der DFG und der Universität Tübingen danke ich für die großzügige Förderung durch ein Promotionsstipendium, für Sachmittel und Reisestipendien.

Ich danke Prof. Dr. W. Lindner und Dr. N. M. Maier (Institut für Analytische Chemie und Lebensmittelchemie, Universität Wien) für die wertvolle und erfolgreiche Kooperation auf dem Gebiet der enantioselektiven HPLC Forschung.

Prof. Dr. Uccello-Barretta und S. Nazzi danke ich für die wertvolle Kooperation auf dem Gebiet der Synthese und NMR Untersuchungen des chiralen Selektor Valdex.

Prof. Dr. K. Albert, Prof. Dr. C. Ochsenfeld, Prof. Dr. M. Maier, Prof. Dr. E. Schweda, Prof. Dr. E. Lindner (Universität Tübingen), Prof. Dr. Coquerel (University Rouen, France), Prof.

Dr. B. Chankvetadze (Tbilisi State University, Georgien), Prof. Dr. V. Davankov (INEOS, RAS, Moskau) danke ich für nützliche Diskussionen und Ratschläge.

Mein besonderer Dank gilt meinen Eltern für die großzügige Unterstützung meiner akademischen Ausbildung.

für meine Frau

CONTENT

Abbreviations.....	17
Introduction, Scope and Aims.....	19
1. Practice of the enantioseparation on single- and binary-selector gas-chromatographic (GC) chiral stationary phases (CSPs). Combining the enantioselective properties of different chiral selectors.....	37
1.1 Chirasil-DexVal: combining heptakis(2,3,6-tri- <i>O</i> -methyl)- β -cyclodextrin and <i>L</i> -valine-diamide chiral selectors in one CSP.....	37
1.1.1 Synthesis of <i>L</i> -valine-diamide selector and single-selector CSP Chirasil-Val-C ₁₁	37
1.1.2 GC investigation of Chirasil-Val-C ₁₁	39
1.1.3 Synthesis of the single-selector CSP Chirasil-Dex and binary-selector CSP Chirasil-DexVal.....	40
1.1.4 Comparison of the enantioselective properties of the single- and binary-selector CSPs: Chirasil-Dex, Chirasil-Val-C ₁₁ and Chirasil-DexVal, respectively.....	41
1.1.5 Refinement of the enantioseparation of α -amino acid derivatives on Chirasil-Val-C ₁₁ using the binary-selector approach.....	46
1.2 Chirasil-CalixDex: combining resorcinearene-based <i>L</i> (or <i>D</i>)-valine-diamide and heptakis(2,3,6-tri- <i>O</i> -methyl)- β -cyclodextrin chiral selectors in one CSP.....	49
1.2.1 Synthesis of Chirasil-Calix and Chirasil-CalixDex CSPs.....	49
1.2.2 Comparison of the enantioselective properties of the single- and binary-selector CSPs: Chirasil-Calix, Chirasil-Dex and Chirasil-CalixDex, respectively.....	53
1.2.3 Study of matched and mismatched cases.....	63
1.3 Chirasil-Val(γ -Dex): combining <i>L</i> -valine-diamide and octakis(3- <i>O</i> -butanoyl-2,6-di- <i>O</i> - <i>n</i> -pentyl)- γ -cyclodextrin chiral selectors in one CSP.....	69
1.3.1 Comparison of the enantioselective properties of the single- and binary-selector CSPs: Chirasil-Val-C ₁₁ , Lipodex E and Chirasil-Val(γ -Dex), respectively.....	71

1.4 Valdex: combining <i>L</i> -valine-diamide and heptakis(2,3,6-tri- <i>O</i> -methyl)- β -cyclodextrin chiral selectors in one molecule.....	81
1.4.1 Synthesis of Valdex.....	82
1.4.2 Valdex as a chiral solvating agent for NMR determination of enantiomeric compositions.....	82
2. Theory of the enantioseparation on single- and binary-selector gas-chromatographic chiral stationary phases.....	89
2.1 Introduction.....	91
2.2 Determination of the distribution and association constants.....	94
2.3 Single-selector GC systems.....	97
2.3.1 Determination of the apparent enantioseparation factor, α_{app} Dependence of α_{app} on the concentration of the chiral selector present in the achiral solvent.....	97
2.3.2 Determination of the true enantioseparation factor, α_{true}	100
2.4 Binary-selector GC systems.....	103
2.4.1 Determination of the apparent enantioseparation factor, α_{app}	103
2.4.1.1 Analysis of the behavior of α_{app} upon varying ratio and the association strengths of two different chiral selectors, A and B, present in an achiral solvent.....	108
a) Case I: the same elution order of the selectand enantiomers D and L on the chiral selectors A and B (matched case)	109
b) Case II: opposite elution order of the selectand enantiomers D and L on the chiral selectors A and B (mismatched case)	112
c) Case III: chiral selector is not enantiomerically pure. Analysis of the apparent enantioseparation factor, α_{app} , as a function of the enantiomeric excess, <i>ee</i> , of the chiral selector.....	114
2.4.1.2 Experimental verification of the equation for the calculation of the apparent enantioseparation factor, α_{app} , on a CSP containing an <i>L</i> -valine diamide and a permethylated- β -cyclodextrin.....	118
2.4.2 Determination of the true enantioseparation factor, α_{true}	120
3. Influence of temperature on the enantioseparation by GC.....	123
3.1 Introduction.....	125

3.2 Temperature-induced inversion of the elution order of enantiomers.....	128
3.2.1 Enantioseparation of <i>N</i> -ethoxycarbonyl propyl amides of α -amino acids on Chirasil-Val-C ₁₁ CSP.....	128
3.2.2 Enantioseparation of <i>N</i> -trifluoroacetyl ethyl esters of α -amino acids on Chirasil-Dex CSP.....	139
3.3 Study of the non-linear behavior of $\ln(\alpha_{\text{true}})$ as a function of the reciprocal temperature.....	144
4. Enantiomerization of 1,2-di-<i>tert</i>-butylpyrazolidine and 1,2-di-<i>iso</i>-propyl-3,5- dimethylpyrazolidine by dynamic GC.....	147
5. Experimental investigation of the influence of the enantiomeric purity of a chiral selector on the enantioseparation by liquid chromatography.....	153
5.1 Introduction.....	155
5.2 Results and discussion.....	155
6. Evaluation of nonenantioselective <i>versus</i> enantioselective interactions in liquid chromatography.....	163
6.1 Introduction.....	165
6.2 Results and discussion.....	167
7. Differentiation between racemic compounds and conglomerates by enantioselective GC.....	177
7.1 Introduction.....	179
7.2 Results and discussion.....	180
8. Experimental part.....	185
8.1 Materials and methods.....	185
8.2 Synthetic procedures.....	186
<i>N</i> -Trifluoroacetyl amino acid ethyl esters.	186
<i>N</i> -Alkoxycarbonyl alkylamide derivatives	187
<i>N</i> -Boc- <i>L</i> (<i>D</i>)-valine (1)	187
<i>N</i> -Boc- <i>L</i> (<i>D</i>)-valine- <i>tert</i> -butylamide (2)	187
<i>L</i> (<i>D</i>)-Valine- <i>tert</i> -butylamide (3)	188
<i>N</i> -(Undec-10-enoyl)- <i>L</i> -valine- <i>tert</i> -butylamide (4)	188

<i>N</i> -Bromoacetyl- <i>L</i> (<i>D</i>)-valine- <i>tert</i> -butylamide (5)	189
<i>C</i> -dec-9-enylresorcinarene (6)	190
Octakis- <i>O</i> -(<i>N</i> -acetyl- <i>D</i> -valine- <i>tert</i> -butylamide)- <i>C</i> -decenyl- resorcinarene (D').....	190
Octakis- <i>O</i> -(<i>N</i> -acetyl- <i>L</i> -valine- <i>tert</i> -butylamide)- <i>C</i> -decenyl- resorcinarene (L')	191
Monokis-2- <i>O</i> -undec-10-enyl-permethyl- β -cyclodextrin (CD).....	191
Heptakis[6- <i>O</i> -(<i>tert</i> -butyldimethylsilyl)]- β -cyclodextrin.....	191
Heptakis[6- <i>O</i> -(<i>tert</i> -butyldimethylsilyl)-2,3-di- <i>O</i> -methyl]- β -cyclodextrin....	192
Heptakis(2,3-di- <i>O</i> -methyl)- β -cyclodextrin	192
Octakis(3- <i>O</i> -butanoyl-2,6-di- <i>O</i> - <i>n</i> -pentyl)- γ -cyclodextrin (Lipodex E).....	193
Heptakis(6- <i>O</i> -(<i>N</i> -acetyl- <i>L</i> -valine- <i>tert</i> -butylamide)-2,3-di- <i>O</i> -methyl)- β - cyclodextrin (Valdex)	193
2,3:6,7-dibenzobicyclo[3.3.1]nona-2,6-diene-4,8-dione (28).....	194
4,8-bis(methylene)-2,3:6,7-dibenzobicyclo[3.3.1]nona-2,6-diene (29).....	195
General procedure for the immobilization of chiral selectors to dimethylhydromethylpolysiloxane by platinum-catalyzed hydrosilylation.....	195
8.3 Preparation of the single- and binary-selector CSPs.....	196
Chirasil-Dex.....	196
Chirasil- <i>L</i> (<i>D</i>)-Val-C ₁₁	196
Chirasil-DexVal	196
Chirasil-CalixDex.....	196
Chirasil- γ -Dex	196
Chirasil-Val(γ -Dex)	196
Reference stationary phase.....	196
Supplementary material	197
Conclusions	201
References	207

ABBREVIATIONS AND SYMBOLS:

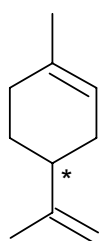
α_{app}	Apparent enantioseparation factor
α_{true}	True enantioseparation factor
$\Delta G^{\#}$	Activation Gibbs energy
$\Delta H^{\#}$	Activation enthalpy
$\Delta S^{\#}$	Activation entropy
$\Delta_{\text{D,L}}\Delta G$	Gibbs energy difference
$\Delta_{\text{D,L}}\Delta H$	Enthalpy difference
$\Delta_{\text{D,L}}\Delta S$	Entropy difference
BOC ₂ O	Di- <i>tert</i> -butyldicarbonate
CD	Cyclodextrin selector
CE	Capillary electrophoresis
CEC	Capillary electrochromatography
Chirasil-Dex	Single-selector CSP containing permethyl- β -cyclodextrin chemically linked to a polysiloxane
Chirasil-Calix	Single-selector CSP containing resorcinarene-based valine-diamide selector chemically linked to a polysiloxane
Chirasil-CalixDex	Binary-selector CSP containing a resorcinarene-based valine-diamide and permethyl- β -cyclodextrin selectors chemically linked to a polysiloxane
Chirasil-DexVal	Binary-selector CSP containing permethyl- β -cyclodextrin and valine-diamide chemically linked to a polysiloxane
Chirasil-Val-C ₁₁	Single-selector CSP containing valine-diamide selector chemically linked to a polysiloxane
Chirasil-Val(γ -Dex)	Binary-selector CSP containing Lipodex E dissolved in Chirasil-Val-C ₁₁
“Compound B”	1,1,1,3,3-pentafluoro-2-(fluoromethoxy)-3-methoxypropane
CSA	Chiral solvating agent
CSP	Chiral stationary phase
DA	Diamide selector
DCC	<i>N,N'</i> -Dicyclohexylcarbodiimide
DCM	Dichloromethane
DGC	Dynamic gas chromatography
DMF	Dimethylformamide
DMSO	Dimethylsulfoxide
<i>ee</i>	Enantiomeric excess

ECD	Electron capture detector
<i>er</i>	Enantiomeric ratio
EtOH	Ethanol
FID	Flame ionization detector
GC	Gas chromatography
HPLC	High-performance liquid chromatography
i.d.	Internal diameter
<i>K</i>	Distribution constant
<i>k</i>	Retention factor
LC	Liquid chromatography
Lipodex E	Octakis(3- <i>O</i> -butanoyl-2,6-di- <i>O</i> - <i>n</i> -pentyl)- γ -cyclodextrin
Valine-diamide	<i>N</i> -acyl- <i>L</i> (or <i>D</i>)-valine- <i>tert</i> -butyl amide
MeOH	Methanol
NMR	Nuclear magnetic resonance
MS	Mass spectroscopy
<i>R'</i>	Retention increment
<i>R</i>	Gas constant
<i>r</i>	Relative retention
<i>R_s</i>	Resolution factor
SFC	Supercritical fluid chromatography
sfGC	Stopped-flow GC
<i>T</i>	Temperature
<i>T_{iso}</i>	Isoenantioselective temperature
<i>t</i>	Time; retention time
<i>t'</i>	Adjusted retention time
<i>t_d</i>	Hold-up time
TBDMS	<i>tert</i> -Butyldimethylsilyl
TFA	Trifluoroacetic acid
THF	Tetrahydrofuran
TLC	Thin-layer chromatography
Valdex	Heptakis(6- <i>O</i> -(<i>N</i> -acetylyl- <i>L</i> -valine- <i>tert</i> -butylamide)-2,3-di- <i>O</i> -methyl)- β -cyclodextrin
<i>x</i>	Molar fraction
<i>w_h</i>	Width of a peak at a half height

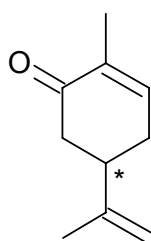
Introduction, Scope and Aims

Introduction, Scope and Aims

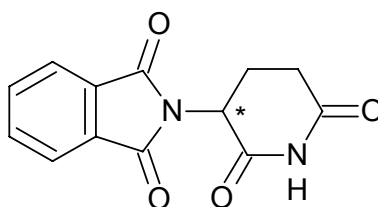
Modern enantioselective chromatography, as a part of the field of chiral analysis, is a powerful technique for both preparative separations of enantiomers and for high-resolution analyses of their complex mixtures. Why is this important? The targets of enantioselective chromatography are chiral compounds, i.e. molecules which are not superimposable on their mirror images. Such molecules are called enantiomers. With the exception of their chiroptical properties, the characteristics of enantiomers in an achiral environment are strictly equivalent. However, in a chiral environment, the physical and chemical properties of the enantiomers become distinct. Since most of the building blocks in living organisms are homochiral (e.g. *L*-amino acids, *D*-carbohydrates, etc), the biosphere represents a perfect chiral environment and, as a consequence, pharmacological properties, odor and taste of enantiomers are often significantly different. For example, (R)-(-)-carvone smells like spearmint while (S)-(+)-carvone has the odor of caraway. (R)-(+)-Limonene smells like orange, whereas (S)-(-)-limonene has the odor of turpentine [1, 2]. The different pharmacological properties of enantiomers may have much more severe consequences. Thus, one enantiomer of thalidomide (Contergan), a well-known drug, has a sedative effect, while the other is believed to have a strong teratogenic effect, causing birth defects. Administration of racemic thalidomide to pregnant women in the late fifties led to a tragedy: approximately 10,000 children were born with severe malformations. However, it has been found that the enantiomers of thalidomide are interconverted *in vivo*, therefore, administering only one enantiomer would not have prevented the teratogenic effect [3a]. Another chiral substance, ibuprofen, is a non-steroidal anti-inflammatory drug (NSAID). It has been found that only (S)-(+)-ibuprofen is the active form, whereas the (R)-(-)-ibuprofen has no pharmacological activity [3b] but is transformed to the (S)-enantiomer in the body.



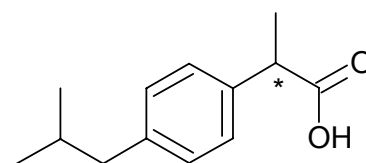
Limonene



Carvone



Thalidomide



Ibuprofen

There are many other examples of chiral drugs in which the opposite enantiomers have completely different pharmacological properties. Therefore, it is obligatory to treat enantiomers as different compounds in the assessment of chiral pharmaceuticals. Thus, it is

not surprising that the world market of the chiral technology has constantly increased over the last decades and that today chirality is one of the central issues of organic and pharmaceutical chemistry, especially in the development of new drugs. According to Stinson, “worldwide sales of chiral drugs in single-enantiomer dosage forms continued growing at an annual rate of more than 13%. With a sales volume of \$133 billion in 2000, “this figure could hit \$200 billion in 2008” [4]. In 1999, the turnover in the Chiral Technology business (Geoffrey Winkler, Business Commun., Norwalk, CT USA) amounted to \$150 billions. Of this sum, chiral analyses accounted for \$150 millions per annum with an annual increase of 15%.

Figure 1 shows further areas of research topics that require precise chiral analysis for various different purposes. The most important techniques used for the analysis of enantiomers nowadays are liquid chromatography (LC, HPLC) [5,6], high-resolution gas chromatography (GC) [7,8,9], capillary electrophoresis (CE) [10,11,12], supercritical fluid chromatography (SFC) [13-18] and ligand-exchange chromatography (LEC) [19-22]. The present PhD thesis will deal mainly with practical and theoretical aspects of enantioseparation by GC and HPLC as the central tools of the field of chiral analysis.

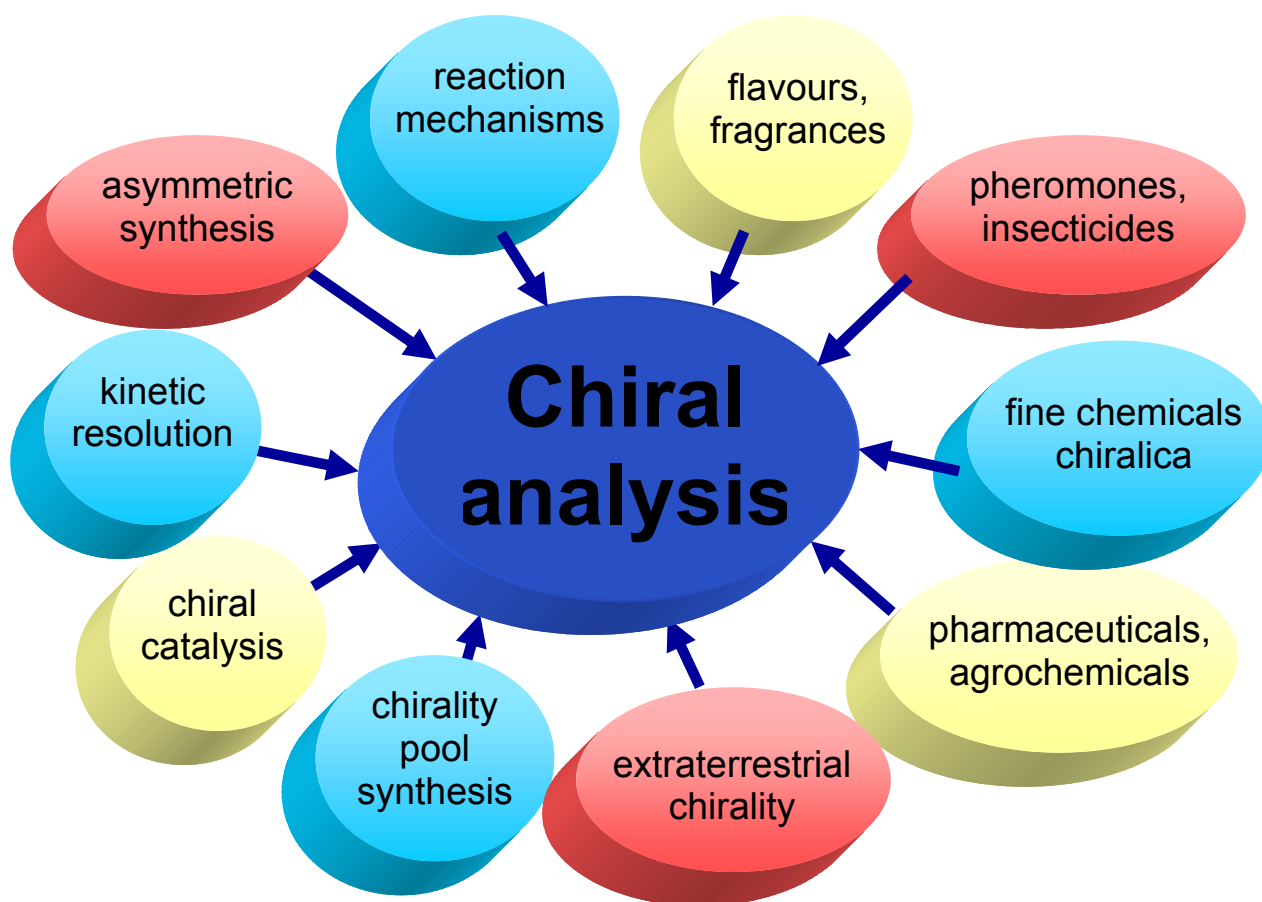


Figure 1 Different areas of research that require precise methods for analysis of enantiomers.

As previously mentioned, the properties of enantiomers are rendered different only in a chiral environment. Therefore, to be able to separate enantiomers by chromatography, the stationary phase or mobile phase must be chiral and non-racemic. One of the main strategy of introducing chirality into stationary phases is the use of chiral and non-racemic selectors capable of forming transient diastereomeric associates with the enantiomers of selectand (analyte) enantiomers during the separation process.

In enantioselective GC, the first chiral selectors that showed a reproducible and quantitative ability for the separation of enantiomers were derivatives of natural α -amino acids as introduced by Gil-Av, Feibush and Charles-Sigler in 1966 [23]. These selectors showed enantioselectivity towards derivatives of amino acids, diols, amino alcohols and other classes of compounds on the basis of stereoselective hydrogen-bonding [24-29]. The scope of the enantioseparations was further substantially expanded by Schurig et al. with the development of complexation-GC with metal chelates as chiral selectors [30-33]. The enantioselectivity of metal chelates is based on different complexation strengths of the selectand enantiomers with the metal ions. Later on, Sybilska et al. [34,35], Juvancz et al. [36,37], Venema et al. [38], Schurig et al. [39,40] and König et al. [41,42] introduced derivatives of cyclodextrins as chiral selectors. The approach of Schurig et al. has the advantage that modified cyclodextrins are dissolved or bonded to polysiloxanes. Enantioselectivity of cyclodextrins is believed to be the result of inclusion into the cavity and external interactions.

A breakthrough in enantioselective GC was achieved in 1977 by Frank, Nicholson and Bayer [29,43] when the most important amino acid diamide chiral selector, *N*-acyl-valine-*tert*-butyl amide, was linked to a polysiloxane, thereby combining the enantioselectivity of the selector with the high efficiency of the polymer. The chiral polysiloxane containing the valine selector in the *L*- or *D*-form was termed Chirasil-Val (**Figure 2**).

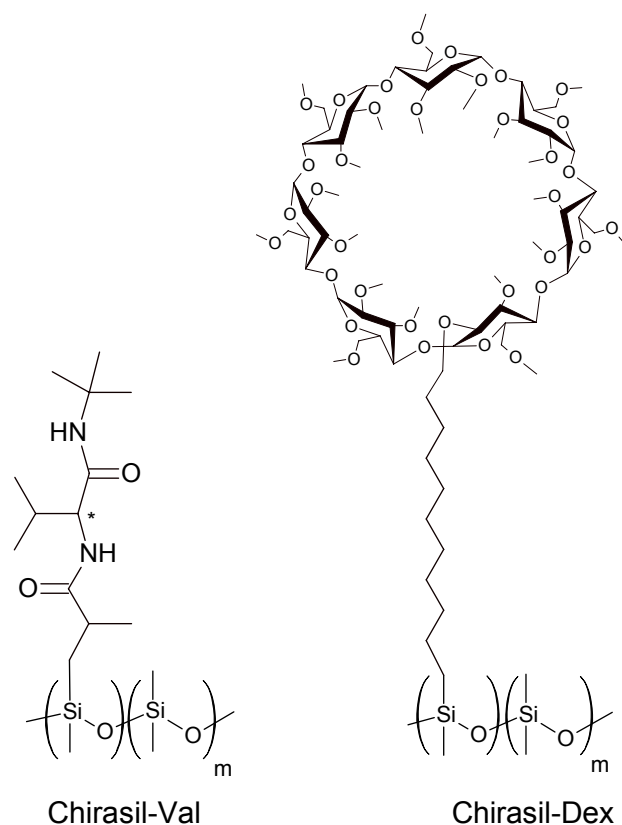


Figure 2 Chirasil-Val (left) and Chirasil- β -Dex (right) chiral stationary phases.

Chirasil-Val represents the most valuable chiral stationary phase (CSP) for the enantioselective analysis of amino acid derivatives. GC using Chirasil-Val is the only method allowing the enantioseparation of all proteinogenic α -amino acids in a temperature-programmed run within half an hour (**Figure 3**)! Since the enantioselectivity of Chirasil-Val is based on hydrogen-bonding, the enantioseparation of chiral compounds lacking at least two hydrogen-bonding sites is very difficult.

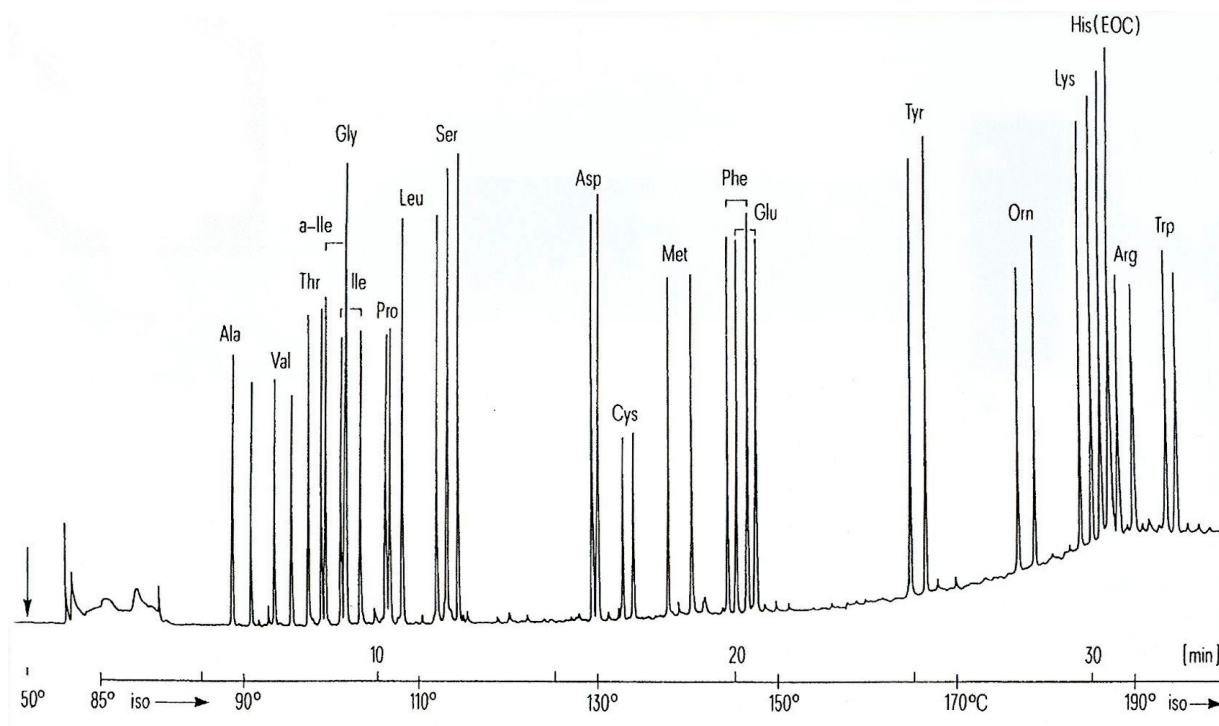


Figure 3 Gas-chromatogram of the enantioseparation of a mixture of 20 proteinogenic α -amino acids in the form of *N*-trifluoroacetyl isopropyl esters on Chirasil-*L*-Val CSP [29, 44].

Chirasil- β -Dex represents another versatile CSP based on permethylated- β -cyclodextrin [45-47], chemically attached to a polysiloxane (**Figure 2**) and capable of the enantioseparation of different classes of chiral selectands, e.g. underivatized alcohols, ketones, amines and even hydrocarbons devoid of any functional groups (**Figure 4**) [48].

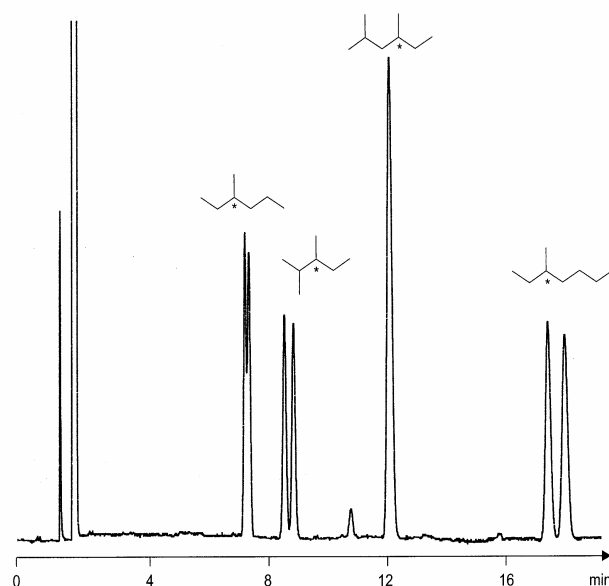


Figure 4 Gas-chromatogram of the enantioseparation of the smallest unfunctionalized hydrocarbons on Chirasil-Dex CSP. 25m x 0.25mm i.d. -capillary, T=30°C, P=40kPa [unpublished results].

The two CSPs, Chirasil-Val and Chirasil- β -Dex, are commercially available and are routinely used in analytical and research laboratories around the world. In 2005, a spacecraft aimed at the search for extraterrestrial homochirality in outer space was launched toward the 67P/Churyumov-Gerasimenko comet (Rosetta mission [48]). The spacecraft carries a gas-chromatograph equipped *inter alia* with two miniaturized enantioselective capillary columns (**Figure 5**), one coated with Chirasil-Val, the other with Chirasil- β -Dex.

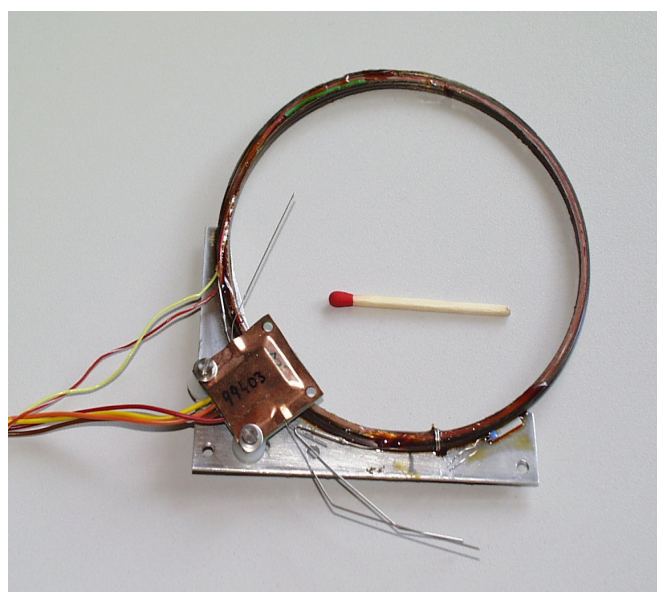


Figure 5 Enantioselective capillary column for the Rosetta/COSAC instrumentation including heater and thermo-conductivity-detector [49]

The reason for using two columns instead of one is the fact that despite high enantioselectivity of Chirasil- β -Dex toward different classes of racemates, this CSP possesses very low enantioselectivity toward derivatized proteinogenic α -amino acids, important markers to be found in space. This reflects a general fact that despite the significant progress in enantioselective chromatography, and particularly in GC, until now there exists no universal chiral selector and all the CSPs available are enantioselective only toward a certain class, or several classes, of chiral compounds.

Mixed or binary-selector CSPs^{(footnote: Stationary phase containing one kind of chiral selectors is called chiral stationary phase (CSP) or single-selector CSP. If a stationary phase contains two different chiral selectors, it is termed a binary-selector CSP. A simple mixture of different single-selector CSPs is termed as a mixed CSP.)} can be used to combine and, therefore, to expand the enantioselective properties of single-selector CSPs. One of the main intention of the present work was to develop the theoretical background and the practical implementation of the use of binary-selector CSPs, i.e. CSPs containing two different chiral selectors.

In 1975 Purnell and Laub [50,51] suggested the use of *achiral* mixed stationary phases in GC for the improvement of the separation of complex blends of compounds. Many nonpolar and polar stationary phases have been combined in this manner. For liquid chromatography (LC), there are greater constraints because the stationary phases must have compatible mobile phases. Mixed *achiral* stationary phases that have been successfully used in LC include reversed-phase with size-exclusion materials [52-55], cation- or anion-exchange with size-exclusion materials [54], reversed phase with cation- or anion-exchange materials [56-64], and cation- with anion-exchange materials [57,60,65].

Attempts to combine the enantioselective properties of different *chiral* selectors in mixed and binary-selector CSPs have been realized in liquid chromatography [66-73] and in gas-chromatography [74-80]. Many reports on using different enantioselective columns coupled in series (tandem arrangement) appeared in the literature [81-85]. In a lucid account, Pirkle and Welch treated the merits and limitations of coupling of dissimilar enantioselective columns or mixing different CSPs for the separation of enantiomers in the realm of LC [73]. The coupled-column approach, and hence the mixed approach, was considered to be advantageous only when complex mixtures of selectands had to be enantioseparated [73]. This clearly applies in attempts to enantioseparate different classes of compounds simultaneously. For GC, however, simple mixing of CSPs may be disadvantageous due to the frequent incompatibility of different polymers resulting in non-homogeneity of the produced binary mixture. Thus, because of the immiscibility, the versatile CSPs, Chirasil-Val and Chirasil- β -Dex, as well as Chirasil-Val and Chirasil- γ -Dex [86,44], another important CSP,

could not be used as simple homogeneous mixtures [unpublished results]. In 1994 Karpf [87] succeeded in the preparation of a binary-selector CSP by means of copolymerization of benzoyl-*L*-valine-bornylamide and permethyl- β -cyclodextrin both linked to dialkylcyclosiloxanes. Another rational way to overcome the problem of the immiscibility of different polymers is the chemical linking of suitable precursors of the selectors simultaneously to a polymeric matrix. Thus, Pfeiffer [86] combined resorcinarene-based *L*-valine-diamide with permethylated- β -cyclodextrin selectors by simultaneous linking them to a polysiloxane (Chirasil-Calix).

In the present work, three different ways for the combination of enantioselective properties of different chiral selectors were investigated: (a) the simultaneous immobilization of two different chiral selectors on a polymeric matrix, (b) the dissolution of a *chiral* selector in a *chiral* stationary phase and (c) the direct chemical linking of different selectors to each other.

Chirasil-Val and Chirasil- β -Dex, possessing complementary enantioselectivities, were chosen for the aim to combine the enantioselective properties by simultaneous attachment the chiral selectors to a polysiloxane. The synthesis of Chirasil-Val usually done by copolymerization of monomers [29] was modified in order to be able to use platinum-catalyzed hydrosilylation (Section 1.1.1), the method used for the synthesis of Chirasil- β -Dex. Therefore, a modified valine-diamide chiral selector bearing a long olefinic spacer, *N*-undec-10-enoylvaline-*tert*-butyl amide, was synthesized and attached to a polysiloxane by platinum-catalyzed hydrosilylation. The GC investigation of the Chirasil-Val-C₁₁ CSP thus produced showed that the important enantioselective properties of the valine-diamide chiral selector toward derivatives of α -amino acids were preserved (Section 1.1.1.1). The next step was the simultaneous attachment to a polysiloxane of the permethylated- β -cyclodextrin, also bearing a long olefinic spacer, and the valine-diamide chiral selector. This was done by platinum-catalyzed hydrosilylation leading to a novel binary-selector CSP Chirasil-DexVal combining the enantioselectivities of both Chirasil-Dex and Chirasil-Val-C₁₁ (Section 1.1).

The valine-diamide moiety was also chemically linked to a resorcin[4]arene to produce a macromolecular resorcinarene-based chiral selector possessing a cavity composed of aromatic groups and a chiral environment based on the valine-diamide moieties (**Figure 6**). The *L*-form of this selector was first synthesized by Pfeiffer et al. [86].

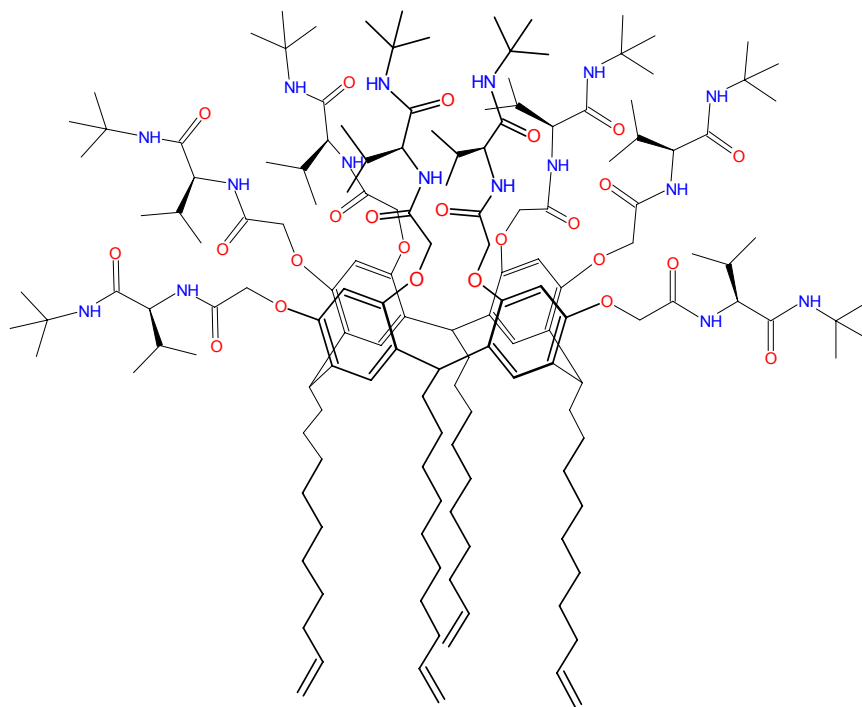


Figure 6 Octakis-*O*-(*N*-acetyl-*L*-valine-*tert*-butylamide)-*C*-decenyl-resorcinarene. Red – oxygens; blue – NH-groups.

In the present work, this selector was synthesized in both enantiomerically pure forms. Two diastereomeric binary-selector CSPs, Chirasil-Calix(*L*)Dex and Chirasil-Calix(*D*)Dex containing both resorcinarene-based chiral selectors (*L* or *D* forms, respectively) and heptakis(2,3,6-tri-*O*-methyl)- β -cyclodextrin were synthesized by platinum-catalyzed hydrosilylation. Comprehensive GC investigation of the performance of the produced binary-selector CSPs has been performed (Section 1.2). In order to analyse the influence of the presence of the diamide selector on the enantioselectivity of the cyclodextrin selector, a ternary-selector CSP containing the cyclodextrin-selector and the *racemic* mixture of the resorcinarene-based chiral selectors has been prepared and investigated (Section 1.2).

Octakis(3-*O*-butanoyl-2,6-di-*O*-*n*-pentyl)- γ -cyclodextrin first utilized by König et al.[88] is an important cyclodextrin-based chiral selector commonly used in the field of GC analysis of different classes of racemates and especially for the enantioseparation of the components of essential oils [88,89]. The feasibility of combining the enantioselective properties of this selector with those of the valine-diamide chiral selector was investigated on a binary-selector CSP obtained by dissolving the cyclodextrin selector in Chirasil-Val-C₁₁ CSP. This work is described in Section 1.3.

Direct chemical linking of different chiral selectors is the third approach that may lead to the combination of their enantioselective properties. In this case, however, one can also anticipate a change of the mechanism of the enantiorecognition, i.e. the close arrangements of chiral selectors may influence their enantioselective properties by cooperative effects. Thus, the valine-diamide moiety was chemically attached to heptakis(2,3-di-*O*-methyl)- β -cyclodextrin. The produced bifunctional valine-cyclodextrin chiral selector called **ValDex** (**Figure 7**) was prepared with the intention of combining the apolar enantioselective properties of the methylated- β -cyclodextrin cavity with the polar hydrogen-bonding chiral entities of the valine-diamide chiral selector. In order to study the enantioselective properties of ValDex, it was used as a chiral solvating agent (CSA) in NMR. This work is described in Section 1.4.

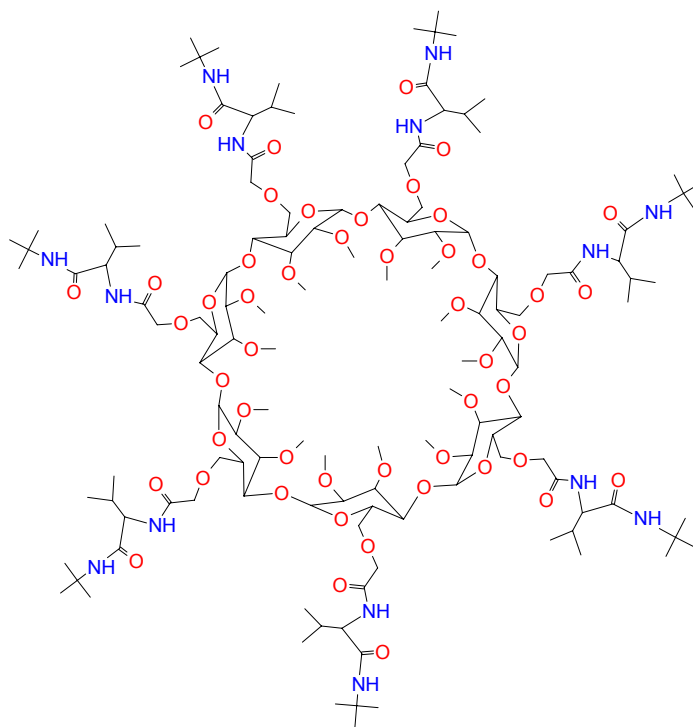


Figure 7 Heptakis[6-*O*-(*N*-acetyl-L-valine-*tert*-butylamide)-2,3-di-*O*-methyl]- β -cyclodextrin. Red – oxygens; blue – NH-groups

Chiral selectors used in enantioselective GC are often dissolved in, or chemically bonded, to achiral polymers, thereby improving the efficiency and thermal stability of the CSPs. However, the retention on such CSPs is composed of the enantioselective contribution, arising from the interaction of the selectand enantiomers with the chiral selector, and of the nonenantioselective contribution, resulting from the interaction of the selectand enantiomers with the achiral polymer [30,33,90-93]. As the result, the apparent enantioselectivity of the CSP related to the apparent enantioseparation factor, α_{app} , is different from the

enantioselectivity of the chiral selector determined from the true enantioseparation factor, α_{true} . Therefore it is mandatory to separate nonenantioselective and enantioselective contributions to retention in chromatographic selector–selectand systems displaying enantioselectivity [33].

In binary-selector CSPs, due to the presence of two chiral selectors along with an achiral polymer, the apparent enantioseparation factor, α_{app} , depends not only on the amount of the chiral selectors but also on the molar ratio between them. The theory of the enantioseparation on binary-selector CSPs including determination of the apparent and true enantioseparation factors, α_{app} and α_{true} , respectively, is discussed (Chapter 2). Using an equation for the calculation of the apparent enantioseparation factor, α_{app} , the analysis of the behavior of α_{app} upon varying the ratio and the association strengths of the two different chiral selectors present in the achiral solvent is described in Section 2.4.1.1.

Chapter 6 describes the development of a method for distinguishing between enantioselective and nonenantioselective interactions in liquid chromatography on brush-type CSPs. This method is based on the retention increment approach advanced by Schurig et al. [30,33] known for the calculation of the true enantioseparation factor, α_{true} , in enantioselective GC. Equations are derived that account for two equilibrium processes, including the nonenantioselective adsorption of the analyte on the achiral parts of the CSP and the enantioselective association of the analyte with the chiral selector present on the surface of the CSP. To verify the method, three compounds (*N*-fmoc-phenylalanine, *N*-[(3,5-dipropoxybenzyloxy)carbonyl]leucine and 2-(2,4-dichlorophenoxy)propanoic acid) were studied in three different mobile phase modes (organic polar, reversed and normal) on quinine-based CSPs with different loadings of the chiral selector.

Enantioselective chromatography is important not only for separation purposes. Since the establishment of this technique, it is widely used for the investigation of the enantiorecognition mechanisms between CSPs or chiral selectors and the selectand enantiomers. Temperature-dependent studies allow the determination of the thermodynamic parameters of the interactions between the chiral selector and the selectand enantiomers [7,33]. This information can be used for the elucidation of the mechanism of enantiorecognition and, therefore, for the optimization of the enantioseparation. An important phenomenon caused by the variation of temperature is the inversion of the elution order of enantiomers [94-99]. The reason for such an inversion is the enthalpy-entropy compensation at a certain temperature. The inversion of the elution order of enantiomers is important, e.g., for trace analyses where the trace enantiomer should be eluted as the first peak in order to

attain the high precision of the analysis. The temperature-induced inversion of the elution order of enantiomers was experimentally observed upon analysis of different derivatives of α -amino acids on Chirasil-Val-C₁₁ and Chirasil- β -Dex CSPs. The results of the comprehensive thermodynamic investigation of this phenomenon are presented in Section 3.2.

The temperature dependent study of the enantioseparation of *N*-ethoxycarbonyl propylamide derivatives of a number of α -amino acids on Chirasil-Val-C₁₁ CSP revealed nonlinearity of the plots of the natural logarithm of the enantioseparation factor as a function of the reciprocal temperature. The results of the investigation of this rare phenomenon using the retention increment method are presented in Section 3.3.

Enantioselective chromatography has been widely used for the investigation of dynamic processes occurring during the separation, e.g. chemical reactions or interconversion of enantiomers [100, 101]. The latter phenomenon has been studied for a long time in the present laboratory and is based on the calculation of the rate constants and the activation parameters from the shape of a plateau formed between the chromatographic peaks of the interconverting enantiomers [101-108]. In the present work, enantiomerization was studied on 1,2-di-*tert*-butylpyrazolidine with stereogenic centers located on the stereolabile nitrogen atoms. The GC enantioseparation of the racemate of 1,2-di-*tert*-butylpyrazolidine on the Chirasil- β -Dex CSP above 100°C revealed the characteristic plateau formation. The activation parameters were determined using the approximation function [108]. This work is described in Chapter 4.

An important problem of enantioselective chromatography is the use of enantiomerically impure chiral selectors. It should be noted that a CSP containing an enantiomerically impure chiral selector represents the simplest case of a binary-selector CSP in which different selectors are nothing else but the opposite enantiomers. Contrary to the chiral selectors based on carbohydrates that are present in the enantiomerically pure forms, synthetic chiral selectors may contain significant amounts of the opposite enantiomer. This is especially important for amino acid-based chiral selectors that are prone to racemization. A recent investigation of the enantiomeric purity of commercial compounds showed that more than half of the non-racemic substances available on the market contained more than 0.1% of the undesirable enantiomer [109,110]. The theoretical and liquid-chromatographic experimental investigation (Chapter 5) of the influence of the presence of the opposite enantiomer on the enantioseparation showed that for highly enantioselective systems, even traces of the opposite enantiomer dramatically reduces the apparent enantioseparation factor, α_{app} . This observation is especially important in the light of the high enantioselectivity of newly developed synthetic “receptor-like” chiral selectors [111-13].

Chapter 7 describes the application of enantioselective chromatography and ESR spectroscopy for distinguishing between two important crystalline modifications of chiral substances: the racemic conglomerate (crystalline modification of a chiral substance where each single crystal is composed of only one enantiomer) and racemic compound (crystalline modification of a chiral substance where each single crystal is composed of both enantiomers) [114,115]. As it is known, until now the easiest and cheapest way of separation of racemates into pure enantiomers is still the “spontaneous resolution” or “preferential crystallization” of racemates using a chiral seed [114-117]. However, a prerequisite for obtaining spontaneous resolution is the formation of a racemic conglomerate upon crystallization, i.e. precipitation of the racemate in the form of a conglomerate of enantiomerically pure single crystals. Detection of the conglomerate formation using enantioselective GC is experimentally shown in Section 7.2.

Chapter 1

1. Practice of the enantioseparation on single- and binary-selector gas-chromatographic (GC) chiral stationary phases (CSPs). Combining the enantioselective properties of different chiral selectors

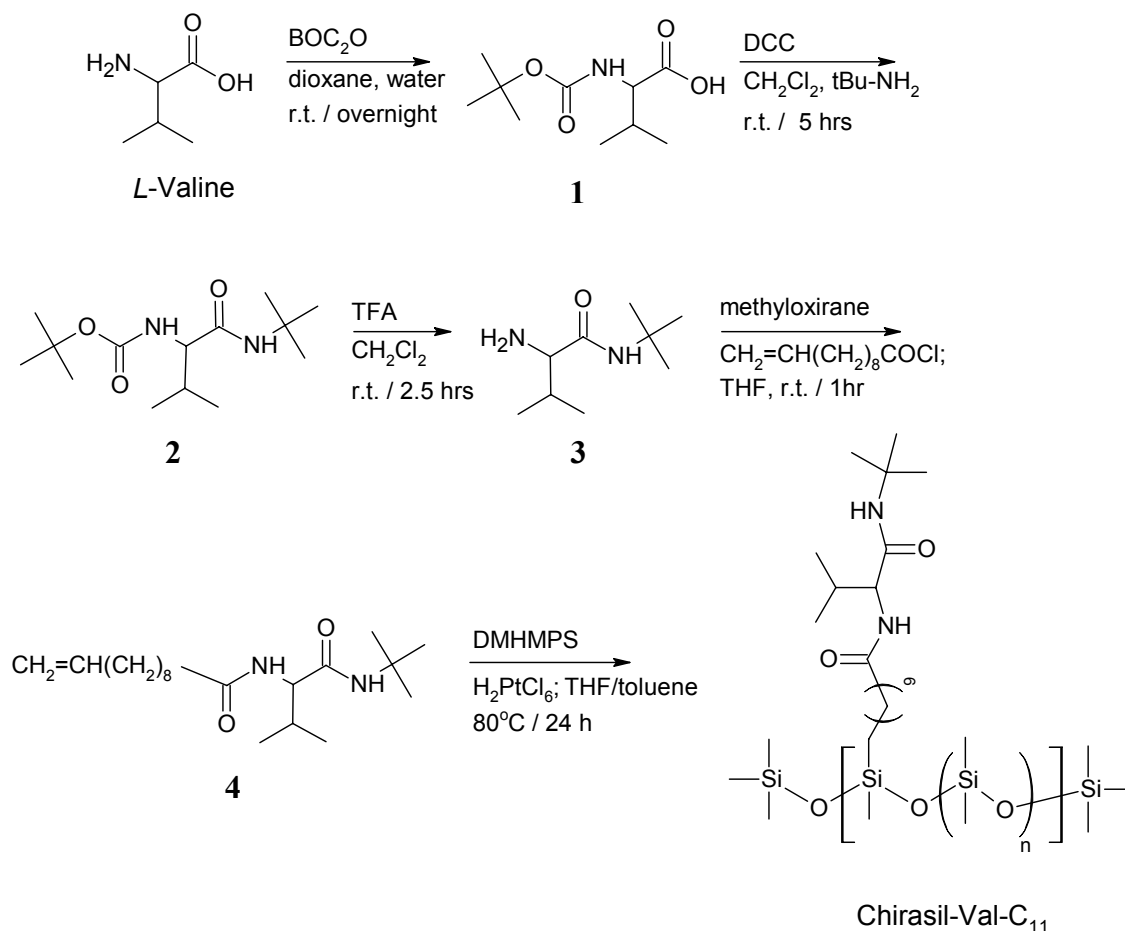
1.1 Chirasil-DexVal: combining heptakis(2,3,6-tri-*O*-methyl)- β -cyclodextrin and *L*-valine-diamide chiral selectors in one CSP

1.1.1 Synthesis of *L*-valine-diamide selector and single-selector CSP

Chirasil-Val-C₁₁

N-Acyl-*L*(*D*)-valine-*tert*-butyl amide was found to be a versatile chiral selector for the enantioseparation of amino acids as their *N*-trifluoroacetyl (*N*-TFA) alkyl esters by gas chromatography. [25] Linking this selector to a polysiloxane via polymer-analogous reaction gave rise to Chirasil-Val CSP which possessed greatly improved properties (higher thermal stability, lower solidification point). [29,43] Nowadays, Chirasil-Val is one of the most important CSP being used in enantioselective gas-chromatographic α -amino acid analyses. The strategy of the synthesis of Chirasil-Val, using a polymerization reaction of the corresponding monomers including the chiral selector itself, renders it relatively difficult to control and vary the content of the selector in the produced CSP. An alternative way to CSPs rests on the attachment of selector molecules, bearing terminal olefinic groups, to a dimethylhydromethylpolysiloxane by platinum-catalyzed hydrosilylation. [118] This approach permits the easy variation of the amount and the nature of a selector in the polymer. Previously, both the diamide CSP Chirasil-Nova, [118] the cyclodextrin-based CSPs, Chirasil-Dex, [45-47] Chirasil- γ -Dex, [119] as well as the complexation CSPs such as Chirasil-Metal [31,120] were obtained using platinum-catalyzed hydrosilylation. In addition, the hydrosilylation approach allows one to link *different* chiral selectors to one polymer, thereby combining their enantioselective properties within the same CSP as shown for Chirasil-Calix. [121] In the present section, synthesis and gas-chromatographic investigation of a novel CSP based on the *L*-valine-diamide selector chemically attached to a polysiloxane using platinum-catalyzed hydrosilylation is described. The synthesis of Chirasil-Val-C₁₁ was shown to be more straightforward than that of the commercially available CSP, Chirasil-Val, and the enantioselective properties were found to be excellent for the enantioseparation of α -amino acids.

The synthesis of the Chirasil-Val-C₁₁ CSP is schematically shown in **Scheme 1.1**. Protection of the amino group of valine with BOC is followed by amidation of the carboxylic group with *tert*-butylamine to yield the diamide **2**. After deprotection, the free amino group was acylated with undec-10-enoyl chloride to give **4** (diamide (DA) chiral selector), which was immobilized on dimethylhydromethylpolysiloxane (DMHMPS) by platinum-catalyzed hydrosilylation leading to Chirasil-Val-C₁₁. The long hydrocarbon C₁₁-spacer connecting the selector molecules to the polymer increases the mobility of the selector in the stationary phase. In addition, the spacer renders the polymer less polar and decreases the solidification temperature. The polysiloxane containing 30% (w/w) of the selector is still liquid at room temperature. That allows GC analyses of highly volatile racemates at low (ambient) temperatures. In addition, embedding of apolar components into CSPs (e.g. hydrocarbons) may even improve their enantioselective properties. Such a phenomenon is known as *squalane effect* [122] and was previously used to amend the enantioseparation of several CSPs. [118,123] To check the thermal stability of the CSP, a 20-m Chirasil-Val-C₁₁ column was conditioned at 200°C for five days whereby no decrease in the enantioseparation factor α was observed.



Scheme 1.1 Synthesis of Chirasil-Val-C₁₁ starting from *L*-valine

1.1.2 GC investigation of Chirasil-Val-C₁₁

Chirasil-Val-C₁₁ CSP was found to have very good enantioselective properties towards derivatives of all investigated proteinogenic amino acids. A representative chromatogram is shown in **Figure 1.1** (His and Arg are not included). Enantioseparation of the proline (as *N*-TFA alkyl ester) bearing a secondary amino group has been always a problem on the diamide-type CSPs, [44] nevertheless, this could be overcome in a binary CSP (*vide infra*). A frequent degradation of derivatized Ser and Cys during GC experiments [118] could be solved by thorough purification of the produced CSP. However, it should be noted that occasionally an increase of the enantiomeric excess of racemic cysteine from zero, caused by enantioselective decomposition of the amino acid during the chromatographic experiments, was observed. The same effect has been recently observed on a commercial Chirasil-Val column (unpublished results).

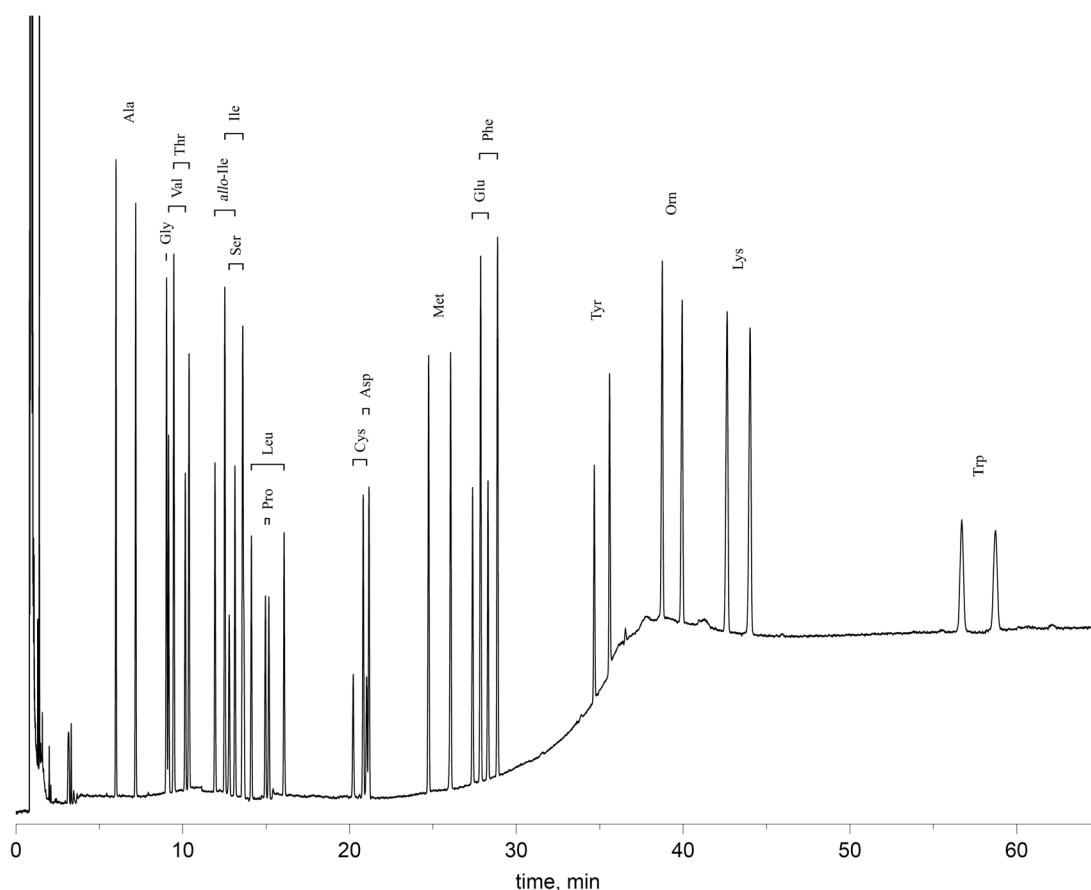
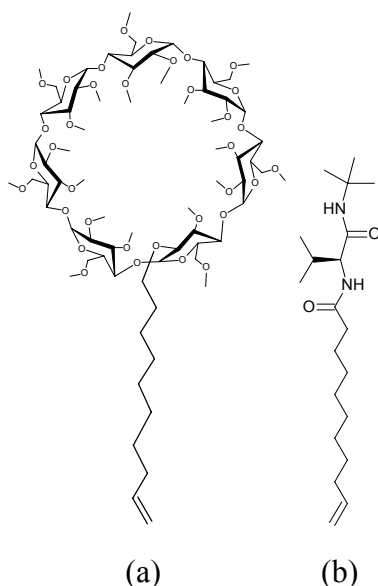


Figure 1.1 Enantiomeric separation of proteinogenic amino acids as *N*-trifluoroacetyl ethyl esters on Chirasil-Val-C₁₁ (30%). Carrier gas H₂, 50 kPa; temperature program: 70°C/3 min isothermal, then 3°/min up to 170°C followed by 30 min isothermally. Column: fused silica 20 m, 0.25 mm i.d., 0.25 μm polymer film thickness.

Thus, a diamide CSP, Chirasil-Val-C₁₁, has been synthesized by means of attachment of the *L*-valine-diamide selector to dimethylhydromethylpolysiloxane matrix using platinum-catalyzed hydrosilylation. The enantioselective properties of this readily accessible CSP have been found to be similar to that of the commercially available Chirasil-Val CSP. The developed synthesis of the valine-diamide selector and its subsequent attachment to a polysiloxane can now be used for the combination of different selectors in the same polymer (*vide infra*).

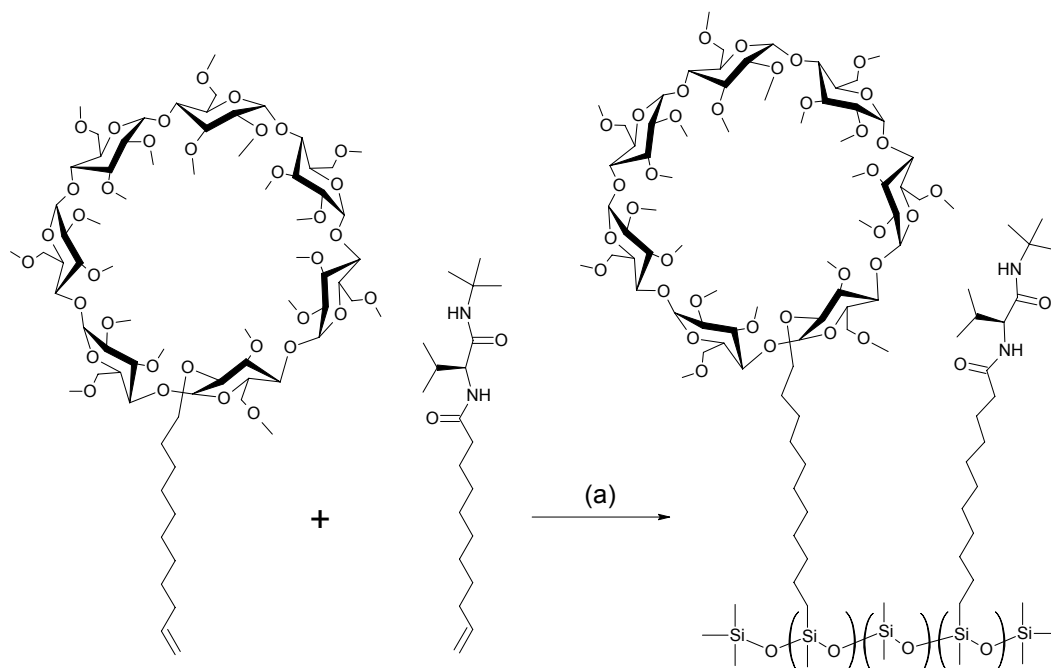
1.1.3 Synthesis of the single-selector CSP Chirasil-Dex and binary-selector CSP Chirasil-DexVal

The valine-diamide selector (DA) (**Scheme 1.2**) and the corresponding CSP, Chirasil-Val-C₁₁, were prepared as described in Section 1.1.1. The cyclodextrin selector (CD) was prepared according to a described procedure [47,124] using 10-undecenylbromide [125] instead of 7-octenylbromide. It should be mentioned that mono-undecenylation in the 2-position of β -cyclodextrin followed by permethylation is confirmed for CD (cf. **Scheme 1.2**) in contrast to the previous assignment [125]. Chemical immobilization of CD on the dimethylhydromethylpolysiloxane gave Chirasil-Dex CSP. The percentage of CD in the polymeric matrix was 20% (w/w).



Scheme 1.2 (a) The cyclodextrin selector monokis-2-*O*-undecenyl-permethylated- β -cyclodextrin (CD); (b) the valine-diamide chiral selector (DA).

To produce the binary-selector CSP, Chirasil-DexVal-C₁₁, a mixture of DA and CD selectors were simultaneously attached to dimethylhydromethylpolysiloxane by one-pot platinum-catalyzed hydrosilylation under ultrasonic conditions (**Scheme 1.3**).



Scheme 1.3 Synthesis of the binary-selector CSP Chirasil-DexVal; (a) dimethylhydromethylpolysiloxane, hexachloroplatinic acid (cat.), 50°C, ultrasonic bath, 24h.

1.1.4 Comparison of the enantioselective properties of the single- and binary-selector CSPs: Chirasil-Dex, Chirasil-Val-C₁₁ and Chirasil-DexVal, respectively

Underivatized alcohols and hydrocarbons are known to be enantioseparated on the CD selector, [45-47] while enantioseparation of α -amino acid derivatives is a prerogative of the DA selector. [25,26,44] To demonstrate the preservation of the enantioselective properties of the DA selector in the binary CSP, a mixture of seventeen proteinogenic amino acids was analyzed on Chirasil-Val-C₁₁ (**Figure 1.1**), Chirasil-Dex (**Figure 1.2**) and on Chirasil-DexVal (**Figure 1.3**). Although there is an inherent decrease in the enantioselectivity of the binary-selector CSP, all the amino acids (except Asp) were baseline enantioseparated on Chirasil-DexVal containing 20% (w/w) of the CD selector and 15% (w/w) of the DA selector.

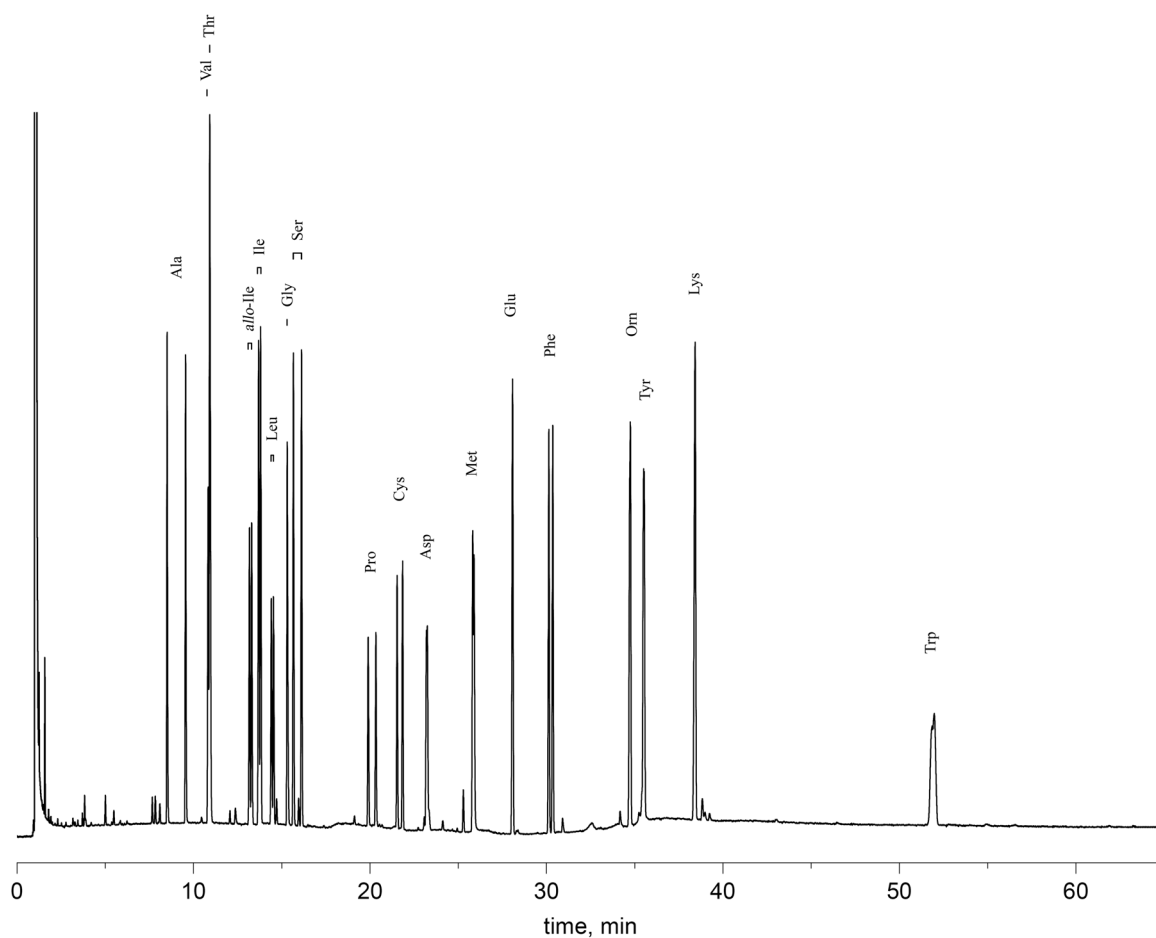


Figure 1.2. Enantiomeric separation of proteinogenic α -amino acids as *N*-trifluoroacetyl ethyl ester on Chirasil-Dex (20%, w/w). Carrier gas H_2 , 50 kPa; temperature program: $70^\circ C/3$ min isothermal, then $3^\circ/min$ up to $170^\circ C$ followed by 30 min isothermally. Column: fused silica 20 m, 0.25 mm i.d., 0.25 μm polymer film thickness.

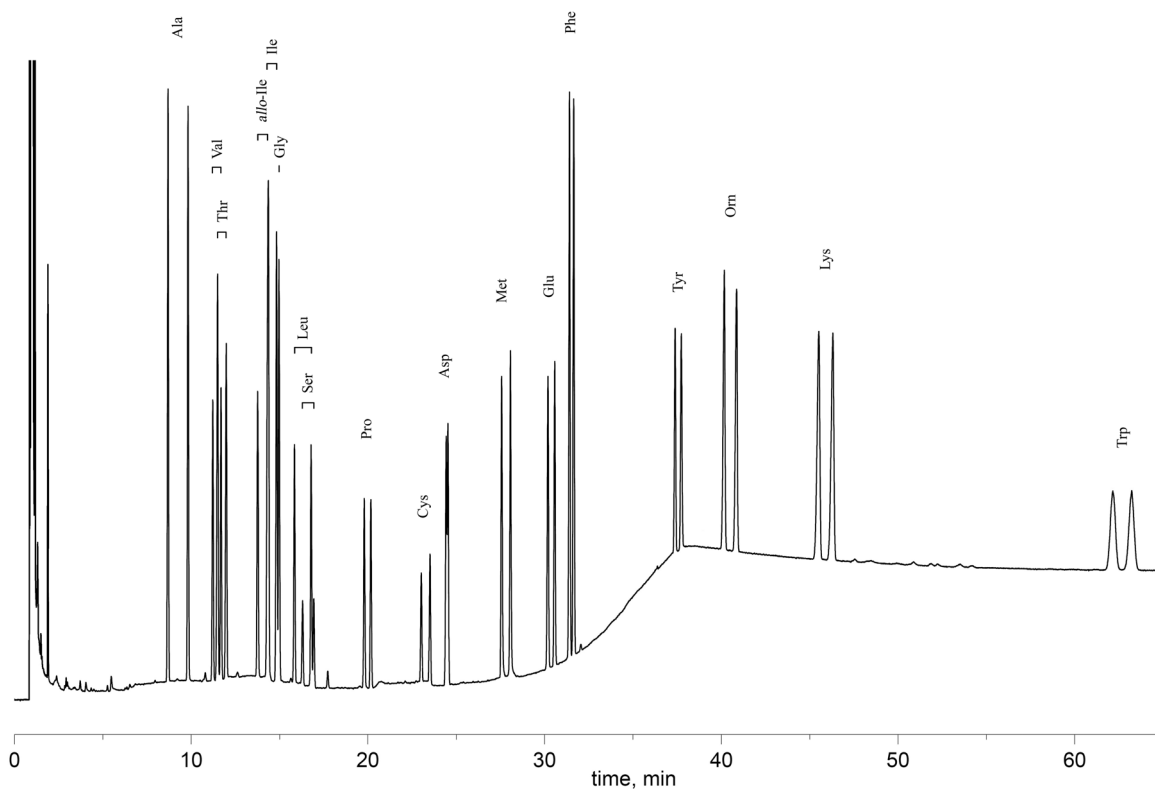


Figure 1.3 Enantiomeric separation of proteinogenic α -amino acids as *N*-trifluoroacetyl ethyl ester on Chirasil-DexVal CSP (20% of CD and 15% of DA selector, w/w). Carrier gas H_2 , 50 kPa; temperature program: $70^\circ C/3$ min isothermal, then $3^\circ/\text{min}$ up to $170^\circ C$ followed by 30 min isothermally. Column: fused silica 20 m, 0.25 mm i.d., $0.25 \mu\text{m}$ polymer film thickness.

In order to meet the imposed requirements, the binary-selector CSP Chirasil-DexVal had also to preserve the enantioselective properties of the CD selector. Therefore, a set of underivatized alcohols (Table 1.1) was analyzed on Chirasil-DexVal and the results were compared with that obtained on the single CSPs. Contrary to the CD, the DA selector displays no enantioselectivity towards the alcohols. Nevertheless, all the underivatized alcohols studied are enantioseparated on the binary-selector CSP Chirasil-DexVal, thus, confirming the preservation of the enantioselective properties of the CD selector.

Table 1.1 Enantioseparation of underivatized alcohols on Chirasil-Dex, Chirasil-Val-C₁₁ and Chirasil-DexVal CSPs

Alcohols	T (°C)*	Chirasil-Dex			Chirasil-Val-C ₁₁			Chirasil-DexVal (CD – 20%, DA – 15%, w/w)		
		α	R_s	k_I	α	R_s	k_I	α	R_s	k_I
1-(4-methoxyphenyl)ethanol	120	1.10	1.07	17.12	1.00	-	5.75	1.06	2.29	17.30
1-(4-methylphenyl)ethanol	100	1.20	5.53	20.10	1.00	-	5.22	1.15	4.57	17.65
1-(2-methylphenyl)ethanol	110	1.34	5.40	16.99	1.02	0.79	3.93	1.26	4.36	14.70
1-(2-chlorophenyl)-ethanol	140	1.11	3.27	11.42	1.00	-	4.71	1.07	2.85	11.15
1-phenylpropanol	100	1.09	2.25	25.14	1.00	-	4.87	1.07	2.68	21.42
1-(2-furyl)ethanol	80	1.07	1.70	9.68	1.00	-	1.77	1.06	1.79	7.78
1-phenylprop-2-en-1-ol	120	1.09	1.07	7.66	1.00	-	2.23	1.04	1.37	7.33
<i>trans</i> -1,2-cyclohexanediol	120	1.10	2.07	10.14	1.00	-	1.64	1.07	2.29	9.52

* The experiments were carried out isothermally.

Finally, a test-mixture of racemates containing both hydrocarbons (*trans*- and *cis*- 1,3-dimethylcyclohexane and 1,2-dimethylcyclohexane), ketone (3,5-dimethylcyclohex-2-en-1-one), alcohol (1-(2-methylphenyl)ethanol) and α -amino acids (Pro, Glu, Orn, Lys as *N*-trifluoroacetyl ethyl esters) was prepared and analyzed on the single- and binary-selector CSPs. As one can see from **Figures 1.4-1.6**, the enantioselective properties of the CD and the DA selectors are successfully combined in Chirasil-DexVal leading to the baseline enantioseparation of all the racemates from the test mixture.

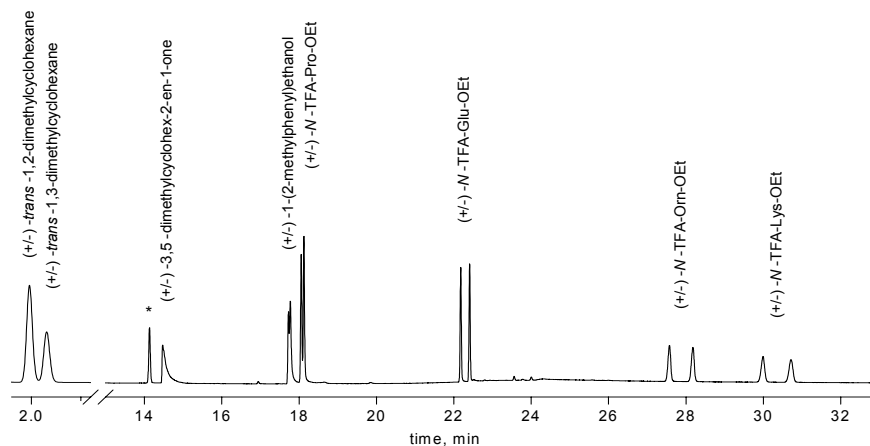


Figure 1.4 Enantiomeric separation of racemates of the test-mixture on Chirasil-Val-C₁₁, 30% (w/w), * - unknown impurity. Carrier gas H₂, 50 kPa; temperature program: 40°C/10 min isothermal, then 10°/min up to 170°C followed by 20 min isothermally. Column: fused silica 20 m, 0.25 mm i.d., 0.25 µm polymer film thickness.

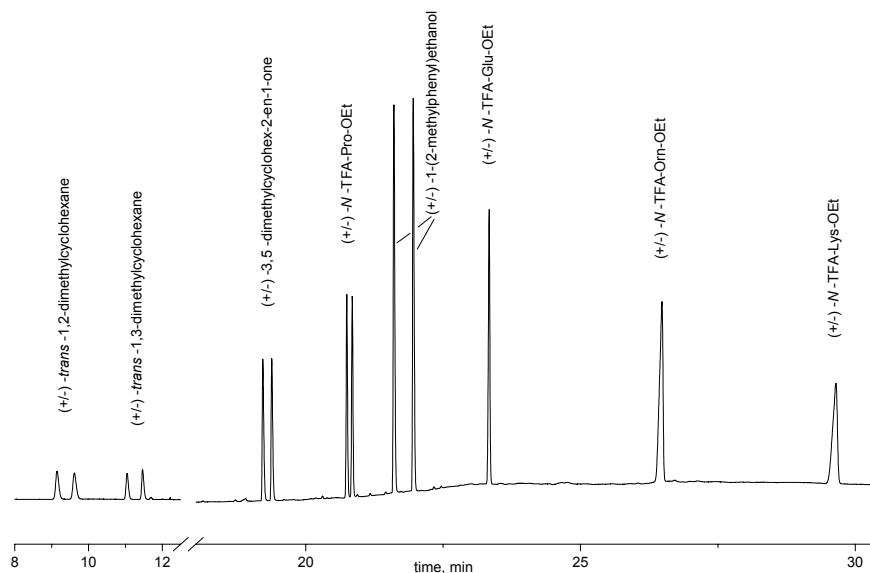


Figure 1.5 Enantiomeric separation of racemates of the test-mixture on Chirasil-Dex, 20% (w/w). Carrier gas H₂, 50 kPa; temperature program: 40°C/10 min isothermal, then 10°/min up to 170°C followed by 20 min isothermally. Column: fused silica 20 m, 0.25 mm i.d., 0.25 µm polymer film thickness.

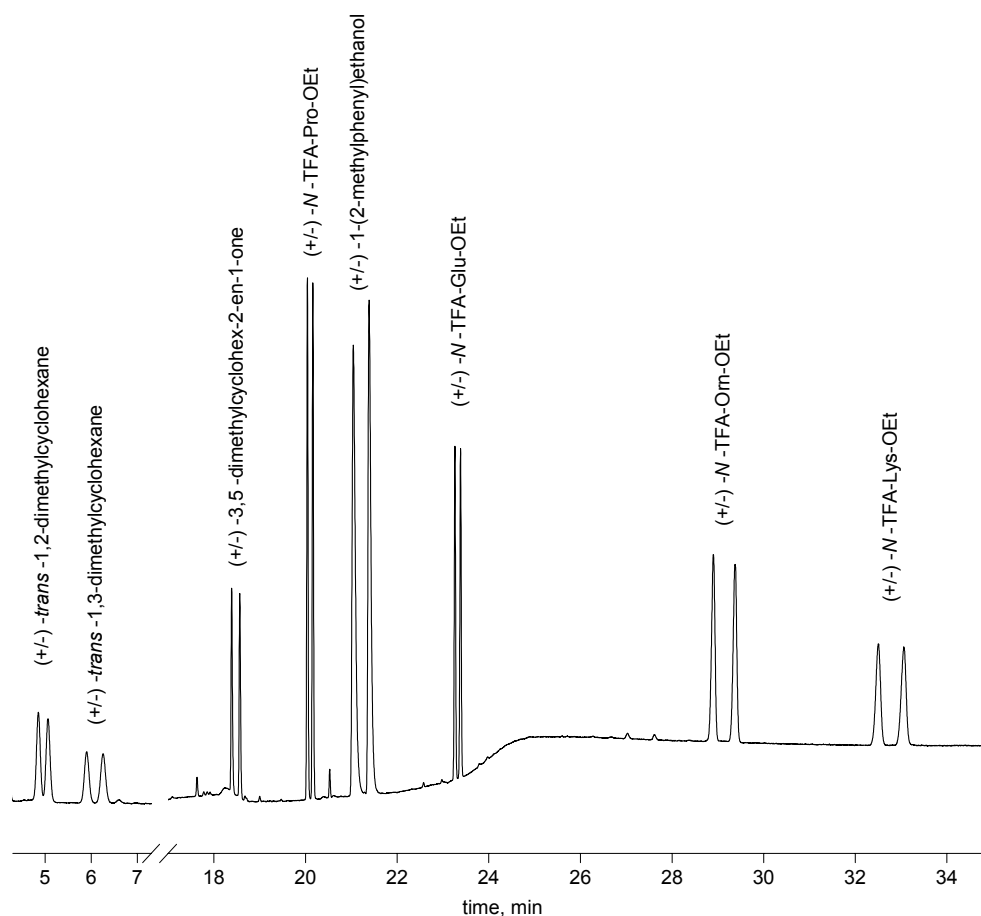


Figure 1.6 Enantiomeric separation of racemates of the test-mixture on Chiral-DexVal CSP, (20% of the CD and 15% of the DA selector, w/w). Carrier gas H₂, 50 kPa; temperature program: 40°C/10 min isothermal, then 10°/min up to 170°C followed by 20 min isothermally. Column: fused silica 20 m, 0.25 mm i.d., 0.25 μm polymer film thickness.

1.1.5 Refinement of the enantioseparation of α-amino acid derivatives on Chiral-Val-C₁₁ using the binary-selector approach

The binary-selector approach used to combine the enantioselectivity of different chiral selectors in one CSP can also be applied to improve the enantioseparation of a certain racemate in a complex mixture. In this case a small amount of a chiral selector possessing high enantioselectivity towards the problematic racemate is added to a CSP. For example, the proteinogenic α-amino acids (as *N*-TFA alkyl esters) are very well enantioseparated on the DA CSPs including Chiral-Val-C₁₁, the only problematic α-amino acid derivative being proline ($\alpha = 1.03$, $R_s = 1.1$ at 100°C on Chiral-Val-C₁₁). On the contrary, the CD selector

possesses much better enantioselectivity towards the proline derivative ($\alpha = 1.08$, $R_s = 5.0$ at 100°C) without inversion of the elution order of enantiomers. Thus, incorporation of a small amount of the CD selector into Chirasil-Val-C₁₁ should improve the enantioseparation of proline. To demonstrate this notion, a binary-selector CSP which contains predominantly the DA selector (24% w/w) and a minor amount of the CD selector (8%, w/w) has been synthesized by means of simultaneous attachment of both selectors to a dimethylhydromethylpolysiloxane using platinum-catalyzed hydrosilylation. Chromatographic examination of a mixture of the derivatives of proteinogenic α -amino acids on the obtained binary-selector CSP revealed considerable improvement of the enantioseparation of proline ($\alpha = 1.05$, $R_s = 2.2$ at 100°C), while the enantioseparation of the other α -amino acids was not significantly affected (**Figure 1.7**). Moreover, the addition of a small quantity of the CD selector also improved the nonenantioselective separation of the α -amino acids. Thus, all the seventeen proteinogenic amino acids studied were separated from each other without considerable overlapping (**Figure 1.7**).

Surprisingly, despite the relatively small amount of the CD selector added to the CSP, the enantioseparation of underivatized alcohols on the produced binary CSP was still observed and six out of eight alcohols from a test mixture were enantioseparated with resolution factor R_s higher than 1.3 (**Table 1.2**).

Table 1.2 Enantioseparation of underivatized alcohols on Chirasil-DexVal (CD – 8%, DA – 24%, w/w) CSPs

Alcohols:	T ($^\circ\text{C}$)*	α	R_s	k_I
1-(4-methoxyphenyl)ethanol	120	1.03	1.38	9.84
1-(4-methylphenyl)ethanol	100	1.07	3.11	10.18
1-(2-methylphenyl)ethanol	110	1.13	2.87	8.03
1-(2-chlorophenyl)-ethanol	140	1.04	2.11	7.20
1-phenylpropanol	100	1.04	1.24	10.50
1-(2-furyl)ethanol	80	1.03	0.90	3.68
1-phenylprop-2-en-1-ol	120	1.02	1.01	4.05
<i>trans</i> -1,2-cyclohexanediol	120	1.05	2.34	4.75

* The experiments were carried out isothermally.

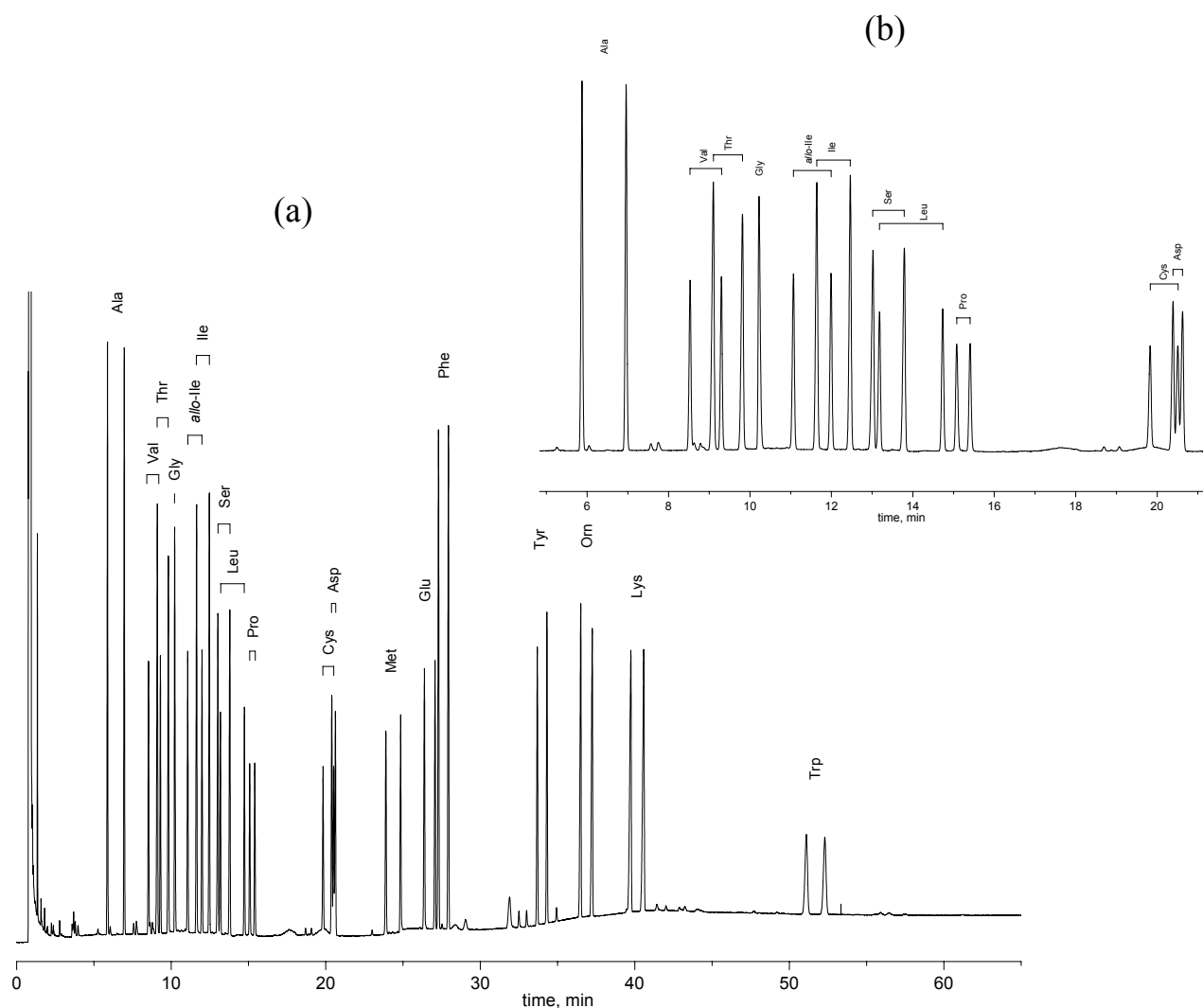


Figure 1.7 Enantiomeric separation of proteinogenic amino acids as *N*-trifluoroacetyl ethyl ester on the binary-selector CSP Chirasil-DexVal (8% of the cyclodextrin and 24% of the diamide selector, w/w): (a) the whole chromatogram, (b) enlarged initial part of the chromatogram. Carrier gas H₂, 50 kPa; temperature program: 70°C/3 min isothermal, then 3°/min up to 170°C followed by 30 min isothermally. Column: fused silica 20 m, 0.25 mm i.d., 0.25 μm polymer film thickness.

1.2 Chirasil-CalixDex: combining resorcinearene-based *L*(or *D*)-valine-diamide and heptakis(2,3,6-tri-*O*-methyl)- β -cyclodextrin chiral selectors in one CSP

Resorcinearene with pendant *L*-valine diamide groups (**L'** selector, **Figure 1.8**) and a binary-selector CSP containing **L'** and a permethylated- β -cyclodextrin chiral selector (**CD** – selector) were first synthesized by Pfeiffer et al. [121,78] The following section describes the synthesis of both enantiomers of the resorcinearene-based chiral selectors, **L'** and **D'**, (**Figure 1.8**) and their employment for the preparation and GC investigation of two diastereomeric binary-selector CSPs Chirasil-*L*-CalixDex (**CD-L'**) and Chirasil-*D*-CalixDex (**CD-D'**), respectively. In addition, a ternary-selector CSP containing **CD** and the racemic mixture of **D'** and **L'** [**CD-D'L'**] has been prepared in order to probe the influence of the racemic mixture of the resorcinearene-selectors **D'** and **L'** on the enantioselectivity displayed solely by the cyclodextrin-selector **CD** in the polymeric matrix.

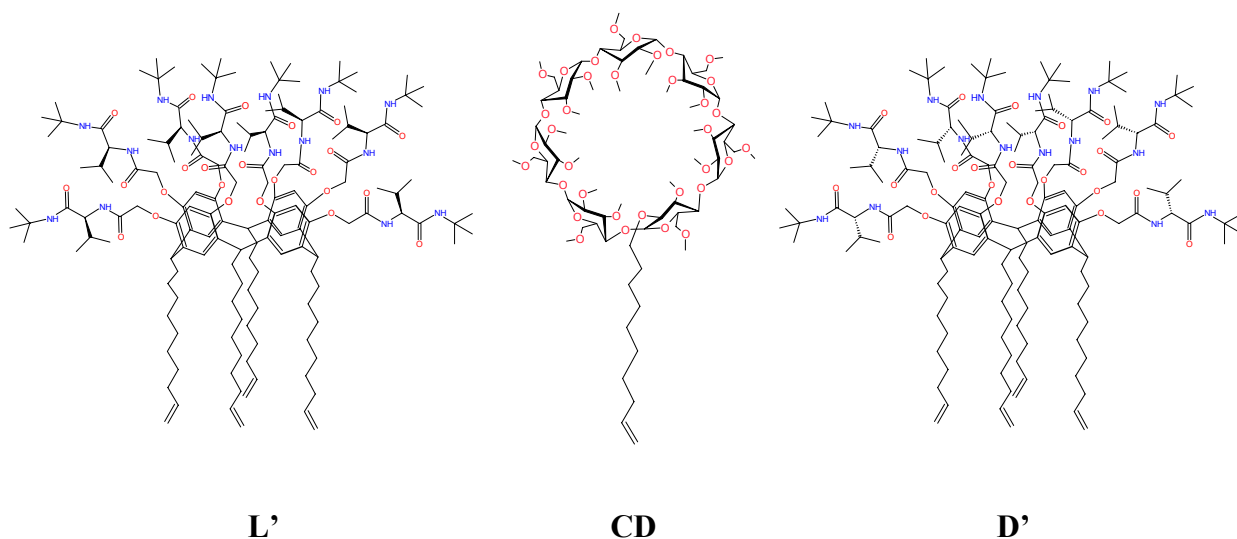
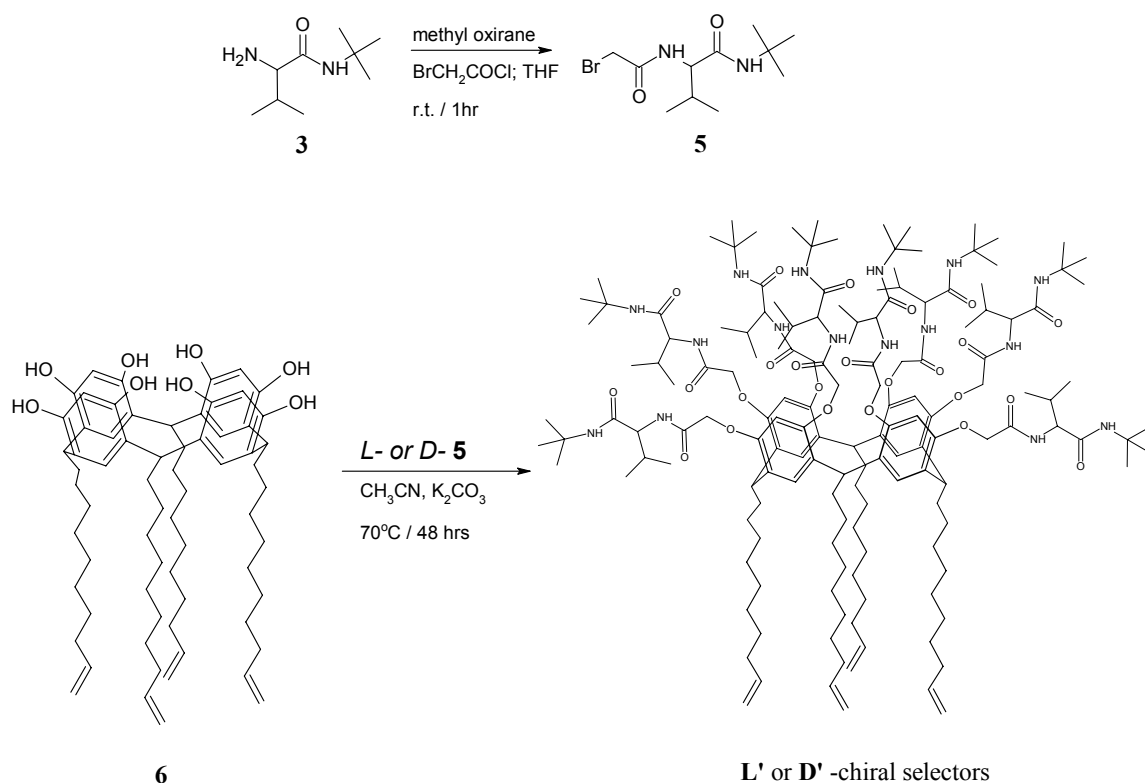


Figure 1.8 **L'** – octakis-*O*-(*N*-acetyl-*L*-valine-*tert*-butylamide)-*C*-decenyl-resorcinearene (Chirasil-*L*-Calix); **D'** – octakis-*O*-(*N*-acetyl-*D*-valine-*tert*-butylamide)-*C*-decenyl-resorcinearene (Chirasil-*D*-Calix); **CD** – monokis-2-*O*-undecenyl-permethyl- β -cyclodextrin (Chirasil- β -Dex with an 11 spacer at the 2 position of CD). Oxygens are marked with red, NH groups - with blue.

1.2.1 Synthesis of Chirasil-Calix and Chirasil-CalixDex CSPs

The same length of the spacers (C_{11}) for **CD**, **D'** and **L'** selectors was chosen to guarantee the same accessibility of the selectors by selectands in the polymeric matrix. Selectors **D'** and **L'** (**Figure 1.8**) were prepared using a modified procedure [126] starting

from *D*- or *L*-valine, respectively (**Scheme 1.4**). Acylation of the free amino group of compound **3**, which was prepared as described above (see **Scheme 1.1**), with bromoacetylchloride gave **5**. Derivatization of resorcin[4]arene **6** with **5** gave rise to selectors **L'** or **D'** depending on the configuration of the initial valine. The platinum-catalyzed hydrosilylation of **D'**-selector (or **L'**-selector) with hydromethyl(7.4%)dimethylpolysiloxane (PS) gave rise to the corresponding **D'** (or **L'**) CSP. The percentage of **D'** or **L'** in the polymeric matrix was 15% (w/w).



Scheme 1.4 Synthesis of the chiral selector **L'** (**D'**).

The binary-selector CSPs **CD-D'** and **CD-L'** were prepared by one-pot platinum-catalyzed hydrosilylation of the selector **CD** (20% w/w) and **D'** or **L'** (15% w/w), respectively, with PS. In addition, **CD-D'L'** CSP was prepared from the selector **CD** (20% w/w) and a 1:1 mixture of the selectors **D'** and **L'** (15% of the mixture in PS, w/w). The racemic nature of the 1:1 mixture of **D'** and **L'** has been proved by GC as follows. The mixture of the selectors was hydrolyzed with $\text{DCl}/\text{D}_2\text{O}$ (6 N) and the liberated free valine was examined by GC-MS on **D'** CSP.

It should be noted that if a chiral selector is diluted in a matrix (e.g., a polysiloxane), the enantioseparation factor α is rendered concentration dependent and it increases with a higher

selector loading [127]. Therefore, in the present work the individual selector concentrations of **CD** and **D'** (20% and 15%, respectively) were maintained in the binary-selector CSP **CD-D'** (or **CD-L'**) assuming the overall concentration of the selectors of 35%.

The average molecular weight of PS used for the preparation of the CSPs is 3000 g/mol and the percentage of the hydromethylsilyl groups (-SiHMe-O-) in the polymer is 7.3% (according to NMR). Based on these data the ratio between the selector molecules, individual polymeric chains, number of spacers bearing the double bonds and the binding sites (hydromethylsilyl moieties) on each polymeric chain can be roughly calculated as follows. If the terminal groups are neglected and the polysiloxane used is represented by the structure $-(\text{SiMeH-O})_X-(\text{SiMe}_2\text{-O})_Y-$, the following expression can be written $3000 = 60 \cdot X + 74 \cdot Y$. 3000 g/mol is the molecular weight of the polymer and 60 g/mol and 74 g/mol are the molecular weights of the -SiMeH-O- and -SiMe₂-O- groups, respectively. On the other hand, the percentage of the -SiMeH-O- groups in the polymer is 7.3%, therefore, the ratio X:Y is equal to 7.3:92.7. Thus, the following combined equations can be written:

$$\begin{cases} 3000 = 60 \cdot X + 74 \cdot Y \\ Y = X \cdot (92.7/7.3) \end{cases}$$

Solution of this set of equations leads to $X = 3$ and $Y = 38$, i.e. three -SiMeH-O- groups and 38 -SiMe₂-O- groups constitute one polymeric chain. Thus, it is obvious that in case of the **D'** selector, bearing four olefinic spacers, cross-linking of the polymeric chains must occur.

The binary-selector CSPs **CD-D'** and **CD-L'** are composed of 20% of **CD**, 15% of **D'** or **L'** and 65% of PS (w/w). Transformation of the weight-to-weight percentage into the molar ratio gives approximately the following proportion **CD** : **D'** : PS = 2 : 1 : 4. The previous calculation identified in each polymeric chain three hydromethylsilyl groups capable of the reaction with the double bonds of the selectors. As the **CD** selector bears one spacer and the **D'** selector contains four spacers, altogether only six spacers of the three selectors (**D'** : **CD** = 2 : 1) must be accommodated by twelve existing binding sites of the four polymer chains, i.e., only half of them are required.

Since the resorcinarene selector **D'** (or **L'**) bears four spacers, four different possibilities for a statistical linking the selectors to the polymeric chains are schematically shown in **Figure 1.9**. The probabilities of the four cases are not equal. In the case A the selector can be linked to the four polymeric chains in 81 different ways (3 possibilities for each spacer). The number of the possible ways leading to the structures B, C and D are 27, 9 and 3, respectively. The total number of the possibilities in which **L'** can be linked to a maximum of four

polysiloxane chains carrying each three binding sites is 120. Therefore, the probabilities P of the structures A, B, C and D (**Figure 1.9**) are 0.675, 0.225, 0.075 and 0.025, respectively.

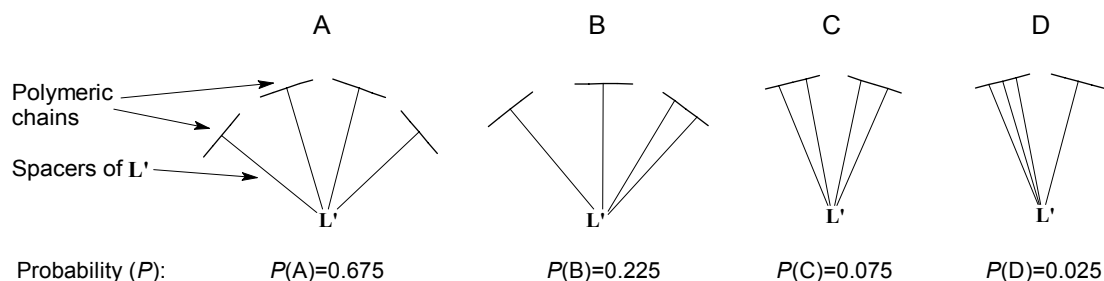


Figure 1.9 Schematic representation of the possible structures formed by reaction of selector **L'** or **D'** (having four spacers) and a maximum of four polymeric chains (having three binding sites). P is statistical probability of the structures.

Therefore, ignoring entropy effects and assuming that statistics governs the distribution of the different structures in the binary-selector CSPs **CD-D'** and **CD-L'**, the most likely structure can be drawn (**Figure 1.10**).

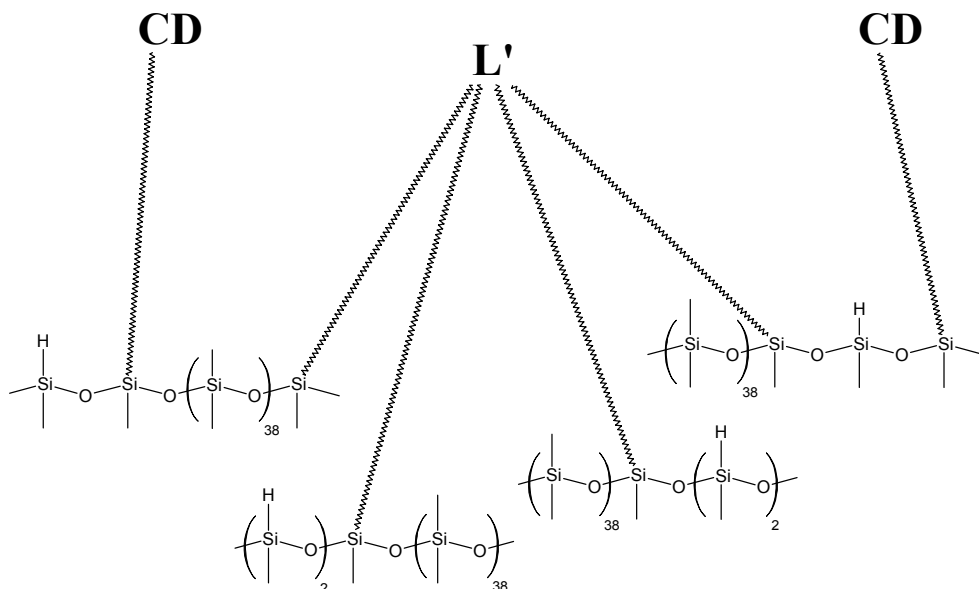


Figure 1.10 Schematic representation of the most probable structure of the binary-selector CSP **CD-L'** (20% of **CD** and 15% of **L'**). The figure shows the ratio between the selectors, polymeric chains, spacers of the selectors and the hydromethylsilyl groups capable of the reaction with the spacers.

It should be pointed out that the structure depicted in **Figure 1.10** is not a mixture of individual polymers but it is a single branched chain of a new polymer bearing two different chiral selectors. It is surprising that, despite predicted crosslinking of the polymer, it is still very good soluble in many organic solvents.

1.2.2 Comparison of the enantioselective properties of the single- and binary-selector CSPs: Chirasil-Calix, Chirasil-Dex and Chirasil-CalixDex, respectively

The purpose of this work was to expand the enantioseparation ability of both single diamide and single CD selectors by means of fixing them to a polymeric matrix in a simultaneous reaction. In order to demonstrate the versatility of such an approach, both single and binary-selector CSPs were examined by enantioselective GC and the results were compared. The chromatographic data obtained for the four CSPs **CD**, **D'**, **CD-D'** and **CD-L'** are summarized in **Table 1.3**.

Table 1.3 Chromatographic data obtained on the single- and binary-selector CSPs (Chirasil-Dex (CD), Chirasil-Val-C₁₁ (D'), Chirasil-L-CalixDex (CD-L'), Chirasil-D-CalixDex (CD-D'))

Racemates	CSPs	T(°C)	CD			D'			CD-L'			CD-D'		
			α	Rs	k ₁	α	Rs	k ₁	α	Rs	k ₁	α	Rs	k ₁
GROUP 1														
<i>Alcohols</i>														
1-(3-methylphenyl)ethanol		100	1.124	2.64	24.3	1.000	-	7.11	1.109	2.85	25.84	1.112	2.69	23.23
2-methyl-2-hepten-6-ol		80	1.082	1.92	10.9	1.000	-	4.77	1.071	1.88	11.70	1.064	1.67	9.83
2-nonanol		80	1.024	0.80	15.8	1.000	-	10.45	1.020	0.78	25.88	1.020	0.59	20.89
4-methoxy- α -methylbenzyl alcohol		120	1.096	1.07	17.1	1.000	-	8.38	1.072	2.52	21.69	1.074	2.25	20.29
1-(4-methylphenyl)ethanol		100	1.203	5.53	20.1	1.000	-	7.19	1.172	5.65	21.91	1.171	5.02	19.84
1-(2-naphthyl)ethanol		150	1.057	3.47	19.3	1.000	-	11.91	1.045	2.95	26.09	1.049	2.49	24.43
3-octen-2-ol		80	1.050	0.84	11.0	1.000	-	5.11	1.043	2.05	11.61	1.044	1.28	9.71
α -tetralol		120	1.066	2.08	26.0	1.000	-	10.23	1.053	2.60	30.64	1.053	2.72	29.22
3-methylcyclopentanol		70	1.000	-	11.0	1.023	0.50	2.55	1.000	-	10.24	1.000	-	-
1-hepten-3-ol		70	1.045	0.80	10.1	1.000	-	3.35	1.040	0.50	9.85	1.025	0.67	6.28
1-(2-methylphenyl)ethanol		110	1.343	5.40	17.0	1.000	-	5.34	1.302	6.30	18.92	1.305	4.73	16.96
1-(4-pyridyl)ethanol		120	1.089	1.53	14.0	1.000	-	5.72	1.071	2.41	17.88	1.022	1.27	12.33
1-indanol		120	1.030	0.71	11.9	1.000	-	5.57	1.024	1.25	14.75	1.026	1.24	13.74
1-phenylpropanol		100	1.092	2.25	25.1	1.000	-	6.43	1.087	2.24	26.52	1.089	2.14	22.81
<i>trans</i> -1,2-cyclohexandiol		120	1.102	2.07	10.1	1.036	0.66	3.10	1.094	2.46	12.00	1.074	1.20	10.94
3-methyl-1,5-heptadien-4-ol (1st diast.)		80	1.034	0.89	10.9	1.018	0.64	3.69	1.035	1.65	10.49	1.037	0.90	8.34
1-(2-furyl)ethanol		80	1.072	1.70	9.7	1.000	-	2.43	1.065	1.51	10.18	1.064	1.46	8.56
1-(2-bromophenyl)-ethanol		130	1.440	6.85	16.9	1.000	-	6.10	1.382	10.44	19.84	1.380	6.15	18.44
phenyl- <i>n</i> -butyl-carbinol		120	1.046	0.71	19.7	1.000	-	9.42	1.040	1.46	24.76	1.036	1.03	22.34
phenyl- <i>n</i> -propyl-carbinol		120	1.020	0.28	11.7	1.000	-	5.73	1.020	0.81	14.75	1.020	0.87	13.61
1-(2-chlorophenyl)ethanol		140	1.107	3.27	11.4	1.000	-	6.28	1.088	5.01	14.38	1.079	2.52	13.43
cyclopentyl-phenyl-carbinol		110	1.017	1.06	18.7	1.000	-	27.15	1.015	1.16	23.02	1.005	0.32	21.40
3-methyl-1-phenyl-butan-2-ol		120	1.030	0.10	11.6	1.000	-	6.68	1.030	1.07	14.28	1.021	0.86	13.07
methylheptan-3-ol		80	1.038	0.76	9.4	1.000	-	3.69	1.030	0.69	9.20	1.033	0.69	7.89
2,2-dimethylhexan-3-ol		70	1.082	1.82	12.2	1.000	-	3.56	1.069	1.48	11.96	1.071	1.82	9.50
2,2-dimethyloctan-3-ol		100	1.062	1.51	9.1	1.000	-	4.19	1.050	1.58	9.46	1.054	1.33	8.19

1-phenylethanol	100	1.140	2.80	13.1	1.000	-	1.70	1.120	2.60	13.64	1.121	4.34	13.06
<i>Others</i>													
4-hydroxy-2-pentanone	60	1.095	0.98	17.0	1.081	1.16	3.33	1.077	2.06	10.61	1.069	1.42	8.48
4-hydroxy-2-heptanone	90	1.061	1.80	9.0	1.000	-	3.88	1.047	1.60	9.63	1.050	1.37	8.47
3-methyl-2-pentanone	40	1.072	1.13	5.4	1.000	-	2.66	1.066	2.44	5.68	1.038	0.83	3.54
3-methyl-5-hepten-4-one	80	1.107	3.16	4.1	1.000	-	3.26	1.092	3.97	4.31	1.084	2.11	3.59
3,5-dimethyl-2-cyclohexen-1-one	90	1.110	2.63	13.7	1.000	-	6.30	1.097	3.26	14.64	1.092	2.13	12.28
2-bromopentane	50	1.067	1.68	4.3	1.000	-	1.89	1.086	2.24	26.20	1.034	0.94	2.62
1,2-dimethylcyclohexane (<i>trans</i>)	50	1.053	2.22	5.2	1.000	-	2.30	1.040	1.37	2.06	1.045	1.26	3.75
1,3-dimethylcyclohexane (<i>trans</i>)	50	1.066	3.25	6.7	1.000	-	1.93	1.051	2.33	4.55	1.059	1.67	4.50
2-methyl-2-ethyloxirane	40	1.053	1.33	1.1	1.000	-	2.44	1.065	1.17	4.79	1.000	-	3.37
2,2-dimethyl-3-methyloxirane	40	1.050	1.05	1.1	1.000	-	2.52	1.044	1.08	0.95	1.000	-	3.31
2-methyl-2-vinyloxirane	40	1.030	1.07	2.9	1.000	-	2.46	1.035	0.91	1.29	1.000	-	3.45
1,2-diethyloxirane (<i>trans</i>)	40	1.072	1.71	3.4	1.000	-	2.25	1.063	1.93	3.26	1.028	0.92	2.66
<i>n</i> -propyl mandelate	130	1.102	4.77	9.2	1.000	-	6.62	1.080	5.39	11.54	1.074	3.21	11.18
diethyl malate	120	1.032	0.54	9.0	1.000	-	6.21	1.020	1.00	11.61	1.023	0.86	10.29
GROUP 2													
<i>N</i> -Trifluoroacetyl, ethyl ester derivatives of amino acids													
Ala-TFA-Et	80	1.239	12.02	6.2	1.080	2.10	5.28	1.202	10.12	7.42	1.100	3.51	7.02
Val-TFA-Et	80	1.010	0.76	10.2	1.048	1.88	10.28	1.045	2.55	11.54	1.046	1.87	10.29
Ile-TFA-Et -allo	100	1.020	1.18	5.7	1.034	1.89	6.71	1.031	1.71	6.69	1.046	1.91	5.88
Ile-TFA-Et	100	1.018	1.10	6.2	1.031	1.53	7.05	1.027	1.58	7.22	1.041	1.78	6.36
Pro-TFA-Et	100	1.079	5.02	16.5	1.015	0.87	12.38	1.068	4.35	18.11	1.048	2.25	16.51
Leu-TFA-Et	100	1.024	1.46	6.7	1.066	2.81	7.34	1.057	3.38	8.67	1.072	2.99	7.57
Ser-TFA-Et	90	1.134	6.64	18.3	1.051	1.47	9.25	1.101	5.36	20.16	1.047	1.85	15.43
Thr-TFA-Et	80	1.020	1.14	10.1	1.043	1.68	12.19	1.036	1.86	13.06	1.031	1.19	10.98
Asp-TFA-Et	100	1.012	0.93	29.5	1.019	0.97	21.72	1.000	-	36.14	1.019	1.01	30.94
Cys-TFA-Et	100	1.067	3.89	22.7	*	-	-	1.067	3.84	29.33	1.031	1.41	26.45
Met-TFA-Et	120	1.014	0.81	15.3	1.000	-	14.35	1.039	2.05	19.68	*	-	-
Phe-TFA-Et	120	1.045	3.00	29.5	1.031	1.56	23.50	1.000	-	34.95	1.057	2.93	34.48
Glu-TFA-Et	120	1.000	-	21.6	1.043	2.09	20.39	1.036	2.34	26.95	1.039	1.96	27.53
Tyr-TFA-Et	140	1.010	0.84	23.2	1.033	1.85	19.91	1.023	1.56	30.24	1.041	2.19	12.68
Orn-TFA-Et	150	1.000	-	12.3	1.080	2.72	17.73	1.060	2.72	25.68	1.053	2.37	24.20
Lys-TFA-Et	160	1.000	-	12.2	1.054	2.83	15.37	1.043	2.81	23.28	1.036	3.31	22.43

Trp-TFA-Et	160	1.009	0.74	33.8	1.056	1.82	14.97	1.016	1.03	46.65	1.024	1.38	47.07
Nva-TFA-Et	80	1.016	1.12	14.9	1.085	2.83	14.85	1.081	4.92	18.12	1.059	2.48	16.13
2-Abu-TFA-Et	80	1.087	5.15	9.2	1.089	2.08	8.75	1.113	6.19	10.86	1.000	-	10.01
<i>N-Trifluoroacetyl, iso-propyl ester derivatives of amino acids</i>													
Ala-TFA-iPr	80	1.184	10.08	8.4	1.087	3.17	6.46	1.185	10.05	9.21	1.072	2.56	8.72
Val-TFA-iPr	80	1.014	0.98	12.1	1.059	2.75	12.71	1.054	3.29	13.63	1.059	2.38	11.90
Ileu-TFA-iPr -allo	100	1.024	1.31	6.9	1.038	1.99	7.93	1.033	1.84	7.68	1.053	2.36	6.63
Ileu-TFA-iPr	100	1.026	1.40	7.3	1.036	1.86	8.41	1.027	1.59	8.29	1.052	2.28	7.15
Pro-TFA-iPr	100	1.022	1.41	17.4	1.010	0.67	14.58	1.029	1.87	19.21	1.000	-	18.50
Leu-TFA-iPr	100	1.038	2.12	7.7	1.073	3.16	8.46	1.057	3.15	9.59	1.089	3.62	8.34
Ser-TFA-iPr	90	1.184	10.55	17.3	1.047	1.68	10.42	1.146	8.12	20.47	1.103	4.06	17.71
Thr-TFA-iPr	80	1.048	2.75	11.6	1.043	1.65	12.19	1.027	1.48	14.78	1.058	2.15	12.17
Asp-TFA-iPr	100	1.044	2.89	39.7	1.015	0.93	30.02	1.015	1.06	45.43	1.043	2.03	39.70
Cys-TFA-iPr	100	1.105	5.72	26.5	*	-	-	1.090	5.13	32.03	1.056	2.51	29.20
Met-TFA-iPr	120	1.018	1.03	16.5	1.056	1.20	15.27	1.037	2.58	19.96	*	-	-
Phe-TFA-iPr	120	1.022	1.53	32.7	1.035	1.83	26.87	1.020	1.37	35.77	1.044	2.32	36.63
Glu-TFA-iPr	120	1.016	1.16	28.2	1.043	2.30	25.50	1.031	2.06	32.84	1.049	2.44	32.38
Tyr-TFA-iPr	140	1.000	-	24.5	1.025	1.42	20.66	1.034	2.38	30.17	1.030	1.65	30.16
Orn-TFA-iPr	150	1.000	-	12.5	1.084	3.71	17.08	1.062	3.87	25.03	1.060	2.98	23.60
Lys-TFA-iPr	160	1.000	-	12.3	1.059	3.04	15.87	1.045	2.90	23.02	1.042	2.22	22.29
Trp-TFA-iPr	160	1.000	-	34.4	*	-	-	1.020	1.37	45.50	*	-	-
Nva-TFA-iPr	80	1.025	1.62	17.7	1.094	3.82	17.64	1.073	4.47	21.04	1.095	3.91	18.20
<i>N-Pentafluoropropionate(PFP), iso-propyl ester derivatives of amino acids</i>													
Ala-PFP-iPr	80	1.194	10.59	8.1	1.056	2.32	6.22	1.171	9.07	8.44	1.087	3.53	8.14
Val-PFP-iPr	80	1.000	-	12.2	1.034	1.69	12.62	1.033	1.99	12.58	1.036	1.55	11.33
Ileu-PFP-iPr -allo	100	1.020	1.19	6.8	1.020	1.10	7.70	1.015	0.92	6.95	1.037	1.69	6.29
Ileu-PFP-iPr	100	1.019	1.17	7.2	1.020	1.11	8.09	1.015	0.94	7.40	1.036	1.62	6.70
Pro-PFP-iPr	100	1.040	2.57	16.5	1.012	0.82	14.03	1.043	2.74	17.51	1.021	1.12	16.91
Leu-PFP-iPr	100	1.030	1.65	7.3	1.055	2.52	8.09	1.038	2.11	8.55	1.068	2.86	7.43
Ser-PFP-iPr	90	1.099	5.77	14.3	1.020	0.89	11.28	1.090	5.03	18.12	1.149	1.96	19.84
Thr-PFP-iPr	80	1.031	1.78	13.0	1.016	0.93	13.29	1.000	-	14.43	1.027	1.15	12.44
Asp-PFP-iPr	100	1.025	1.64	37.8	1.000	-	29.52	1.000	-	41.01	1.025	1.22	36.76
Cys-PFP-iPr	100	1.054	9.21	27.0	*	-	-	1.111	7.31	30.73	1.099	4.49	27.54

Met-PFP-iPr	120	1.022	1.03	15.3	1.000	-	15.57	1.020	1.09	18.03	1.000	-	17.76
Phe-PFP-iPr	120	1.022	1.55	30.7	1.024	1.38	25.42	1.023	1.64	29.88	1.037	1.94	33.94
Glu-PFP-iPr	120	1.021	1.40	25.4	1.028	1.53	23.56	1.017	1.16	28.67	1.044	2.14	28.22
Tyr-PFP-iPr	140	1.010	0.88	23.6	1.026	1.44	21.86	1.029	1.88	25.46	1.021	1.13	27.40
Orn-PFP-iPr	150	1.000	-	9.8	1.063	2.99	11.54	1.049	3.10	16.59	1.047	2.40	16.13
Lys-PFP-iPr	160	1.000	-	9.9	1.041	2.07	11.40	1.030	1.95	15.74	1.034	1.77	15.51
Trp-PFP-iPr	160	1.000	-	28.6	*	-	-	1.018	1.90	32.93	*	-	-
Nva-PFP-iPr	80	1.033	2.09	16.9	1.060	2.75	17.02	1.041	2.52	18.83	1.078	3.37	16.90
<i>Other amino acid derivatives</i>													
Abu-TFA-Me	80	1.091	4.35	6.0	1.057	1.56	5.13	1.076	1.85	10.84	1.020	0.87	6.63
Nva-TFA-Me	90	1.000	-	6.2	1.049	1.55	5.93	1.119	5.42	7.89	1.036	1.19	6.83
Met-TFA-Me	130	1.010	0.55	7.3	1.000	-	7.35	1.026	1.48	10.39	1.039	1.63	9.83
Ala-TFA-Me	80	1.000	-	4.9	1.062	1.37	3.24	1.000	-	6.41	1.089	2.31	4.65

In order to facilitate the evaluation of the multitude of the obtained chromatographic data, these were depicted graphically (**Figure 1.11**) showing the percentages of the racemates separated with $\alpha \geq 1.02$ on the four CSPs (**CD**, **D'**, **CD-D'** and **CD-L'**). The racemates were subdivided into two groups:

- group 1 involves underivatized alcohols, ketones, hydrocarbons etc, i.e. chiral compounds which are preferentially resolved on the cyclodextrin-based CSP **CD**;
- group 2 includes derivatized α -amino acids which are customarily resolved well on the diamide selector **D'** or, with peak inversion, [7] on **L'**.

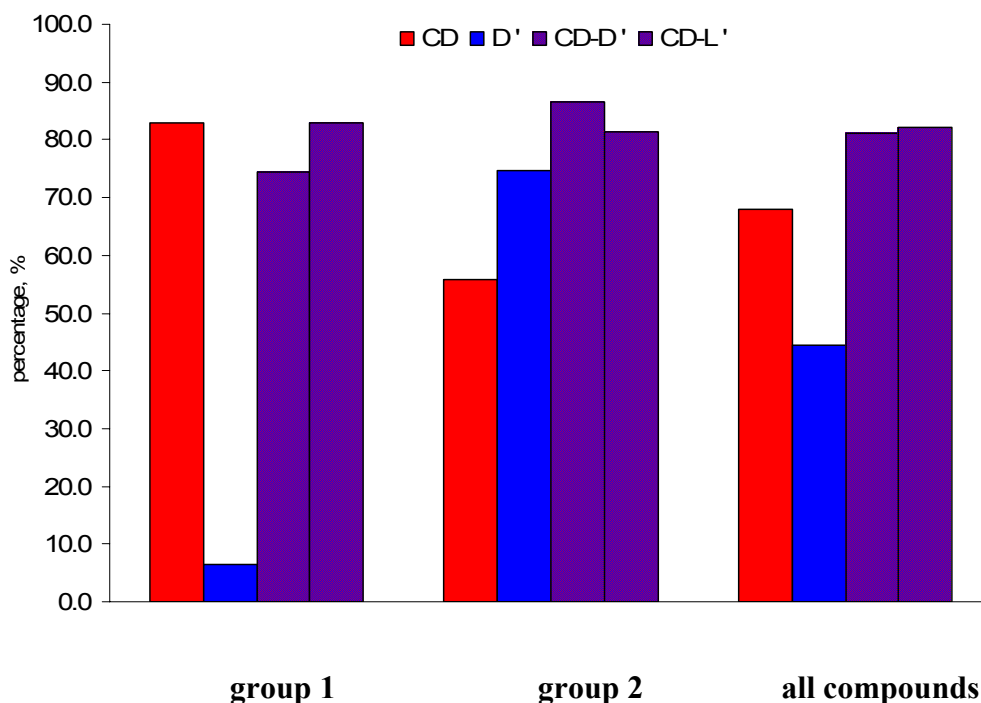


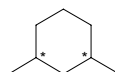
Figure 1.11 Percentage of racemates separated with $\alpha \geq 1.02$ on the single- and binary-selector CSPs: **CD**, **D'**, **CD-D'** and **CD-L'**. Group 1 includes alcohols, ketones, lactones, hydrocarbons and others (not including derivatized amino acids); group 2 includes all the investigated derivatized α -amino acids (see **Table 1.3**). The diagram is drawn on the basis of the retention data obtained from the analysis of 100 racemates.

As can be seen from **Figure 1.11**, despite the evident inability of the diamide selector **D'** to enantioseparate racemates from the group 1, the inherent enantioselectivity of the selector **CD** towards the same racemates is maintained in both binary-selector CSPs. On the other

hand, the unsurpassed enantioseparation ability of the diamide phase **D'** towards amino acid derivatives of group 2 was not only maintained but even increased in both binary-selector CSPs (**Figure 1.11**). It should be pointed out that the derivative of proline (Pro) represents the most problematic proteinogenic α -amino acid for the valine-diamide phases [44] (the enantioseparation factor α of *N*-TFA-Pro-OEt on **D'** is only 1.015). However, the cyclodextrin-based single-selector CSP shows a very good enantioseparation of proline with α as high as 1.079. As a consequence, both diastereomeric binary-selector CSPs showed better enantioseparation of the important α -amino acid in comparison to the single-selector CSPs **D'** or **L'**. Thus, the enantioseparation ability of the diamide phases **D'** or **L'** towards α -amino acid derivatives based on the hydrogen bonding can be enhanced in the binary-selector CSPs due to the inherent enantioselectivity of the inclusion-type cyclodextrin selector **CD**. Each of the binary-selector CSPs **CD-D'** and **CD-L'** were able to separate underivatized alcohols, ketones, lactones, derivatized α -amino acids, hydrocarbons etc., thereby pointing the way to the development of a single universal chiral stationary phase combining enantioselectivities of different chiral selectors. To demonstrate the unification of the enantioselective properties of the chiral selectors **D** and **D'** (or **L'**) in the binary-selector CSPs, a test mixture of different classes of racemates have been prepared (**Table 1.4**) and analyzed on the single- and binary-selector CSPs (**CD**, **L'**, **CD-D'** and **CD-L'**) (**Figures 1.12-1.15**).

Table 1.4 Components of a test mixture of racemate

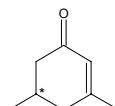
trans- and *cis*-1,3-dimethylcyclohexane



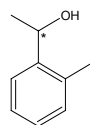
trans- and *cis*-1,2-dimethylcyclohexane



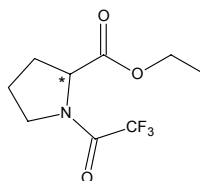
3,5-dimethylcyclohex-2-en-1-one



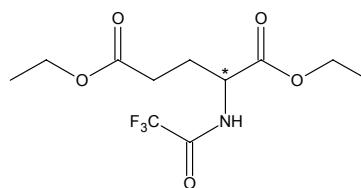
1-(2-methylphenyl)ethanol



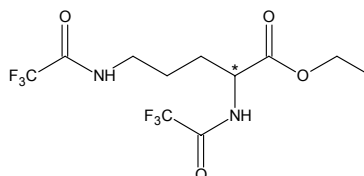
N-TFA-Pro-OEt



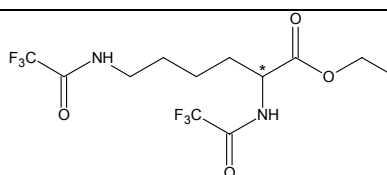
N-TFA-Glu-OEt



N-TFA-Orn-OEt



N-TFA-Lys-OEt



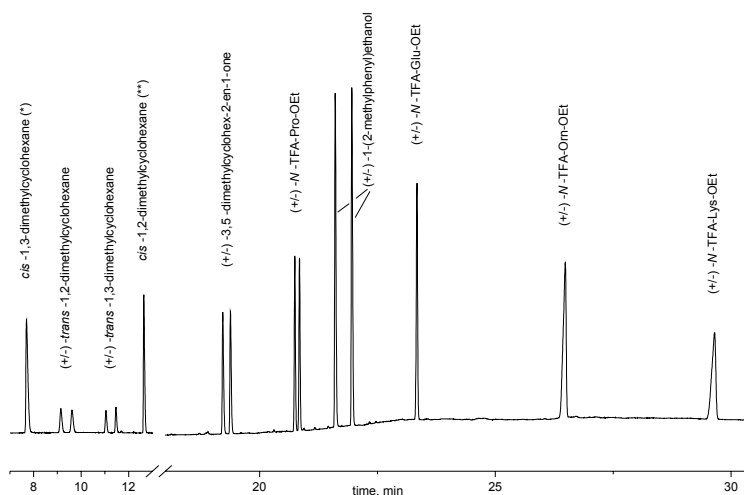


Figure 1.12 Enantiomeric separation of racemates from the test mixture (**Table 1.4**) on the single-selector CSP **CD** (Chirasil-Dex) containing 20% (w/w) of the cyclodextrin selector. Carrier gas H_2 , 50 kPa; temperature program: $40^\circ C/10$ min isothermal, then $10^\circ/min$ up to $170^\circ C$ followed by 20 min isothermally. Column: fused silica 20 m, 0.25 mm i.d., 0.25 μm polymer film thickness. (*)- Achiral; (**) - fast enantiomerization.

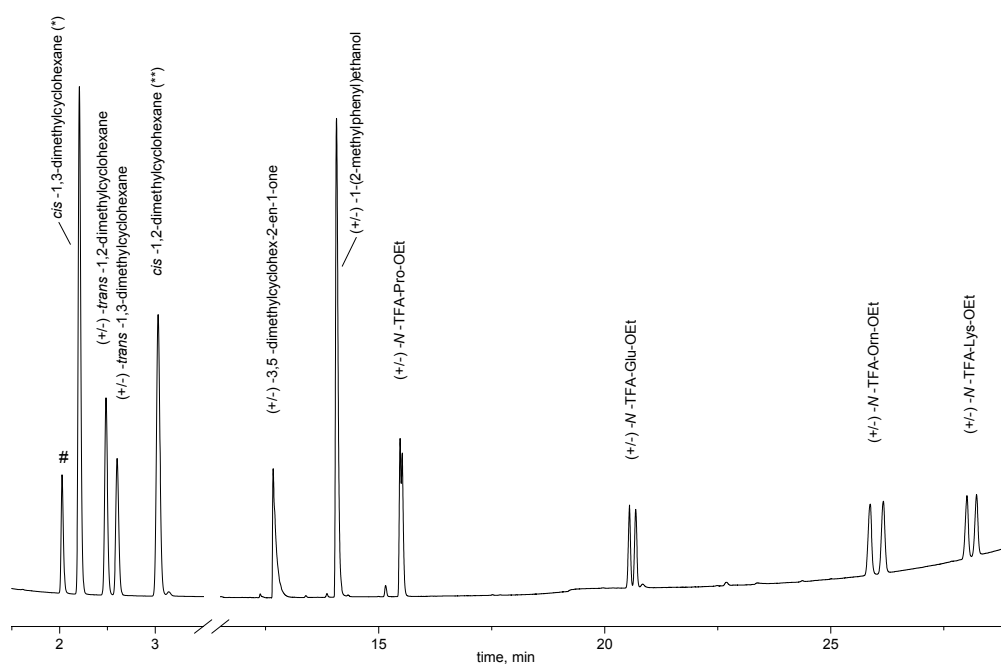


Figure 1.13 Enantiomeric separation of racemates from the test mixture (**Table 1.4**) on the single-selector CSP **L'** (Chirasil-L-Calix) containing 15% (w/w) of the diamide selector. Conditions: see caption to **Figure 1.12**. (*)- Achiral; (**) - fast enantiomerization.

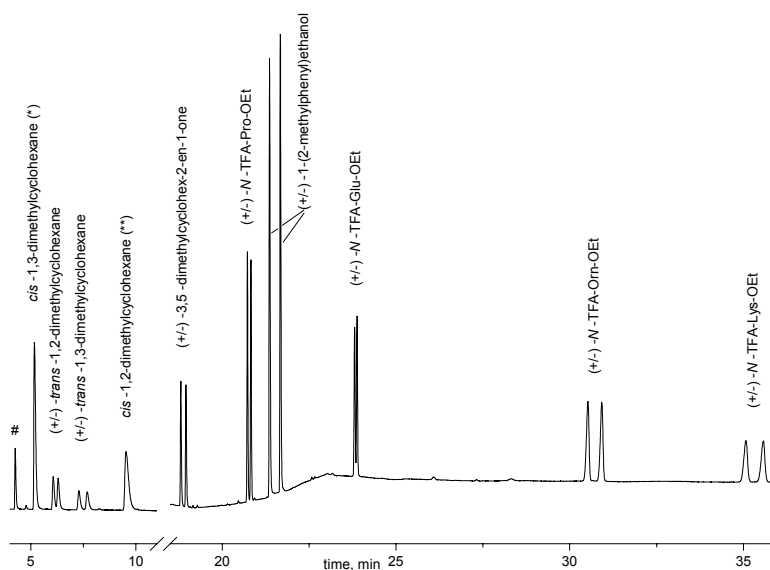


Figure 1.14 Enantiomeric separation of racemates from the test mixture (Table 1.4) on the binary-selector CSP **CD-L'** (Chirasil-*L*-CalixDex) containing 20% (w/w) of the cyclodextrin and 15% (w/w) of the diamide selectors. Conditions: see caption to Figure 1.12. (*)- Achiral; (**)- fast enantiomerization.

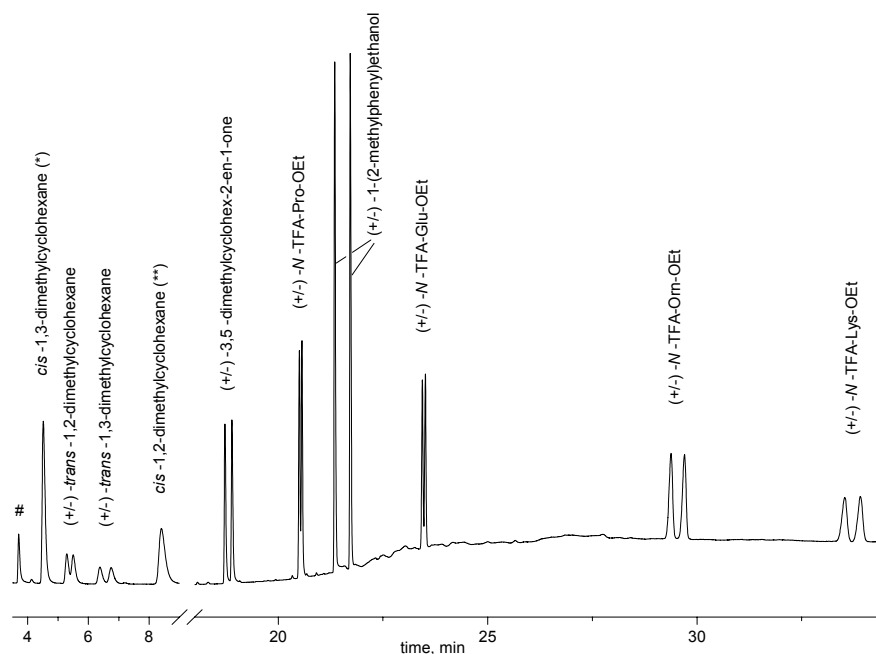


Figure 1.15 Enantiomeric separation of racemates from the test mixture (Table 1.4) on the binary-selector CSP **CD-D'** (Chirasil-*D*-CalixDex) containing 20% (w/w) of the cyclodextrin and 15% (w/w) of the diamide selectors. Conditions: see caption to Figure 1.12. (*)- Achiral; (**)- fast enantiomerization.

Examination of the ternary-selector CSP **CD-D'L'** showed an expected [73] drastic decrease of the enantioseparation factor α towards all the racemates studied. Thus, separation of enantiomers with $\alpha > 1.02$ on **CD-D'L'** was only observed for the racemates separated on the single-selector CSP **CD** with a high enantioseparation factor ($\alpha > 1.1$). The extra molecular interaction of the analytes with the *racemic* **D'L'** part of the CSP **CD-D'L'** reduced the enantioseparation factors arising entirely from the **CD** part. In other words, the nonenantioselective interaction of the analytes with the racemic part of the CSPs causes an unnecessary increase in the retention times not affecting enantioselectivity (see Chapter 2). Thus, hypothetical elongation of an enantioselective GC column with an achiral part containing a nonenantioselective selector (coupling in a series [73]) would have exactly the same result on the enantioseparation factor. This effect is clearly evident for the racemates analyzed from the group 1 which were very poorly enantioseparated on **D'** and as a consequence the decrease of the enantioseparation factor α on the binary-selector CSPs **CD-D'** and **CD-L'**, in comparison with that on the single-selector CSP **CD**, is observed (**Table 1.3**).

1.2.3 Study of matched and mismatched cases

An important phenomenon inherent to the use of more than one chiral selector present in a stationary phase is the differentiation between the mismatched case, i.e. decrease of the enantioseparation factor α on a binary-selector CSP due to the opposite elution order of enantiomers on single-selector CSPs, and the matched case, i.e. increase of the enantioseparation factor α on a binary-selector CSP due to the same elution order of the enantiomers on single-selector CSPs. Whereas the matched case always leads to a better peak separation due to increased concentration (35%), the mismatched case may lead either to peak coalescence or to peak inversion scenarios. Some examples of the matched and mismatched cases for the enantioseparation of TFA-Et amino acids are summarized in **Table 1.5** (the configurational assignment of the eluted fractions was done by GC using a mixture of non-racemic amino acid derivatives). A typical undesired mismatched case, i.e. peak coalescence, is observed for *N*-TFA-Phe-OEt and *N*-TFA-Asp-OEt (**Table 1.5** and **Figures 1.16-1.19**). The elution order of the enantiomers and the enantioseparation factor α on the single-selector CSPs are roughly additive in the binary-selector CSPs. Thus, the elution order of *N*-TFA-Leu-OEt on **CD** and **D'** CSP is the same ($\alpha = 1.024$ on **CD** and 1.066 on **D'**) and consequently an increase of α to 1.072 on **CD-D'** (matched case) and a decrease of α to 1.057 on **CD-L'** (mismatched case) is indeed observed. It should be noted that the elution order of the

enantiomers on the binary-selector CSPs for all the amino acids studied is in agreement with that on the single-selector CSP which displays the higher enantioseparation factor α (**Table 1.5**).

The calculation of the apparent enantioseparation factor α_{app} on binary-selector CSPs based on the retention data obtained on the corresponding single-selector CSPs is discussed in Chapter 2. Yet, qualitatively matched and mismatched cases can readily be observed in **Figures 1.16-1.19** which represent temperature programmed enantiomeric separations of selected derivatized α -amino acids on the single- and binary-selector CSPs. Surprisingly, there is almost no influence of the matched and mismatched cases on the overall performance of the binary-selector CSPs **CD-D'** and **CD-L'**, if all the studied racemates are compared (cf. **Figure 1.11**). It should be noted that some compounds (namely Cys, Met and Trp derivatives) have not been eluted on **D'** and **L'**, nevertheless, these racemates (except Met) were eluted on the binary-selector CSPs.

Table 1.5 Elution order of the enantiomers of α -amino acids (*N*-trifluoroacetyl ethyl ester (*N*-TFA-AA-OEt)) on the single- and binary-selector CSPs (CD, D', CD-D' and CD-L').

α -Amino acids, (<i>N</i> -trifluoroacetyl ethyl ester)	Configuration of the <i>first</i> eluted enantiomer and enantioseparation factor α of <i>N</i> -TFA-, <i>O</i> -Et amino acids on the four CSPs.			
	CD CSP	D' CSP	CD-D' CSP	CD-L' CSP
<i>N</i> -TFA-Ala-OEt (80°C)	<i>D</i> ^a 1.239	<i>L</i> 1.080	<i>D</i> 1.100	<i>D</i> 1.202
<i>N</i> -TFA-Val-OEt (80°C)	n.r.* 1.010	<i>L</i> 1.048	<i>L</i> 1.046	<i>D</i> 1.045
<i>N</i> -TFA-Ile-OEt (100°C)	<i>L</i> 1.018	<i>L</i> 1.031	<i>L</i> 1.041	<i>D</i> 1.027
<i>N</i> -TFA-Pro-OEt (100°C)	<i>D</i> 1.079	<i>L</i> 1.015	<i>D</i> 1.048	<i>D</i> 1.068
<i>N</i> -TFA-Leu-OEt (100°C)	<i>L</i> 1.024	<i>L</i> 1.066	<i>L</i> 1.072	<i>D</i> 1.057
<i>N</i> -TFA-Ser-OEt (90°C)	<i>D</i> 1.134	<i>L</i> 1.051	<i>D</i> 1.047	<i>D</i> 1.101
<i>N</i> -TFA-Thr-OEt (80°C)	n.r. 1.020	<i>L</i> 1.043	<i>L</i> 1.031	<i>D</i> 1.036
<i>N</i> -TFA-Asp-OEt (100°C)	n.r. 1.012	<i>L</i> 1.019	<i>L</i> 1.019	n.r. 1.000
<i>N</i> -TFA-Cys-OEt (100°C)	<i>D</i> 1.067	n.e.** -	<i>D</i> 1.031	<i>D</i> 1.067

<i>N</i> -TFA-Met-OEt (120°C)	<i>L</i> 1.014	n.e. 1.000	n.e. *)	<i>D</i> 1.039
<i>N</i> -TFA-Phe-OEt (120°C)	<i>L</i> 1.045	<i>L</i> 1.031	<i>L</i> 1.057	n.r. 1.000
<i>N</i> -TFA-Glu-OEt (120°C)	n.r. 1.000	<i>L</i> 1.043	<i>L</i> 1.039	<i>D</i> 1.036
<i>N</i> -TFA-Tyr-OEt (140°C)	n.r. 1.010	<i>L</i> 1.033	<i>L</i> 1.041	<i>D</i> 1.023
<i>N</i> -TFA-Orn-OEt (150°C)	n.s. 1.000	<i>L</i> 1.080	<i>L</i> 1.053	<i>D</i> 1.060
<i>N</i> -TFA-Lys-OEt (160°C)	n.r. 1.000	<i>L</i> 1.054	<i>L</i> 1.036	<i>D</i> 1.043
<i>N</i> -TFA-Trp-OEt (160°C)	<i>L</i> 1.009	<i>L</i> 1.056	<i>L</i> 1.024	<i>D</i> 1.016

^a*D* or *L* designate the configuration of the *first* eluted enantiomer. The configurational assignment was done by GC using a mixture of nonracemic α -amino acid derivatives. All the chromatograms were recorded isothermally – the temperature is given in the brackets. *n.r. – not resolved racemate. **n.e. – not eluted racemate.

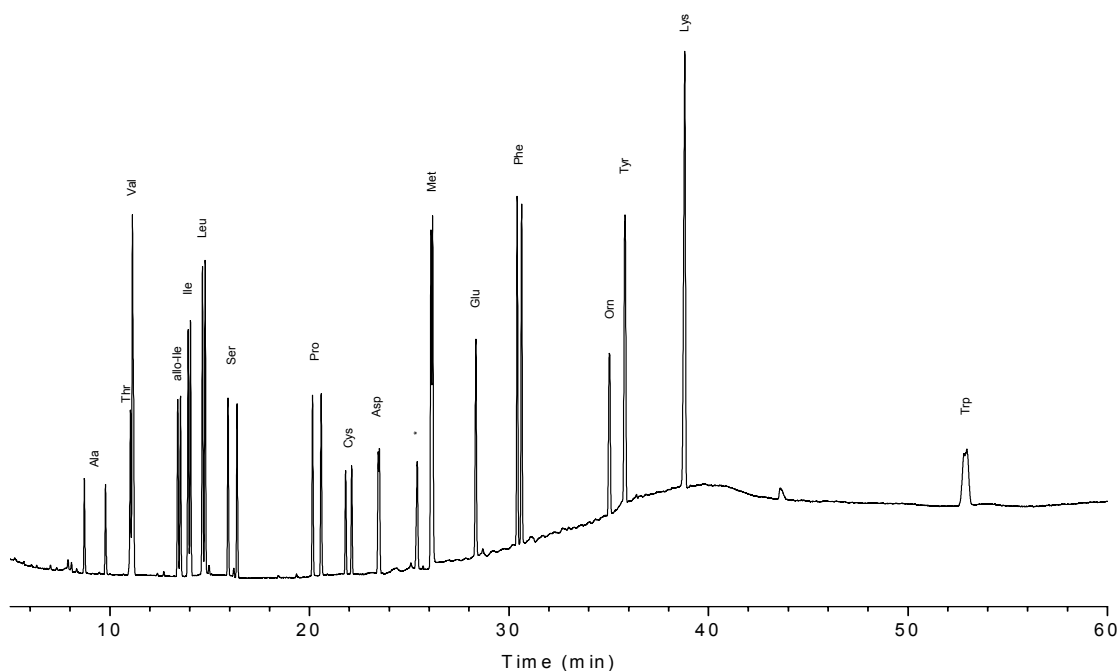


Figure 1.16 Enantiomeric separation of a mixture of α -amino acids as *N*-trifluoroacetyl ethyl ester on the single-selector CSP **CD** (Chirasil-Dex) containing 20% (w/w) of the cyclodextrin selector. Carrier gas H_2 , 50 kPa; temperature program: 70°C/3min isothermal, then 3°/min up to 170°C followed by 20 min isothermally. Column: fused silica 20 m, 0.25 mm I.D., 0.25 μ m polymer film thickness.

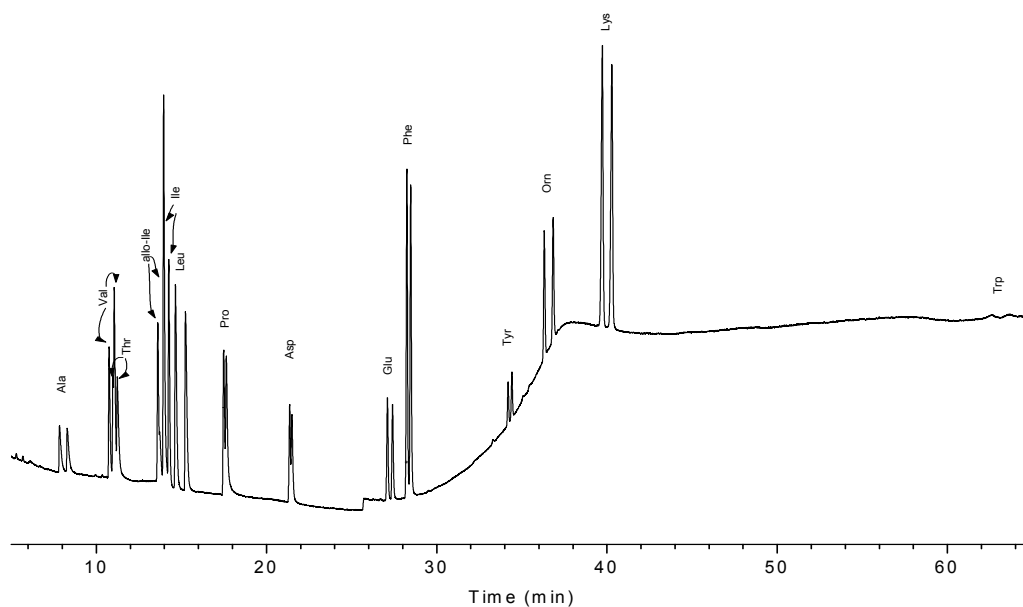


Figure 1.17 Enantiomeric separation of a mixture of α -amino acids as *N*-trifluoroacetyl ethyl ester on the single-selector CSP **D'** (Chirasil-*D*-Calix) containing 15% (w/w) of the *D*-diamide selector. Conditions: see caption to **Figure 1.16**.

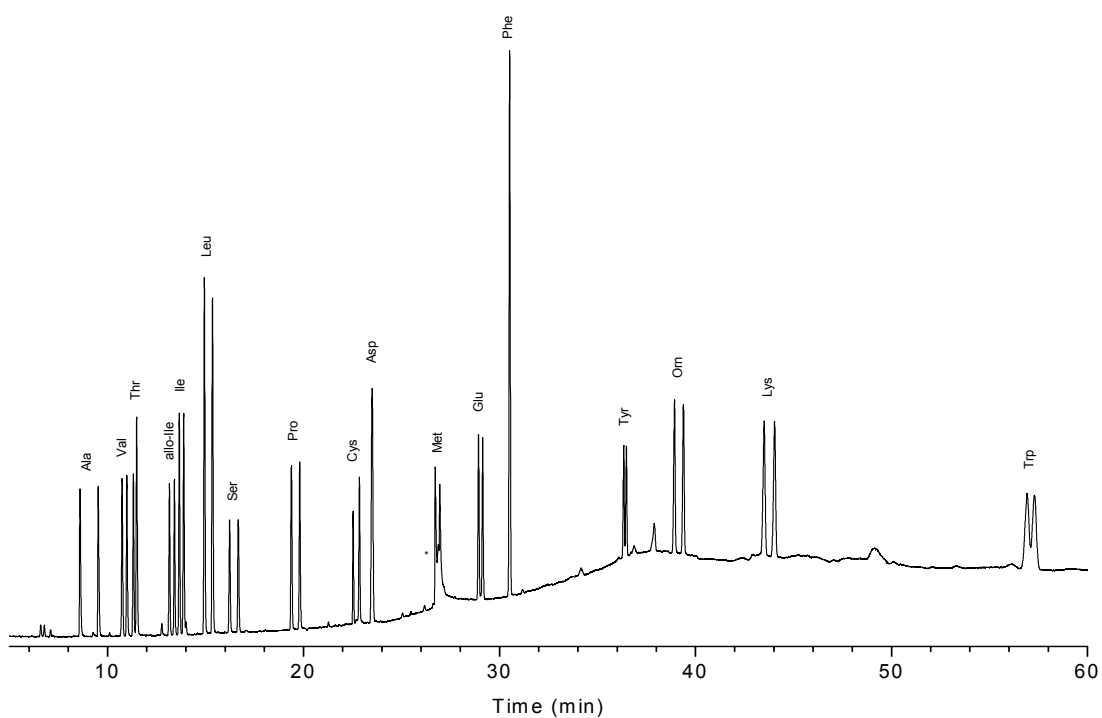


Figure 1.18 Enantiomeric separation of a mixture of α -amino acids as *N*-trifluoroacetyl ethyl ester on the binary-selector CSP **CD-L'** (Chirasil-*L*-CalixDex) containing 20% (w/w) of the cyclodextrin and 15% (w/w) of the *L*-diamide selectors. Conditions: see caption to **Figure 1.16**.

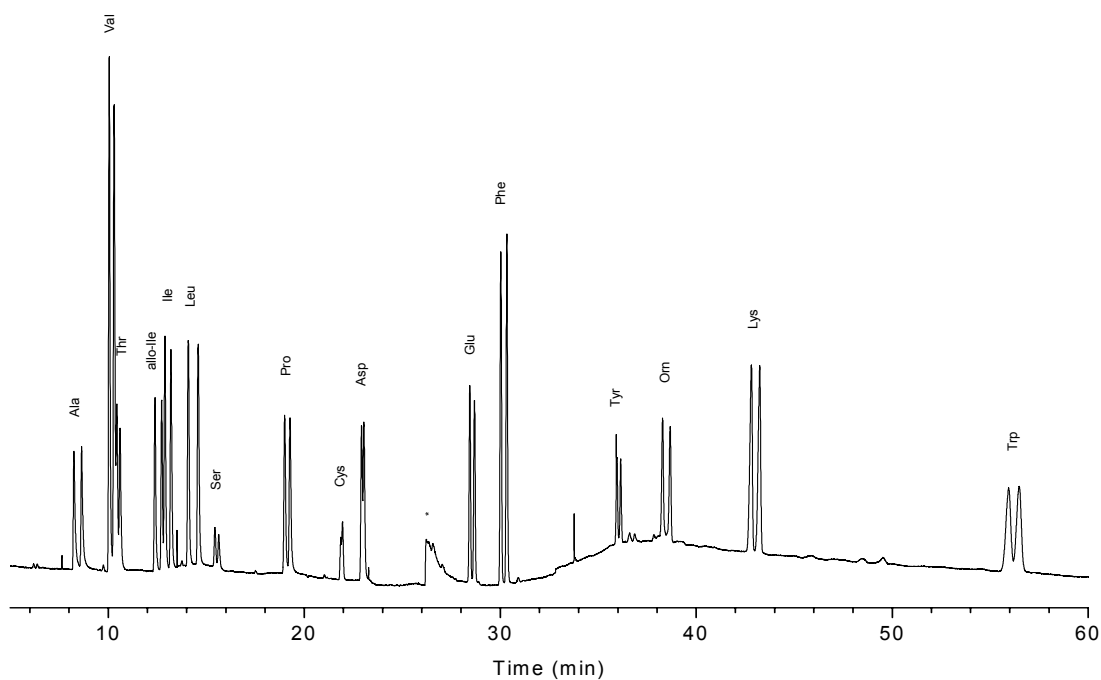


Figure 1.19 Enantiomeric separation of a mixture of α -amino acids as *N*-trifluoroacetyl ethyl ester on the binary-selector CSP **CD-D'** (Chirasil-*D*-CalixDex) containing 20% (w/w) of the cyclodextrin and 15% (w/w) of the diamide selectors. Conditions: see caption to **Figure 1.16**

1.3 Chirasil-Val(γ -Dex): combining *L*-valine-diamide and octakis(3-*O*-butanoyl-2,6-di-*O*-*n*-pentyl)- γ -cyclodextrin chiral selectors in one CSP

Octakis(3-*O*-butanoyl-2,6-di-*O*-*n*-pentyl)- γ -cyclodextrin (γ CD) (Figure 1.20), first described by König et al. in 1989 [88], is a versatile chiral selector commonly used in enantioselective GC. The γ CD was employed for the enantioseparation of many different classes of racemates [88, 128] including constituents of essential oils [89,129,130] and α -amino acid derivatives [88,44]. However, in comparison with Chirasil-Val-type CSPs (based on the *L*- or *D*-valine diamide selectors), α -amino acids Trp, Tyr, Phe, Cys and His were only partially enantioseparated [88,44]. The extraordinary enantioselectivity of γ CD toward halogenated ethers [131,132] permitted the use of the simulated moving bed (SMB) technology in preparative GC for enflurane [133] and of enantioselective sensor devices for ‘compound B’, a degradation product of sevoflurane [134]. The low solidification point of γ CD allowed the use of the selector in its undiluted form, thereby increasing the apparent enantioselectivity of the CSP [88]. However, to improve the efficiency and thermal stability of the CSP, γ CD was either dissolved in a polar polysiloxane [135] or chemically linked to an apolar polysiloxane by means of platinum-catalyzed hydrosilylation [119]. The immobilization of polysiloxane-anchored γ CD enabled its use in supercritical fluid chromatography (SFC) [119].

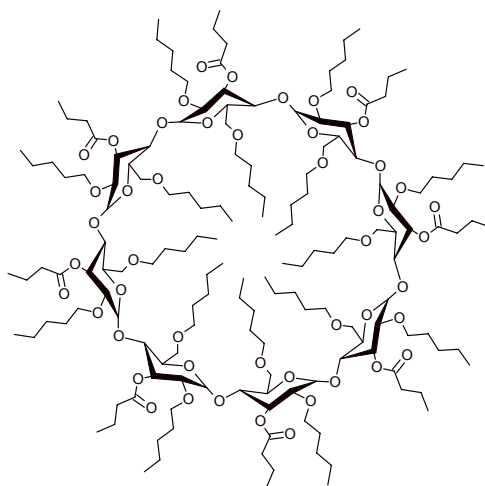


Figure 1.20 Octakis(3-*O*-butanoyl-2,6-di-*O*-*n*-pentyl)- γ -cyclodextrin (γ CD).

CSPs based on the valine-diamide chiral selector are capable of simultaneous enantioseparation of nineteen derivatized proteinogenic α -amino acids in one run. Routine usage of Chirasil-Val CSP for almost 30 years unambiguously proves its importance in the field of the enantiomeric analysis of α -amino acids. Unfortunately, the valine-diamide selector is prone to racemization which is affected by elevated temperatures and by acidic contamination introduced during injections. The racemization causes a decrease of the apparent enantioseparation factor α_{app} which is already low for proline and aspartic acid derivatives on the valine-diamide selectors. Therefore the increase of the enantioselectivity of this selector towards derivatives of proline and aspartic acid is of great practical importance. In Sections 1.1 and 1.2, a combination of the enantioselective properties of permethylated- β -cyclodextrin and *L*-valine-diamide chiral selectors [78,136,137], resulting in an improvement of the enantioseparation of the derivative of proline, was already described. The combination was achieved by simultaneous chemical linking the corresponding cyclodextrin and the *L*-valine diamide selector to an achiral polysiloxane to yield the binary-selector CSP. The use of mixed-mode CSPs has received considerable attention [72,73,75-79,136,137]. Herein another approach toward the combination of the enantioselective properties of different selectors is presented. It has previously been demonstrated that dissolution of chiral selectors in achiral polymers (e.g. OV-1701) greatly improves the efficiency and performance of enantioseparations [135]. The use of a *chiral* polymer as a matrix for the dissolution of another *chiral* selector may improve not only the efficiency but also the enantioselectivity. In the present work, the preparation of a binary-selector CSP Chirasil-Val(γ -Dex) (**DA γ CD**) by means of the dissolution of the cyclodextrin selector γ CD in the chiral polymer, Chirasil-*L*-Val-C₁₁ (**DA**), is described. It will be shown that **DA γ CD** obtained by doping **DA** with γ CD indeed possesses an improved enantioseparation ability towards *N*-trifluoroacetyl (TFA) alkyl esters of proline and aspartic acid because of the high enantioselectivity of γ CD towards these compounds whereby for proline the elution order is reversed on **DA γ CD** as compared to **DA**. In addition, it will be demonstrated that the enantioselective properties of γ CD towards some other classes of racemates are essentially retained in the binary-selector CSP, thereby expanding the scope of the applicability of the binary-selector CSP in comparison with that of the single-selector CSPs.

1.3.1 Comparison of the enantioselective properties of the single- and binary-selector CSPs: Chirasil-Val-C₁₁, Lipodex E and Chirasil-Val(γ -Dex), respectively

Two single-selector CSPs containing γ CD (20% of octakis(3-*O*-butanoyl-2,6-di-*O*-*n*-pentyl)- γ -cyclodextrin dissolved in PS-255 polymer) [88, 131] and DA (30% (w/w) of the *L*-valine-diamide selector) [136] were prepared as previously described. To prepare the binary-selector CSP DA γ CD, 20 mg of a mixture of 8% of the neat γ CD (w/w) and 92% (w/w) of the CSP DA was dissolved in 5 ml of dichloromethane/*n*-pentane (1:1 v/v). After shaking for 5 min the solution was used for the coating of a fused silica capillary by a static method [75].

A host of racemates (Table 1.6) belonging to different classes of compounds (α -amino acids, alcohols, halogenated ethers, terpenes etc.) have been analyzed on the single-selector CSPs, γ CD and DA, and on the binary-selector CSP DA γ CD. The chromatographic results are summarized in Table 1.6 and in Figures 1.21-1.26.

Table 1.6 Chromatographic data obtained on the single-selector CSPs γ CD and DA and on the binary-selector CSP DA γ CD for selected analytes.^a

Analytes:	T(°C)	CSP DA			CSP γ CD			CSP DA γ CD		
		α	k_1	R_s	α	k_1	R_s	α	k_1	R_s
1-Phenylethanol	85	1.01	7.25	0.9	1.04	21.3	2.1	1.03	8.77	1.5
2-Pentanol	40	1.00	3.37	-	1.06	4.50	1.5	1.02	3.31	0.6
2-Heptanol	40	1.00	22.4	-	1.03 ^b	26.0	1.0	1.01	21.2	0.5
Pro-TFA-Et	100	1.03	9.07	1.8	1.44	37.7	20	1.18	12.9	9.4
Asp-TFA-Me	130	1.03	3.31	1.1	1.19	6.96	9.3	1.09	3.48	4.5
Tyr-TFA-Me	175	1.07	4.29	2,7	1.00	6.32	-	1.06	4.73	3.4
Trp-TFA-Me	155	1.09	52.9	3.4	1.01	65.2	0.5	1.08	49.5	5.2
Isoflurane ^d	40	1.00	0.22	-	1.17	0.93	1.3	1.12	0.26	0.9
Enflurane ^d	40	1.00	0.23	-	1.61	1.54	3.7	1.47	0.37	3.4
Desflurane ^d	40	1.00	0.11	-	1.35	0.22	1.3	1.21	0.06	0.5
„Compound B“ ^d	40	1.00	0.79	-	6.24 ^b	8.49	12	5.46	1.81	16
Linalool	40	1.00	97.9	-	1.05	232	1.8	1.02	104	1.1
Carvone	60	1.00	47.3	-	1.04 ^c	152	1.5	1.02	54.9	1.3
Pulegone	60	1.00	44.7	-	1.16	42.5	3.2	1.03	49.5	2.0
Phenyloxirane	90	1.00	3.17	-	1.09	10.5	5.2	1.04	3.76	2.1
Methylactat	60	1.05	1.32	1.6	1.26	7.66	5.2	1.20	2.17	2.6

^athe chromatograms were recorded isothermally at 50 kPa if not otherwise stated

^bthe chromatogram was recorded at 100 kPa

^cthe chromatogram was recorded at 150 kPa

^dfor chemical structures see text

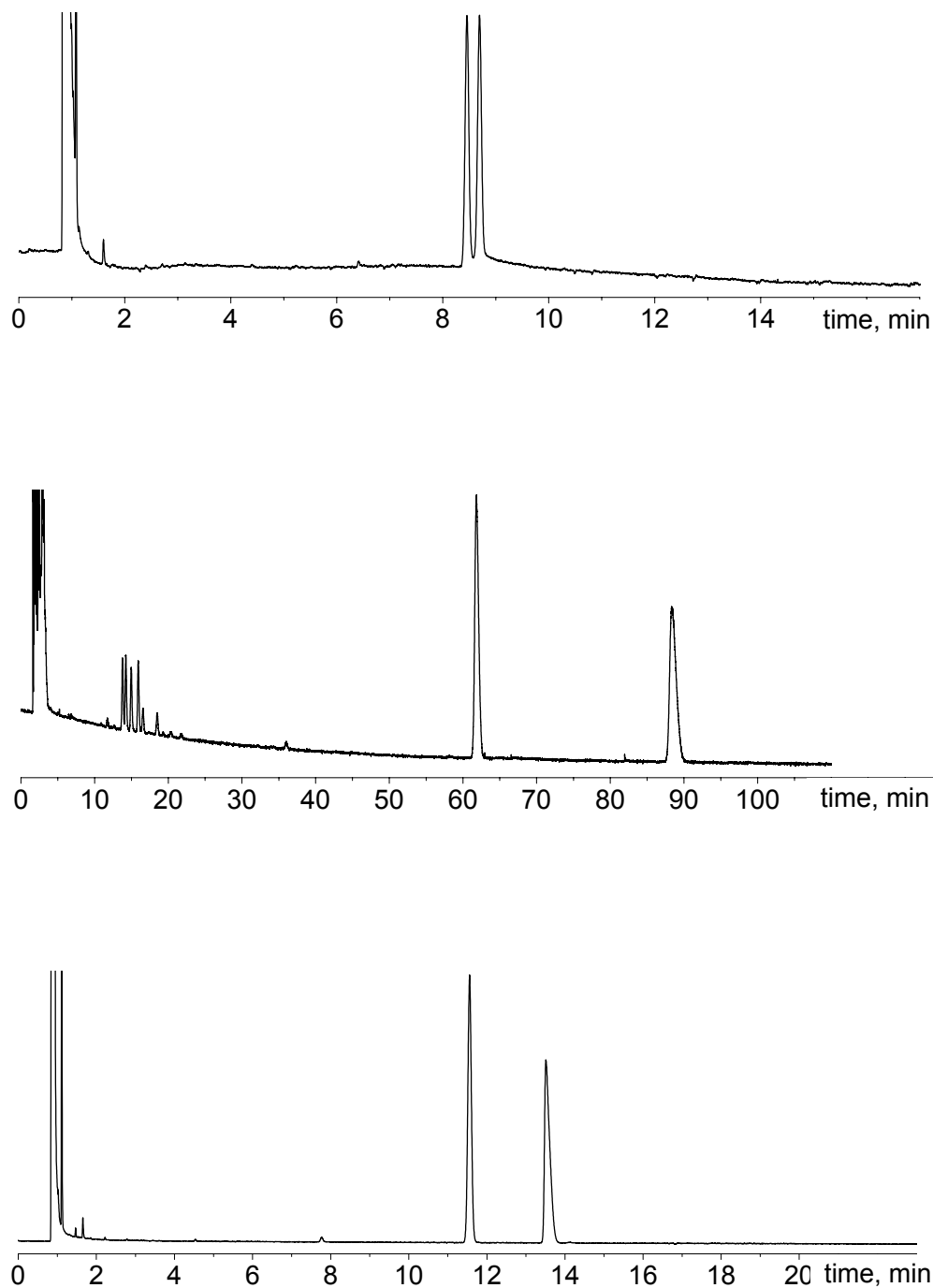


Figure 1.21 Gas-chromatograms of the enantioseparation of proline (as *N*-trifluoroacetyl ethyl ester) on the single-selector CSPs γ CD (middle) and DA (up), and on the binary-selector CSP DA γ CD (bottom). The gas-chromatograms are recorded isothermally at 100°C and 50 kPa pressure of H₂. The elution order of the enantiomers is *D* after *L* on γ CD and DA γ CD and *L* after *D* on DA. Capillaries: 20 m and 30 m for DA γ CD, DA and for γ CD, respectively, 0.25 mm i.d. and 0.25 μ m polymer film thickness.

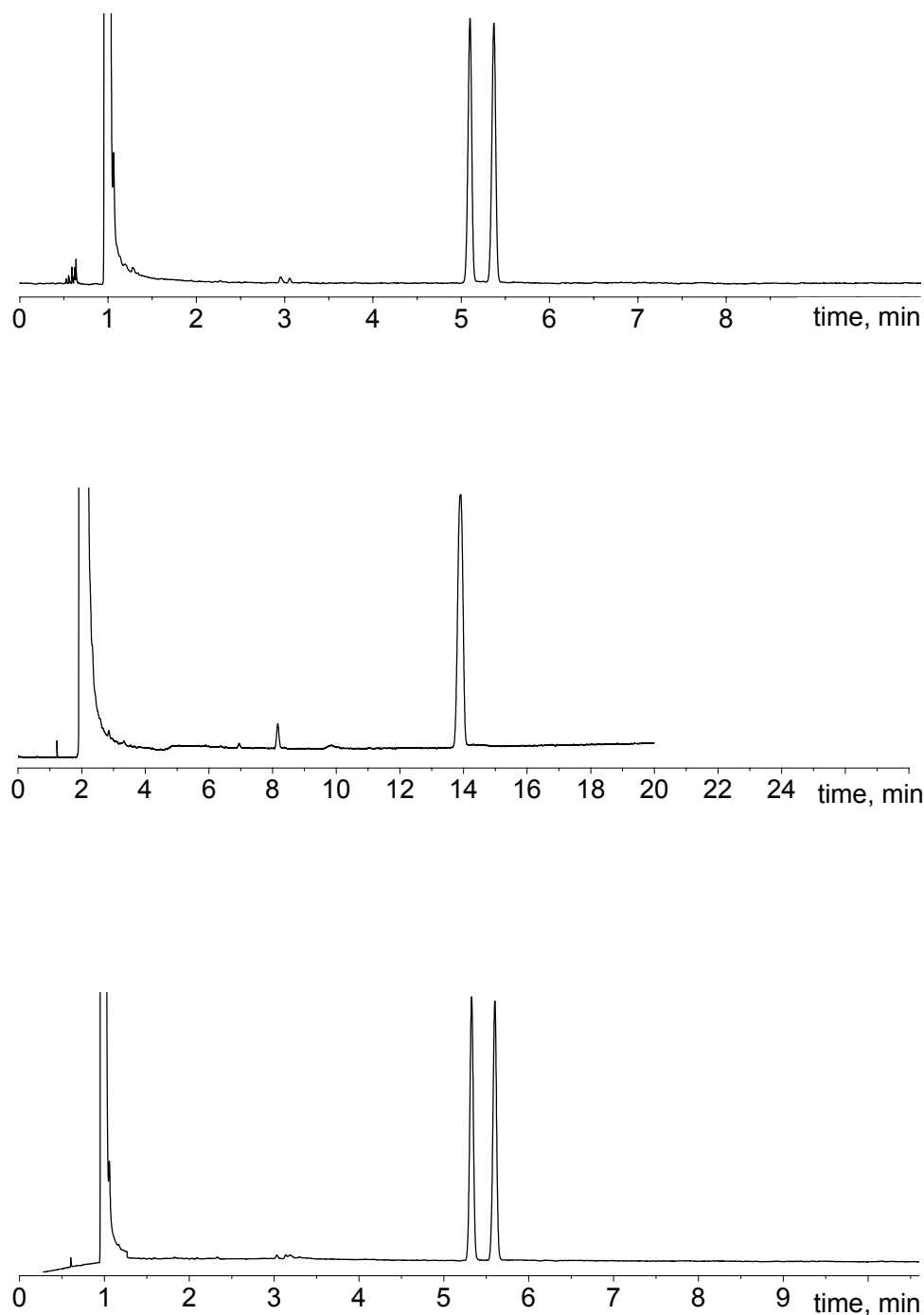


Figure 1.22 Example of a racemate not resolved on the CSP γ CD. Gas-chromatograms of the enantioseparation of tyrosine (as *N*-trifluoroacetyl methyl ester) on the single-selector CSPs γ CD (middle) and DA (up), and on the binary-selector CSP DA γ CD (bottom). The gas-chromatograms are recorded isothermally at 175°C and 50kPa pressure of H₂. The elution order is *L* after *D* for all the chromatograms. Capillaries: 20 m and 30 m for DA γ CD, DA and for γ CD, respectively, 0.25 mm i.d. and 0.25 μ m polymer film thickness.

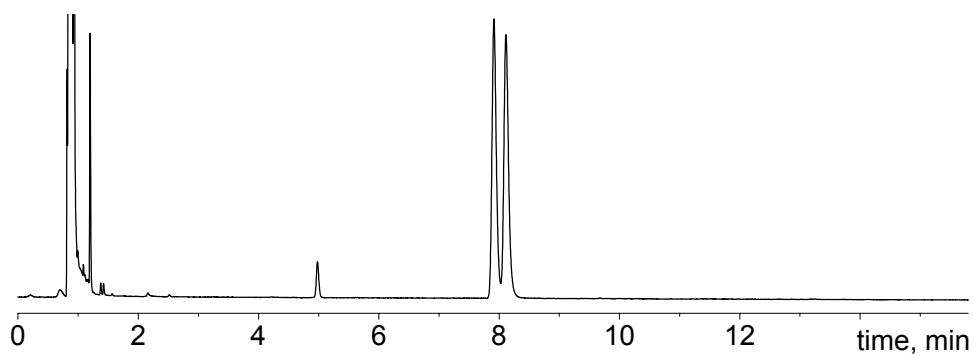
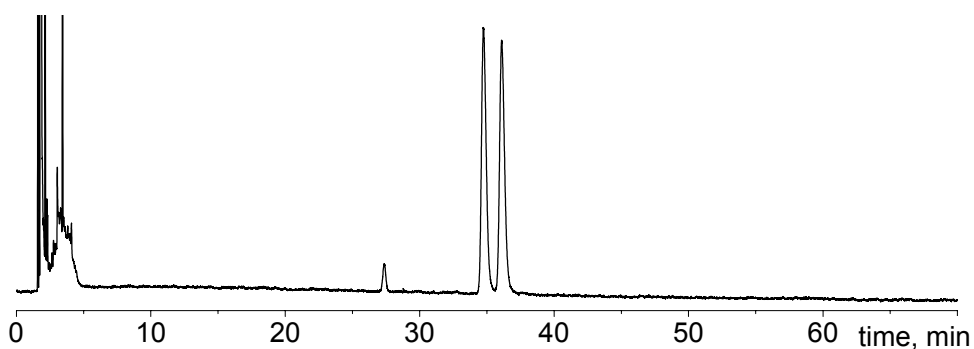
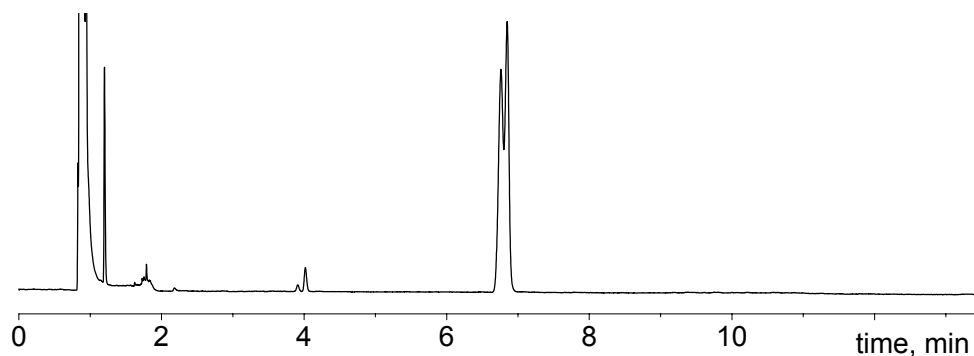


Figure 1.23 Example of a racemate not resolved on the CSP **DA**. Gas-chromatograms of the enantioseparation of 1-phenylethanol on the single-mode CSPs γ CD (middle) and **DA** (up), and on the mixed-mode CSP **DA** γ CD (bottom). The gas-chromatograms were recorded at 85°C and 50 kPa of the carrier gas (H_2). Capillaries: 20 m and 30 m for **DA** γ CD, **DA** and for γ CD, respectively, 0.25 mm i.d. and 0.25 μ m polymer film thickness.

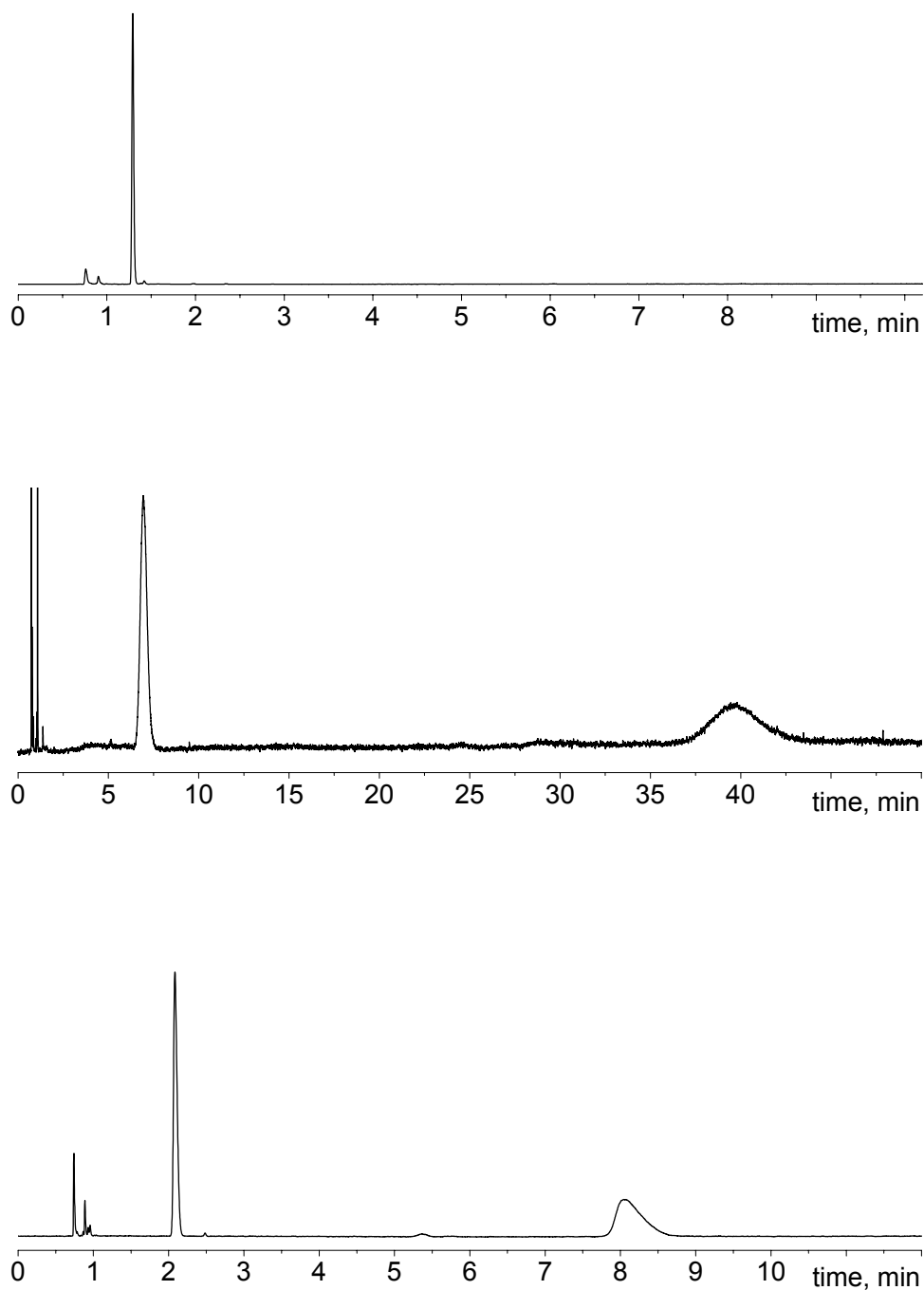


Figure 1.24 Gas-chromatograms of the enantioseparation of “compound B” on the single-selector CSPs γ CD (middle) and DA (up), and on the binary-selector CSP DA γ CD (bottom). The gas-chromatograms are recorded isothermally at 40°C and 50 kPa for DA and DA γ CD and 100 kPa for γ CD of H₂. Capillaries: 20 m and 30 m for DA γ CD, DA and for γ CD, respectively, 0.25 mm i.d. and 0.25 μ m polymer film thickness.

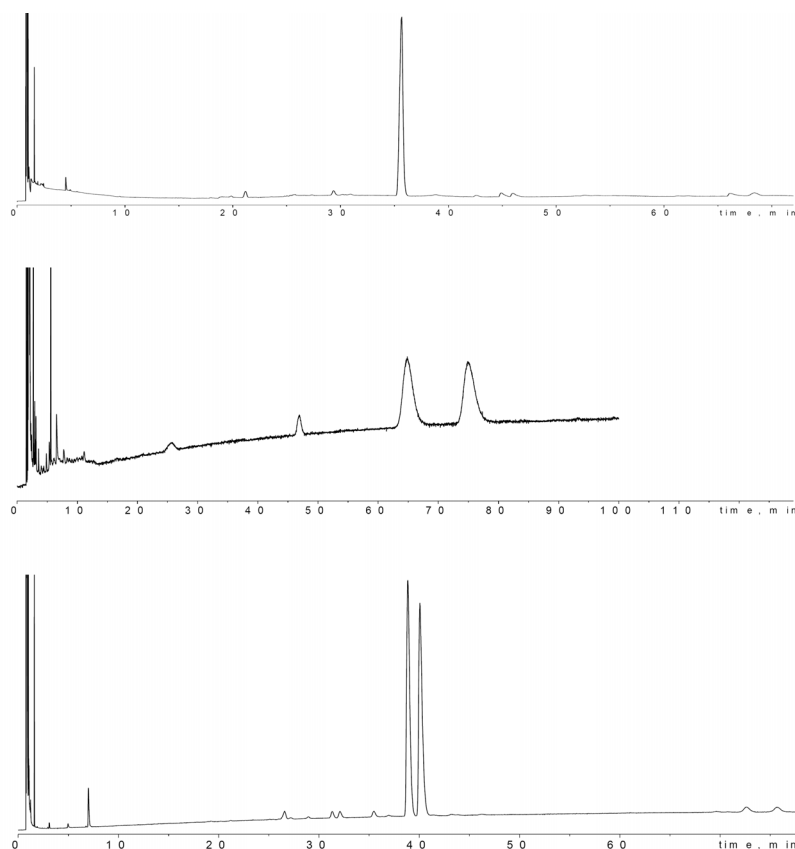


Figure 1.25 Gas-chromatograms of the enantioseparation of pulegone on the single-selector CSPs γ CD (middle) and DA (up) and on the binary-selector CSP DA γ CD (bottom). The gas-chromatograms were recorded at 60°C and 50 kPa of the carrier gas (H₂). Capillaries: 20 m and 30 m for DA γ CD, DA and for γ CD, respectively, 0.25 mm i.d. and 0.25 μ m polymer film thickness.

As can be seen from **Table 1.6** the resolution (R_s) of the enantiomers of proline and aspartic acid (as *N*-trifluoroacetyl ethyl and methyl esters, respectively) is improved from 1.75 and 1.11 on DA, to 9.37 and 4.47 on DA γ CD, respectively (*cf.* **Figure 1.21** for Pro). On the other hand, very low enantioselectivity of γ CD towards tyrosine and tryptophane derivatives does not impair the enantioseparation of these amino acids on DA γ CD (**Table 1.6**, **Figure 1.22** for tyrosine). In contrast to DA, selector γ CD exhibits high enantioselectivity toward some underivatized alcohols. As a consequence, the binary-selector CSP DA γ CD containing the cyclodextrin selector also displays enantioselectivity toward the underivatized alcohols (1-phenylethanol, 2-pentanol and 2-heptanol) (**Table 1.6** and **Figure 1.23** for 1-phenylethanol). Selector γ CD is renowned for the extremely high enantioselectivity towards halogenated ethers that represent important inhalation anesthetics (enflurane (CHF₂-O-CF₂-C*HClF), isoflurane (CHF₂-O-C*HCl-CF₃) and desflurane (CHF₂-O-C*HF-CF₃)) [131,132]. It is interesting to note that the highest enantioseparation factor α ever observed in GC was found

for a decomposition product of sevoflurane, i.e. “compound B” ($\text{CH}_3\text{-O-CF}_2\text{-C}^*\text{H}(\text{CF}_3)\text{-O-CH}_2\text{F}$) on γCD ($\alpha = 10.6$, $T = 26^\circ\text{C}$) [131]. Quite expectedly, such predominant enantioselectivity is retained in $\text{DA}\gamma\text{CD}$ (Table 1.6). Representative chromatograms of the enantioseparation of “compound B” on the single- and binary-selector CSPs are shown in Figure 1.24. As mentioned before, γCD is commonly used for the chiral analysis of flavours [89,129,130]. The chromatographic data of the enantioseparation of some of the monoterpenes (linalool, carvone and pulegone) on the binary-selector CSP $\text{DA}\gamma\text{CD}$ are depicted in Table 1.6 and on Figure 1.25 (for pulegone). Thus, by doping the CSP based on the diamide chiral selector with the cyclodextrin selector, γCD , the scope of the enantioselectivity of the diamide **DA** was greatly expanded. The decrease of the enantioseparation factor on $\text{DA}\gamma\text{CD}$ for racemates that are only enantioseparated on γCD is the result of a smaller concentration of the selector in the binary-selector CSP (8% w/w) in comparison with the single-selector phase (20% w/w). In addition, the presence of the diamide selector **DA** may cause non-enantioselective interactions, e.g. with underivatized alcohols, thereby reducing the apparent enantioseparation factor (see Chapter 2) [137]. In principle, a higher concentration of γCD in the binary-selector CSP $\text{DA}\gamma\text{CD}$ is feasible. However, it may lead to an undesired decrease of the impact of the diamide selector **DA** in the binary-selector CSP on the enantioseparation of the derivatives of α -amino acids.

To demonstrate that the enantioselective properties of the valine-diamide selector were not impeded by the presence of the cyclodextrin selector, a mixture of sixteen proteinogenic amino acids was analyzed on $\text{DA}\gamma\text{CD}$. As can be seen in Figure 1.26, among 16 α -amino acids analyzed in one run only peaks of *L*-Leu and *D*-Ser were found to overlap which may be overcome by temperature tuning. Thus, the enantioselective properties invoked by **DA** are retained in the binary-selector CSP $\text{DA}\gamma\text{CD}$. Moreover, the presence of the cyclodextrin selector γCD in $\text{DA}\gamma\text{CD}$ greatly improved the enantioseparation of the derivatives of proline and aspartic acid. The elution order of the derivatized α -amino acids on $\text{DA}\gamma\text{CD}$ is in agreement with that on **DA**, i.e. *L* after *D* except for proline. Due to the presence of the cyclodextrin selector, the elution order of proline is *D* after *L* both on γCD and on $\text{DA}\gamma\text{CD}$, i.e. an inversion of the elution order is observed as compared to **DA**. The elution order of threonine is *D* after *L* on γCD but *L* after *D* on **DA**. Due to the stronger impact of selector **DA** in the binary-selector CSP, the elution order is *L* after *D* on $\text{DA}\gamma\text{CD}$.

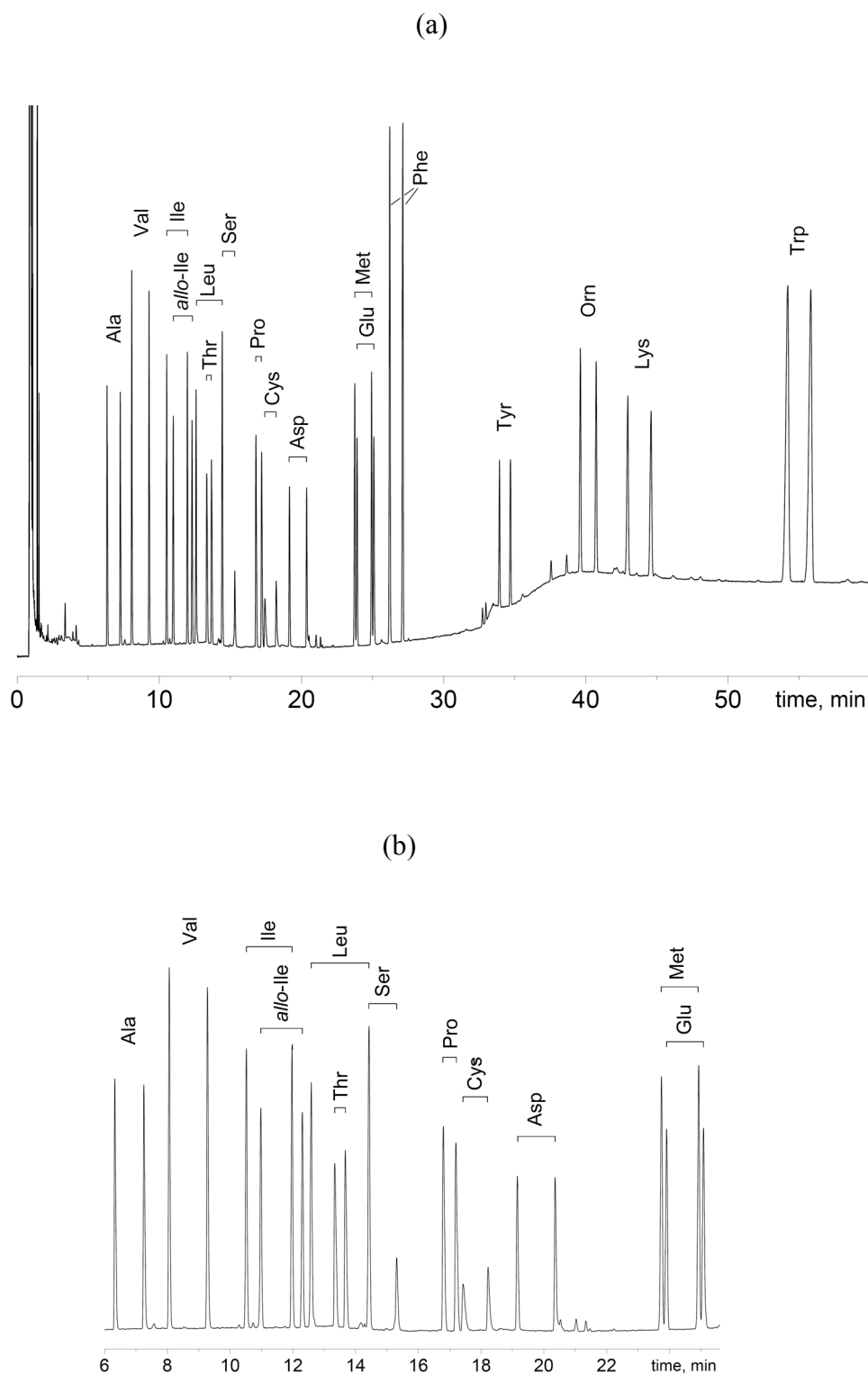


Figure 1.26 Gas-chromatogram of the enantioseparation of 16 proteinogenic amino acids (as *N*-trifluoroacetyl methyl esters) on the binary-selector CSP **DA γ CD**; (a) complete gas-chromatogram (b) enlarged first part of the gas-chromatogram. Carrier gas H₂, 50 kPa; temperature program: 70°C/3 min isothermal, then 3°/min up to 170°C followed by 30 min isothermally. Column: fused silica 20 m, 0.25 mm i.d., 0.25 μ m polymer film thickness.

Since the enantioselectivities of the two chiral selectors (all-*D*-cyclodextrin and *L*-valine-diamide) are to a great extent complementary (except for proline and threonine), the mismatched cases, i.e. strong decrease of the enantioselectivity due to the opposite elution order of enantiomers on single selectors, were not observed. Due to the low concentration of γ CD in **DA** γ CD, exceedingly long retention times on single-mode γ CD are reduced in binary-selector **DA** γ CD resulting in shorter analysis times at acceptable resolution.

1.4 Valdex: combining *L*-valine-diamide and heptakis(2,3,6-tri-*O*-methyl)- β -cyclodextrin chiral selectors in one molecule

Direct chemical linking of different chiral selectors is the third approach that may lead to the combination of their enantioselective properties. In this case, however, one can also anticipate a change of the mechanism of the enantiorecognition, i.e. the close arrangements of chiral selectors can also influence their enantioselective properties by cooperative effects. Thus, the valine-diamide moiety was chemically attached to heptakis(2,3-di-*O*-methyl)- β -cyclodextrin. The produced bifunctional valine-cyclodextrin chiral selector called **Valdex** (**Figure 1.27**) was prepared with the intention to combine the apolar enantioselective properties of the methylated- β -cyclodextrin cavity with the polar hydrogen-bonding chiral groups of the valine-diamide chiral selector. Because of the low solubility of **Valdex** in all the polymers examined as solvents, the GC measurements were not possible. However, using **Valdex** as a chiral solvating agent (CSA), NMR spectroscopy could be utilized in order to study the enantioselective properties of the molecule. The results of the synthesis and the NMR investigation are presented in the following section.

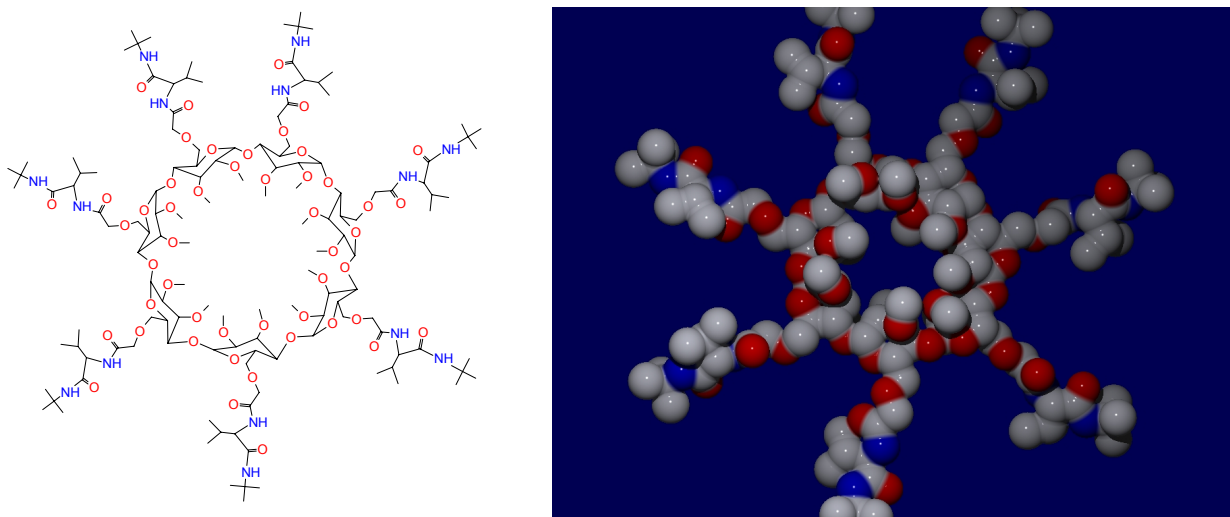
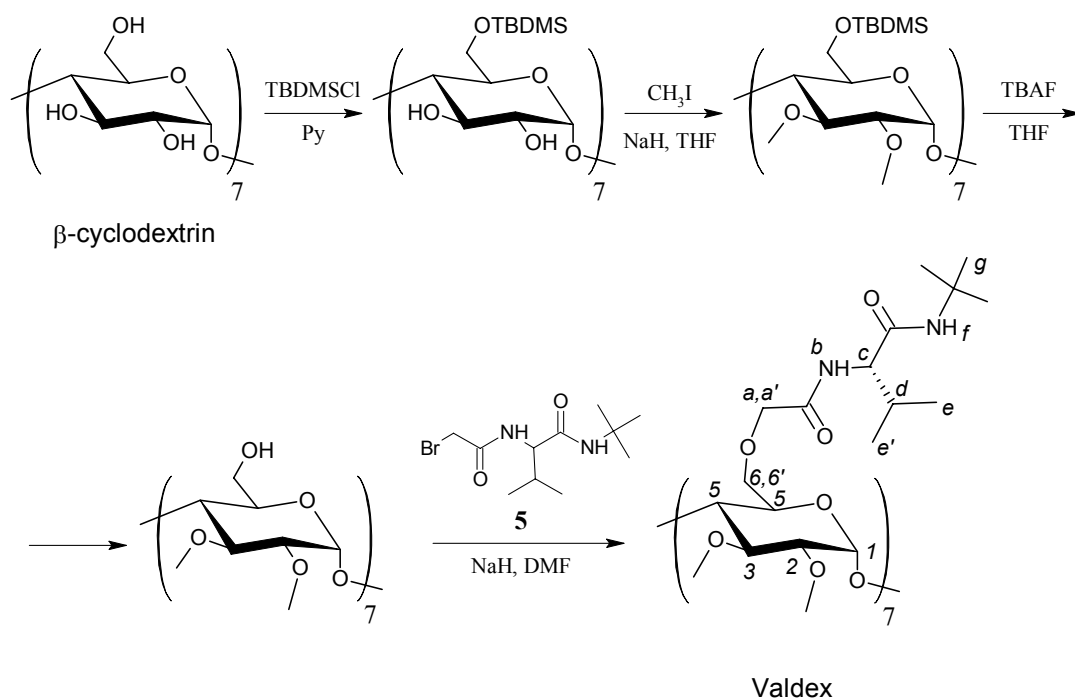


Figure 1.27 Heptakis[6-*O*-(*N*-acetyl-*L*-valine-*tert*-butylamide)-2,3-di-*O*-methyl]- β -cyclodextrin (**Valdex**). Right: “Stick and ball” 3D-model of **Valdex** representing the sizes of the apolar cavity and the polar valine-diamide “arms”. Red – oxygens, Blue – NH groups.

1.4.1 Synthesis of Valdex

The synthesis of heptakis(2,3-di-*O*-methyl)- β -cyclodextrin was carried out using the classical procedure (**Scheme 1.5**) [138] of the selective protection of primary hydroxyls as *tert*-butyldimethylsilyl (TBDMS) ethers, methylation of the secondary ones and, finally, deprotection of the primary sites. **Valdex** was then prepared by alkylation of the primary hydroxyl groups of heptakis(2,3-di-*O*-methyl)- β -cyclodextrin with *N*-bromoacetyl-*L*-valine-*tert*-butylamide (**5**) (**Scheme 1.5**). Compound **5** was prepared as discussed above (see **Scheme 1.4**).



Scheme 1.5 Synthesis of **Valdex** (heptakis[6-*O*-(*N*-acetyl)-*L*-valine-*tert*-butylamide]-2,3-di-*O*-methyl]- β -cyclodextrin)

1.4.2 Valdex as a chiral solvating agent for NMR determination of enantiomeric compositions

Chiral auxiliaries for NMR spectroscopy, the enantiodiscriminating ability of which is based on solvation or complexation processes occurring in solution, are called Chiral Solvating Agents (CSAs), whereas the use of Chiral Derivatizing Agents (CDAs) relies on the formation of covalent bonds [139,140]. Since the mixtures of the CSAs with the chiral compounds to be analysed can be prepared directly inside an NMR tube, the use of the CSAs is particularly attractive from the application point of view. During the last twenty years, cyclodextrin CSAs gained great popularity [139,140,141] by virtue of the effect of their

unique structural features on complexation processes in solution. The three hydroxyl groups of every glucose unit of cyclodextrins have very different reactivities and can be suitably derivatized giving the opportunity of modulating and tailoring cyclodextrin complexing and enantiodiscriminating features as well as their physicochemical properties [142,143].

Recently, derivatized cyclodextrins, bearing both methyl and carbamoyl groups, have been proposed [144-146] as CSAs for the enantiodiscrimination of both polar and apolar chiral substrates. The results [144-146] revealed the necessity of having methyl groups on both cyclodextrin secondary sites in order to obtain NMR differentiation of enantiomers of apolar trisubstituted allenes devoid of hydrogen bonding groups, and raised the problem of finding optimal derivatizing groups to be introduced into the primary sites of the cyclodextrin in order to obtain the simultaneous efficient enantiodiscrimination of polar substrates.

In the present section the results of the NMR investigation of heptakis[6-*O*-(*N*-acetylyl-*L*-valine-*tert*-butylamide)-2,3-di-*O*-methyl]- β -cyclodextrin (**Valdex**) (**Figure 1.27**), a methylated cyclodextrin containing the chiral *L*-valine-diamide moiety chemically attached to the primary hydroxy groups, are presented. The racemates of polar α -amino acid derivatives and apolar trisubstituted allenes used as the analytes for the NMR study are shown in **Figure 1.28**.

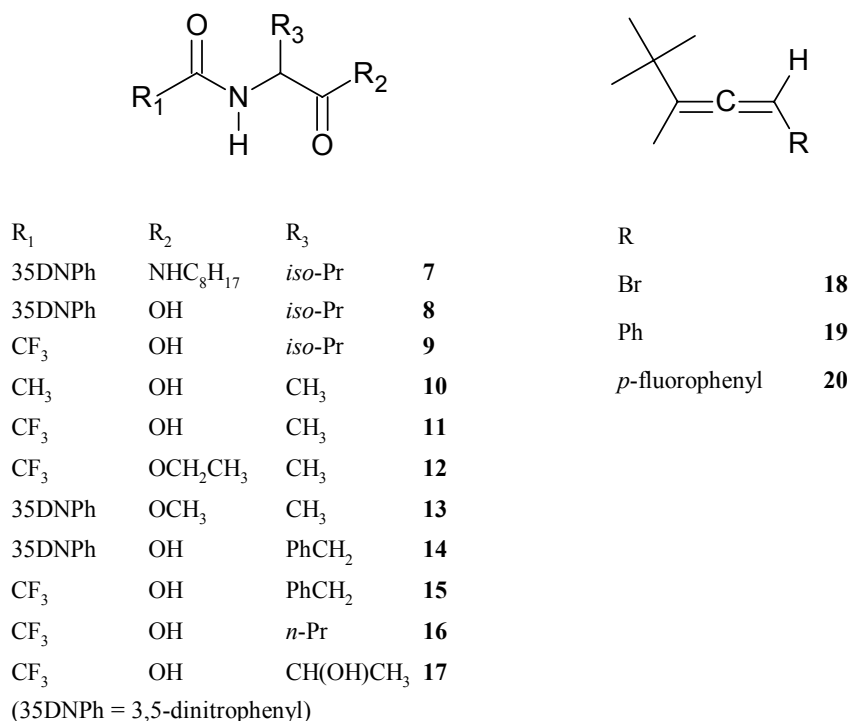


Figure 1.28 Racemic substrates 7-20

Enantiodiscrimination experiments were carried out by comparing NMR spectra of pure racemic compounds **7-20** (**Figure 1.28**) and that of their mixtures with **Valdex**. Comparison with analogous mixtures containing pure enantiomers or their enantiomerically enriched mixtures confirmed assignments of signals to the two enantiomers. Enantiodiscriminating efficiency of chiral auxiliaries was evaluated by measuring chemical shift nonequivalences ($\Delta\delta$).

Different kinds of α -amino acid derivatives have been investigated. Compound **7** represented a diamide compound similar to the diamide compound **5**, whereas compounds **8-17** were monoamide derivatives with a free carboxyl function in **8-11** and **14-17** or with an ester group in **12** and **13**, in order to find out the optimal combination of derivatizing functional groups to improve enantiodiscrimination. The compounds were analysed in CDCl_3 , as their solubility was too low in less polar solvents (CCl_4 , C_6D_{14} or C_6D_{12}), which, in principle, could favour complexation processes by the chiral auxiliaries and, hence, enhance the enantiodiscrimination. Experiments with trisubstituted allenes were carried out in CD_3OD . The use of methanol as solvent also gave the opportunity of enhancing the enantiodiscrimination at low temperatures.

Analysis of racemic diamide derivative of valine **7** revealed doublings of all its signals in the presence of one equivalent of the **Valdex**. Nonequivalences were remarkably high (240 Hz at 20 mM, **Figure 1.29d** and **Table 1.7**) for the amide proton bound to the chiral center. Even in diluted equimolar solutions (up to 1 mM), which is out of the concentration range commonly involved in the use of CSAs, a strong non-equivalence of the amide proton was observed (about 50 Hz, **Table 1.7** and **Figure 1.29a**).

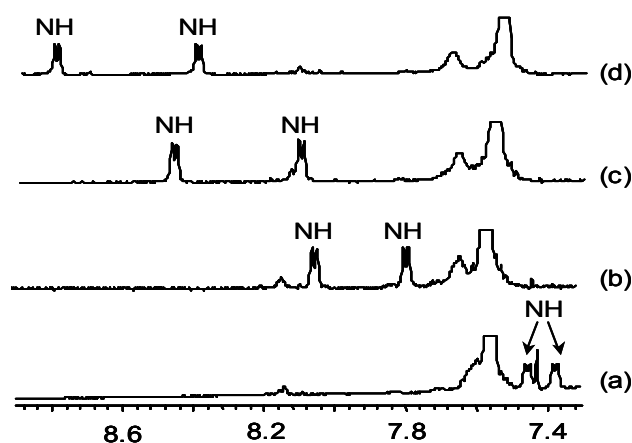


Figure 1.29 ^1H NMR (600 MHz, CDCl_3 , 25 °C) spectral regions corresponding to the NH proton bound to the stereogenic center of **7** in the presence of the equimolar amount of **Valdex** at 1 mM (a), 5 mM (b) 10 mM (c), and 20 mM (d).

Strong nonequivalence of the amide protons was also observed for other derivatives of the same amino acid (**Table 1.7**, **Figure 1.30**) in the presence of **Valdex**. In the case of the trifluoroacetyl derivative **9**, with the free carboxyl group, nonequivalence measured for the amide proton was 214 Hz in the equimolar 5 mM mixture, even higher than that for the derivative **7** at the same concentration.

Chemical shift nonequivalences of the amide protons of trifluoroacetyl derivative of alanine **11** and threonine **17** were similarly high (about 140 Hz, **Table 1.7**). Differentiation was lower (about 20-30 Hz) in the case of phenylalanine (**15**) and of norvaline (**16**) derivatives.

Table 1.7 Chemical shift nonequivalences ($\Delta\delta = |\delta_R - \delta_S|$, Hz; 600 MHz, CDCl₃) of NH protons (bound to the stereogenic center) of α -amino acid derivatives 7-17 in the presence of equimolar amount of Valdex.

compound	mM	$\Delta\delta$
7^a	1	46.7
7^a	5	154.8
7^a	10	215.5
7^a	20	240.0
9	5	214.0
8	5	139.1
10	5	161.3
11	5	141.2
12	20	36.8
13	20	30.0
14	5	40.8
15	5	25.9
16	5	18.7
17	5	107.9

^a NH bound to the chiral centre

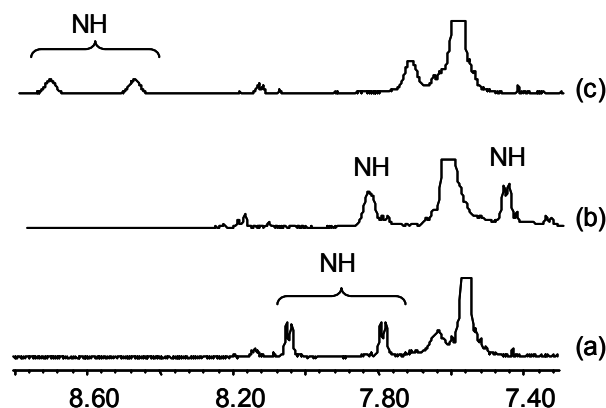


Figure 1.30 ^1H NMR (600 MHz, CDCl_3 , 25 $^\circ\text{C}$, 5 mM) spectral regions corresponding to the NH proton bound to the stereogenic center of **7** (a), **9** (b) and **8** (c) in the presence of the equimolar amount of **Valdex**.

In the case of alanine, nonequivalence of the amide protons was virtually insensitive to the kind of the derivatization of the amino group (**Table 1.7**). This result suggests that the stabilization of the diastereoisomeric associate mainly involves the NH moiety of the amino acid derivatives as a hydrogen bond donor group, whereas the role of the carbonyl amide group as hydrogen bond acceptor group is less important. This is in accordance with the GC experiments where the presence of the amide protons was found to be crucial for the observation of the enantioselectivity (see Chapter 3). Nonequivalences of the amide proton of the alanine derivative **12**, which has the *N*-trifluoroacetyl group as in **11**, but with an ester function in place of the free carboxyl group, were remarkably lower (about 40 Hz at 20 mM), indicating that the efficient enantiodiscrimination by **Valdex** required the presence of two hydrogen bond donor groups, i.e. either two amide groups or one amide and one carboxyl functions.

Investigation of compound **13** confirms the above conclusions: the magnitude of nonequivalence of the amide proton at 20 mM in the presence of one equivalent of **Valdex** was 30 Hz, i.e. very similar to the value obtained at the same concentration in the case of **12**.

The enantiodiscrimination of trisubstituted allenes **18-20** (**Figure 1.28**) in CD_3OD equimolar solutions (**Table 1.8**) could also be achieved using **Valdex** (60 mM) as the CSA.

Table 1.8 Chemical shift nonequivalences ($\Delta\delta = |\delta_R - \delta_S|$, Hz; 600 MHz, CD₃OD, 60 mM) of protons of allenes **18-20** in the presence of one equivalent of **Valdex**.

allene	proton	$\Delta\delta$		
		25 °C	-20 °C	-40 °C
18	H	1.7	8.6	17.1
	Me	0	3.5	6.7
	Bu ^t	0	2.0	4.3
19	H	1.7	11.1	22.8
	Me	2.9	5.2	9.8
	Bu ^t	0	3.4	6.8
20	H	4.2	27.8	54.7
	Me	2.5	12.9	23.1
	Bu ^t	2.1	8.9	16.5

Nonequivalences ranged from 2 to about 4 Hz and, even though quite small, were comparable to the ones obtained by using heptakis[2,3-di-*O*-methyl-6-*O*-(3,5-dimethylphenylcarbamoyl)]- β -cyclodextrin **21**, which was most efficient [146] towards trisubstituted allenes among mixed methylated-carbamoylated cyclodextrins. An important difference between **Valdex** and **21** was revealed by low-temperature experiments. Thus, nonequivalence of the allene proton of **18** changed from 1.7 Hz at room temperature to 8.6 Hz at -20 °C, reaching the value of 17.1 Hz at -40 °C (**Figure 1.31** and **Table 1.8**). The latter value was comparable to the splitting (18.1 Hz) obtained [147] for the same proton of **18** in the equimolar (40 mM) mixture containing fully methylated cyclodextrin, heptakis(2,3,6-tri-*O*-methyl)- β -cyclodextrin **22**, which was the most efficient CSA in the differentiation of allene enantiomers [147,148]. However, **22** was devoid of polar groups and, hence, the enantiodiscrimination of polar substrates was prevented. This trend was confirmed in the

case of racemate **19**: in the presence of **Valdex** splitting of allene proton increased from 1.7 Hz at room temperature (to be compared to 3.3 Hz in the 40 mM mixture (*R,S*)-**19/22**) [147] up to 11.1 Hz at $-20\text{ }^{\circ}\text{C}$ and 22.8 Hz at $-40\text{ }^{\circ}\text{C}$ (**Table 1.8**), reaching the nonequivalence value comparable to that obtained (23.4 Hz) [147] in the presence of **22** 40 mM at the same temperature. Temperature gradients produced even more marked effects in the case of compound **20** enantiomers of which were differentiated by 4.2 Hz in the presence of **Valdex** at room temperature (comparable with 4.9 Hz obtained in the presence of **22**), [148] but a surprisingly higher nonequivalence of 54.7 Hz was measured at $-40\text{ }^{\circ}\text{C}$ (**Table 1.8**) with respect to that measured (5.1 Hz at $-40\text{ }^{\circ}\text{C}$) in the presence of **21** [146]. Therefore, even though CSAs **Valdex** and **21** have comparable efficiency in the enantiodiscrimination of trisubstituted allenes at room temperature, **Valdex** clearly surpasses the mixed carbamoylated-methylated cyclodextrin **21** at lower temperatures, becoming comparable to permethylated cyclodextrin **22**.

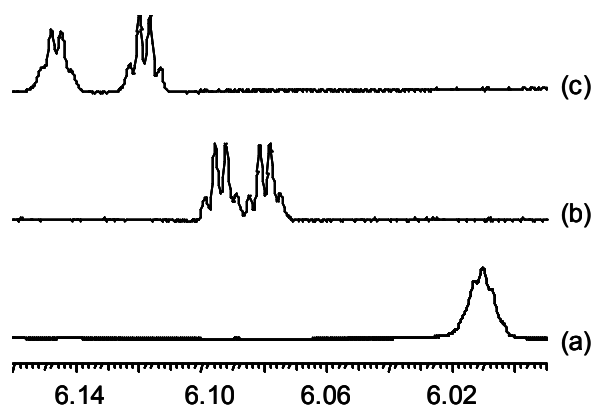


Figure 1.31 ^1H NMR (600 MHz, CD_3OD , 60 mM) spectral regions corresponding to the allene proton of **19** in presence of the equimolar amount of **Valdex** at $25\text{ }^{\circ}\text{C}$ (a), $-20\text{ }^{\circ}\text{C}$ (b), and $-40\text{ }^{\circ}\text{C}$ (c)

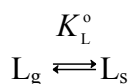
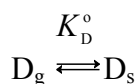
Chapter 2

2. Theory of the enantioseparation on single- and binary-selector gas-chromatographic chiral stationary phases

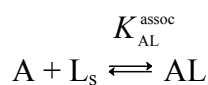
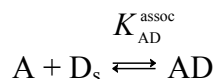
2.1 Introduction

Since four decades, enantioselective GC has been established as a versatile technique for the analysis of volatile chiral compounds. A GC column is a capillary coated with a thin layer of a CSP, enantiopure selector A present in an achiral solvent S. The separation of enantiomers in enantioselective GC is based on the different thermodynamic stability of transient diastereomeric associates, AD and AL, formed between A and the selectand enantiomers, D and L, passing through the GC column. The greater the difference, the higher is the apparent enantioseparation factor, α_{app} , experimentally obtained as the ratio of the retention factors, k_{D} and k_{L} , of the second and the first eluted enantiomers, respectively ($\alpha_{\text{app}} = \frac{k_{\text{D}}}{k_{\text{L}}}$). Thus, enantioselective GC, in addition to the practical applications as an analytical tool, has proven to be an important method for the investigation of mechanisms of enantiorecognition. Depending on the selectors employed, non-covalent molecular interactions such as hydrogen-bonding [28], complexation [33] or inclusion [127] have previously been studied.

In contemporary enantioselective GC, the chiral selectors are either dissolved in [40,149,150], or chemically bonded to [47,151,31], the achiral solvent S (often a polysiloxane) and only in earlier studies they are used undiluted [23,24,152]. The distribution of the selectand enantiomers, D and L, between the gas phase (g) and the neat achiral solvent (s) is characterized by the distribution constants, K_{D}° and K_{L}° , respectively. Due to the achiral nature of S, K_{D}° and K_{L}° are identical.

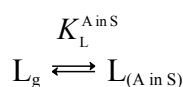
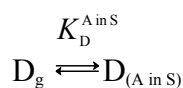


The association occurring between the selectand enantiomers, D and L, and the enantiopure selector A are characterized by the association constants, $K_{\text{AD}}^{\text{assoc}}$ and $K_{\text{AL}}^{\text{assoc}}$, respectively. If the enantiopure selector A is enantioselective toward the selectand enantiomers D and L, the constants, $K_{\text{AD}}^{\text{assoc}}$ and $K_{\text{AL}}^{\text{assoc}}$, are rendered dissimilar.



The ratio of the association constants determines the *true enantioseparation factor* of the selectand enantiomers D and L on the *chiral selector* A, i.e. $\alpha_{true} = \frac{K_{AD}^{assoc}}{K_{AL}^{assoc}}$. The enantioselectivity of the *chiral selector* A is quantitatively determined as the Gibbs energy difference between the diastereomeric associates AD and AL by the expression $-\Delta_{AD,AL}(\Delta G) = RT\ln(\alpha_{true})$, where R is the gas constant and T is the absolute temperature.

If the chiral selector A is diluted with the achiral solvent S, the apparent distribution of the selectand enantiomers D and L between the gas phase and the CSP, A in S (i.e. chiral selector A dissolved in achiral solvent S), is described by the apparent distribution constants, $K_D^{A\text{ in }S}$ and $K_L^{A\text{ in }S}$, respectively. If the enantiopure selector A is enantioselective towards the selectand enantiomers, the apparent distribution constants, $K_D^{A\text{ in }S}$ and $K_L^{A\text{ in }S}$, are rendered dissimilar.



The ratio of the apparent distribution constants $K_D^{A\text{ in }S}$ and $K_L^{A\text{ in }S}$ determines the *apparent enantioseparation factor* of the selectand enantiomers D and L on the *chiral stationary phase*, A in S, i.e. $\alpha_{app} = \frac{K_D^{A\text{ in }S}}{K_L^{A\text{ in }S}}$. The enantioselectivity of the *chiral stationary phase*, A in S, is quantitatively determined as the Gibbs energy difference between the transfer of the selectand enantiomers D and L from the gas phase into the CSP, A in S, by the expression $-\Delta_{D,L}(\Delta G) = RT\ln(\alpha_{app})$, where R is the gas constant and T is the absolute temperature. Despite the above elaboration, the expression $-\Delta_{D,L}(\Delta G) = RT\ln(\alpha_{app})$ has been often erroneously used for the assessment of the Gibbs energy difference between the diastereomeric associates AD and AL, i.e., for the determination of the enantioselectivity of the chiral selector A. Since the selector A is diluted with S and the latter contributes to the retention of the selectand enantiomers to the

same extent, the apparent enantioseparation factor, α_{app} , does not correspond to the enantioselectivity of the chiral selector A. This notion has been expressed many times in the literature [30,33,90-93]. Thus, whereas the apparent enantioselectivity, α_{app} , is important from the practical point of view, because it reflects the observed separation capabilities of the entire enantioselective chromatographic system, the true enantioseparation factor, α_{true} , is of theoretical importance and can be used for the investigation of enantioselective recognition mechanisms.

Because of some obscurity in the literature around the terms enantioselectivity and the enantioseparation factor and their relationship, these terms are defined here as follows. The apparent enantioseparation factor, α_{app} , is related to the enantioselectivity of the total CSP, composed of a chiral selector and an achiral support, as $-\Delta\Delta G_{\text{app}} = RT\ln(\alpha_{\text{app}})$. The true enantioseparation factor, α_{true} , is related to the enantioselectivity of the chiral selector as part of an achiral matrix as $-\Delta\Delta G_{\text{true}} = RT\ln(\alpha_{\text{true}})$.

The apparent distribution constants, $K_{\text{D}}^{\text{A in S}}$ and $K_{\text{L}}^{\text{A in S}}$, in contrast to the association constants, $K_{\text{AD}}^{\text{assoc}}$ and $K_{\text{AL}}^{\text{assoc}}$, can be easily determined experimentally as the product of the phase ratio and the retention factor (i.e. $K_{\text{D}}^{\text{A in S}} = \beta^{\text{A in S}} \cdot k_{\text{D}}^{\text{A in S}}$ where β is the ratio of the volumes of the gas and stationary phases).

Purnell and Laub [50] suggested in 1975 the use of mixed stationary phases, in GC in the realm of achiral separations, for the improvement of the separation of complex mixtures of compounds. Since then, many reports on the preparation and use of stationary phases containing more than one *chiral* selector (binary-selector CSPs – in the case of using two chiral selectors) appeared in the literature [72,73,76-79,136,137,153]. The idea behind the binary-selector stationary phases is the endeavor to combine complementary enantioselectivities of two different selectors in one stationary phase, thereby expanding the scope of the enantioseparations [136,137,153].

In this chapter, a theoretical treatment of the enantioseparation on single- and binary-selector CSPs is presented. The apparent and true enantioseparation factors are described for both single- and binary-selector CSPs. Analysis of the variation of the apparent enantioseparation factor, α_{app} , of a binary-selector system as a function of the ratio between the selectors and the strength of their interactions with the selectand enantiomers is advanced.

In the present treatise, a gas-chromatographic column is determined as a capillary coated with a thin film of a chiral stationary phase (CSP). The CSP consists of a chiral selector A or B, or a mixture of them, A and B, diluted with an achiral solvent S. Such CSPs will be referred to as CSP “A in S”, “B in S” and “AB in S”,

respectively. The CSPs containing a single selector will be termed single-selector CSPs, the CSPs containing two selectors will be called binary-selector CSPs and the CSPs composed of more than two selectors will be called multi-selector CSPs. A CSP prepared by mixing two single-selector CSPs will be termed as a mixed CSP. The selectors A and B are considered to be enantiomerically pure. The chiral selectand DL (considered to be racemic) consists of the first eluted enantiomer L and the second eluted enantiomer D, irrespective of their absolute configuration. Note, that in Section 2.2, in order to introduce a method for the determination of the association constants, D and A are considered to be achiral. The terms used in this paper have subscripts that show “relation to” and superscripts that refer to the location of the action. For example, subscripts (g) and (s) refer to the gas phase and the achiral solvent S, respectively. D_g (L_g) and D_s (L_s) correspond to the selectand enantiomer D (L) present in the gas phase and in the achiral solvent S, respectively. AD and BD (AL and BL) relate to the corresponding associates (complexes) formed between selectors A or B and enantiomer D (L), respectively. The following terms correspond equally to the L enantiomer provided the subscript “L” is used. If selector B is used instead of selector A, the following terms will contain the corresponding super- or subscript “B”. For the binary-selector CSP, AB in S, the corresponding superscript will be used.

The terms c_A , c_{AD} and c_{D_s} are the concentrations of A, AD and D_s , respectively. The use of concentrations instead of activities is a simplification which is only permitted at low values. The K_D^0 is the apparent distribution constant of D corresponding to its partitioning between the gas phase and the achiral solvent S devoid of the chiral selector. $K_D^{A\text{ in }S}$ is the apparent distribution constant of D corresponding to its partitioning between the gas phase and the CSP A in S. K_{AD}^{assoc} is the association constant corresponding to the reversible formation of the associate AD. $\beta^{A\text{ in }S}$ is the phase ratio of a GC column containing the CSP A in S. $k_D^{A\text{ in }S}$ and $k_{St}^{A\text{ in }S}$ are retention factors of the selectand D and a standard compound not interacting with the selectors, respectively, on the CSP A in S. $r_D^{A\text{ in }S}$ refers to the relative retention of D on the CSP A in S. R is the gas constant. T is absolute temperature. x_A^{AB} and x_B^{AB} are the mole fractions of A and B in the mixture of A plus B, respectively. n_A and n_B are the mole amounts of A and B, respectively.

2.2 Determination of the distribution and association constants

The method for the determination of the association constants in achiral GC was developed by Gil-Av and Herling [154] and by Muhs and Weiss [155]. According to this method, a volatile selectand D is capable of reversible association with a selector A. In the original work of Gil-Av [154], the selectand was designated with the letter B and it was achiral as was the selector A. In the present section, the selectand D and the selector A are considered to be achiral too, although, the same equations can be applied to chiral selectands and selectors (see Section 2.3) dissolved in the solvent S and migrating through a GC column. In this case, two different equilibria can be distinguished [154]:

a) nonselective distribution of the selectand D between the gas phase and the solvent S:



b) selective association of the selectand D with the selector A:

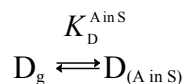


where subscripts g and s refer to the gas phase and the solvent S, respectively. AD is the associate formed between D and A. K^o is the distribution constant of D between the gas phase and the neat solvent S, i.e. it reflects the nonselective contribution to the retention. K_{AD}^{assoc} is the association constants of the selectand D with the selector A present in the solvent S. c_A is the concentration of the selector A in the solvent S. c_{AD} is the concentration of the associate AD in the solvent S. c_{D_s} is the concentration of the selectand D in the solvent S.

Equation (1.2) can be rewritten into equation (1.3).

$$K_{AD}^{assoc} c_A = \frac{c_{AD}}{c_{D_s}} \quad (1.3)$$

The total concentration of D present in S is the sum of the concentrations c_{D_s} and c_{AD} . Consequently, assuming no volume change on dissolution of D, the distribution of D between the gas phase and the stationary phase A in S, described by the apparent distribution constant $K_D^{A \text{ in } S}$, can be defined using the following expressions:



$$K_D^{A \text{ in } S} = \frac{c_{D_s} + c_{AD}}{c_{D_g}} \quad (1.4)$$

Where $D_{(A \text{ in } S)}$ is the selectand D present in the stationary phase A in S. Substituting (1.1) and (1.3) into (1.4) gives (1.5).

$$K_D^{A \text{ in } S} = K_D^o + K_D^o K_{AD}^{\text{assoc}} c_A \quad (1.5)$$

Experimentally, the apparent distribution constant, $K_D^{A \text{ in } S}$, is obtained as a product of the phase ratio, $\beta^{A \text{ in } S}$, and the retention factor, $k_D^{A \text{ in } S}$, of the selectand D on the stationary phase A in S, i.e. $K_D^{A \text{ in } S} = \beta^{A \text{ in } S} \cdot k_D^{A \text{ in } S}$. The phase ratio, $\beta^{A \text{ in } S}$, is determined as the ratio of the volume of the gas mobile phase and that of the stationary phase A in S. Thus, a plot of $K_D^{A \text{ in } S}$ vs. c_A yields a straight line of the slope $K_D^o K_{AD}^{\text{assoc}}$, and the intercept K_D^o , from which the association constant, K_{AD}^{assoc} , can be calculated. This method of distinguishing between selective and non-selective interactions was developed by Gil-Av and Herling [154] and by Muhs and Weiss [155] and was used for the determination of complexation constants of various olefins with silver nitrate dissolved in ethylene glycol by argentation GC. Schurig used this method for the determination of the stability constants of π -complexation of alkenes and alkynes with various metal complexes [156,157]. It should be mentioned that the requirement for the validity of the model and, hence, the linearity of the plot, $K_D^{A \text{ in } S}$ versus c_A , is the low concentration of the selector A in S, whereas upon increasing the concentration of the selector deviation of this plot from linearity may be observed [155].

A similar method for distinguishing between selective and nonselective interactions in liquid chromatography on brush-type CSPs has been described in this work (see Chapter 6). Another method that can be used for the differentiation between selective and nonselective interactions occurring between the selectand and the components of the stationary phase in liquid chromatography is based on the determination of adsorption isotherms by frontal analysis technique and has been described by Guiochon et al. [158].

2.3 Single-selector GC systems

2.3.1 Determination of the apparent enantioseparation factor, α_{app} .

Dependence of α_{app} on the concentration of the chiral selector present in the achiral solvent

In the following section, the apparent enantioseparation factor, α_{app} , and its dependence on the concentration of a chiral selector present in a CSP is described. The discussion is based on the equations derived in the previous section. However, in the following section the selectand D and L now represent enantiomers. Selector A is considered to be chiral and enantioselective towards the racemate DL. The first application of the method of Gil-Av for enantioselective GC was done by Schurig et al. [30] studying the enantioseparation of chiral cyclic ethers by complexation GC on a manganese(II)-*bis*(3-heptafluorobutyryl-1R-camphorate chiral selector).

Thus, if two selectand enantiomers D and L compete for the same enantiopure selector A present in the solvent S (CSP A in S), equations identical to (1.5) can be written for the enantiomers D and L.

$$K_D^{A\text{ in } S} = K_D^o + K_D^o K_{AD}^{\text{assoc}} c_A \quad (1.5)$$

$$K_L^{A\text{ in } S} = K_L^o + K_L^o K_{AL}^{\text{assoc}} c_A \quad (1.5a)$$

Where subscripts D and L correspond to the enantiomers D and L, respectively. c_A is the concentration of the chiral selector A in the solvent S. c_{AD} is the concentration of the associate AD formed between A and D in the solvent S. c_{Ds} is the concentration of the selectand enantiomer D in the solvent S. $K_D^{A\text{ in } S}$ is the apparent distribution constant of the selectand enantiomer D partitioned between the gas phase and the CSP A in S. K_D^o is the distribution constant of the selectand enantiomer D between the gas phase and the neat solvent S, i.e. it reflects the nonenantioselective contribution to the retention. Since the nonenantioselective contribution is the same for both enantiomers, then $K_D^o = K_L^o$. K_{AD}^{assoc} is the association constant of the interaction of the selectand enantiomer D with the chiral selector A present in the solvent S. Expression $K_D^o \cdot K_{AD}^{\text{assoc}} \cdot c_A$ defines the enantioselective contribution to the retention.

Plotting distribution constants for the two enantiomers, $K_D^{A \text{ in } S}$ and $K_L^{A \text{ in } S}$, as functions of the concentration of A, c_A , yields two straight lines of different slopes $K_D^\circ \cdot K_{AD}^{\text{assoc}}$ and $K_L^\circ \cdot K_{AL}^{\text{assoc}}$, respectively, but with the same intercept, $K_D^\circ = K_L^\circ$ (**Figure 2.1**).

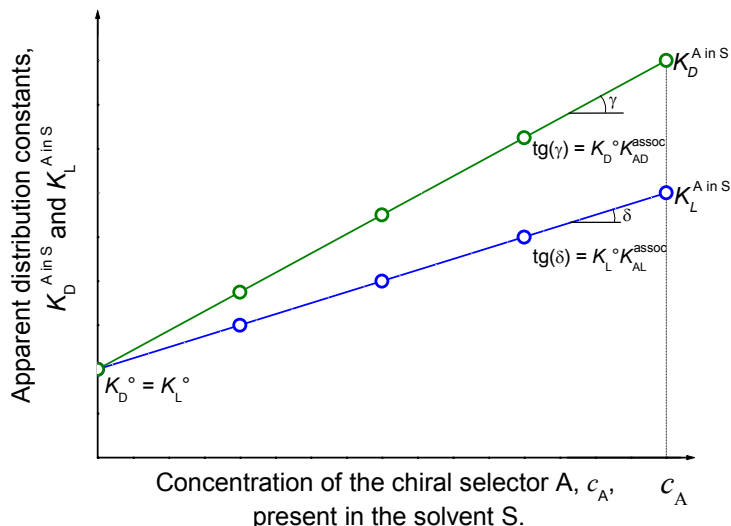


Figure 2.1 Plot of the apparent distribution constants $K_D^{A \text{ in } S}$ and $K_L^{A \text{ in } S}$ as a function of the concentration of the selector A, c_A , in the solvent S

The apparent enantioseparation factor, α_{app} , is determined as the ratio of the apparent distribution constants, $K_D^{A \text{ in } S}$ and $K_L^{A \text{ in } S}$, or the retention factors, $k_D^{A \text{ in } S}$ and $k_L^{A \text{ in } S}$, i.e.

$$\alpha_{\text{app}} = \frac{K_D^{A \text{ in } S}}{K_L^{A \text{ in } S}} = \frac{k_D^{A \text{ in } S}}{k_L^{A \text{ in } S}} \quad (1.6) \text{ (cf. Figure 2.1).}$$

Substitution of (1.5) and (1.5a) into (1.6) gives an expression (1.7) for the apparent enantioseparation factor, α_{app} , in terms of the association constants K_{AD}^{assoc} and K_{AL}^{assoc} and the concentration of the selector A, c_A , in the solvent S:

$$\alpha_{\text{app}} = \frac{1 + K_{AD}^{\text{assoc}} c_A^{A \text{ in } S}}{1 + K_{AL}^{\text{assoc}} c_A^{A \text{ in } S}} \quad (1.7)$$

From (1.7) it can be seen that α_{app} becomes larger with increasing the concentration of the selector in the stationary phase. Provided the association constants, K_{AD}^{assoc} and K_{AL}^{assoc} , are known, equation (1.7) can be used for the determination of the apparent enantioseparation factor, α_{app} , of a CSP, A in S, at different concentrations of the chiral selector A. A plot of α_{app} versus c_A is schematically shown in **Figure 1.2**. It is a convex upward curve. Equation analogous to (1.7) was first derived and experimentally studied by Jung et al. [127]

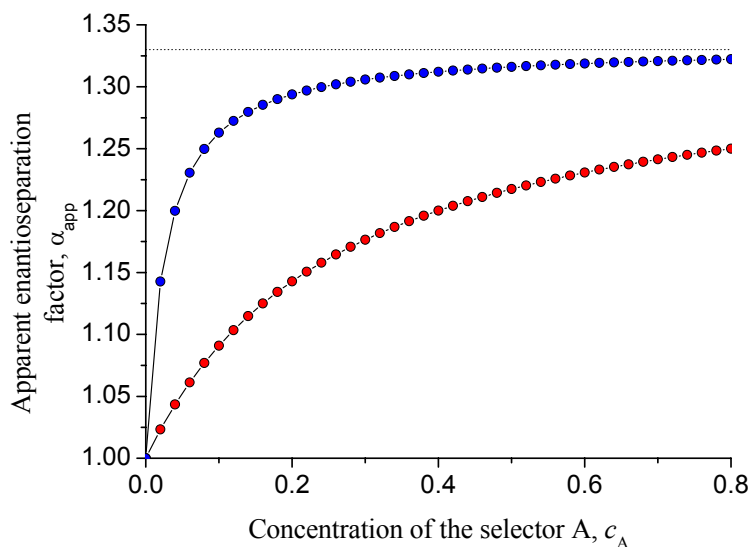


Figure 2.2 Plot of the apparent enantioseparation factor, α_{app} , as a function of the concentration of the chiral selector A in the solvent S. Eq. 1.7 was used for the simulation with the following parameters: $K_{AD}^{assoc} = 5$, $K_{AL}^{assoc} = 3.75$ (red curve); $K_{AD}^{assoc} = 50$, $K_{AL}^{assoc} = 37.5$ (blue curve); $\alpha_{true} = \frac{K_{AD}^{assoc}}{K_{AL}^{assoc}} = 1.33$ for both curves (dotted line).

As one can see from **Figure 2.2**, upon increasing the concentration of the chiral selector A the apparent enantioseparation factor, α_{app} , approaches a constant value. For both examples (**Figure 2.2**, red and blue curves) this constant was chosen 1.33 and this value is nothing else but the true enantioseparation factor, α_{true} , determined as $\alpha_{true} = \frac{K_{AD}^{assoc}}{K_{AL}^{assoc}}$ (1.8). Here, it should be reminded that the apparent enantioseparation factor, α_{app} , is related to the enantioselectivity of the total CSP, composed of a chiral selector and an achiral support, as $-\Delta\Delta G_{app} = RT \cdot \ln(\alpha_{app})$, while the true enantioseparation factor, α_{true} , is related to the enantioselectivity of the chiral selector as a part of an achiral matrix as $-\Delta\Delta G_{true} = RT \cdot \ln(\alpha_{true})$.

As one can see, the larger the value of the association constant, K_{AL}^{assoc} , the more rapidly α_{app} approaches the value of α_{true} (**Figure 2.2**, blue curve). The product of the association constant and the activity of the selector (e.g. $K_{AD}^{assoc} a_A$) is also called retention increment, R' , [30,33,127,156] and can be determined experimentally as $\frac{r_D^{A in S} - r^o}{r^o}$, where $r_D^{A in S}$ and r^o are

the relative retention factors of D on the CSP, A in S, and on the reference column coated with

the neat solvent S, respectively. The relative retention is defined as the ratio of the retention factors of the selectand to the retention factor of a standard compound that does not interact with the selector present in the CSP, i.e. $r_D^{A \text{ in } S} = \frac{k_D^{A \text{ in } S}}{k_{St}^{A \text{ in } S}}$ [127].

The value of the association constant that determines the initial slope of the curve α_{app} versus c_A , depends on the temperature and on the selector. Cyclodextrin selectors used in GC usually show low values of the association constants and, therefore, the slope of the curve α_{app} versus c_A , is usually flat [127]. On the contrary, the metal complexes used as chiral selectors in complexation GC [33] often display very high association constants [157,30] and hence should reveal a fast increase of the plot of α_{app} versus c_A . Thus, the optimization of the enantioseparation on CSPs containing one chiral selector consists in raising the concentration of the chiral selector. It should be noted, however, that a large increase of the concentration of the selector can often impair the efficiency of the CSP [135,40]. Therefore, neat selectors are seldom used in modern GC. Usually chiral selectors are either dissolved in or chemically bound to achiral polymers [151,31,40].

2.3.2 Determination of the true enantioseparation factor, α_{true}

The importance of the true enantioseparation factor, α_{true} , consists in its direct relation to the enantioselectivity of the chiral selector quantitatively determined as the Gibbs energy difference between the diastereomeric associates AD and AL $-\Delta_{AD,AL}(\Delta G) = -RT \ln(\alpha_{true})$, where R is the gas constant and T is absolute temperature. Enantioselective chromatography (see also Chapter 6) is one of the techniques allowing the exact experimental determination of the true enantioseparation factor, α_{true} , and hence the enantioselectivity of a chiral selector as a part of an achiral matrix. The true enantioseparation factor, α_{true} , is determined as the ratio of the association constants, i.e. $\alpha_{true} = \frac{K_{AD}^{assoc}}{K_{AL}^{assoc}}$. As has been mentioned above, the association constants K_{AD}^{assoc} and K_{AL}^{assoc} can be calculated from the plot of the apparent distribution constant $K_D^{A \text{ in } S}$ and $K_L^{A \text{ in } S}$, respectively, versus the concentration of the chiral selector A, c_A , present in the solvent S [30,33]. Therefore, preparation of several CSPs with different concentrations of the selector A is required. On the other hand, the linearity of the plot $K_D^{A \text{ in } S}$ (or $K_L^{A \text{ in } S}$) versus c_A allows using only two points on the graph to determine the association constants. These two points can be the apparent distribution constants obtained by using two columns, i.e., (a) a reference column devoid of

the chiral selector and a column containing the chiral selector or (b) by using two columns with different concentration of the chiral selector. In the latter case, the achiral contribution to retention, K° , can be obtained by the following equation derived by Schurig et al. [33]:

$$K^{\circ} = \frac{K_L^{A_2 \text{ in S}} \cdot K_D^{A_1 \text{ in S}} - K_L^{A_1 \text{ in S}} K_D^{A_2 \text{ in S}}}{(K_D^{A_1 \text{ in S}} + K_L^{A_2 \text{ in S}}) - (K_D^{A_2 \text{ in S}} + K_L^{A_1 \text{ in S}})} \quad (1.9)$$

where subscripts D and L designate two enantiomers (D is arbitrary eluted after L) and subscripts 1 and 2 correspond to the CSPs with different concentrations of the chiral selector A.

To derive an expression for the determination of the association constant, K_{AD}^{assoc} , using the retention data obtained on two columns containing different concentrations of the chiral selector, one should write eq (1.5) for the two columns:

$$\begin{cases} K_D^{A_1 \text{ in S}} = K_D^{\circ} + K_D^{\circ} K_{AD}^{\text{assoc}} c_{A_1} \\ K_D^{A_2 \text{ in S}} = K_D^{\circ} + K_D^{\circ} K_{AD}^{\text{assoc}} c_{A_2} \end{cases}$$

where c_{A_1} and c_{A_2} correspond to the concentrations of the chiral selector A in the two CSPs. Solving this set of equations in terms of the association constant, K_{AD}^{assoc} , one obtains eq (1.10):

$$K_{AD}^{\text{assoc}} = \frac{K_D^{A_2 \text{ in S}} - K_D^{A_1 \text{ in S}}}{K_D^{A_1 \text{ in S}} c_{A_2} - K_D^{A_2 \text{ in S}} c_{A_1}} \quad (1.10)$$

If the concentration of the chiral selector in one of the CSPs is zero, an expression (1.11) is obtained. This equation can be used for the determination of the association constant, K_{AD}^{assoc} , based on the use of a reference column devoid of the chiral selector.

$$K_{AD}^{\text{assoc}} = \frac{K_D^{A \text{ in S}} - K_D^{\circ}}{K_D^{\circ} c_A} \quad (1.11)$$

Substituting (1.10) and (1.11) written for both selectand enantiomers D and L into the expression for the true enantioseparation factor, α_{true} , two equations are obtained:

$$\alpha_{\text{true}} = \frac{K_{\text{D}}^{\text{A in S}} - K^{\circ}}{K_{\text{L}}^{\text{A in S}} - K^{\circ}} \quad (1.10a)$$

$$\alpha_{\text{true}} = \frac{K_{\text{D}}^{\text{A}_2 \text{ in S}} - K_{\text{D}}^{\text{A}_1 \text{ in S}}}{K_{\text{L}}^{\text{A}_2 \text{ in S}} - K_{\text{L}}^{\text{A}_1 \text{ in S}}} \quad (1.11a)$$

The use of eq (1.10a) requires a reference column devoid of the chiral selector and a column containing the chiral selector, while for eq (1.11a) two columns coated with CSPs with different concentration of the chiral selector A are necessary. A favorable feature of these methods is that the value of the concentration of the chiral selector A is not included in eq (1.10a) and (1.11a).

The apparent distribution constants are experimentally determined as the product of the retention factor and the phase ratio of the column being used, i.e. $K_{\text{D}}^{\text{A in S}} = \beta^{\text{A in S}} \cdot k_{\text{D}}^{\text{A in S}}$. In gas chromatography, however, the exact determination of the phase ratios is difficult. Hence, an indirect route leading to the determination of α_{true} avoiding the use of the phase ratios has been developed [33]. This method is based on the concept of the retention increment, R' , and relative retentions, r [30,99,127,131,156,159]. The relative retentions are independent of all operating conditions (column dimensions, flow-rate and film thickness) except the temperature. Writing eqs (1.10a) and (1.11a) in terms of R' and r leads to equations 1.12 and 1.13, respectively.

$$\alpha_{\text{true}} = \frac{r_{\text{D}}^{\text{A in S}} - r^{\circ}}{r_{\text{L}}^{\text{A in S}} - r^{\circ}} = \frac{R_{\text{D}}^{\text{A in S}}}{R_{\text{L}}^{\text{A in S}}} \quad (1.12)$$

$$\alpha_{\text{true}} = \frac{r_{\text{D}}^{\text{A}_2 \text{ in S}} - r_{\text{D}}^{\text{A}_1 \text{ in S}}}{r_{\text{L}}^{\text{A}_2 \text{ in S}} - r_{\text{L}}^{\text{A}_1 \text{ in S}}} = \frac{R_{\text{D}}^{\text{A}_2 \text{ in S}} - R_{\text{D}}^{\text{A}_1 \text{ in S}}}{R_{\text{L}}^{\text{A}_2 \text{ in S}} - R_{\text{L}}^{\text{A}_1 \text{ in S}}} \quad (1.13)$$

where $r_{\text{D}}^{\text{A in S}}$ ($r_{\text{L}}^{\text{A in S}}$) and r° are the relative retentions of the selectand D (L) on the CSP, A in S, and on the reference column coated with the neat solvent S, respectively. The relative retention is defined as the ratio of the retention factors of the selectand to the retention factor of a standard compound that does not interact with the chiral selector A present in S, i.e.

$r_{\text{D}}^{\text{A in S}} = \frac{k_{\text{D}}^{\text{A in S}}}{k_{\text{St}}^{\text{A in S}}}$. The term $R_{\text{D}}^{\text{A in S}}$ is the retention increment of the selectand D on the CSP A in S.

The retention increment is determined as the ratio $\frac{r_D^{\text{A in S}} - r^{\circ}}{r^{\circ}}$. Subscript 1 and 2 correspond to the two CSPs with different concentration of the chiral selector A.

2.4 Binary-selector GC systems

2.4.1 Determination of the apparent enantioseparation factor, α_{app}

The presence of different chiral selectors in the solvent S renders the apparent enantioseparation factor, α_{app} , dependent not only on the overall concentration of the selectors (cf. **Figure 2.2**) but also on the ratio between them. In the foregoing section, an expression for the determination of the apparent enantioseparation factor, α_{app} , of a CSP composing of two selectors, A and B, and the solvent S (CSP: AB in S) will be derived. Thus, if a volatile selectand D, capable of fast and reversible association with both selectors A and B, is migrating through a GC column, three different equilibria can be distinguished:

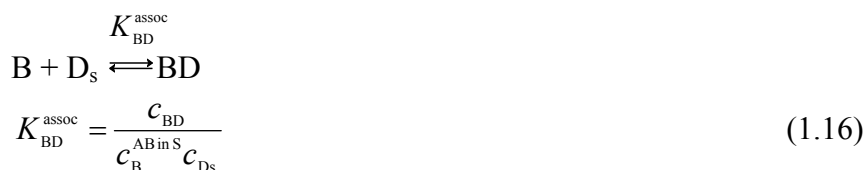
a) nonenantioselective distribution of the selectand D between the gas phase and the solvent S:



b) enantioselective association of the selectand D with the selector A:



c) enantioselective association of the selectand D with the selector B:



where subscripts g and s refer to the gas phase and the solvent S devoid of the chiral selector, respectively. AD and BD are the associates formed between D and A or B, respectively. c_A^{ABinS} and c_B^{ABinS} are the concentrations of the selector A and B in the CSP AB in S, respectively. c_{BD} and c_{AD} are the concentrations of the associates BD and AD, respectively. c_{Ds} is the concentration of the selectand D in the solvent S. K^o is the distribution constant of D between the gas phase and the neat solvent S. K^o reflects the nonenantioselective contribution to the retention. K_{AD}^{assoc} and K_{BD}^{assoc} are the association constants of the selectand D with the selector A or B, respectively, present in the solvent S. Equations (1.15) and (1.16) can be rewritten into the equations (1.17) and (1.18), respectively.

$$K_{AD}^{assoc} c_A^{ABinS} = \frac{c_{AD}}{c_{Ds}} \quad (1.17)$$

$$K_{BD}^{assoc} c_B^{ABinS} = \frac{c_{BD}}{c_{Ds}} \quad (1.18)$$

The total concentration of the selectand D present in the stationary phase is the sum of the concentrations c_{Ds} , c_{AD} and c_{BD} . Consequently, the apparent distribution constant K_D^{ABinS} of the selectand D between the gas phase and the CSP AB in S, assuming no volume change on dissolution of D, is

$$K_D^{ABinS} = \frac{c_{Ds} + c_{AD} + c_{BD}}{c_{Dg}} \quad (1.19)$$

Substituting equations (1.14), (1.17) and (1.18) into (1.19) gives

$$K_D^{ABinS} = K_D^o + K_D^o K_{AD}^{assoc} c_A^{ABinS} + K_D^o K_{BD}^{assoc} c_B^{ABinS} \quad (1.20)$$

Substituting eqs (1.20) written for the selectand enantiomers D and L into the expression for the apparent enantioseparation factor, α_{app} , on the CSP, AB in S, ($\alpha_{app} = \frac{K_D^{ABinS}}{K_L^{ABinS}}$) gives equation (1.21):

$$\alpha_{\text{app}}^{\text{AB in S}} = \frac{1 + K_{\text{AD}}^{\text{assoc}} c_{\text{A}}^{\text{AB in S}} + K_{\text{BD}}^{\text{assoc}} c_{\text{B}}^{\text{AB in S}}}{1 + K_{\text{AL}}^{\text{assoc}} c_{\text{A}}^{\text{AB in S}} + K_{\text{BL}}^{\text{assoc}} c_{\text{B}}^{\text{AB in S}}} \quad (1.21)$$

Since the association constants $K_{\text{AD}}^{\text{assoc}}$ and $K_{\text{BD}}^{\text{assoc}}$ as well as $K_{\text{AL}}^{\text{assoc}}$ and $K_{\text{BL}}^{\text{assoc}}$ can be experimentally determined on single-selector CSPs A in S and B in S, respectively, equation (1.21) can be used for the calculation of $\alpha_{\text{app}}^{\text{AB in S}}$ related to the binary-selector CSP AB in S at any ratio and values of the concentrations $c_{\text{A}}^{\text{AB in S}}$ and $c_{\text{B}}^{\text{AB in S}}$. Similar equation can be produced for more than two chiral selectors present in the solvent S. When the concentration of one of the selectors present in S equals zero, i.e. $c_{\text{B}}^{\text{AB in S}} = 0$, equation (1.21) transforms into equation (1.7) known for single-selector CSPs (vide supra). Substitution of equation (1.11) and the same equation for L-enantiomer into (1.21) leads to the expression for $\alpha_{\text{app}}^{\text{AB in S}}$ in terms of the apparent distribution constants obtained on single-selector CSPs:

$$\alpha_{\text{app}}^{\text{AB in S}} = \frac{K^{\circ} + \frac{c_{\text{A}}^{\text{AB in S}}}{c_{\text{A}}^{\text{A in S}}} (K_{\text{D}}^{\text{A in S}} - K^{\circ}) + \frac{c_{\text{B}}^{\text{AB in S}}}{c_{\text{B}}^{\text{B in S}}} (K_{\text{D}}^{\text{B in S}} - K^{\circ})}{K^{\circ} + \frac{c_{\text{A}}^{\text{AB in S}}}{c_{\text{A}}^{\text{A in S}}} (K_{\text{L}}^{\text{A in S}} - K^{\circ}) + \frac{c_{\text{B}}^{\text{AB in S}}}{c_{\text{B}}^{\text{B in S}}} (K_{\text{L}}^{\text{B in S}} - K^{\circ})} \quad (1.22)$$

where $c_{\text{B}}^{\text{A in S}}$ and $c_{\text{B}}^{\text{AB in S}}$ are the concentrations of the selector B in the single-selector CSP A in S and in the binary-selector CSP AB in S, respectively. $K_{\text{D}}^{\text{B in S}}$ and $K_{\text{L}}^{\text{B in S}}$ are the apparent distribution constants of the selectand D and L, respectively, on the single-selector CSP B in S. Since the distribution constants obtained on the reference column are the same for D and L enantiomers, the corresponding subscripts are omitted.

In turn, equation (1.22) can be modified in terms of the mole fractions of the selectors A and B in their mixture to give (1.23):

$$\alpha_{\text{app}}^{\text{AB in S}} = \frac{K_{\text{D}}^{\text{A in S}} x_{\text{A}}^{\text{AB}} + K_{\text{D}}^{\text{B in S}} (1 - x_{\text{A}}^{\text{AB}})}{K_{\text{L}}^{\text{A in S}} x_{\text{A}}^{\text{AB}} + K_{\text{L}}^{\text{B in S}} (1 - x_{\text{A}}^{\text{AB}})} \quad (1.23)$$

where $x_{\text{A}}^{\text{AB}} = \frac{n_{\text{A}}}{n_{\text{A}} + n_{\text{B}}}$ is the mole fraction of the selector A in the mixture A and B; n_{A}

and n_{B} are the mole amounts of the selector A and B present in the solvent S, respectively. The apparent distribution constants present in eq (1.23) are determined on single-selector CSPs. The concentrations of the selector A and B in the binary-selector and single-selector

CSPs, however, become interrelated with each other. Therefore, the sum of the concentrations of A and B in the binary-selector CSP AB in S has to be constant and must be equal to the concentration of A or B in the single-selector CSPs A in S and B in S, respectively, i.e. $c_A^{A \text{ in } S} = c_B^{B \text{ in } S} = (c_A^{AB \text{ in } S} + c_B^{AB \text{ in } S})$ (1.24). In this case, the distribution constant, K° , is cancelled.

Since the apparent distribution constant in chromatography is determined as the product of the phase ratio, β , and the retention factor, k , equation (1.23) can be written in terms of the retention factors provided the phase ratios $\beta^{A \text{ in } S}$, $\beta^{B \text{ in } S}$ and $\beta^{AB \text{ in } S}$ are the same [72]:

$$\alpha_{\text{app}}^{AB \text{ in } S} = \frac{k_D^{A \text{ in } S} x_A^{AB} + k_D^{B \text{ in } S} (1 - x_A^{AB})}{k_L^{A \text{ in } S} x_A^{AB} + k_L^{B \text{ in } S} (1 - x_A^{AB})} \quad (1.25)$$

where $k_D^{A \text{ in } S}$ and $k_L^{A \text{ in } S}$ ($k_D^{B \text{ in } S}$ and $k_L^{B \text{ in } S}$) are the retention factors of the selectand enantiomers D and L, respectively, on the CSP A in S (B in S) [67,72]. If the phase ratios are not the same, relative retentions (vide supra) can be used instead of the retention factors:

$$\alpha_{\text{app}}^{AB \text{ in } S} = \frac{r_D^{A \text{ in } S} x_A^{AB} + r_D^{B \text{ in } S} (1 - x_A^{AB})}{r_L^{A \text{ in } S} x_A^{AB} + r_L^{B \text{ in } S} (1 - x_A^{AB})} \quad (1.26)$$

If the selectors A and B are used undiluted, the condition (1.24) is fulfilled. In this case, however, the molar ratios in equation (1.23) should be substituted with volume fractions:

$$\alpha_{\text{app}}^{AB} = \frac{\phi^A K_D^A + \phi^B K_D^B}{\phi^A K_L^A + \phi^B K_L^B} \quad (1.27)$$

where K_D^A and K_L^A (K_D^B and K_L^B) are the apparent distribution constants of the selectand enantiomers D and L, respectively, between the gas phase and the undiluted selector A (B); ϕ^A and ϕ^B represent the volume fractions of the undiluted selectors A and B, respectively, in their mixture - the mixed CSP AB. Note that $\phi^A = \frac{V^A}{V^A + V^B}$ and $\phi^A + \phi^B = 1$,

where V^A and V^B are volumes of the selectors A and B, respectively. Equation (1.27) was derived by Purnell and Laub in 1975 [50] and was used for the optimization of solvent compositions used as stationary phases in achiral GC for separations of complex mixtures of analytes (up to 30 components) [50,160-164]. Some solvent mixtures, however, did not obey

the equation [165-169,122]. Similar equation was used in liquid chromatography for the optimization of the protein separation on a column packed with a mixture of ion exchangers [61].

Mixed undiluted selectors were also used in enantioselective GC. König et al. used 1:1 mixture of per-*O*-methylated- and per-*O*-pentylated- β -cyclodextrins as the CSP for the enantioseparation of a mixture of phenoxypropionic acid herbicides [80]. A mixture of heptakis(2,6-di-*O*-methyl-3-*O*-pentyl)- β -cyclodextrin and octakis(2,6-di-*O*-methyl-3-*O*-trifluoroacetyl)- γ -cyclodextrin was applied for the analysis of a multicomponent system of flavours and it was found to be superior to the separate use of the selectors [77]. Contrary to the examples above, the enantioselective properties of a mixture of 6-*O*-*tert*-butyldimethylsilyl-2,3-*O*-diacetyl- and 6-*O*-*tert*-butyldimethylsilyl-2,3-*O*-dimethyl- β -cyclodextrins were found to be unfavorable to that of the single selectors used separately [170].

Equation (1.27) can be applied for the calculation of the apparent enantioseparation factor, α_{app} , of two columns coupled in series based on the retention data obtained on the single columns. In this particular case ϕ^A and ϕ^B become length ratios of the columns containing selector A and B, respectively [82]. Investigation of the (enantio)separation using columns coupled in series was a frequent topic in GC and LC because of its ease of realization accompanied by useful results [67,73,82-85].

Equation (1.21) and the related equations are based on the assumption that there are no interactions between the mixed selectors that could lead to non-additive effects, i.e. the absence of synergistic effects. Therefore, a deviation of the experimental data from the predicted one on binary-selector CSPs may be a sign of synergistic effects. Thus, using equation (1.23) Gil-Av et al. observed the deviation of the experimental retention data from the predicted one that was attributed to the self-association of the chiral selectors [122,167-169]. Laub et al. [165, 166] observed deviations from the linearity of the plot of the apparent distribution constant, K , versus the volume fraction, ϕ , (see eq 1.27) for several pairs of binary solvent mixtures. Nevertheless, one should be careful when claiming for observed synergistic effects on the basis of the deviations of experimental data from the calculated ones. As it was mentioned, equation (1.25) can only be used providing the columns being compared have identical phase ratios. Further, the equations using molar fraction, x , can only be applied if the condition (1.24) is satisfied. Recently, a series of works [75,76,171-175] describing the observation of synergistic effects was published. The conclusion was made on the basis of the discrepancies found between experimental and calculated values of the separation factors on

binary-selector stationary phases. Eq. (1.25) was used for the calculation of the apparent separation factors, yet the identity of the phase ratios of the columns used was not stated. In addition, concentrations of the selectors were different on all the single-selector stationary phases compared, i.e. eq. (1.25) could not be used under such conditions and, therefore, attribution of the disagreement of α_{calc} with α_{observed} to synergistic effects was premature. It should also be noted that for the investigation of the synergistic effects it would be more reliable to compare calculated and observed retention factors (or relative retentions) instead of enantioseparation factors. The reason for that is that the possible deviations of the observed retention factors from the calculated ones for both enantiomers have often the same sign. Therefore, when dividing the retention factors of the enantiomers to obtain the enantioseparation factor, the deviations may cancel [176].

2.4.1.1 Analysis of the behavior of α_{app} upon varying ratio and the association strengths of two different chiral selectors, A and B, present in an achiral solvent

Provided the absence of synergistic effects, the apparent enantioseparation factor, α_{app} , on a binary-selector CSP is always smaller than that on a single-selector CSP containing the more enantioselective selector. Therefore, it may appear unfavorable to combine different selectors in the same CSP. This notion was expressed by Pirkle and Welch in their note on “mixing of CSPs for the separation of enantiomers” [73]. On the other hand, however, combination of chiral selectors with complementary enantioselectivity in the same CSP can endow this CSP with a broader scope of the enantioselectivity than that of either of the single-selector CSPs. Therefore, when combining different selectors in the same solvent S, it is important to reach a compromise between a decreased absolute value of the apparent enantioseparation factor, α_{app} , and the extended scope of possible enantioseparations. Consequently, the optimization of the ratio between chiral selectors present in a binary-selector CSP is necessary. Such optimization can be performed using one of the equations presented in Section 2.4.1. In the given section, the behavior of α_{app} upon varying ratio between selectors A and B and the values of the apparent distribution constants, $K_{\text{D}}^{\text{BinS}}$ ($K_{\text{L}}^{\text{BinS}}$) and $K_{\text{D}}^{\text{AinS}}$ ($K_{\text{L}}^{\text{AinS}}$), is studied. The examination is performed using equation (1.25).

$$\alpha_{\text{app}}^{\text{ABinS}} = \frac{k_{\text{D}}^{\text{AinS}} x_{\text{A}}^{\text{AB}} + k_{\text{D}}^{\text{BinS}} (1 - x_{\text{A}}^{\text{AB}})}{k_{\text{L}}^{\text{AinS}} x_{\text{A}}^{\text{AB}} + k_{\text{L}}^{\text{BinS}} (1 - x_{\text{A}}^{\text{AB}})} \quad (1.25)$$

The matched case, i.e. the case when the elution order of the enantiomers D and L on the selectors A and B is the same, will be described before the mismatched case – the case of the opposite elution order of the enantiomers on the combined selectors.

a) Case I: the same elution order of the selectand enantiomers D and L on the chiral selectors A and B (matched case)

In the case of the identical retention factors of the first eluted enantiomer on the single-selector CSPs, A in S and B in S (i.e. $k_L^{A \text{ in } S} = k_L^{B \text{ in } S}$), the apparent enantioseparation factor, $\alpha_{\text{app}}^{AB \text{ in } S}$, obtained on the binary-selector CSP, AB in S, is linearly dependent on the molar fraction of the selector B, x_B^{AB} , in the mixture of the selectors (**Figure 2.3**). The linearity of the plot is preserved irrespectively of the value of the difference between the enantioseparation factors, $\alpha_{\text{app}}^{A \text{ in } S}$ and $\alpha_{\text{app}}^{B \text{ in } S}$.

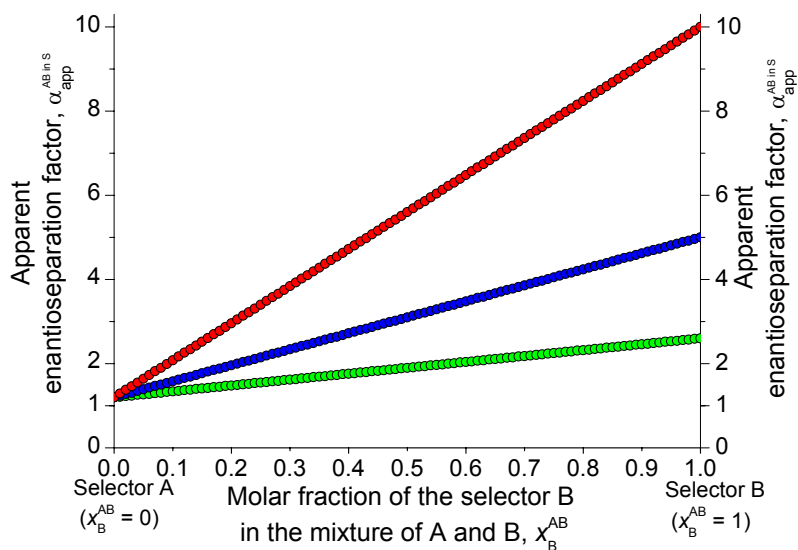


Figure 2.3 Plot of the apparent enantioseparation factor, $\alpha_{\text{app}}^{AB \text{ in } S}$, on the binary-selector CSP, AB in S, as a function of the fraction of the selector B in the mixture of A and B, x_B^{AB} . Green plot: $\alpha_{\text{app}}^{A \text{ in } S} = 1.2$, $\alpha_{\text{app}}^{B \text{ in } S} = 2.6$, $k_L^{A \text{ in } S} = 4$, $k_L^{B \text{ in } S} = 4$; blue plot: $\alpha_{\text{app}}^{A \text{ in } S} = 1.2$, $\alpha_{\text{app}}^{B \text{ in } S} = 5$, $k_L^{A \text{ in } S} = 4$, $k_L^{B \text{ in } S} = 4$; red plot: $\alpha_{\text{app}}^{A \text{ in } S} = 1.2$, $\alpha_{\text{app}}^{B \text{ in } S} = 10$, $k_L^{A \text{ in } S} = 4$, $k_L^{B \text{ in } S} = 4$. Where $\alpha_{\text{app}}^{A \text{ in } S}$ and $\alpha_{\text{app}}^{B \text{ in } S}$ are the apparent enantioseparation factors on the single-selector CSPs, A in S and B in S, respectively; $k_L^{A \text{ in } S}$ and $k_L^{B \text{ in } S}$ are the retention factors of the first eluted enantiomer on the CSPs A in S and B in S, respectively.

However, if the selectors A and B retain the first eluted enantiomer of the selectand with different strengths (i.e. $k_L^{A \text{ in } S} \neq k_L^{B \text{ in } S}$), the plot $\alpha_{\text{app}}^{\text{AB in } S}$ vs. x_B^{AB} becomes nonlinear (**Figure 2.4**). The stronger the interaction of one of the selectors with the selectand, the greater is the influence of this selector on the apparent enantioseparation factor, $\alpha_{\text{app}}^{\text{AB in } S}$, on the binary-selector CSP AB in S. For example, the apparent enantioseparation factors of a racemic selectand on the single-selector CSPs A in S and B in S are 1.2 and 5.0, respectively. If the first eluted enantiomer is retained 20 times stronger on the CSP A in S than on B in S, the addition of only 10% of the selector A to the CSP B in S reduces the apparent enantioseparation factor, $\alpha_{\text{app}}^{\text{B in } S}$, from 5.0 to 2.4, i.e. more than twice. It should be emphasized that in this case the elution order of the selectand enantiomers on the single-selector CSPs A in S and B in S is the same.

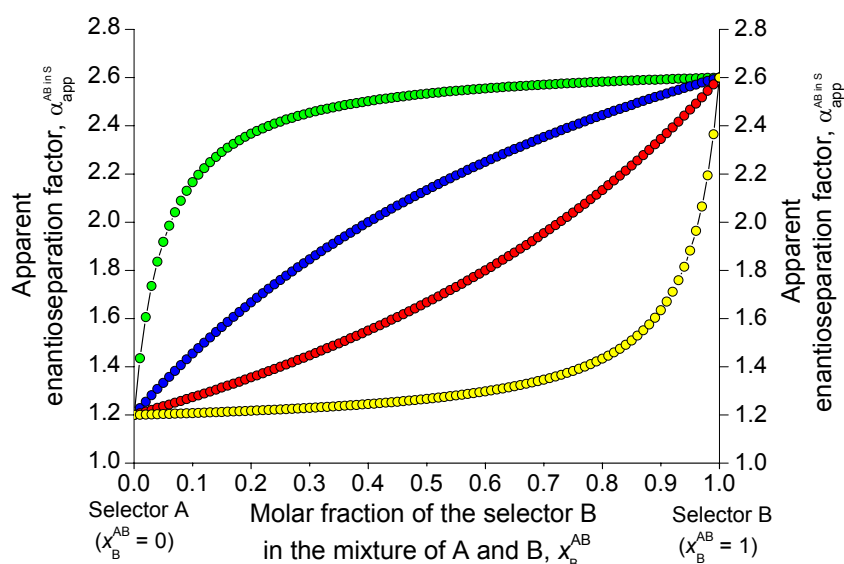


Figure 2.4 Plot of the apparent enantioseparation factor, $\alpha_{\text{app}}^{\text{AB in } S}$, on the binary-selector CSP, AB in S, as a function of the fraction of the selector B in the mixture of A and B, x_B^{AB} . Green plot: $\alpha_{\text{app}}^{\text{A in } S} = 1.2$, $\alpha_{\text{app}}^{\text{B in } S} = 2.6$, $k_L^{\text{A in } S} = 4$, $k_L^{\text{B in } S} = 80$; blue plot: $\alpha_{\text{app}}^{\text{A in } S} = 1.2$, $\alpha_{\text{app}}^{\text{B in } S} = 2.6$, $k_L^{\text{A in } S} = 4$, $k_L^{\text{B in } S} = 8$; red plot: $\alpha_{\text{app}}^{\text{A in } S} = 1.2$, $\alpha_{\text{app}}^{\text{B in } S} = 2.6$, $k_L^{\text{A in } S} = 8$, $k_L^{\text{B in } S} = 4$; yellow plot: $\alpha_{\text{app}}^{\text{A in } S} = 1.2$, $\alpha_{\text{app}}^{\text{B in } S} = 2.6$, $k_L^{\text{A in } S} = 80$, $k_L^{\text{B in } S} = 4$. For descriptions see **Figure 2.3**.

In the case of a binary-selector CSP containing a *chiral* selector B and an *achiral* selector A (racemic or nonenantioselective towards the selectand) the same behavior of the apparent enantioseparation factor, $\alpha_{\text{app}}^{\text{ABinS}}$, can be observed. Namely, the stronger the achiral selector retains the selectand (in comparison with that of the chiral selector), the lower will be the apparent enantioseparation factor, $\alpha_{\text{app}}^{\text{ABinS}}$ (**Figure 2.5**).

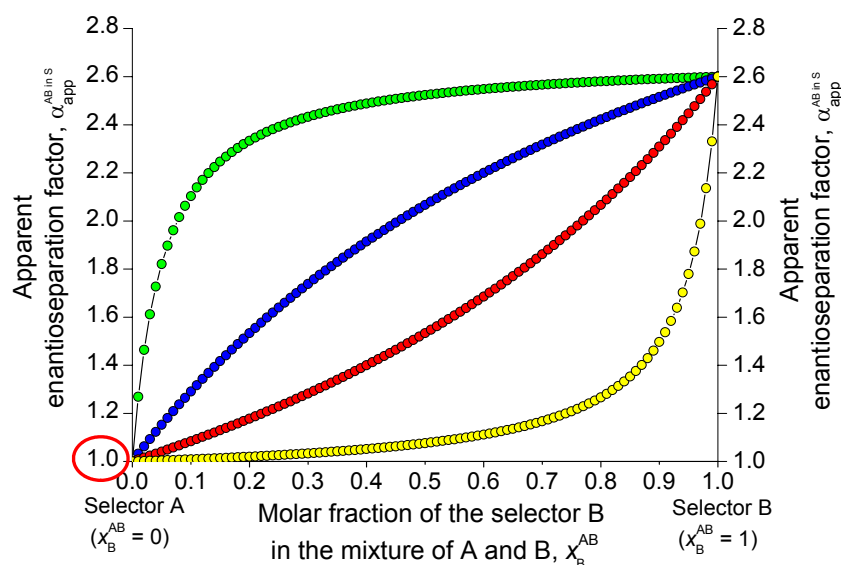


Figure 2.5 Plot of the apparent enantioseparation factor, $\alpha_{\text{app}}^{\text{ABinS}}$, on the binary-selector CSP, AB in S, as a function of the fraction of the selector B in the mixture of A and B, x_B^{AB} . Green plot: $\alpha_{\text{app}}^{\text{AinS}} = 1.0$, $\alpha_{\text{app}}^{\text{BinS}} = 2.6$, $k_L^{\text{AinS}} = 4$, $k_L^{\text{BinS}} = 80$; blue plot: $\alpha_{\text{app}}^{\text{AinS}} = 1.0$, $\alpha_{\text{app}}^{\text{BinS}} = 2.6$, $k_L^{\text{AinS}} = 4$, $k_L^{\text{BinS}} = 8$; red plot: $\alpha_{\text{app}}^{\text{AinS}} = 1.0$, $\alpha_{\text{app}}^{\text{BinS}} = 2.6$, $k_L^{\text{AinS}} = 8$, $k_L^{\text{BinS}} = 4$; yellow plot: $\alpha_{\text{app}}^{\text{AinS}} = 1.0$, $\alpha_{\text{app}}^{\text{BinS}} = 2.6$, $k_L^{\text{AinS}} = 80$, $k_L^{\text{BinS}} = 4$. For descriptions see **Figure 2.3**.

The role of the achiral selector can be fulfilled by any achiral “impurity” that interacts with the selectand enantiomers. Achiral solvents, usually used in GC for dissolving or binding chiral selectors, may also nonenantioselectively interact with the selectand enantiomers. It is interesting to draw an analogy between the achiral selector in **Figure 2.5** and a racemic selector (*vide infra*). In this case, a convex downwards curve is expected because the retention factor of the first eluted enantiomer on the enantiopure selector is, by definition, smaller than that on the corresponding racemic selector. However, the presence of homo- and/or

heterochiral interactions between the selector molecules, e.g. formation of homochiral dimers in case of the enantiopure selector and heterochiral dimers in the case of the racemic one, may lead to interesting unexpected results. For example, if the formation of heterochiral dimers makes them indifferent towards the interaction with the selectand molecules, the plot of $\alpha_{\text{app}}^{\text{ABinS}}$ vs. x_{B}^{AB} can become convex upwards (cf. blue or green curve in **Figure 2.5**).

b) Case II: opposite elution order of the enantiomers D and L on the chiral selectors A and B (mismatched case)

The foregoing discussion deals with the behavior of the apparent enantioseparation factor, $\alpha_{\text{app}}^{\text{ABinS}}$, on a binary-selector CSP, AB in S, where the two chiral selectors, A and B, possess opposite enantioselectivity (mismatched case), i.e. the elution order of the enantiomers is opposite on the single-selector CSPs. In this case, the behavior of $\alpha_{\text{app}}^{\text{ABinS}}$ obeys the same rule as in the matched cases, i.e. the stronger the interaction of the selectand with the selector, the greater is the influence of the apparent enantioseparation factor, $\alpha_{\text{app}}^{\text{ABinS}}$, on the binary-selector CSP, AB in S. An important difference of the mismatched case, distinguishing it from the matched case, is the inevitability of the inversion of the elution order of the enantiomers when turning between the single-selector CSPs A in S and B in S. **Figure 2.6** displays the behavior of the apparent enantioseparation factor, $\alpha_{\text{app}}^{\text{ABinS}}$, as a function of the molar fraction of selector B in the mixture of A and B, the apparent enantioseparation factors on the single-selector CSPs, A in S and B in S, being the same by the magnitude but opposite by the sign. For convenience, the convention of $\alpha \geq 1$ is retained, i.e. the points where the plots cross the X-axis correspond to the inversion of the elution order of the enantiomers. As one can see (**Figure 2.6**, green curve), equimolar mixture of the selectors loses completely its enantioselectivity if the retention factors of the first eluted enantiomer on the single-selector CSPs are the same, i.e. $k_1^{\text{AinS}} = k_1^{\text{BinS}}$. In the other cases, despite the same apparent enantioseparation factors on the single-selector CSPs, i.e. $\alpha_{\text{app}}^{\text{AinS}} = \alpha_{\text{app}}^{\text{BinS}}$, equimolar mixture of the selectors can be still highly enantioselective towards the selectand (**Figure 2.6**, blue and red curves).

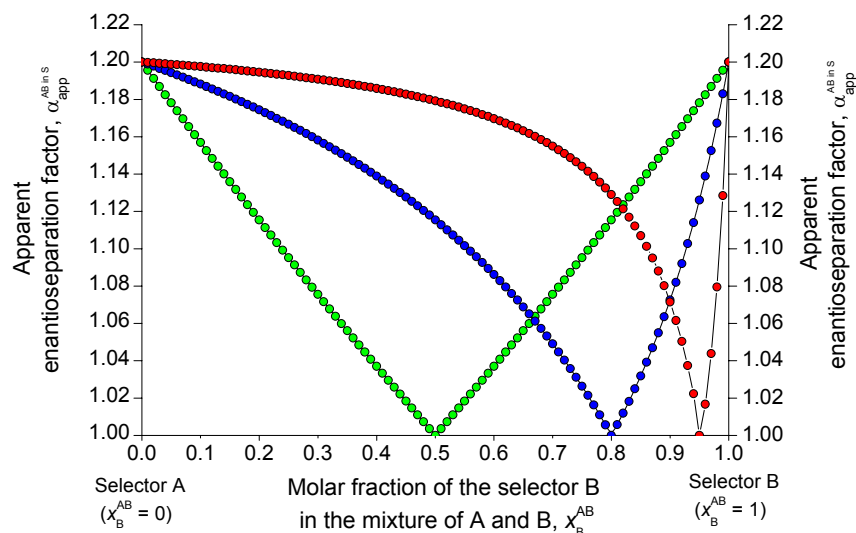


Figure 2.6 Plot of the apparent enantioseparation factor, $\alpha_{\text{app}}^{\text{AB in S}}$, on the binary-selector CSP AB in S as a function of the fraction of the selector B in the mixture of A and B, x_B^{AB} . Green plot: $\alpha_{\text{app}}^{\text{A in S}} = 1.2$, $\alpha_{\text{app}}^{\text{B in S}} = 1.2$, $k_1^{\text{A in S}} = 4$, $k_1^{\text{B in S}} = 4$; blue plot: $\alpha_{\text{app}}^{\text{A in S}} = 1.2$, $\alpha_{\text{app}}^{\text{B in S}} = 1.2$, $k_1^{\text{A in S}} = 16$, $k_1^{\text{B in S}} = 4$; red plot: $\alpha_{\text{app}}^{\text{A in S}} = 1.2$, $\alpha_{\text{app}}^{\text{B in S}} = 1.2$, $k_1^{\text{A in S}} = 80$, $k_1^{\text{B in S}} = 4$; where $k_1^{\text{A in S}}$ and $k_1^{\text{B in S}}$ are the retention factors of the first eluted enantiomer on the stationary phases A in S and B in S, respectively. Enantioselectivity of A and B is opposite towards the selectand enantiomers.

It is interesting that contrary to the matched case with the same retention factors of the first eluted enantiomer, where linearity of the plot $\alpha_{\text{app}}^{\text{AB in S}}$ vs. x_B^{AB} is not disrupted even if the apparent enantioseparation factors on the single-selector CSPs are very different (**Figure 2.3**, red line), in the mismatched case with the same retention factors of the first eluted enantiomer the visual linearity of the plot at low apparent enantioseparation factors (**Figure 2.6**, green line) is dramatically upset at high enantioseparation factors (**Figure 2.7**). The green curves depicted in **Figures 2.6** and **2.7** were simulated using the same retention data but different enantioseparation factors on the single-selector CSPs, i.e. $\alpha_{\text{app}}^{\text{A in S}} = \alpha_{\text{app}}^{\text{B in S}} = 1.2$ (**Figure 2.6**), $\alpha_{\text{app}}^{\text{A in S}} = \alpha_{\text{app}}^{\text{B in S}} = 50$ (**Figure 2.7**). The ideal example of the two chiral selectors possessing opposite enantioselectivity but displaying the same retention factor for the first eluted enantiomer is nothing else but a pair of opposite enantiomers. That means that the predicted strong non-linearity of the plot $\alpha_{\text{app}}^{\text{AB in S}}$ vs. x_B^{AB} (**Figure 2.7**) should be observed for a

chromatographic system where the mixed selectors are highly enantioselective opposite enantiomers. The behaviour of the apparent enantioseparation factor, $\alpha_{app}^{AB\text{ in } S}$, on a CSP as a function of the enantiomeric excess, ee , of the chiral selector will be discussed in the next section.

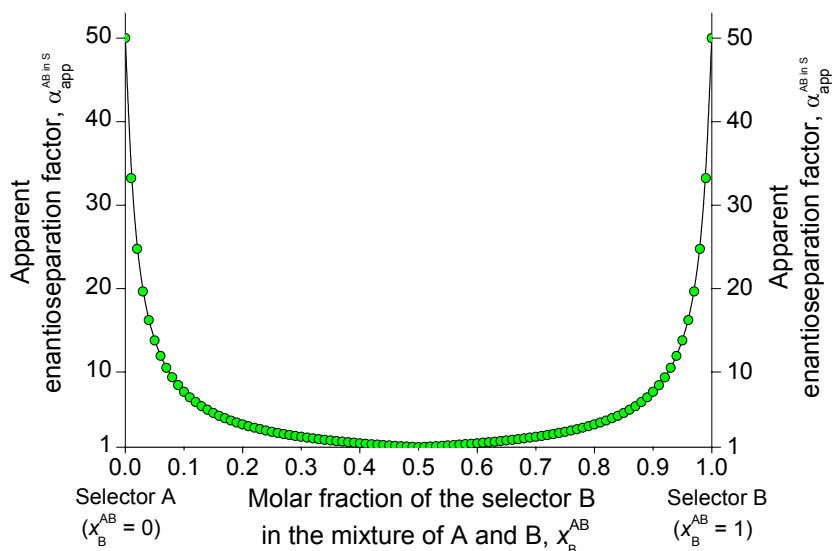


Figure 2.7 Plot of the apparent enantioseparation factor, $\alpha_{app}^{AB\text{ in } S}$, on the binary-selector CSP, AB in S, as a function of the fraction of the selector B in the mixture of A and B, x_B^{AB} . The highly enantioselective selectors A and B ($\alpha_{app}^{A\text{ in } S} = \alpha_{app}^{B\text{ in } S} = 50$) display the same retention factor for the first eluted enantiomer ($k_1^{A\text{ in } S} = k_1^{B\text{ in } S} = 4$) but possess opposite enantioselectivity toward the selectand; where $k_1^{A\text{ in } S}$ and $k_1^{B\text{ in } S}$ are the retention factors of the first eluted enantiomer on the stationary phases A in S and B in S, respectively. Enantioselectivity of A and B is opposite towards the selectand enantiomers.

c) Case III: chiral selector is not enantiomerically pure. Analysis of the apparent enantioseparation factor, α_{app} , as a function of the enantiomeric excess, ee , of the chiral selector

The simplest binary-selector CSP contains a chiral selector which is enantiomerically impure, i.e. the enantiomers of the selector behave as different chiral selectors with opposite enantioselectivity. In the present section, the opposite enantiomers of the chiral selector will be referred to as R and S. An analysis of the behavior of the apparent enantioseparation factor, α_{app}^{RS} , as a function of the enantiomeric excess of the chiral selector, ee , will be presented. To describe the dependence of the apparent enantioseparation factor, α_{app}^{RS} , obtained on a CSP

containing both selector R and S on the enantiomeric excess of the chiral selector, i.e. $\alpha_{\text{app}}^{\text{RS}}$ vs. ee , equation (1.25) can be modified as follows. Molar fraction of the selector R, x_{R}^{RS} , expressed in terms of the enantiomeric excess, ee , is $x_{\text{R}}^{\text{RS}} = \frac{ee+1}{2}$. Substitution this expression into (1.25) gives

$$\alpha_{\text{app}}^{\text{RS}} = \frac{k_{\text{D}}^{\text{R}}(1+ee) + k_{\text{D}}^{\text{S}}(1-ee)}{k_{\text{L}}^{\text{R}}(1+ee) + k_{\text{L}}^{\text{S}}(1-ee)} \quad (1.28)$$

where k_{D}^{R} and k_{L}^{R} are retention factors of D and L selectand enantiomers, respectively, on a CSP containing the enantiopure selector of R configuration. k_{D}^{S} and k_{L}^{S} are retention factors of D and L selectand enantiomers, respectively, on a CSP containing the enantiopure selector of S configuration.

For a chromatographic system where the selectors R and S are opposite enantiomers the following expressions hold true: $k_{\text{D}}^{\text{R}} = k_{\text{L}}^{\text{S}}$ and $k_{\text{L}}^{\text{R}} = k_{\text{D}}^{\text{S}}$. Thus, dividing numerator and denominator of (1.28) by k_{L}^{S} , the expression (1.29) is obtained.

$$\alpha_{\text{app}}^{\text{RS}} = \frac{\alpha_{\text{app}}^{\text{ee}=1}(1+ee) + (1-ee)}{\alpha_{\text{app}}^{\text{ee}=1}(1-ee) + (1+ee)} \quad (1.29)$$

where $\alpha_{\text{app}}^{\text{RS}}$ is the apparent enantioseparation factor obtained on the CSP containing both R and S, i.e. the chiral selector R with the enantiomeric excess, ee , being less than unity; $\alpha_{\text{app}}^{\text{ee}=1}$ is the apparent enantioseparation factor obtained on a CSP containing enantiomerically pure selector R.

The same equation can also be derived by the following thought experiment. A chromatographic column containing a nonracemic mixture of a chiral selector enriched, e.g., with the enantiomer R, can be subdivided into two virtual segments containing the enantiomerically pure selector R in the first part, and the racemic selector RS in the second part of the column (or *vice versa*). For example, a column of the length l , containing a selector with $ee = 0.5$ (75% R and 25% S), is thought to be equivalent (in the absence of non-linear effects not yet observed in enantioselective chromatography [177]) to a column comprising of two segments of the length $l/2$, containing enantiomerically pure selector R, and racemic selector RS, respectively. When the same column contains a selector with $ee = 0.98$ (99% R

and 1% S), it can be subdivided into a segment with the length of $0.98 l$ containing R, and a segment with the length of $0.02 l$ containing RS. Thus, the length of the segment containing the pure enantiomer R is related to the ee of the selector whereas the length of the segment containing the racemate RS is related to $(1-ee)$, respectively.

The adjusted retention times (t'_r) of the enantiomers separated on a chiral selector with $ee < 1$ can be calculated as follows. The adjusted retention time is $x \cdot ee$ for the first eluted enantiomer and $y \cdot ee$ for the second eluted enantiomer, respectively, on the enantiomerically pure selector R present in the segment with the length $l \cdot ee$. The adjusted retention time is $(x + y)/2 \cdot (1 - ee)$ for both *unresolved* enantiomers on the racemic selector RS present in the segment with the length $l \cdot (1 - ee)$. Hence, the apparent enantioseparation factor, α_{app}^{RS} , is:

$$\alpha_{app}^{RS} = \frac{t'_{r2}}{t'_{r1}} \quad \text{or} \quad \alpha_{app}^{RS} = \frac{y \cdot ee + \frac{(x+y)}{2} \cdot (1-ee)}{x \cdot ee + \frac{(x+y)}{2} \cdot (1-ee)} \quad (1.30)$$

The apparent enantioseparation factor, $\alpha_{app}^{ee=1}$, of the selectand on the enantiomerically pure selector R is:

$$\alpha_{app}^{ee=1} = y/x \quad (1.31)$$

As apparent enantioseparation factors are independent of the column length, equation (1.31) can be inserted into equation (1.30) furnishing expression (1.29).

Equation (1.29) is compatible with an expression derived by Beitler and Feibush in 1976 [178]. The authors extrapolated the apparent enantioseparation factor $\alpha_{app}^{ee=1}$ of a chiral selectand on an elusive enantiomerically pure selector from the apparent enantioseparation factor α_{app}^{RS} obtained on a real enantiomerically impure selector ($ee < 1$) according to:

$$\alpha_{app}^{ee=1} = \frac{(\alpha_{app}^{RS} + 1) ee + (\alpha_{app}^{RS} - 1)}{(\alpha_{app}^{RS} + 1) ee - (\alpha_{app}^{RS} - 1)} \quad (1.32)$$

According to equation (1.29), α_{app}^{RS} is rendered equivalent to $\alpha_{app}^{ee=1}$ for $ee = 1$. For values of $\alpha_{app}^{ee=1} = 1.01 - 2.0$, usually encountered in enantioselective GC, the function of α_{app}^{RS} vs. ee is

almost linear and hence an enantiomerically pure chiral selector is not strictly required. However, for large values of $\alpha_{\text{app}}^{\text{ee}=1}$ a striking drop of the apparent enantioseparation factor, $\alpha_{\text{app}}^{\text{RS}}$, is encountered as the result of minute deviations from $ee = 1$ of the selector. Thus, the apparent enantioseparation factor, $\alpha_{\text{app}}^{\text{RS}}$, of a chiral selectand drops from 100 to 49.8 on a chiral selector of $ee = 0.98$, i.e. containing only 1% of the enantiomeric impurity (cf. **Figure 2.8**). This large difference can further be appreciated by the following thought experiment. In the hypothetical case that one enantiomer is eluted with the void volume of the column, whereas the other enantiomer is retained, the apparent enantioseparation factor, α_{app} , becomes infinite. However, only a tiny amount of an enantiomeric impurity present in the selector ($ee \cong 1$) causes a minute retention of the first eluted enantiomer and the infinite separation factor is now rendered finite. A plot of $\alpha_{\text{app}}^{\text{RS}}$ vs. ee of the chiral selector is shown in **Figure 2.8**. Such behaviour was predicted by Davankov [21] and by Welch and Pirkle [73]. It should be noted, however, that the equations (1.29) and (1.32) can only be used provided the condition (1.24) is satisfied.

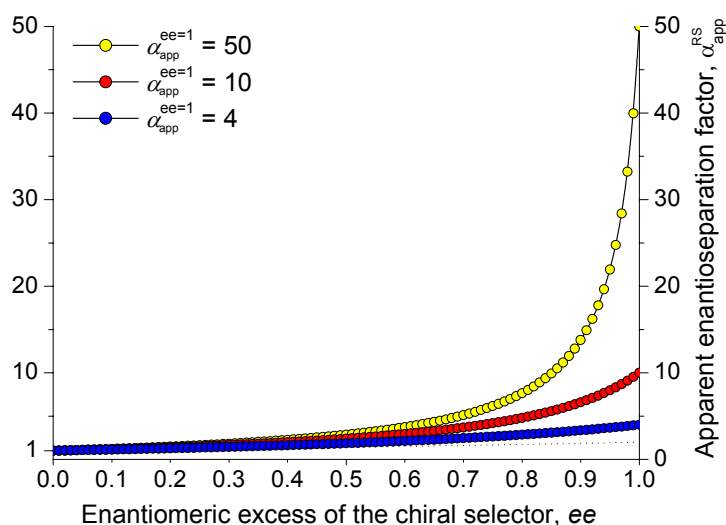


Figure 2.8 Plot of the apparent enantioseparation factor, $\alpha_{\text{app}}^{\text{RS}}$, as a function of the enantiomeric excess of a chiral selector, ee ; $\alpha_{\text{app}}^{\text{ee}=1}$ is the apparent enantioseparation factor of the enantiomerically pure selector

It is important to recognize that according to a recent examination [109,110], over a half of commercially available non-racemic chiral compounds contain more than 0.1% of the undesired enantiomer.

Despite the decrease of the apparent enantioseparation factors on enantiomerically impure chiral selectors, coupling of two columns with enantiopure and racemic CSPs in series, which is equivalent to a longer column with enantiomerically impure chiral selector, can be useful for improving the *diastereoselectivity* of the CSP [73,81,82,84,85].

It is interesting to note that in enantioselective catalysis, governed by kinetics, an enantiomerically pure product can not be obtained from a prochiral educt if the chiral catalyst is not enantiomerically pure ($ee \neq 1$). In enantioselective chromatography, governed by thermodynamics, however, enantiomerically pure fractions can still be obtained when the chiral selector is not enantiomerically pure as only the apparent enantioseparation factor α_{app} is reduced according to equation 1.29. This is schematically shown in **Figure 2.9** [177].

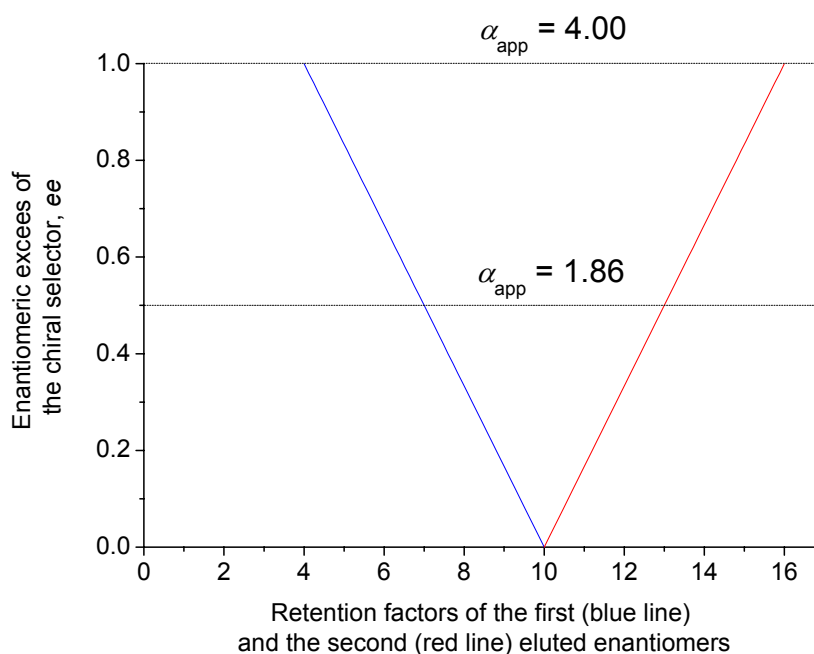


Figure 2.9 This figure is an amended previously published version [177].

2.4.1.2 Experimental verification of the equation for the calculation of the apparent enantioseparation factor, α_{app} , on a CSP containing an *L*-valine diamide and a permethylated- β -cyclodextrin

In order to verify the equation for the calculation of the apparent enantioseparation factors (1.22), six different chiral polymers were prepared: polymer containing 20% (w/w) of the permethylated- β -cyclodextrin selector (CD) [151] bonded to dimethylhydromethylpolysiloxane (polysiloxane) (CSP1) through an undecenyl spacer; polymer containing 19.9% (w/w) of *N*-(undec-10-enoyl)-*L*-valine-*tert*-butylamide selector

(DA) [136, 92] (cf. Section 1.1) bonded to the polysiloxane (CSP2); three polymers containing both CD and DA selectors bonded to the polysiloxane, the concentrations of CD and DA selectors being 6.2 and 18.5 (CSP3), 10.1 and 9.9 (CSP4), 14.4 and 4.9% (w/w) (CSP5), respectively; a reference polysiloxane polymer devoid of any selectors (SP6). The bonding of the selectors to the polysiloxane was performed by platinum-catalyzed hydrosilylation [118]. The polymers were coated onto six fused-silica GC capillaries which were used for the analysis of four different α -amino acids (proline, phenylalanine, ornithine and lysine) derivatized as *N*-trifluoroacetyl ethyl esters. The retention data obtained on CSP1, CSP2 and SP6 were used for the calculation of the apparent enantioseparation factors of four racemates enantioseparated on CSP3-5. In order to avoid measuring the phase ratios of the six gas-chromatographic columns, relative retentions, r , were used instead of the retention factors. In the case of the derivatives of proline and phenylalanine, *n*-undecane was used as the inert standard for the calculation of the relative retentions. For lysine and ornithine derivatives, *n*-hexadecane was used. In addition, the concentration of the selectors in the polysiloxane, c (mol/L), was substituted by the molality, m (mol/kg). Thus, equation (1.33) was used instead of (1.22). The calculated and experimental results are presented in **Table 2.1**. Although the calculation was based on the retention data obtained on three different columns, the agreement of the calculated and the experimental enantioseparation factors is satisfactory.

$$\alpha_{\text{app}}^{\text{ABinS}} = \frac{r^{\circ} + \frac{m_{\text{A}}^{\text{ABinS}}}{m_{\text{A}}^{\text{AinS}}} (r_{\text{D}}^{\text{AinS}} - r^{\circ}) + \frac{m_{\text{B}}^{\text{ABinS}}}{m_{\text{B}}^{\text{BinS}}} (r_{\text{D}}^{\text{BinS}} - r^{\circ})}{r^{\circ} + \frac{m_{\text{A}}^{\text{ABinS}}}{m_{\text{A}}^{\text{AinS}}} (r_{\text{L}}^{\text{AinS}} - r^{\circ}) + \frac{m_{\text{B}}^{\text{ABinS}}}{m_{\text{B}}^{\text{BinS}}} (r_{\text{L}}^{\text{BinS}} - r^{\circ})} \quad (1.33)$$

For description see eq (1.22).

Table 2.1 Calculated and experimental values of the apparent enantioseparation factors obtained for α -amino acid derivatives¹ enantioseparated on CSP1-5

Chiral stationary phases ²	Proline		Phenylalanine		Ornithine		Lysine	
	T = 80°C		T = 100°C		T = 130°C		T = 140°C	
	α_{exp}	α_{calc}	α_{exp}	α_{calc}	α_{exp}	α_{calc}	α_{exp}	α_{calc}
CSP1 (0%)	1.02		1.18 ³		1.15		1.11	
CSP3 (25%)	1.05	1.05	1.13	1.13	1.14	1.14	1.11	1.10
CSP4 (50.4%)	1.07	1.06	1.07	1.05	1.11	1.12	1.08	1.08
CSP5 (74.5%)	1.06	1.08	1.02	1.00	1.07	1.09	1.05	1.06
CSP2 (100%)	1.10		1.05 ³		1.01		1.00	

¹as *N*-trifluoroacetyl ethyl esters; ²in the brackets are weight fractions of the CD selector in the mixture of CD and DA selectors; ³mismatched case – opposite elution order of the enantiomers on DA and CD selectors;

2.4.2 Determination of the true enantioseparation factor, α_{true} .

In binary-selector CSPs where two different chiral selectors, e.g. A and B, are present in an achiral solvent S, the selectand enantiomers, D and L, compete for the association with the selectors. For each pair of the selector-selectand associate formed in the CSP a ratio of the association constants, determining the true enantioseparation factor, α_{true} , can be written, i.e.

$$\alpha_{\text{true}}^{\text{AD,AL}} = \frac{K_{\text{AD}}^{\text{assoc}}}{K_{\text{AL}}^{\text{assoc}}} \quad \text{and} \quad \alpha_{\text{true}}^{\text{BD,BL}} = \frac{K_{\text{BD}}^{\text{assoc}}}{K_{\text{BL}}^{\text{assoc}}}. \quad \text{Each true enantioseparation factor can be used for the}$$

calculation of the enantioselectivity of a separate chiral selector, i.e. the Gibbs energy difference between the diastereomeric associates. For example, the enantioselectivity of the

chiral selector A will be determined as $-\Delta_{\text{AD,AL}}(\Delta G) = RT \ln(\alpha_{\text{assoc}}^{\text{AD,AL}}) = RT \ln\left(\frac{K_{\text{AD}}^{\text{assoc}}}{K_{\text{AL}}^{\text{assoc}}}\right)$, while that

of B will be $-\Delta_{\text{BD,BL}}(\Delta G) = RT \ln(\alpha_{\text{assoc}}^{\text{BD,BL}}) = RT \ln\left(\frac{K_{\text{BD}}^{\text{assoc}}}{K_{\text{BL}}^{\text{assoc}}}\right)$. To determine the true

enantioseparation factors corresponding to different chiral selectors, eq. (1.20) should be written in terms of the required association constant (eq. 1.34). Recognizing that

$K^{\circ} K_{\text{BD}}^{\text{assoc}} c_{\text{B}}^{\text{ABinS}} = K_{\text{D}}^{\text{BinS}} - K^{\circ}$, eq. (1.34) can be transformed into (1.35). Substituting (1.34) and (1.35) into the expression for the true enantioseparation factor, α_{true} , gives (1.36) and (1.37), respectively.

$$K_{\text{AD}}^{\text{assoc}} = \frac{K_{\text{D}}^{\text{ABinS}} - K^{\circ} - K^{\circ} K_{\text{BD}}^{\text{assoc}} c_{\text{B}}^{\text{ABinS}}}{K^{\circ} c_{\text{A}}^{\text{ABinS}}} \quad (1.34)$$

$$K_{\text{AD}}^{\text{assoc}} = \frac{K_{\text{D}}^{\text{ABinS}} - K_{\text{D}}^{\text{BinS}}}{K^{\circ} c_{\text{A}}^{\text{ABinS}}} \quad (1.35)$$

$$\alpha_{\text{true}}^{\text{AD,AL}} = \frac{K_{\text{AD}}^{\text{assoc}}}{K_{\text{AL}}^{\text{assoc}}} = \frac{K_{\text{D}}^{\text{ABinS}} - K^{\circ} - K^{\circ} K_{\text{BD}}^{\text{assoc}} c_{\text{B}}^{\text{ABinS}}}{K_{\text{L}}^{\text{ABinS}} - K^{\circ} - K^{\circ} K_{\text{BL}}^{\text{assoc}} c_{\text{B}}^{\text{ABinS}}} \quad (1.36)$$

$$\alpha_{\text{assoc}}^{\text{AD,AL}} = \frac{K_{\text{AD}}^{\text{assoc}}}{K_{\text{AL}}^{\text{assoc}}} = \frac{K_{\text{D}}^{\text{ABinS}} - K_{\text{D}}^{\text{BinS}}}{K_{\text{L}}^{\text{ABinS}} - K_{\text{L}}^{\text{BinS}}} \quad (1.37)$$

It should be noted that the apparent distribution constants $K_{\text{D}}^{\text{ABinS}}$ and $K_{\text{D}}^{\text{BinS}}$ ($K_{\text{L}}^{\text{ABinS}}$ and $K_{\text{L}}^{\text{BinS}}$) in (1.35) and (1.37) have to be measured at the same concentration of the selector B in the solvent S, i.e. $c_{\text{B}}^{\text{ABinS}}$ must be equal to $c_{\text{B}}^{\text{BinS}}$. Thus, using (1.36) or (1.37), the true enantioseparation factor, $\alpha_{\text{true}}^{\text{AD,AL}}$, corresponding to the chiral selector A can be determined on a CSP containing both chiral selector A and B.

Since the exact determination of the phase ratios required for the measurement of the distribution constants ($K = \beta \cdot k$) is difficult in GC, relative retentions should be used (1.38).

$$\alpha_{\text{true}}^{\text{AD,AL}} = \frac{K_{\text{AD}}^{\text{assoc}}}{K_{\text{AL}}^{\text{assoc}}} = \frac{r_{\text{D}}^{\text{AB in S}} - r_{\text{D}}^{\text{B in S}}}{r_{\text{L}}^{\text{AB in S}} - r_{\text{L}}^{\text{B in S}}} \quad (1.38)$$

Equation (1.38) can also be applied to other cases. For example, the selectors A and B being the same (e.g. B = A), binary-selector CSP AB becomes just a more concentrated CSP containing selector A and, therefore, eq (1.38) can be transformed into (1.39) (cf. eq 1.13).

$$\alpha_{\text{true}}^{\text{AD,AL}} = \frac{r_{\text{D}}^{\text{A}_2 \text{ in S}} - r_{\text{D}}^{\text{A}_1 \text{ in S}}}{r_{\text{L}}^{\text{A}_2 \text{ in S}} - r_{\text{L}}^{\text{A}_1 \text{ in S}}} \quad (1.39)$$

Where $r_{\text{D}}^{\text{A}_2 \text{ in S}}$ ($r_{\text{L}}^{\text{A}_2 \text{ in S}}$) and $r_{\text{D}}^{\text{A}_1 \text{ in S}}$ ($r_{\text{L}}^{\text{A}_1 \text{ in S}}$) are the relative retentions of the selectand enantiomer D(L) on two CSPs with different concentration of the selector A. Eq. (1.39) can be especially useful for the calculation of the true enantioseparation factor, $\alpha_{\text{true}}^{\text{AD,AL}}$, on CSPs for which the reference stationary phase, i.e. the achiral polymer S, is not available.

It is worth noting that eq. (1.12) is just a special case of eq. (1.39), i.e. the case where the relative retentions, $r_{\text{D}}^{\text{A}_1 \text{ in S}}$ ($r_{\text{L}}^{\text{A}_1 \text{ in S}}$), are determined on the reference stationary phase devoid of the chiral selector A (i.e. $c_{\text{A}}^{\text{A}_1 \text{ in S}} = 0$).

Chapter 3

3. Influence of temperature on the enantioseparation by GC

3.1 Introduction

The separation of enantiomers in chromatography is the result of different stabilities of transient diastereomeric associates formed between the selectand enantiomers, D and L, and the enantiopure selector present in a CSP. Association equilibrium constants, K_D^{assoc} and K_L^{assoc} , characterize the formation of the diastereomeric associates. The ratio of these constants is defined as the true enantioseparation factor (footnote: in the present Chapter apparent and true enantioseparation factors are determined as the ratio of retention factors or association constants, respectively, of L and D enantiomers, i.e. $\alpha = L/D$, independently of the elution order of the enantiomers), $\alpha_{\text{true}} = \frac{K_L^{\text{assoc}}}{K_D^{\text{assoc}}}$, which quantifies the true enantioseparation factor of

the racemate DL on the chiral selector (cf. Chapter 2). On the contrary, the apparent enantioseparation factor, α_{app} , of a gas-chromatographic system is determined as the ratio of the retention factors of the two enantiomers, k_L and k_D , $\alpha_{\text{app}} = \frac{k_L}{k_D}$. Since the retention factors include both different chiral and identical achiral contributions to retention, α_{app} is always lower than α_{true} . By knowledge of the association enantioseparation factor α_{true} , the Gibbs energy difference, $\Delta_{L,D}(\Delta G)$, between the diastereomeric associates is obtained via

$$\Delta_{L,D}(\Delta G) = -RT \ln(\alpha_{\text{true}})$$

where R is the gas constant and T is absolute temperature. Using the Van't Hoff relation

$$\ln(\alpha_{\text{true}}) = -\frac{\Delta_{L,D}(\Delta H)}{R} \cdot \frac{1}{T} + \frac{\Delta_{L,D}(\Delta S)}{R}$$

the true enantioseparation factor α_{true} is related to the enthalpy $\Delta_{L,D}(\Delta H)$ and entropy $\Delta_{L,D}(\Delta S)$ differences between the diastereomeric selector-selectand associates. Since the formation of a stronger selector-selectand associate implies a gain in enthalpy and a loss in entropy (higher order of the stronger associate), the two contributions to the Gibbs energy difference of the association act in opposite directions and there is a particular temperature at which these contributions cancel each other. Such temperature is called *isoenantioselective*: $T_{\text{iso}} = \Delta_{L,D}(\Delta H) / \Delta_{L,D}(\Delta S)$. Enantioseparation at this temperature is not possible, i.e.

$K_D^{\text{assoc}} = K_L^{\text{assoc}}$, $\Delta_{L,D}(\Delta G) = -RT\ln(\alpha_{\text{true}}) = 0$, and peak coalescence ensues. However, above and below this temperature enantioseparation with the opposite elution order of the enantiomers (inversion) takes place. The existence of the isoenantioselective temperature in enantioselective liquid chromatography was predicted in 1978 by Davankov et al. [95] and in enantioselective gas chromatography in 1984 by Koppenhoefer and Bayer [96]. First examples were independently observed by Musso et al. in liquid chromatography [179], by Gil-Av et al. in hydrogen-bonding GC systems [98] and by Schurig et al. in complexation GC [97] (a report claimed of peak inversion for methyl lactate on a modified cyclodextrin selector (Lipodex E) [180] could not be reproduced in our hands). All the by far known examples of the experimentally observed inversion of the elution order of enantiomers at the isoenantioselective temperature T_{iso} in gas chromatography are summarized in **Table 3.1**.

Table 3.1 Examples of the experimentally observed isoenantioselective temperature, T_{iso} , in gas chromatography.

Racemate:	Chiral stationary phase:	T_{iso} (°C)	Reference:
Tripeptides derived from alanine (<i>LLL</i> and <i>DDD</i>)	Chirasil- <i>L</i> -Val		Koppenhoefer, Bayer et al. [181]
<i>N</i> -Trifluoroacetyl(TFA)- α -amino acids <i>tert</i> -butyl amides of alanine, 2-aminobutyric acid, leucine, valine	<i>N</i> -Docosanoyl- <i>L</i> -leucin-(1,1,3,3-tetramethylbutyl)amide	130-150	Gil-Av et al. [98]
(<i>E</i>)-2-Ethyl-1,6-dioxaspiro[4.4]nonane	Nickel(II)-bis[3-heptafluorbutanoyl]-(1 <i>S</i>)-10-methylencamphorate]	80	Schurig et al. [97]
Isopropylloxirane	Nickel(II)-bis[3-heptafluorbutanoyl]-(1 <i>R</i>)-camphorate]	65	Schurig et al. [32]
<i>sec</i> -Butylloxirane (unlike diastereomer)	Nickel(II)-bis[3-heptafluorbutanoyl]-(1 <i>R</i>)-camphorate]	95	Schurig et al. [32]
2-(2,4-Dichlorophenoxy)propionic acid	Octakis(3- <i>O</i> -butyryl-2,6-di- <i>O</i> -pentyl)- γ -cyclodextrin (Lipodex E)	115	König et al. [80]
2-(4-Chloro-2-methylphenoxy)propionic acid	Octakis(3- <i>O</i> -butyryl-2,6-di- <i>O</i> -pentyl)- γ -cyclodextrin (Lipodex E)	135	König et al. [80]
Methyl lactate (re-investigation necessary)	Octakis(3- <i>O</i> -butyryl-2,6-di- <i>O</i> -pentyl)- γ -cyclodextrin (Lipodex E)	62	König et al. [180]
<i>N</i> -TFA- <i>O</i> - <i>n</i> -butyl valine	Heptakis(2,3,6-trimethyl)- β -cyclodextrin	85	Krupcic et al. [182]
γ -Pentalactone	Octakis(2,6-di- <i>O</i> - <i>tert</i> -butyldimethylsilyl-3- <i>O</i> -methyl)- γ -cyclodextrin	67	Mosandl et al. [183]
Isomenthone	Octakis(2,6-di- <i>O</i> - <i>tert</i> -butyldimethylsilyl)- γ -cyclodextrin	63	Mosandl et al. [184]
1-Phenyl-2,2,2-trifluoroethanol	Octakis (6- <i>O</i> - <i>tert</i> -butyldimethylsilyl-2,3-di- <i>O</i> -methyl)- γ -cyclodextrin	80-90	Schomburg et al. [185]

Despite the smaller range of the applicable temperatures, the isoenantioselective temperature was also observed in liquid chromatography (e.g. see [186,187] and references therein).

Thus, despite the 40 year history of enantioselective gas chromatography and thousands of enantioseparated racemates, until now only a few examples of the temperature-induced inversion of elution order of enantiomers were experimentally observed and even less of them were investigated. On the one hand, this interesting phenomenon may cause many obstacles during the optimization of the enantioseparation notably for multienantiomeric analysis in one run. It is usually observed that a decrease of the temperature in the enthalpy-controlled regime results in the improvement of the enantioselectivity of the system. This is not the case, however, when the observed enantioseparation is governed by the entropy difference, i.e. if the isoenantioselective temperature T_{iso} is already below the experimental temperature. In this event, decrease of temperature will lead to a decline of the enantioselectivity invoked by the CSP. On the other hand, the possibility to invert the elution order of the enantiomers may be very useful, e.g., for trace analysis of enantiomeric impurities. In practice, the configuration of the CSP should be chosen such that the minor component is eluted as the first peak. Carbohydrate CSPs exist only in the *all-D*-configuration and, therefore, a change in the elution order may only be affected by a temperature change in case of a low value of T_{iso} . In the following section, the first comprehensive thermodynamic investigation of the observed inversion of the elution order of enantiomers at the isoenantioselective temperature T_{iso} is presented. The inversion is observed on the diamide-type CSP, Chirasil-*L*-Val- C_{11} [24,25,29,136], with *N*-ethoxycarbonyl propylamide derivatives [188,189] of a number of α -amino acids and on the cyclodextrin-type CSP, Chirasil-Dex [151,31], (for the synthesis of the CSPs see Section 1.1) with *N*-trifluoroacetyl ethyl esters of several α -amino acids.

3.2 Temperature-induced inversion of the elution order of enantiomers

3.2.1 Enantioseparation of *N*-ethoxycarbonyl propyl amides of α -amino acids

on Chirasil-Val-C₁₁ CSP

Chirasil-Val-type CSPs are based on the valine-diamide chiral selector and are important for the enantioseparation of α -amino acids, diols, amino alcohols etc. [29,27,28]. Since the invention of the valine-diamide selector [25,24], α -amino acids have been usually analyzed in the form of *N*-trifluoroacetyl (*N*-TFA) alkyl esters. Recently, Abe et al. showed that *N*-alkyloxycarbonyl alkyl esters (ACAE) [190,191] of α -amino acids could be used for gas-chromatographic investigations. The procedure of the derivatization was significantly simpler in comparison with that for *N*-TFA alkyl esters [137]. The enantioseparation of the ACAE derivatives of amino acids on Chirasil-*L*-Val, however, turned out to be inferior to that of *N*-TFA alkyl esters [190,191]. Later on, Abe et al. proposed a modified procedure for the derivatization of amino acids that led to diamide derivatives, i.e. *N*-alkyloxycarbonyl alkylamide derivatives [188,189]. These derivatives were found to have high enantioseparation factors α_{app} on Chirasil-*L*-Val despite high analysis temperatures. The procedure itself was also simple and did not require heating of the samples as in the case of the preparation of *N*-TFA alkyl esters. Another advantage was the greatly improved enantioseparation of proline ($\alpha = 1.36$, $T = 110^\circ\text{C}$ as *N*-ethoxycarbonyl *n*-propylamide) which was only slightly enantioseparated as *N*-TFA-alkyl ester on Chirasil-*L*-Val ($\alpha = 1.03$, $T = 110^\circ\text{C}$ as *N*-TFA ethyl ester). Above 150°C all the α -amino acid enantiomers in the form of *N*-alkyloxycarbonyl alkylamides were eluted D after L (except for proline enantiomers eluted L after D) on Chirasil-*L*-Val, [188,189] in contrast to the *N*-TFA esters ($L > D$).

All the reported enantioseparations of α -amino acids derivatized as *N*-alkyloxycarbonyl alkylamides were performed at relatively high temperature, i.e. above 150°C . The high enantioseparation factors α_{app} at high temperatures may suggest one to use lower temperature and a shorter column to gain the same α_{app} at shorter times (in line with a miniaturization concept for space applications to detect homochirality in extraterrestrial environment by GC [192]). This idea was attempted in our group with *N*-ethoxycarbonyl *n*-propylamides (ECPA) of several α -amino acids. However, it was found that the decrease of the analysis temperature to approximately 120°C resulted in a decline or complete loss of the enantioselectivity of Chirasil-*L*-Val-C₁₁ for all the analyzed racemates except proline. However, a further decrease of the temperature surprisingly led to the improvement of the enantioseparation along with the inversion of the elution order, i.e. the elution order below 120°C was L after D (**Figure 3.1**).

This is the very first clear visual representation of the increase of the enantioseparation factor α_{app} as the temperature is raised. Note that the increase of α_{app} is accompanied by a concomitant reduction of the retention time. Van't Hoff plots of $\ln(\alpha_{\text{app}})$ versus $1/T$ for eight α -amino acids in the form of ECPA derivatives were constructed (**Figure 3.2**) (plots of Nva-ECPA and Nle-ECPA overlapping with that of Abu-ECPA and Ala-ECPA are not included). The plots show a linear behavior up to approximately 130°C followed by a nonlinear part at higher temperatures. The isoenantioselective temperatures, T_{iso} , were found to lie between 110 and 130°C. That means that the reported enantioseparation of *N*-alkyloxycarbonyl alkylamide derivatives of α -amino acids at the temperatures above 150°C was governed by the entropic term of the Gibbs-Helmholtz equation. Note that the similar behavior of $\ln(\alpha_{\text{app}})$ versus $1/T$ was observed by Gil-Av et al. for *N*-trifluoroacetyl *tert*-butyl amides of α -amino acids on *N*-docosanoyl-*L*-leucin-(1,1,3,3-tetramethylbutyl)amide CSP as one of the first examples of the inversion of the elution order for enantiomers in GC [98].

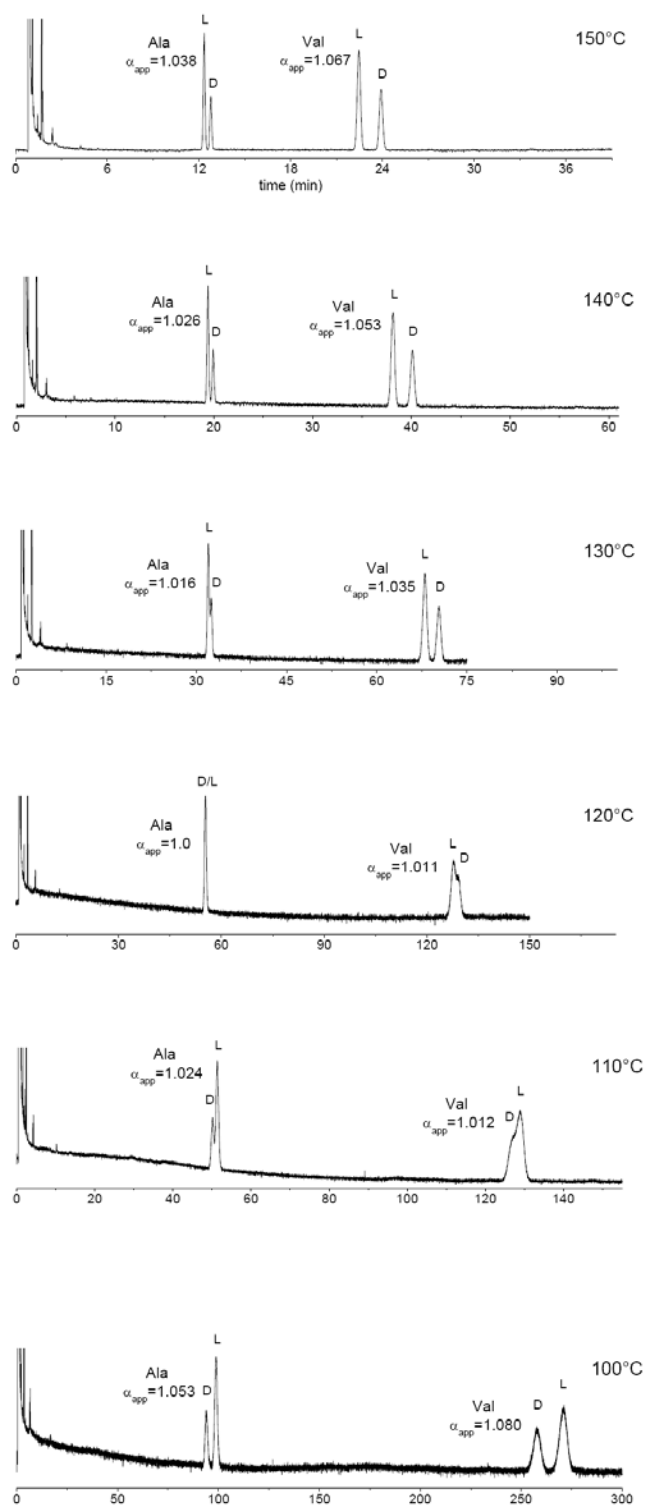


Figure 3.1 Gas chromatograms of the enantioseparation of Ala-ECPA and Val-ECPA on Chirasil-L-Val-C₁₁ in the temperature range from 100 to 150°C with 10°C step-intervals; α -amino acids are enriched in the L-enantiomer. Isoenantioseleective temperatures, T_{iso} , for Ala-ECPA and Val-ECPA are 120 and 114°C, respectively. Column: fused silica, 20 m x 0.25 mm (i.d.) x 0.25 μ m (polymer

thickness); carrier gas: dihydrogen; pressure: 50 kPa (120-170°C) and 100 kPa (100-110°C); detector: FID.

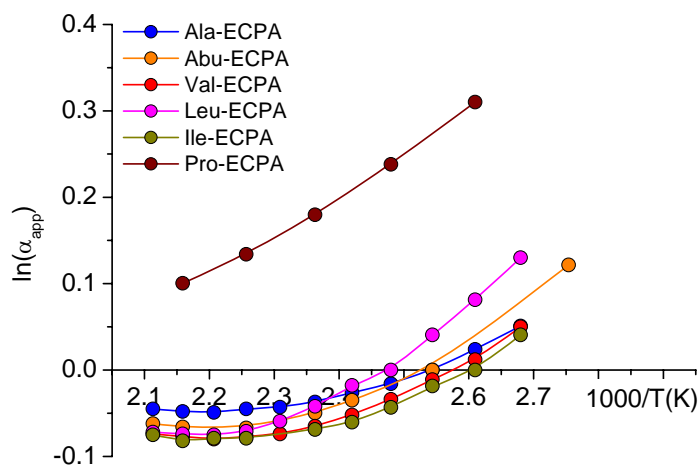


Figure 3.2 Plots of $\ln(\alpha_{app})$ versus $1/T(K)$ for the α -amino acids (as *N*-ethoxycarbonyl *n*-propylamides – ECPA) enantioseparated on Chiralasil-*L*-Val- C_{11} CSP.

In contrast, *N*-trifluoroacetyl ethyl esters (TFA-Et) of the same α -amino acids were found to be enantioseparated under enthalpy control in the temperature range from 70 to 180°C, i.e. the approximated isoenantioselective temperatures T_{iso} were above the analysis temperature. The corresponding plots of $\ln(\alpha_{app})$ versus $1/T$ are shown in **Figure 3.3**.

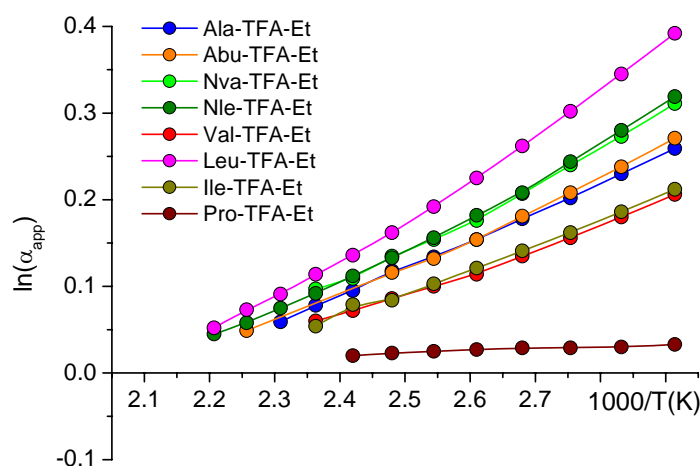


Figure 3.3 Plots of $\ln(\alpha_{app})$ versus $1/T(K)$ for *N*-trifluoroacetyl ethyl esters (TFA-Et) of α -amino acids enantioseparated on Chiralasil-*L*-Val- C_{11} CSP.

Table 3.2 Isoenantioselective temperature, T_{iso} , of the derivatives of α -amino acids enantioseparated on Chirasil-*L*-Val-C₁₁.

Amino acids:	T_{iso}^a (°C) of ECPA derivatives	T_{iso}^b (°C) of <i>N</i> -TFA-Et derivatives
Ala	120	200
Abu ^c	122	220
Nva	121	250
Nle	122	220
Val	114	250
Leu	132	215
Ile	112	200
Pro	240 ^b	230

^adetermined experimentally

^bextrapolated from the plot of $\ln(\alpha_{app})$ vs. $1/T$

^cAbu = 2-aminobutanoic acid

The observed and extrapolated isoenantioselective temperatures, T_{iso} , for ECPA and TFA-Et derivatives of the selected α -amino acids are shown in **Table 3.2**. The values of T_{iso} for TFA-Et derivatives and for proline-ECPA were extrapolated from the $\ln(\alpha_{app})$ vs. $1/T$ plots using a polynomial fit. As one can see from **Table 3.2**, the replacement of the *N*-trifluoroacetyl and ethyl ester groups with *N*-ethoxycarbonyl and propylamide, respectively, reduces the isoenantioselective temperature, T_{iso} , by 80-130°C. Note that similar drop of T_{iso} was observed for *N*-trifluoroacetyl *tert*-butylamide derivatives of α -amino acids on a CSP related to Chirasil-*L*-Val-C₁₁ [98]. This suggests that the presence of the additional NH-amide moiety in the ECPA and *N*-TFA-*tert*-butylamide derivatives of the amino acids is responsible for the decrease of T_{iso} . The importance of NH-amide groups capable of hydrogen bonding for the enantioseparation of the α -amino acid derivatives on Chirasil-Val-type CSPs is also confirmed by the fact that Pro-ECPA having only one NH-amide group behaves very similar to the TFA-Et derivatives of other α -amino acids also bearing only one NH-amide group (**Figure 3.2** and **3.3**). Moreover, Pro-TFA-Et lacking any NH-amide group has dramatically lower enantioseparation factor, α_{app} , on Chirasil-*L*-Val-C₁₁ compared to other α -amino acids and behaves completely different (**Figure 3.3**). It is worth noting that the $\Delta_{L,D}(\Delta H)$ value for Pro-TFA-Et is virtually zero and the enantioseparation is based solely on the different entropy

of the diastereomeric selector-selectand associates (**Figure 3.3**)! This is a very rare instance for a temperature-independent enantiomeric separation. In addition, the sequence of the elution of the ECPA derivatives on the Chirasil-*L*-Val-C₁₁ CSP at 110°C is proline < alanine < valine < leucine, while that on the reference column containing only dimethylpolysiloxane is alanine < valine < proline < leucine. Realizing that among these amino acids only proline has a secondary amino group, the influence of the hydrogen bonding selector-selectand interactions on the retention of the analytes on Chirasil-Val-type CSPs becomes evident.

It can be concluded that for the efficient enantioseparation of α -amino acid derivatives on an α -amino acid-based CSP it is important that in the selector-selectand associates two NH-amide groups interact with at least one NH-amide group. Consequently, it can be predicted that amino acid-monoamide selectors (e.g. *N*-trifluoroacetyl alkyl esters) which show poor enantioselectivity toward mono-amide α -amino acid derivatives (i.e. *N*-trifluoroacetyl alkyl esters) [23] would be highly enantioselective toward α -amino acid derivatives containing two NH-amide groups (reciprocal approach). This has been proven by preparing Pro-diamide selector, containing only one NH-amide group, but displaying high enantioselectivity toward ECPA α -amino acids (except Pro-ECPA containing also one NH-amide group). [unpublished results]

In the following part, a thermodynamic study of the enantioseparation of ECPA versus TFA-Et derivatives of selected α -amino acids on Chirasil-*L*-Val-C₁₁ CSP will be performed with the aim to elucidate the thermodynamic incentives for the observed decrease of the isoenantioselective temperature, T_{iso} , in the case of the ECPA derivatives. In addition, the thermodynamic investigation will be used to shed some light on the observed nonlinearity of the plot $\ln(\alpha_{app})$ vs. $1/T$ observed for ECPA derivatives.

As already mentioned, the analysis of thermodynamically controlled enantiorecognition mechanisms of chiral selector/selectand systems must rely on the true enantioseparation factor, α_{true} . Ignoring this, i.e. resorting to the apparent enantioseparation factor, α_{app} , will lead to underestimated enantioselectivity in the presence of achiral contributions to retention as outlined in Chapter 2. The true enantioseparation factor, α_{true} , can be experimentally obtained using the method of the retention increment, R' (see Chapter 2) [156,33]:

$$\alpha_{true} = \frac{R'_L}{R'_D}$$

$$R' = \frac{r - r^o}{r^o}$$

where R'_D and R'_L are the retention increments of the two enantiomers (D and L subscripts are arbitrary designation of oppositely configured enantiomers, regardless of the observed elution order in the experiments); r and r° are the relative retentions of a single enantiomer on the *enantioselective column* and on a *reference column* containing the polysiloxane used as an achiral matrix for the chiral selector, respectively. Relative retentions, r , are used because they are independent from all chromatographic parameters at a given temperature. They are obtained as the ratio of the retention factors of the enantiomers and that of a standard inert compound devoid of interactions with the chiral selector:

$$r = \frac{k}{k_{st}}$$

where k and k_{st} are the retention factors of the single enantiomer and the standard compound, respectively, whereby *n*-alkanes are usually appropriate for this purpose (see below, however).

The thermodynamic investigation of ECPA vs. TFA-Et derivatives of α -amino acids was performed on alanine and valine. *n*-Octadecane (C18) and *n*-hexadecane (C16) were used as the standard compounds for ECPA derivatives and *n*-dodecane (C12) and *n*-decane (C10) for TFA-Et derivatives. A fused-silica GC column coated with pure dimethylpolysiloxane was used as the reference column. Some experimental and calculated data obtained for alanine and valine ECPA and TFA-Et derivatives on Chirasil-*L*-Val-C₁₁ are summarized in **Table 3.3** (see also supplementary material).

Table 3.3 Experimental details of the enantioseparation of alanine and valine in the form of ECPA and TFA-Et derivatives on Chirasil-L-Val-C₁₁ CSP

Ala-TFA-Et						Ala-ECPA				
T(°C)	R _D ^a	R _L ^a	α _{app}	α _{true} ^a	Δ _{L,D} (ΔG) (kJ·mol ⁻¹) ^a	R _D ^a	R _L ^a	α _{app}	α _{true} ^a	Δ _{L,D} (ΔG) (kJ·mol ⁻¹) ^a
100	1.52	2.01	1.195	1.324	-0.87	10.81	11.43	1.053	1.058	-0.17
110	1.45	1.86	1.167	1.281	-0.79	9.98	10.25	1.024	1.027	-0.08
120	1.35	1.69	1.143	1.249	-0.73	8.81	8.81	1.000	1.000	0.00
130	1.31	1.60	1.125	1.220	-0.67	8.06	7.92	0.984	0.983	0.06
Val-TFA-Et						Val-ECPA				
100	0.98	1.27	1.145	1.292	-0.80	16.29	17.18	1.051	1.055	-0.17
110	0.94	1.17	1.121	1.250	-0.71	14.18	14.35	1.012	1.012	-0.04
120	0.90	1.10	1.105	1.222	-0.66	12.30	12.16	0.989	0.989	0.04
130	0.83	1.00	1.089	1.196	-0.60	10.67	10.28	0.967	0.963	0.13

^a*n*-dodecane and *n*-octadecane were used as standards for TFA-Et and ECPA derivatives, respectively

Van't Hoff plots of $\ln(\alpha_{\text{true}})$ vs. $1/T$ obtained using two different standard compounds (*n*-hexadecane and *n*-octadecane) and that of $\ln(\alpha_{\text{app}})$ vs. $1/T$ are shown in **Figure 3.4**. As predicted, the apparent enantioseparation factor α_{app} does underestimate the enantiodiscrimination of the enantiomers by the chiral selector, i.e. α_{app} is necessarily always lower α_{true} . Note that plots of $\ln(\alpha_{\text{true}})$ vs. $1/T$ obtained by using different hydrocarbon standards are well superimposed confirming the absence of strong interactions between the chiral selector and the hydrocarbons used as the standards. Because of the observed nonlinearity of the plots, the regression analysis was performed in the temperature range from 100 to 130°C where the plots are virtually linear (**Figure 3.5**). The nonlinearity of the plots will be discussed in Section 3.3. The thermodynamic parameters obtained by the regression analysis are summarized in **Table 3.4**.

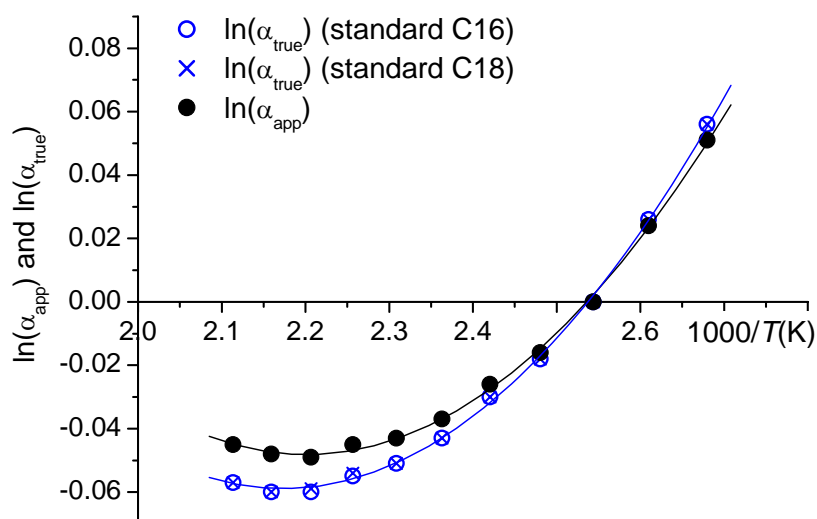


Figure 3.4 Plots of $\ln(\alpha_{\text{true}})$ and $\ln(\alpha_{\text{app}})$ as functions of the reciprocal temperature for Ala-ECPA enantioseparated on Chirasil-*L*-Val- C_{11} CSP. *n*-Hexadecane (C16) and *n*-octadecane (C18) were used as reference standards.

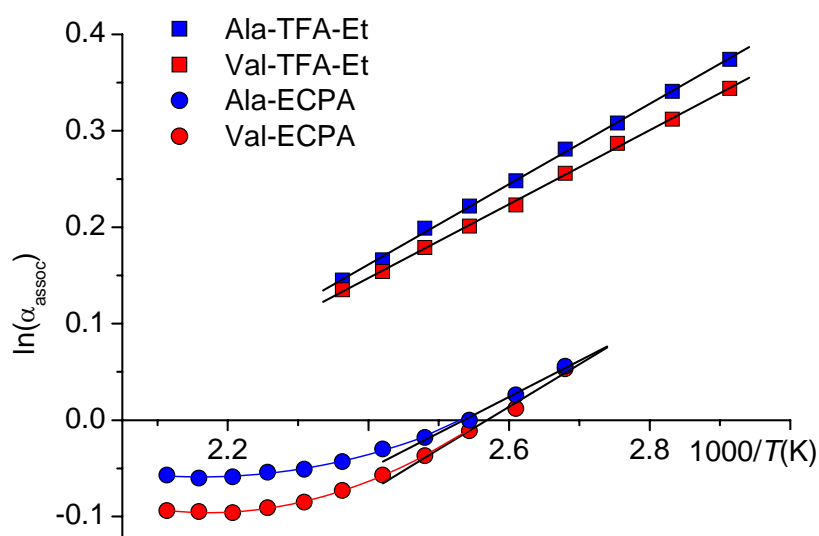


Figure 3.5 Plots of $\ln(\alpha_{\text{true}})$ as a function of the reciprocal temperature for Ala-ECPA and Val-ECPA enantioseparated on Chirasil-*L*-Val- C_{11} CSP. Straight lines represent the linear fits obtained in the temperature range 100–130°C (correlation coefficients $R = 0.995$ and 0.999 for ECPA and TFA-Et derivatives, respectively). *n*-Octadecane and *n*-dodecane were used as the reference standards for ECPA and TFA-Et derivatives, respectively.

Table 3.4 $\Delta_{L,D}(\Delta H)$ and $\Delta_{L,D}(\Delta S)$ for racemates of Ala-ECPA and Val-ECPA as well as for Ala-TFA-Et and Val-TFA-Et obtained by the regression analysis of the $\ln(\alpha_{\text{true}})$ vs. $1/T$ plots (see Figure 3.5) in the temperature range 100-130°C

Amino acid derivatives:	$\Delta_{L,D}(\Delta H)$ (kJ·mol ⁻¹)	$\Delta_{L,D}(\Delta S)$ (J·mol ⁻¹ ·K ⁻¹)	$T \cdot \Delta_{L,D}(\Delta S)$ (kJ·mol ⁻¹); $T = 393\text{K}$
Ala-ECPA	-3.1 ± 0.2	-7.9 ± 0.5	-3.1 ± 0.2
Val-ECPA	-3.7 ± 0.3	-9.4 ± 0.7	-3.7 ± 0.3
Ala-TFA-Et	-3.5 ± 0.1	-7.0 ± 0.1	-2.8 ± 0.1
Val-TFA-Et	-3.2 ± 0.1	-6.5 ± 0.1	-2.6 ± 0.1

As can be seen from **Table 3.4**, the $\Delta_{L,D}(\Delta H)$ values for both ECPA and TFA-Et derivatives of Ala and Val are similar. The $\Delta_{L,D}(\Delta S)$ values for ECPA derivatives are lower than the corresponding values for the TFA-Et derivatives for both alanine and valine. This entropy difference “moves” the plot of $\ln(\alpha_{\text{true}})$ vs. $1/T$ for ECPA derivatives down resulting in the drop of the isoenantioselective temperature, T_{iso} , and, as a consequence, the enthalpic and entropic terms of the Gibbs-Helmholtz equation for ECPA derivatives become the same at 120°C (**Table 3.4** fourth column). To conclude, the difference in the strength ($\Delta_{L,D}(\Delta H)$) of the interactions between the selectand enantiomers and the chiral selector is only slightly changed upon the switch from TFA-Et to ECPA derivatives. On the other hand the entropy difference between the diastereomeric associates of the ECPA derivatives is increased leading to the more negative $\Delta_{L,D}(\Delta S)$ value which is enough to reduce the isoenantioselective temperature, T_{iso} , by 80-130°. Note, that despite the fact that for both ECPA and TFA-Et derivatives the $\Delta_{L,D}(\Delta H)$ values are very similar, the retention increment, R' , values for ECPA derivatives are about ten times higher than that for the TFA-Et derivatives (**Table 3.3**). This behavior represents an example that the increase in the strength of the selector-selectand interactions does not necessarily result in an improved enantioselectivity of the system [193], i.e. the chiral recognition factor $\chi = \Delta_{L,D}\Delta G/\Delta G$ varies at random as found previously in complexation gas chromatography [194].

3.2.2 Enantioseparation of *N*-trifluoroacetyl ethyl esters of α -amino acids on Chirasil-Dex CSP

Further examples of the existence of an isoenantioselective temperature, T_{iso} , were found for TFA-Et derivatives of several α -amino acids enantioseparated on a CSP based on permethylated- β -cyclodextrin, i.e. on Chirasil-Dex CSP. [151,31] Unfortunately, the retention increment method fails for cyclodextrin CSPs, as no inert reference standard, not interacting with the selector, is available. Therefore, only the apparent enantioselectivity can be considered. The plots of $\ln(\alpha_{\text{app}})$ vs. $1/T$ in the range of 25 – 150 °C for twelve α -amino acids are depicted in **Figure 3.6**. As one can see, the behavior of $\ln(\alpha_{\text{app}})$ is strongly nonlinear for all analytes. As the ratio of k_L/k_D has been used throughout, also curves in the negative $\ln(\alpha_{\text{app}})$ region are observed due to an inverted elution order ($L < D$). **Table 3.5** lists the observed and extrapolated values of T_{iso} for the studied α -amino acids. Lysine and glutamic acid were not enantioseparated at the temperatures studied. Ornithine was only slightly enantioseparated between 120 - 130°C.

As one can see from **Figure 3.6**, because of the nonlinearity of the plot $\ln(\alpha_{\text{app}})$ vs. $1/T$, for Val-, Leu- and Ile-TFA-Et there are two intercept points where $\ln(\alpha_{\text{app}}) = 0$. Therefore, it can be predicted that the elution order of the enantiomers of these compounds can be inverted more than one time at two different isoenantioselective temperatures, T_{iso} !

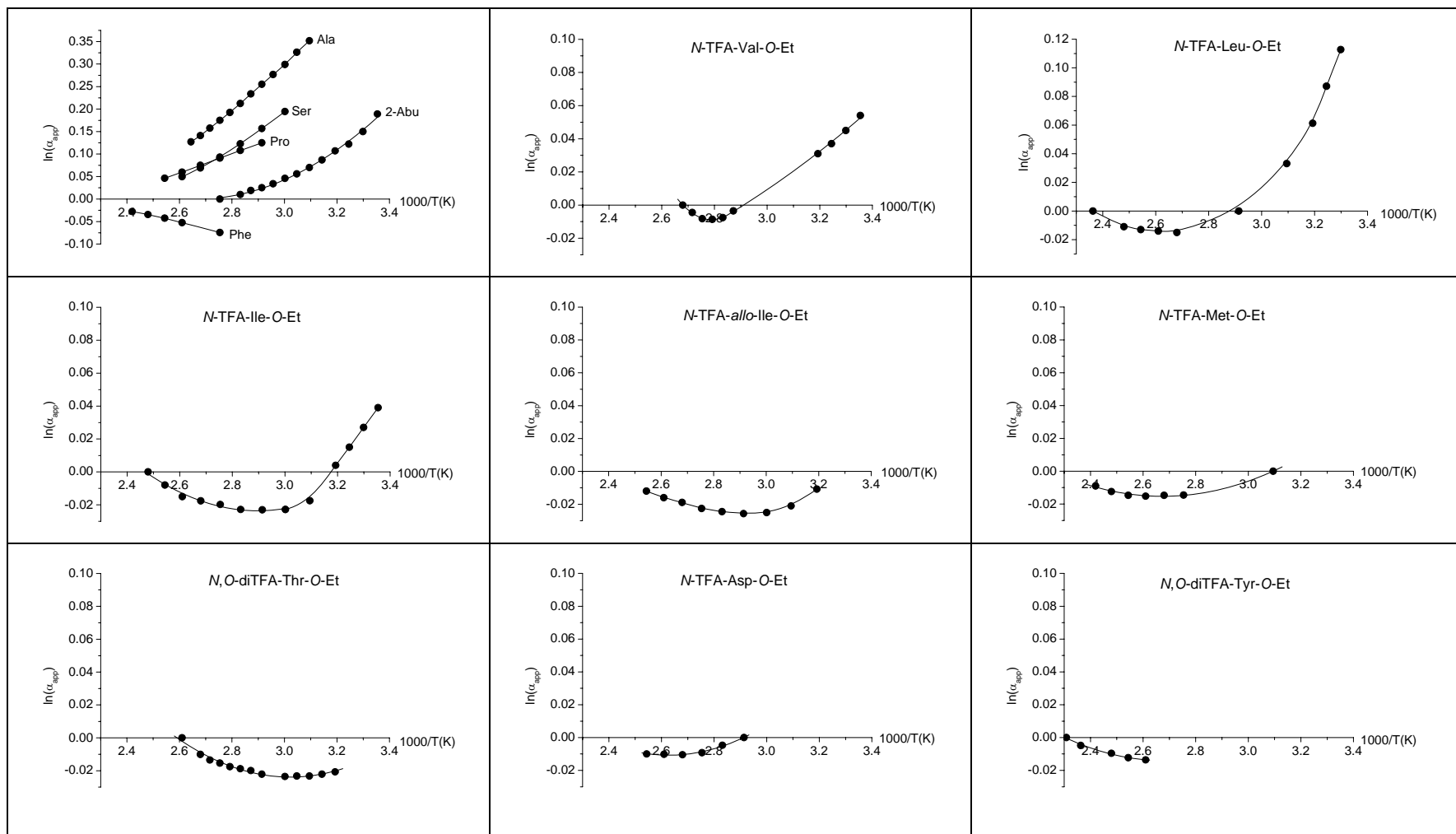


Figure 3.6 Plots of $\ln(\alpha_{app})$ vs. $1/T$ for TFA-Et derivatives of α -amino acids enantioseparated on ChiralSil-Dex CSP. The enantioseparation factor α_{app} was determined as the ratio k_L/k_D independently of the elution order.

Table 3.5 Isoenantioselective temperatures, T_{iso} , of α -amino acid TFA-Et derivatives enantioseparated on Chirasil-Dex CSP experimentally observed or extrapolated from the $\ln(\alpha_{\text{app}})$ vs. $1/T$ plots (see Figure 3.6)

Amino acids :	T_{iso} (°C)
Ala-TFA-Et	160 ^a
Phe-TFA-Et	170 ^a
Pro-TFA-Et	160 ^a
Ser-TFA-Et	140 ^a
Abu-TFA-Et	90 ^b
Val-TFA-Et	70 ^c
Leu-TFA-Et	70 ^c
Asp-TFA-Et	70 ^b
Tyr-TFA-Et	50 ^a
Met-TFA-Et	50 ^b
Ile-TFA-Et	40 ^c
<i>allo</i> -Ile-TFA-Et	30 ^a
Thr-TFA-Et	20 ^a

^aobtained by extrapolation

^bcoalescence temperature (inversion of the elution order of the enantiomers was not observed)

^cexperimentally observed T_{iso}

As mentioned before, a reliable quantitative analysis of the thermodynamic parameters and the use of the retention increment method was not feasible because of the strong discrepancy of the R' and α_{true} values determined using different hydrocarbon standards (*n*-decane (C10) and *n*-dodecane (C12)) (**Figure 3.7b**). Such behavior may be rationalized by two causes. First, it may indicate the presence of the selective interaction between the standard compounds and the cyclodextrin selector [127]. Indeed, simple chiral hydrocarbons have been resolved on Chirasil-Dex previously [48], thereby proving the existence of molecular association. In the case of the Chirasil-*L*-Val-C₁₁ CSP, where such interactions are

improbable, the R' values determined using different hydrocarbon standards were virtually identical as expected (**Figure 3.7a**). Second, the very small values of the retention increment in the case of the TFA-Et derivatives of α -amino acids analyzed on Chirasil-Dex ($R' = 0.1 - 1.5$) could lead to large errors and, hence, to the observed discrepancy.

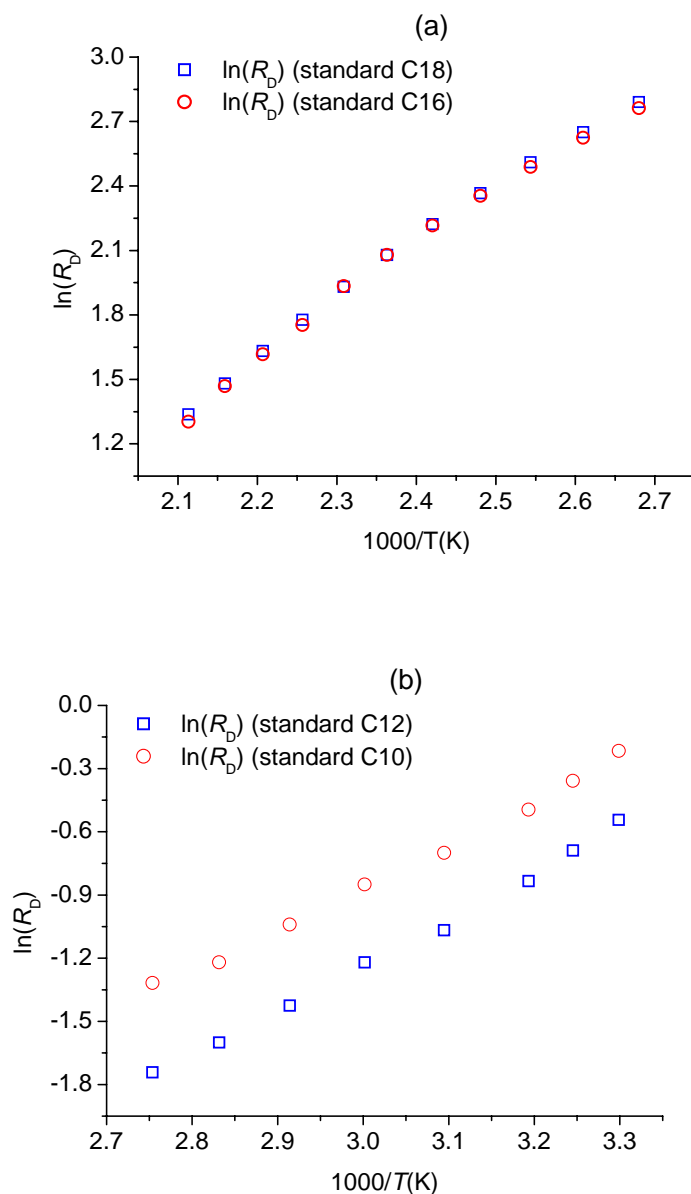


Figure 3.7 Plots of $\ln(R'_D)$ versus $1/T$ determined using two different reference standards: *n*-octadecane (C18) and *n*-hexadecane (C16) for Val-ECPA on Chirasil-*L*-Val-C₁₁ (a) and *n*-dodecane (C12) and *n*-decane (C10) for Leu-TFA-Et on Chirasil-Dex (b).

Nevertheless, qualitative analysis of the retention data is possible. For this purpose it is convenient to compare the behavior of the natural logarithms of the relative retentions of D and L enantiomers, $\ln(r_D)$ and $\ln(r_L)$, respectively, with that of a standard compound, e.g. *n*-dodecane, $\ln(r_{C12})$ (r_{C12} = relative to *n*-decane). In order to cover the temperature range from 30°C to 180°C a short column (10 m) for low temperatures and a long column (50 m) for high temperatures were employed. Therefore, use of the relative retention, which is independent of the phase ratio, pressure, flow rate, etc., is more appropriate in such investigation than the use of the retention factors. The comparison has been performed using Leu-TFA-Et. The relative retentions were obtained as the ratio of the retention factors of the corresponding analyte and that of *n*-decane, i.e. $r_D = \frac{k_D}{k_{C10}}$, $r_L = \frac{k_L}{k_{C10}}$ and $r_{C12} = \frac{k_{C12}}{k_{C10}}$. As one can see from **Figure 3.8**, the plots of $\ln(r)$ vs. $1/T$ for both enantiomers are nonlinear, while that of *n*-dodecane is virtually linear. This indicates that the observed nonlinearity of the plot $\ln(\alpha_{app})$ vs. $1/T$ is the result of the changes in the mechanism of the selector-selectand interactions for both enantiomers. This is to be contrasted with the ECPA derivatives studied on Chirasil-*L*-Val- C_{11} CSP where only the D-enantiomer showed nonlinearity (see Section 3.3). It is interesting to note that at high temperatures the behavior of Leu-TFA-Et enantiomers become similar to that of *n*-dodecane.

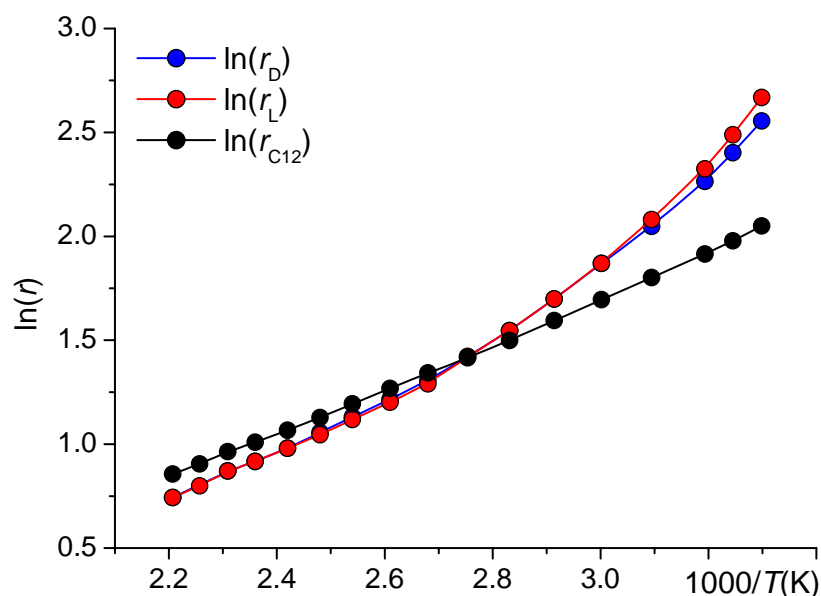


Figure 3.8 Plots of $\ln(r)$ vs. $1/T$ for the enantiomers of Leu-TFA-Et and *n*-dodecane (C12) analyzed on Chirasil-Dex CSP with *n*-decane used as the reference standard.

It should be mentioned that if the mechanism of the selector-selectand interaction is changed, i.e. if the plot $\ln(r)$ vs. $1/T$ is nonlinear, then the lowest enantioselectivity will lead to the strongest nonlinearity of the plot $\ln(\alpha_{\text{app}})$ vs. $1/T$. This may explain the often observed nonlinear behavior of the natural logarithm of the enantioseparation factor α_{app} at high temperatures where α is usually small.

3.3 Study of the non-linear behavior of $\ln(\alpha_{\text{true}})$ as a function of the reciprocal temperature

The following discussion illustrates an application of the retention increment R' concept to the investigation of the nonlinear behavior of the van't Hoff plot, $\ln(\alpha_{\text{true}})$ vs. $1/T$ found for ECPA derivatives of some α -amino acids enantioseparated on Chirasil-*L*-Val- C_{11} (**Figure 3.4 & 3.5**). The retention increment, R' , is determined as the product of the association constant and the activity of the selector in the stationary phase, i.e. $R' = K^{\text{assoc}} \cdot a$ [156,33,127], where K^{assoc} is the association constant between the chiral selector and one of the selectand enantiomers, and a is the activity (or concentration in highly diluted systems) of the chiral selector in the stationary phase. Since $\ln(K^{\text{assoc}})$ is related to ΔH and ΔS of the association process through the Gibbs-Helmholtz equation, the following expression can be written:

$$\ln(R') = -\frac{\Delta H}{R} \frac{1}{T} + \frac{\Delta S}{R} + \ln(a)$$

where ΔH and ΔS are the enthalpy and entropy changes, respectively, caused by the formation of the selector-selectand associate; R' is the retention increment; R is the gas constant; T is the absolute temperature. Since a is a constant for a given CSP, the plot of $\ln(R')$ as a function of $1/T$ should be linear, provided ΔH and ΔS are independent of temperature. Therefore, plotting $\ln(R')$ vs. $1/T$ for both enantiomers one can shed light on the cause of the nonlinearity of the plot $\ln(\alpha_{\text{true}})$ vs. $1/T$. In addition, ΔH and $[\Delta S/R + \ln(a)]$ can be obtained from the slope and the intercept of the Y-axis, respectively. It should be reminded that the use of the retention factor, k , instead of the retention increment R' is inappropriate, since the retention factor, k , is biased by the achiral contribution to retention of the polymer used as the matrix for the chiral selector.

The van't Hoff plots of $\ln(R')$ vs. $1/T$ for the D and L enantiomers of ECPA derivatives of alanine and valine are depicted in **Figures 3.9 and 3.10**. One can see that basically the D enantiomer is responsible for the observed nonlinearity of the plots $\ln(\alpha_{\text{true}})$ vs. $1/T$ in the case

of both alanine and valine ECPA derivatives, i.e. while $\ln(R'_L)$ depends linearly on the reciprocal temperature, the plot of $\ln(R'_D)$ vs. $1/T$ is changing slope above approx. 140°C.

It should be noted that when plotting $\ln(k)$ instead of $\ln(R')$ vs. $1/T$, the nonlinearity of the plot becomes less pronounced. This is the result of the achiral contribution to retention from the polymeric matrix which renders the chiral contribution to retention by the chiral selector as the sole cause of nonlinearity less important.

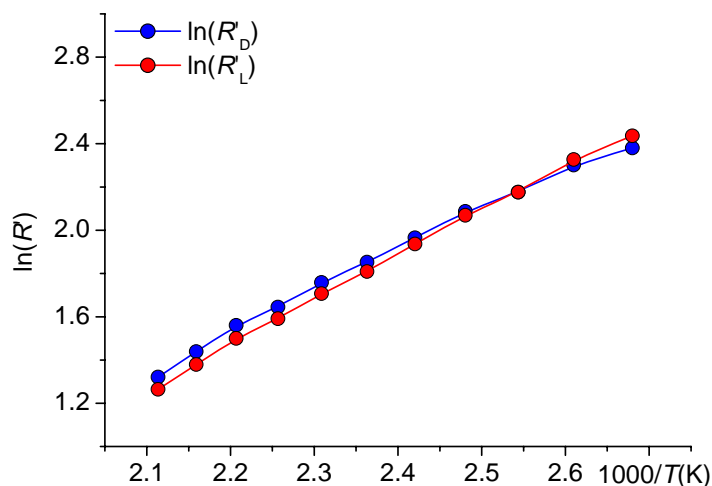


Figure 3.9 Plots of $\ln(R')$ versus $1/T(K)$ for D and L enantiomers of Ala-ECPA enantioseparated on Chirasil-*L*-Val- C_{11} CSP. *n*-Octadecane (C18) was used as the reference standard.

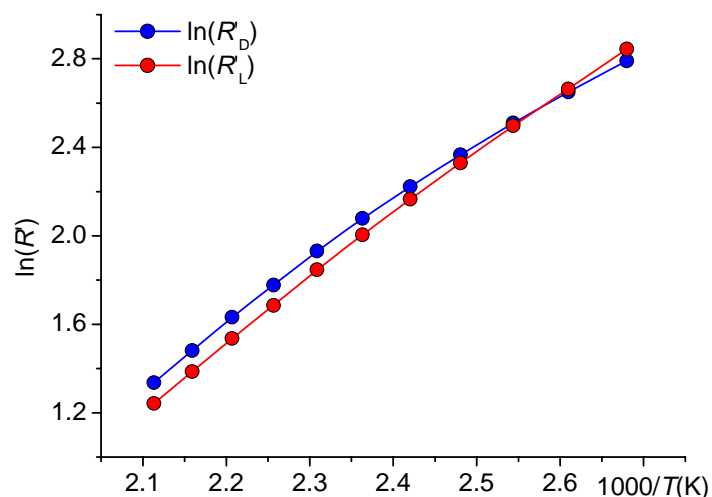
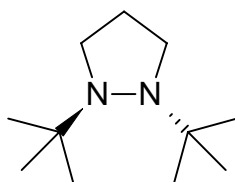


Figure 3.10 Plot of $\ln(R')$ versus $1/T(K)$ for D and L enantiomers of Val-ECPA enantioseparated on Chirasil-*L*-Val- C_{11} CSP. *n*-Octadecane (C18) was used as the reference standard.

Chapter 4

4. Enantiomerization of 1,2-di-*tert*-butylpyrazolidine and 1,2-di-*iso*-propyl-3,5-dimethylpyrazolidine by dynamic GC

The racemate of 1,2-di-*tert*-butylpyrazolidine (**23**) was enantioseparated by gas chromatography on Chirasil-Dex [151] with an enantioseparation factor $\alpha = 1.07$ (100°C). To determine the enantiomerization barrier of **23**, enantioselective dynamic gas chromatography (DGC) was applied [196-198,104].



23

The elution profile of the interconverting enantiomers exhibited a characteristic plateau between the first and the second eluted enantiomers. Based on the chromatographic data and the relative plateau height, computer simulation with ChromWin [106] and direct calculation by the approximation function [108] or the unified equation [199] can be used for the evaluation of the rate constant of the enantiomerization. The rate constants represent a weighted mean of the rate constants in the gas phase and the different rate constants in the CSP ($k_1 \neq k_{-1}$).

Selected experimental data of the enantioselective DGC experiments are presented in **Table 4.1**. Elution profiles between 95°C and 120°C with 5°C steps (18 experiments) used for the evaluation of the rate constants k^{approx} by the approximation function [108,101] are shown in **Figure 4.1**. For the evaluation of the activation parameters, the mean values of the $\ln(k^{\text{approx}}/T)$ were plotted versus $1/T$ according to the Eyring equation. By regression analysis (correlation coefficient $R = 0.999$) (**Figure 4.2**) ΔH^\ddagger was found to be $113.5 \pm 2.0 \text{ kJ}\cdot\text{mol}^{-1}$ and $\Delta S^\ddagger = -14.7 \pm 5.3 \text{ J}\cdot\text{mol}^{-1}\cdot\text{K}^{-1}$. The value of the entropy difference being close to zero indicates that the enantiomerization occurs without breaking bonds and charge separations, the transition state being only slightly more ordered. However, the high value of the activation enthalpy reflects the high volumes of the *tert*-butyl groups rendering the nitrogen inversion very energetic.

Table 4.1 Selected experimental data from the DGC experiment, rate constants of the enantiomerization of 23 in the presence of CSP Chirasil-Dex and enantiomerization barrier of 23 at different temperatures

T	α	t_M	t_1	t_2	w_1	w_2	h_{plateau}	k_1^{approx}	ΔG^\ddagger
[°C]		[min]	[min]	[min]	[s]	[s]	[%]	[10^{-5} s^{-1}]	[kJ mol $^{-1}$]
95	1.076	6.25	49.83	53.16	42.80	46.58	2.01	1.5 ± 0.2	122.8 ± 0.3
100	1.070	6.28	40.92	43.33	35.50	38.30	3.10	2.4 ± 0.3	123.0 ± 0.3
105	1.064	6.31	33.99	35.75	29.92	32.04	5.00	4.0 ± 0.5	123.1 ± 0.4
110	1.057	6.34	28.62	29.89	25.46	27.20	8.29	6.2 ± 0.7	123.3 ± 0.4
115	1.052	6.40	23.39	24.24	20.88	22.00	15.29	10.2 ± 1.2	123.3 ± 0.4
120	1.046	6.36	21.17	21.86	18.56	19.60	28.56	17.4 ± 2.0	123.2 ± 0.4

T is the temperature in °C; α is the apparent enantioseparation factor; t_M is the hold-up time; t_1 and t_2 are the retention times of the first and second eluted enantiomers, respectively; w_1 and w_2 are the width of the peaks at a half height for the first and second eluted enantiomers, respectively; h_{plateau} is the relative height of the plateau formed between the interconverting peaks; k_1^{approx} is the rate constant determined by the approximation function; ΔG^\ddagger is the Gibbs free energy of the enantiomerization

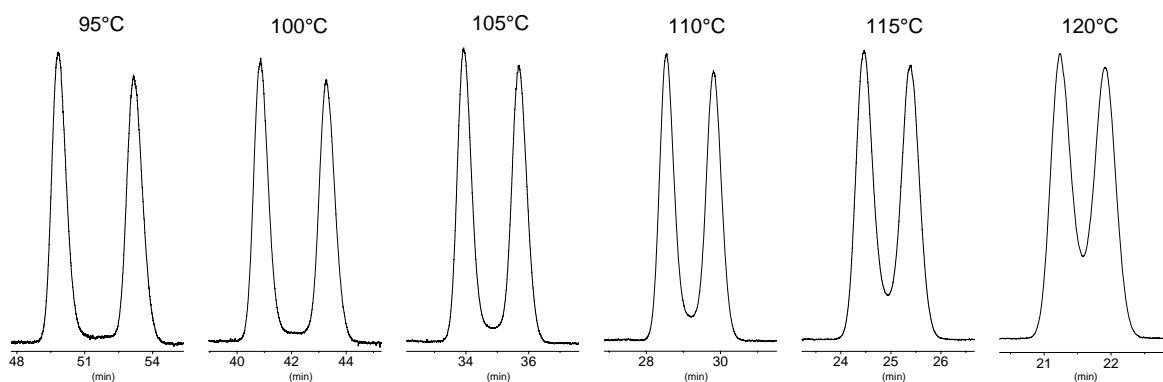


Figure 4.1 Chromatograms from the temperature-dependent DGC experiment for 1,2-di-*tert*-butylpyrazolidine. Chromatographic conditions: 25m Chirasil-Dex (44% (w/w) of the permethylated- β -cyclodextrin as a selector) [151] (0.25 mm i.d., film thickness 0.25 μm). Carrier gas: dihydrogen, $P = 10 \text{ kPa}$.

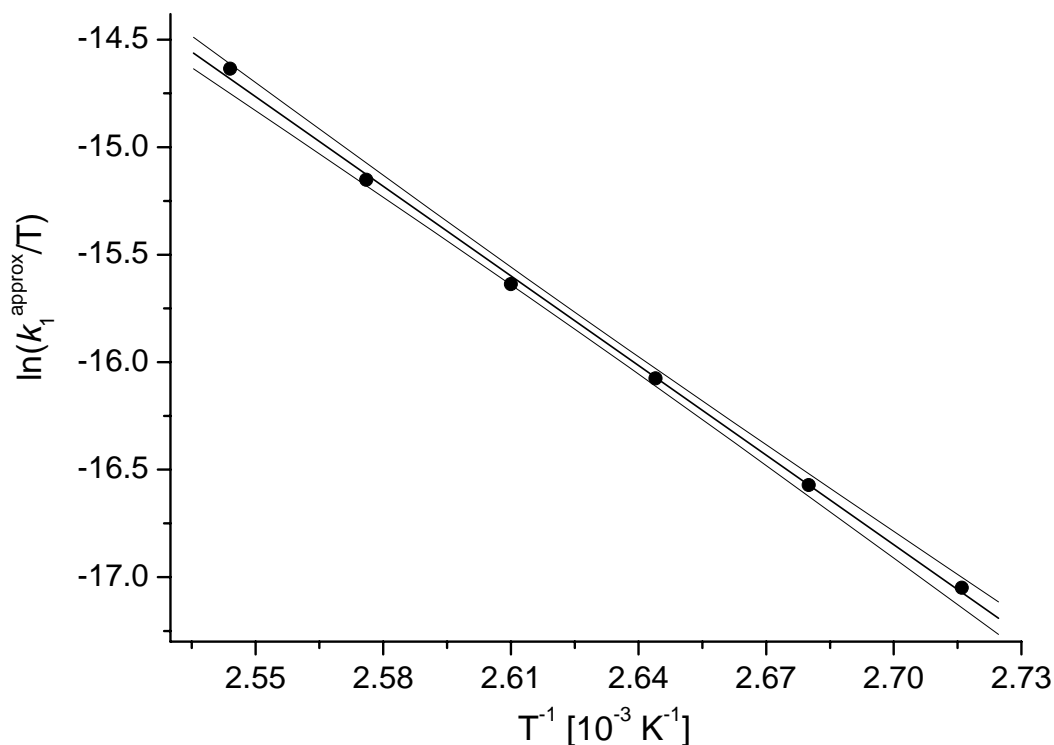
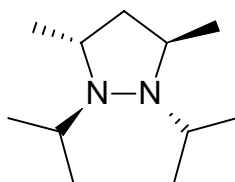


Figure 4.2 Eyring plot for the determination of the activation parameters ΔH^\ddagger and ΔS^\ddagger of 1,2-di-*tert*-butylpyrazolidine (**23**) from the DGC experiment. The upper and lower curves represent the error bands of the linear regression with a level of confidence of 95%. Activation parameters calculated: $\Delta H^\ddagger = 113.5 \pm 2.0$ [kJ·mol⁻¹] and $\Delta S^\ddagger = -14.7 \pm 5.3$ [J·mol⁻¹·K⁻¹].

The racemate of one diastereomer (all-*trans*) of 1,2-di-*iso*-propyl-3,5-dimethylpyrazolidine (**24**) was enantioseparated by gas chromatography on Chirasil-Dex with the enantioseparation factor $\alpha = 1.08$ (40°C) (**Figure 4.3**).



24

In order to examine the possible diastereomerization (nitrogen inversion) of **24**, a stopped-flow experiment was performed as follows. Flow of the carrier gas was switched off exactly at the time when both (already separated) enantiomers were located in the centre of

the gas-chromatographic capillary. The temperature of the oven was quickly increased up to 190°C and kept for 10 min followed by fast cooling to 40°C and proceeding with the separation at 50 kPa of the carrier gas pressure. As the result of the experiment, only two peaks of the enantiomers of **24** were observed, i.e. no diastereomers of **24** were formed at these conditions. Obviously, the reason for the greatly increased inversion barrier of **24** in comparison with that of **23**, despite the lower size of the isopropyl groups than that of *tert*-butyls, is the presence of the methyl substituents in the α -positions which cause additional steric hindrance.

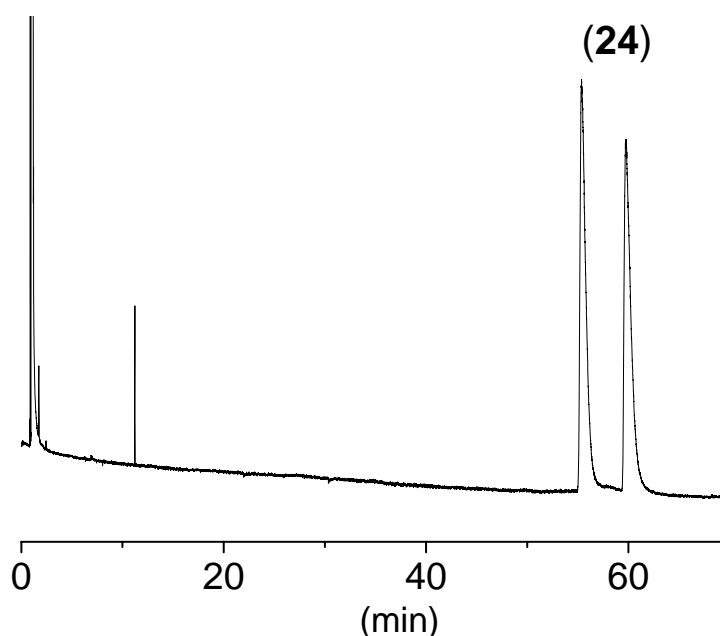


Figure 4.3 Enantioseparation of *N,N'*-di-*iso*-propyl- α,α' -dimethylpyrazolidine (**24**) on Chirasil-Dex. Chromatographic conditions: 25m Chirasil-Dex (0.25mm i.d., film thickness 0.25 μ m). Carrier gas: dihydrogen, P = 50 kPa. Temperature 40°C.

Chapter 5

5. Experimental investigation of the influence of the enantiomeric purity of a chiral selector on the enantioseparation by liquid chromatography

5.1 Introduction

Enantioselectivity^(footnote: in the present chapter apparent enantioselectivity and apparent enantioseparation factor will be implied under the terms of enantioselectivity and enantioseparation factor) is an important concept in separation techniques displaying the ability to distinguish one enantiomer from the other. As outlined in Chapter 2, in chromatography, enantioselectivity is represented by the enantioseparation factor, α , which is measured as the ratio of the retention factors of the second and the first eluted enantiomer. Since three decades enantioselective LC has been greatly advanced and nowadays enantioseparation factors, α , higher than 10 have become quite common [111, 200, 201]. High enantioselectivity is warranted in preparative chromatography [202] (e.g. simulated moving bed [203,204] chromatography) in the chemical and pharmaceutical industries and in membrane separations [205,206] - one of the most promising but challenging method for enantiomer separations. Maximum enantioseparation factors are anticipated for enantiomerically pure chiral selectors. It has been recently reported [109, 110], however, that more than half of chiral building blocks of unnatural origin supposed to be enantiopure contain more than 0.1% (in some cases up to 20%) of the undesired enantiomer. The reason for that is economical because the higher the enantiopurity of a compound, the higher its price. The aim of this work is to investigate experimentally (for theoretical considerations see Section 2.4.1.1c) how the presence of the selector of opposite configuration influences the enantioselectivity of a highly enantioselective chromatographic system [73].

Equation (1.29) [73,178,207] (see Section 2.4.1.1c) represents the dependence of the enantioseparation factor, α , on the enantiomeric excess, ee , of the chiral selector responsible for the enantioseparation and on the enantioseparation factor, $\alpha^{ee=1}$, corresponding to the enantiopure chiral selector.

$$\alpha = \frac{\alpha^{ee=1}(1+ee)+1-ee}{\alpha^{ee=1}(1-ee)+1+ee} \quad (1.29)$$

5.2 Results and discussion

To perform the experimental verification of the predicted drop of the enantioseparation factor the main challenge is to identify a chiral selector possessing an extraordinary enantioselectivity toward a racemic selectand. Another prerequisite is the availability of two

opposite enantiomers of the selector in order to cover the whole range of the enantiomeric compositions.

Chiral anion exchange-type stationary phases based on cinchona alkaloids developed by Lindner et al. are known for very high enantioselectivities toward different classes of chiral acids [200]. Natural quinine and quinidine molecules are in fact diastereomers having four out of five stereogenic centers of opposite configuration. It was shown, however, that QN and QD selectors used in LC possessed opposite enantioselectivity and they were therefore termed “pseudoenantiomers”. The highest enantioseparation factor, α , ever observed in LC (unpublished results) was recently found when derivatives of quinine (QN) or quinidine (QD) (**Figure 5.1**) were used as chiral selectors for the enantioseparation of *N*-3,5-dinitrobenzoyl(DNB)- α -amino acids. The enantioseparation factor of *N*-DNB-4-methylleucine on QN was found as large as 88.5 at 25°C (**Figure 5.2**). Consequently, it was decided to use QN and QD as model selectors for our investigation.

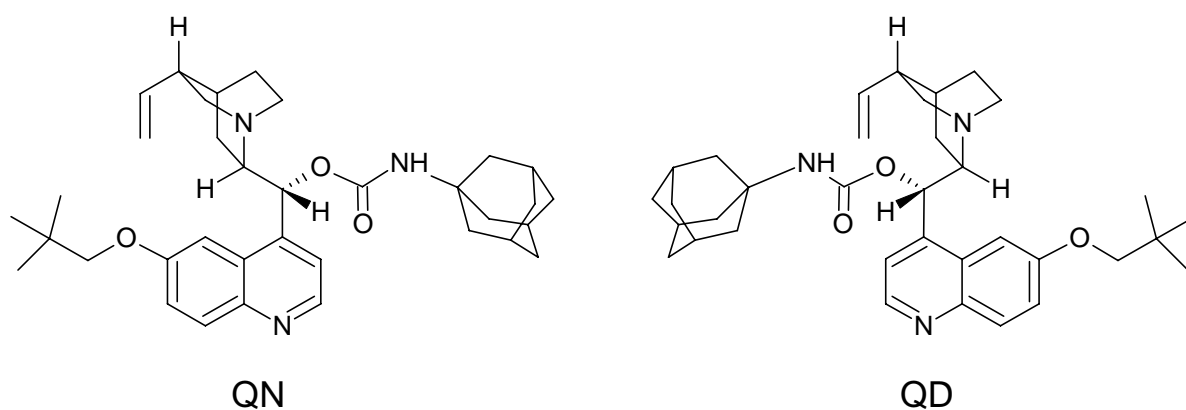


Figure 5.1 “Pseudoenantiomeric” modified quinine (QN) and quinidine (QD) selectors.

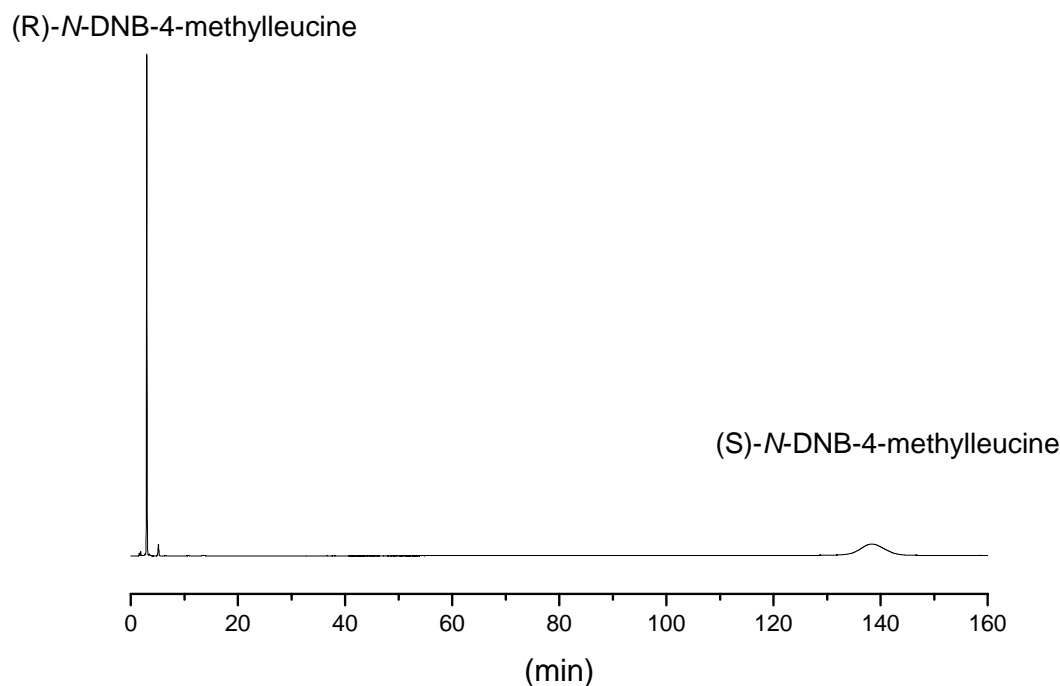


Figure 5.2 Chromatogram of the enantioseparation of (R,S)-N-3,5-dinitrobenzoyl-4-methylleucine on QN100 CSP. Enantioseparation factor $\alpha = 88.5$.

The chiral selectors QN and QD (**Figure 5.1**) were prepared from natural quinine and quinidine, respectively. Enantiomeric excess of QN and QD checked by HPLC was found to be more than 99.9%. The selectors were immobilized onto γ -mercaptopropyl-modified spherical silica (5 μm particle size) using radical initiation with AIBN. The selector loading measured by elemental analysis was found to be 145 ± 0.5 and 158 ± 0.5 $\mu\text{mol/g}$ for QN and QD, respectively. Portions of the silica gel modified with QN and QD were mixed with to yield seven batches of CSPs with different molar fractions, x , of QN in the mixture of QN and QD: $x = 1$ (QN100), 0.989 (QN99), 0.946 (QN95), 0.867 (QN87), 0.736 (QN74), 0.483 (QN48) and 0 (QD100). Thus, the whole range from $ee \cong 0$ to $ee = 1$ has been covered. It should be noted that owing to the “pseudoenantiomeric” nature of QN and QD selectors, the ee values are virtual (footnote: virtual enantiomeric excess ee is in fact the diastereomeric excess de), yet to the best of our knowledge, a selector possessing so high enantioselectivity and present in two enantiomeric forms is not readily available at present. The silica gel batches were used for the preparation of seven HPLC columns (15 cm x 4.0 mm i.d.) using the slurry method. The

eighth column was packed with non-modified γ -mercaptopropyl silica microparticles (SH) and was used as the reference column.

Six racemic (footnote: non-racemic samples were used for assignment of the elution order) α -amino acid derivatives were selected to cover as large as possible range of the enantioseparation factors obtained on the enantiomerically pure CSP QN100: *N*-Fmoc-phenylalanine ($\alpha = 2.46$), *N*-benzoylmethionine ($\alpha = 4.29$), *N*-DNB-alanine ($\alpha = 18.4$), *N*-DNB-2-allylglycine ($\alpha = 30.9$), *N*-DNB-leucine ($\alpha = 51.8$) and *N*-DNB-4-methylleucine ($\alpha = 88.5$). Chromatographic measurements were carried out in a polar organic mode with methanol modified with acetic acid (2% v/v) and ammonium acetate (0.5% w/w) used as the mobile phase. The retention data obtained on stationary phases QN100, QD100 and SH were used for the calculation of the enantioseparation factors at the molar fraction of QN ranging from $x = 0$ to 1. Since the selectors QN and QD are not true enantiomers, the enantioseparation factor was calculated using equation (1.22) that was derived for CSPs containing mixtures of different selectors with unequal concentrations (see Chapter 2 and 6).

$$\alpha^{\text{mix}} = \frac{K^{\circ} + \frac{c_{\text{QN}}^{\text{mix}}}{c_{\text{QN}}} (K_{\text{D}}^{\text{QN100}} - K^{\circ}) + \frac{c_{\text{QD}}^{\text{mix}}}{c_{\text{QD}}} (K_{\text{D}}^{\text{QD100}} - K^{\circ})}{K^{\circ} + \frac{c_{\text{QN}}^{\text{mix}}}{c_{\text{QN100}}} (K_{\text{L}}^{\text{QN100}} - K^{\circ}) + \frac{c_{\text{QD}}^{\text{mix}}}{c_{\text{QD100}}} (K_{\text{L}}^{\text{QD100}} - K^{\circ})} \quad (1.22)$$

where α^{mix} is the enantioseparation factor on the mixed CSP containing both QN and QD selectors; subscripts D and L refer to the opposite enantiomers of the selectand; K° is the distribution constant of a selectand on a reference column containing stationary phase SH; $K_{\text{D}}^{\text{QN100}}$ and $K_{\text{D}}^{\text{QD100}}$ are the distribution constants of enantiomer D on columns containing CSP QN100 and QD100, respectively. The distribution constants are determined as a product of the retention factors and the phase ratio of the corresponding column, e.g. $K_{\text{D}}^{\text{QN100}} = \beta^{\text{QN100}} \cdot k_{\text{D}}^{\text{QN100}}$; $c_{\text{QN}}^{\text{mix}}$ and $c_{\text{QD}}^{\text{mix}}$ are concentrations of selector QN and QD, respectively, in the mixed CSP, while $c_{\text{QN}}^{\text{QN100}}$ and $c_{\text{QD}}^{\text{QD100}}$ are concentrations of selector QN and QD in CSPs QN100 and QD100, respectively. The phase ratios were determined as ratio of the void volume to the volume of the stationary phase (see suppl. material).

As one can see from **Table 5.1**, the agreement of the experimental and the calculated values of enantioseparation factor, α , is excellent. **Figure 5.3** illustrates the behavior of the enantioseparation factor of *N*-Fmoc-phenylalanine (**Figure 5.3a**) and *N*-DNB-4-methylleucine (**Figure 5.3b**) as a function of molar fraction of QN, x . As one can see, the predicted drop of

the enantioseparation factor on the enantiomerically impure chiral selector possessing strong enantioselectivity is fully confirmed. Thus, the enantioseparation factor $\alpha = 88.5$ found for *N*-3,5-dinitrobenzoyl-4-methylleucine on QN100 CSP is dropped to 51.4 on QN99 CSP containing only 1.1% of QD selector. It should be noted that, although QN and QD possess opposite enantioselectivity, QD is somewhat less enantioselective than QN (**Table 5.1**). Therefore, for true enantiomeric selectors with so high enantioselectivity the drop of α would be even more significant.

Table 5.1 Calculated and experimental enantioseparation factors obtained on the CSPs with different molar fraction of QN selector

CSP:	QN100	QD100	QN99	QN95	QN87	QN75	QN50
molar fraction of QN, x :	1.00	0	0.989	0.946	0.865	0.734	0.479
" <i>ee</i> " of QN selector:	1	-1	0.978	0.892	0.73	0.468	-0.042
<i>N</i>-Fmoc-phenylalanine							
α_{exp}	2.46±0.005	2.62±0.005	2.43±0.01	2.21±0.01	1.87±0.01	1.45±0.01	0.92±0.01*
α_{calc}	-	-	2.4±0.01	2.18±0.02	1.85±0.02	1.44±0.02	0.91±0.01
<i>N</i>-benzoylmethionine							
α_{exp}	4.29±0.03	5.00±0.005	4.08±0.03	3.37±0.02	2.47±0.01	1.62±0.01	0.82±0.01*
α_{calc}	-	-	4.06±0.03	3.33±0.02	2.44±0.05	1.59±0.02	0.80±0.01
<i>N</i>-DNB-alanine							
α_{exp}	18.4±0.2	16.4±0.02	15.9±0.02	9.39±0.02	5.05±0.02	2.58±0.01	1.00±0.01
α_{calc}	-	-	15.5±0.2	9.33±0.02	5.08±0.05	2.61±0.02	1.00±0.01
<i>N</i>-DNB-2-allylglycine							
α_{exp}	30.9±0.1	28.8±0.1	24.0±0.2	11.6±0.14	5.56±0.07	2.67±0.01	1.00±0.01
α_{calc}	-	-	23.3±0.2	11.5±0.08	5.54±0.07	2.66±0.02	0.96±0.01**
<i>N</i>-DNB-leucine							
α_{exp}	51.8±0.2	44.6±0.3	36.0±0.1	14.6±0.05	6.47±0.02	2.98±0.01	1.03±0.01
α_{calc}	-	-	34.4±0.3	14.3±0.03	6.39±0.02	2.96±0.02	1.04±0.01
<i>N</i>-DNB-4-methylleucine							
α_{exp}	88.5±0.3	74.3±0.4	51.4±0.2	17.0±0.05	7.07±0.01	3.16±0.01	1.09±0.01
α_{calc}	-	-	48.6±0.3	16.8±0.2	7.03±0.1	3.16±0.03	1.09±0.01

* $\alpha < 1$ means inversion of the elution order

** $\alpha < 1$ because the loading of QD is slightly higher than that of QN

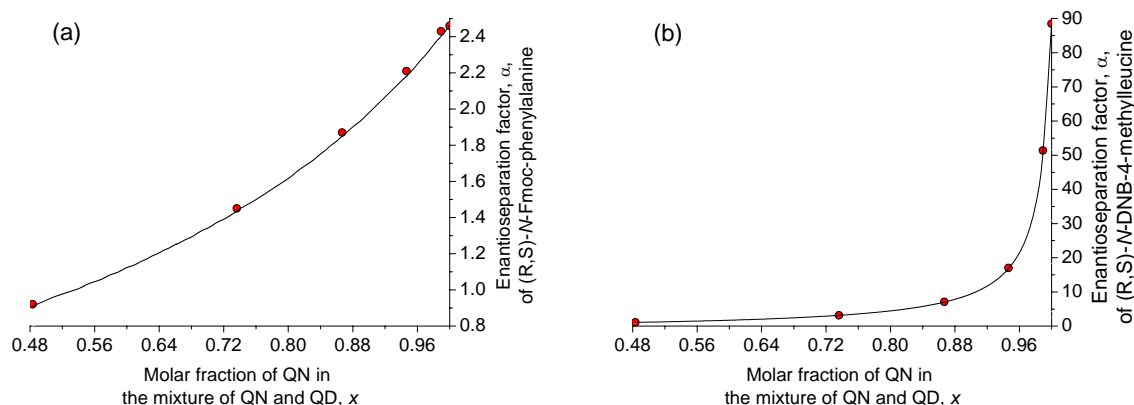


Figure 5.3 Plot of the experimental (red circles) and the calculated (solid black lines) enantioseparation factor, α , versus molar fraction of QN selector in the mixture of QN and QD, x ; analytes: (a) *N*-Fmoc-phenylalanine, (b) *N*-DNB-4-methylleucine.

On the one hand, it is surprising and unexpected that the enantioseparation factor collapse from 88 to 51 after addition of just 1% of the opposite enantiomer of the chiral selector. Intuitively, a linear plot of α versus ee may be expected and this is indeed observed for $\alpha^{ee=1}$ less than 4 (**Figure 5.3a**). Thus, $\alpha = 2.46$ recorded for *N*-Fmoc-phenylalanine on QN100 CSP is only dropped to $\alpha = 2.43$ on QN99 CSP. This peculiarity is a result of the definition of the enantioseparation factor, α , as the ratio of the retention factors, i.e. k_2/k_1 . Thus, the higher α is, the stronger it is influenced by the fluctuation of the retention factor of the first eluted enantiomer, k_1 . This behaviour can further be understood by the following thought experiment: in the hypothetical case that one enantiomer is eluted with the void volume of the column, whereas the other enantiomer is retained, the enantioseparation factor becomes infinite. However, only a minute amount of an enantiomeric impurity present in the selector ($ee \cong 1$) causes a minute retention of the first eluted enantiomer and the infinite separation factor is now rendered finite. Thus, from the practical point of view such a strong drop of α does not seem to be critical because it turned out that the distance between the peaks of the enantiomers is linearly dependent on the enantiomeric excess ee (or molar fraction, x) of the chiral selector. Therefore, for highly enantioselective CSPs the use of the enantioseparation factor, α , might be confusing. Instead, it might be more appropriate to use the ratio (“retention excess”) $\frac{k_2 - k_1}{k_2 + k_1}$, where k_1 and k_2 are retention factors of the first and the

second eluted enantiomer, respectively. The plot of $\frac{k_2 - k_1}{k_2 + k_1}$ vs. molar fraction, x of the selector gives a straight line independently of the enantioselectivity of the selector (**Figure 5.4**). Slight nonlinearity of the lines and the fact that they do not cross X axis at value of 0.5 is the result of the “pseudoenantiomeric” nature of QN and QD selectors.

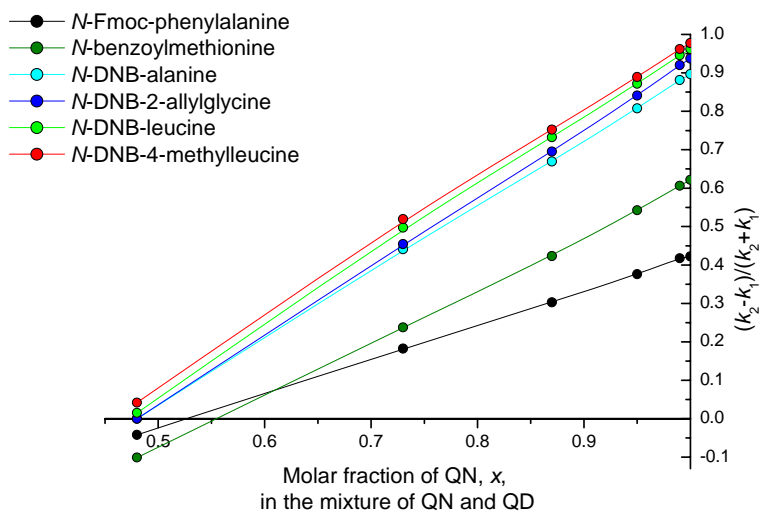


Figure 5.4 Plot of $\frac{k_2 - k_1}{k_2 + k_1}$ vs. molar fraction of QN, x , in the mixture of QN and QD.

Chapter 6

6. Evaluation of nonenantioselective *versus* enantioselective interactions in liquid chromatography

6.1 Introduction

As outlined in Chapter 2, enantioselectivity, $-\Delta_{D,L}\Delta G$, is a strictly thermodynamic quantity, and it is frequently correlated with the apparent enantioseparation factor α_{app} (as before, the subscripts D and L denote enantiomers, irrespective of their absolute configuration; the D enantiomer is arbitrarily eluted after the L enantiomer from the column (below T_{iso}); R = gas constant; T = absolute temperature; k = retention factor; K^{app} = distribution constant).

$$-\Delta_{D,L}\Delta G = RT \cdot \ln(\alpha_{\text{app}}) = RT \cdot \ln\left(\frac{k_D}{k_L}\right) = RT \cdot \ln\left(\frac{K_D^{\text{app}}}{K_L^{\text{app}}}\right) \quad (1.40)$$

In liquid-chromatography on brush-type CSPs, the chiral selectors are chemically linked to an achiral support. Although the achiral support does not participate in enantiomeric recognition, it contributes to the retention of both enantiomers to the same extent. Therefore it is mandatory to separate achiral and chiral contributions to retention in chromatographic selector–selectand systems displaying enantioselectivity [30,33]. In addition, a separate study of the enantioselective and the nonenantioselective interactions is also important for a rational design of new selectors or for the improvement of the enantioselectivity by means of reducing the number and activity of the nonenantioselective sites. Despite the above mentioned notion, eq (1.40) is frequently erroneously used for the determination of the true enantioselectivity of a chiral selector, although for chiral bonded phases in liquid chromatography (LC), Pirkle et al. previously stated that *additional retention mechanisms other than those responsible for chiral recognition attenuate the α value and hence stability differences between diastereomeric solvates calculated from observed α values will represent minimum values* (cf. footnote in ref. [90]). A related argument of distinguishing nonenantioselective from enantioselective interactions in enantioselective liquid-chromatography utilizing protein stationary phases has been advanced by Allenmark [91]. The topic has been reiterated recently by Guiochon et al. to differentiate between apparent and true enantioseparation factors [93]. In enantioselective gas-chromatography (GC), the concept of the retention-increment R' has been used to quantitatively differentiate between nonenantioselective

contributions to retention, arising from gas–liquid partitioning, and enantioselective contributions to retention, arising from enantioselective molecular association defined by the thermodynamic association constant K^{assoc} , whereby only differences of the latter quantity lead to the separation of enantiomers [30,127,131,99]. The concept of the retention-increment R' (formerly called retention-increase [30]) is an extension of an approach to determine complexation constants in argentation GC [154,155]. In enantioselective GC, the true enantioseparation factor, α_{true} , can be assessed by use of two columns, i.e., (a) a reference column devoid of the chiral selector and a column containing the chiral selector or (b) by use of two columns containing the chiral selector with different concentrations (loadings) in the achiral matrix (cf. Chapter 2). In the latter case, the achiral contribution to retention, K° , can be obtained by the following equation [33]:

$$K^{\circ} = \frac{K_{L_2}^{\text{app}} \cdot K_{D_1}^{\text{app}} - K_{L_1}^{\text{app}} K_{D_2}^{\text{app}}}{(K_{D_1}^{\text{app}} + K_{L_2}^{\text{app}}) - (K_{D_2}^{\text{app}} + K_{L_1}^{\text{app}})}$$

where D and L designate two enantiomers (D is arbitrary eluted after L) and subscripts 1 and 2 correspond to the CSPs with different concentrations of the chiral selector.

A method similar to the retention increment approach, based on a “pseudo-phase” model, was recently used in enantioselective GC by Armstrong et al. [208] in order to separate partition equilibria occurring between the gas mobile phase and both components of a CSP (an achiral polymeric matrix and a cyclodextrin selector) and the analyte equilibrium between the achiral polymeric matrix and the cyclodextrin selector.

A method that permits the isolation of enantioselective interactions from the nonenantioselective ones based on the determination of equilibrium isotherms by means of frontal analysis followed by modeling the isotherms was described by Guiochon et al. [158,209,92,93]

In the present Chapter, a method, based by the retention increment approach used in GC, is described for distinguishing between enantioselective and nonenantioselective interactions in liquid chromatography on brush-type CSPs. Despite its similarity with the method described for GC (see Chapter 2), the possibility of the analytes to interact (adsorb) with the selector molecules directly from the mobile phase renders the derived equations different from those obtained for GC applications.

6.2 Results and discussion

If a selectand enantiomer D migrates through a column packed with a brush-type CSP containing enantiopure selector A chemically linked to an achiral support S, two independent equilibria can be distinguished: adsorption of D on S and association of D with A. These processes are described by the corresponding equilibrium constants.



where D_m and D_s represent the selectand in the mobile phase and the selectand adsorbed on S, respectively; A is the chiral selector chemically linked to S; AD is the associate formed between A and D; c_{D_m} (mol/L) is the concentration of D in the mobile phase; c_{D_s} (mol/g) is the molality of D adsorbed on S (mol of D per gram of S); c_A and c_{AD} (mol/g) are the molalities of A and AD present on the surface of S; K_D^o (L/g) is the equilibrium constant of the adsorption of D on the surface of S; K_{AD}^{assoc} (L/mol) is the equilibrium constant of the association between D and A.

It is assumed that the selectand enantiomers form 1:1 associates with the chiral selector. It is also assumed that the selectand is independently adsorbed on the surface of the achiral support and that this adsorption is not changed upon increasing the amount of the chiral selector present on the surface. The latter assumption is only valid at low concentrations of the chiral selector.

The overall adsorption, including enantioselective and nonenantioselective interactions, of the selectand enantiomer D on the CSP composed of the achiral support S and the chiral selector A is described by the apparent adsorption equilibrium constant K_D^{app} (L/g).

$$K_D^{\text{app}} = \frac{c_{\text{Ds}} + c_{\text{AD}}}{c_{\text{Dm}}} \quad (1.43)$$

The value of the apparent adsorption equilibrium constant, K_D^{app} , determines the retention factor of the analyte according with the following expression.

$$K_D^{\text{app}} = \beta \cdot k_D \quad (1.43a)$$

Where β is the phase ratio of the column containing the CSP and k_D is the retention factor of D. Since the concentration of the selector on the silica surface is expressed as mol/g (i.e. as molality), the phase ratio, β , should be determined as the ratio of the volume of the mobile phase (void volume, L) to the mass of the CSP (g).

Substitution of eq (1.41) and (1.42) into (1.43) yields

$$K_D^{\text{app}} = K_D^{\circ} + K_{\text{AD}}^{\text{assoc}} \cdot c_A \quad (1.44)$$

The same considerations for the L enantiomer of the selectand lead to eq (1.45)

$$K_L^{\text{app}} = K_L^{\circ} + K_{\text{AL}}^{\text{assoc}} \cdot c_A \quad (1.45)$$

where subscript L corresponds to the L enantiomer.

The expression for the apparent adsorption equilibrium constant K_D^{app} (eq (1.44)) (and K_L^{app} - eq (1.45)) is composed of two terms. The first term, K_D° , represents the nonenantioselective contribution to the retention arising from the adsorption of D on S, whereas the second term, $K_{\text{AD}}^{\text{assoc}} \cdot c_A$, displays the enantioselective contribution to the retention which is the result of the selector-selectand association.

The ratio of the association equilibrium constants of the enantiomers D and L determines the true enantioselectivity factor [33,207,92,93] of the racemate DL on the CSP,

$$\alpha_{\text{true}} = \frac{K_{\text{AD}}^{\text{assoc}}}{K_{\text{AL}}^{\text{assoc}}}, \text{ which is related to the Gibbs energy difference between the diastereomeric associates AD and AL as } -\Delta_{\text{AD,AL}} \Delta G = RT \ln(\alpha_{\text{true}}).$$

Because of the nonenantioselective contribution of the term K° (see eq (1.44) and (1.45)), the value of the apparent enantioselectivity factor, α_{app} , determined as the ratio of the

apparent adsorption equilibrium constants, i.e. $\alpha_{\text{app}} = \frac{K_{\text{D}}^{\text{app}}}{K_{\text{L}}^{\text{app}}}$, is always lower than that of the true enantioselectivity factor, α_{true} (see Chapter 2). If there were no nonenantioselective sites on the CSP, i.e. K° were zero, the apparent enantioselectivity factor, α_{app} , would be equal to the true enantioselectivity factor, α_{true} . The stronger the nonenantioselective interactions, the lower will be the apparent enantioselectivity factor, α_{app} , on this CSP, although the true enantioselectivity factor will not change.

According to eq (1.44) and (1.45), a plot of $K_{\text{D}}^{\text{app}}$ vs. c_{A} yields a straight line of slope $K_{\text{AD}}^{\text{assoc}}$ and intercept K_{D}° . Thus, using this method, the nonenantioselective and enantioselective contributions to the retention, K° and $K_{\text{AD}}^{\text{assoc}} \cdot c_{\text{A}}$, respectively, can be isolated and studied separately without interference with each other. It should be noted, however, that the nonenantioselective interactions possibly occurring with the achiral parts of the chiral selector, in contrast to the method of Guiochon [92,93,158,209], can not be evaluated.

In order to construct the plot of K^{app} vs. c_{A} , several CSPs loaded with different amount of the quinine selector (**Figure 6.1**) were prepared. Radical immobilization of the selector on the mercaptopropyl silica surface was used to obtain 50, 80, 110 and 150 $\mu\text{mol/g}$ silica batches. The loadings of the selector, c_{QN} ($\mu\text{mol/g}$), determined by elemental analysis, were found to be 48, 78, 111 and 146 $\mu\text{mol/g}$, respectively. The close agreement of the planned selector concentrations and the actually obtained values shows the feasibility of the controlled loading of the selector.

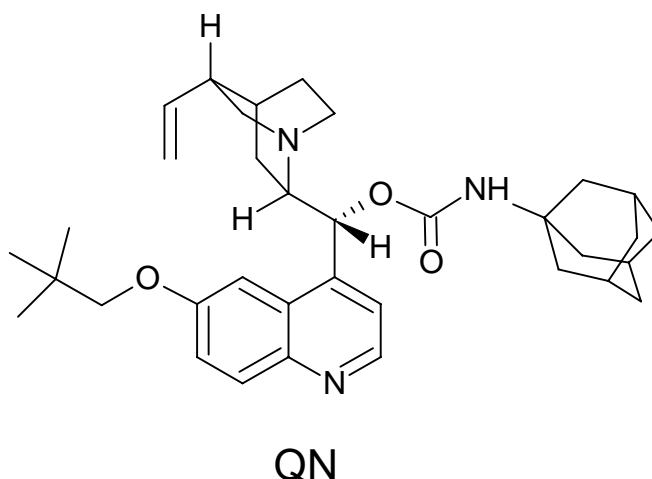


Figure 6.1 Structure of the quinine selector (QN) used for immobilization on the mercaptopropyl silica particles.

Four columns (15 cm x 4 mm i.d.) were packed with the produced CSPs by the slurry method. A reference column was packed with the unmodified mercaptopropyl silica. Under the assumptions mentioned above, the adsorption equilibrium constants obtained on the reference column should correspond to the case with $c_{\text{QN}} = 0$, i.e. to the K° constants.

The following analytes were chosen for the investigation: *N*-Fmoc-phenylalanine (**25**), *N*-{[(3,5-dipropoxybenzyl)oxy]carbonyl}leucine (**26**), 2-(2,4-dichlorophenoxy)propanoic acid (**27**). The racemates were analyzed on the five columns in three different mobile phase modes (for preparation of the mobile phases see experimental part): organic polar mode (methanol : acetic acid : ammonium acetate [98 : 2 : 0.05]), reversed mode (water : methanol : acetic acid : ammonium acetate [40 : 58 : 2 : 0.5]) and normal mode (*n*-heptane : ethanol : acetic acid [90 : 10 : 1]) (see experimental part). All the racemates, except **25** which could not be eluted in the normal mode, could be enantio-separated using the three different mobile phases. All the measurements were performed at $25.0 \pm 0.1^\circ\text{C}$. Each measurement was repeated at least three times. Based on the retention data, plots K^{app} vs. c_{QN} were constructed (**Figure 6.2-6.4**).

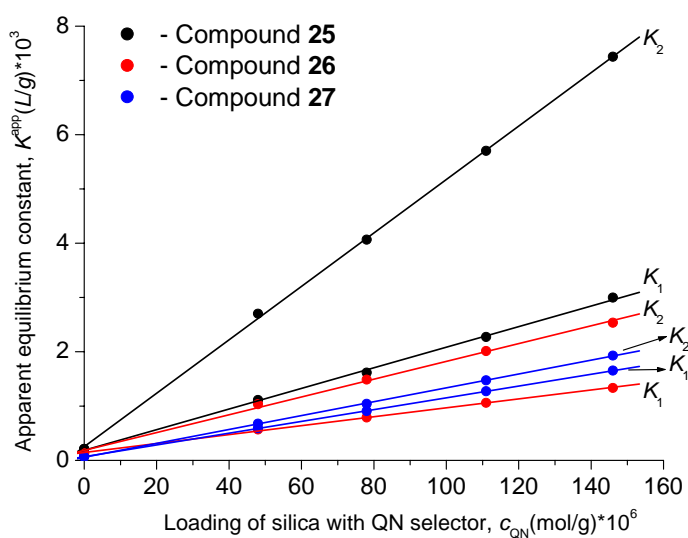


Figure 6.2 Plots of the apparent distribution constants, K^{app} , versus loading of the quinine selector, c_{QN} . Subscripts 1 and 2 correspond to the first and the second eluted enantiomers, respectively. Analyses were performed in organic polar mode.

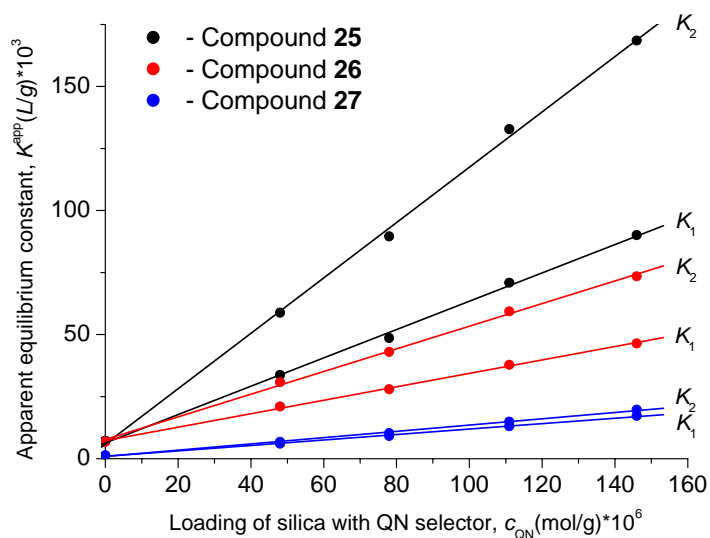


Figure 6.3 Plots of the apparent distribution constants, K^{app} , versus loading of the quinine selector, c_{QN} . Subscripts 1 and 2 correspond to the first and the second eluted enantiomers, respectively. Analyses were performed in reversed mobile phase mode.

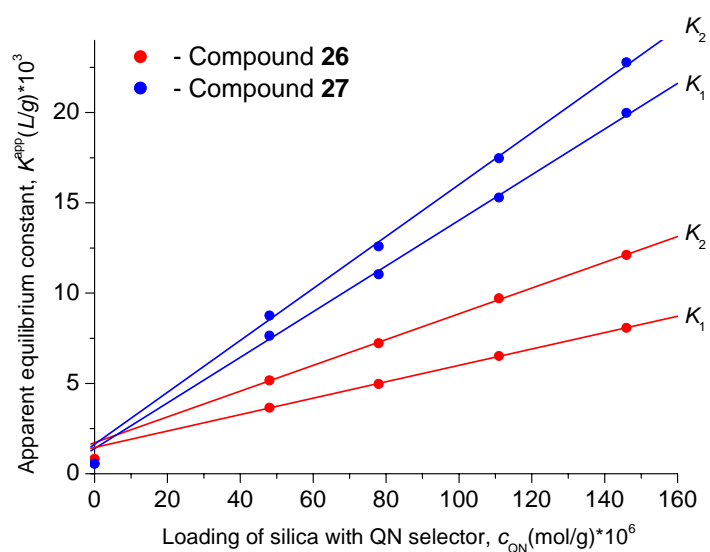


Figure 6.4 Plots of the apparent distribution constants, K^{app} , versus loading of the quinine selector, c_{QN} . Subscripts 1 and 2 correspond to the first and the second eluted enantiomers, respectively. Analyses were performed in normal mobile phase mode. Regression analysis was performed excluding the points at $c_{\text{QN}} = 0$ (see text)

As one can see, all the plots represent straight lines with the correlation coefficient R usually being higher 0.999. This confirms the validity of the equations (1.44 and 1.45) and the precision of the immobilization chemistry and the elemental analysis used for the determination of the loading of the selector on the silica surface. It is also important that the plots corresponding to the opposite enantiomers are converged in the same points, K° .

In the polar organic and reversed modes the values of K° experimentally obtained on the reference column were in good agreement with the extrapolated values obtained from the linear plots constructed excluding the point obtained on the reference column, i.e. the point at $c_{\text{QN}} = 0$. Equilibrium constants, K° , obtained on the reference column in the normal mode, however, were slightly below the approximated values. Presumably, this was caused by the repulsive effect of the acetic acid adsorbed on the pure mercaptopropyl silica surface. In the other cases, ammonium acetate present in the mobile phases served as a competitor to such adsorption. Thus, the linear plots depicted in **Figures 6.2** and **6.3** were constructed on the basis of the retention data obtained on the five columns (including the reference column, i.e. $c_{\text{QN}} = 0$), while the plot represented in **Figure 6.4** was drawn excluding the point at $c_{\text{QN}} = 0$.

From **Figures 6.2-6.4** one can see that when c_{QN} approaches zero, the apparent adsorption equilibrium constants, K^{app} , and selectivity drop significantly. This is also seen from the experimental data summarized in **Table 6.1**. Values of K° and $K_{\text{QN-X}}^{\text{assoc}} \cdot c_{\text{QN}}$ (where $c_{\text{QN}} = 146 \mu\text{mol/g}$ and X is the first eluted enantiomer of the compounds **25-27**) correspond to the nonenantioselective adsorption of the selectand molecules with the achiral support and the enantioselective selector-selectand interactions, respectively. From the data given in **Table 6.1** it becomes apparent that the nonenantioselective interactions are extremely low in these conditions in comparison with the enantioselective ones.

Table 6.1 Chromatographic experimental data

Mobile phase mode:	$K^o \cdot 10^3$ [L/g]	$(K_{QN-X}^{assoc} \cdot c_{QN}) \cdot 10^3$ [L/g] ^a	K_1^{assoc} [L/mol] ^b	K_2^{assoc} [L/mol] ^c	α_{true}	α_{app}^d	$\left(\frac{c_{QN-X}}{c_{Ds}}\right)^a$
Polar organic mode							
Comp. 25	0.22 ± 0.05	2.77 ± 0.06	19.0 ± 0.4	49.3 ± 0.5	2.59 ± 0.06	2.48	12.6
Comp. 26	0.17 ± 0.03	1.20 ± 0.03	8.2 ± 0.2	16.4 ± 0.5	2.00 ± 0.09	1.90	7.1
Comp. 27	0.061 ± 0.004	1.59 ± 0.006	10.9 ± 0.04	12.8 ± 0.1	1.18 ± 0.005	1.17	26.1
Reversed mode							
Comp. 25	6.1 ± 0.3	83.4 ± 2	571 ± 14	1116 ± 24	1.95 ± 0.07	1.87	13.7
Comp. 26	7.5 ± 0.3	39.6 ± 0.9	271 ± 6	457 ± 10	1.69 ± 0.06	1.58	5.3
Comp. 27	0.92 ± 0.04	16.1 ± 0.4	110 ± 3	127 ± 4	1.15 ± 0.005	1.14	17.5
Normal mode							
Comp. 26	1.6 ± 0.2	6.63 ± 0.06	45.4 ± 0.4	71.4 ± 1.0	1.57 ± 0.02	1.50	4.1
Comp. 27	1.5 ± 0.2	18.4 ± 0.4	126 ± 3	144 ± 4	1.14 ± 0.02	1.14	12.3

^aX is the first eluted enantiomers of the racemates **25-27**; $c_{QN} = 146 \mu\text{mol/g}$

^bassociation equilibrium constant corresponding to the first eluted enantiomer

^cassociation equilibrium constant corresponding to the second eluted enantiomer

^d $c_{QN} = 146 \mu\text{mol/g}$; standard deviations of the experimentally obtained apparent enantioseparation factors were ≤ 0.01

The extremely weak nonenantioselective interactions result in virtually complete loss of the retention of the analytes on the reference column devoid of the quinine selector. Such unusual behavior can be explained by the large strength of the interactions of the positively charged quinine selector with the negatively charged selectand molecules. Therefore, the high ionic strength of the mobile phase is necessary for the analytes to be eluted with reasonable retention times, whereas, the contribution of the weak nonselective interactions on the retention in such conditions is very low. Such behavior is not common in liquid chromatography where the nonenantioselective interactions have often pronounced influence on the overall retention [92].

A quantitative characterization of the relative difference between enantioselective and nonenantioselective interactions can be obtained from the following expression derived from eq (1.41) and (1.42).

$$\frac{c_{AD}}{c_{Ds}} = \frac{K^{assoc} \cdot c_A}{K^o} \quad (1.46)$$

Equation (1.46) represents the ratio of the amount of the selector-selectand associates, AD, at a certain concentration of the selector, c_A , to the amount of the selectand molecules, D_s , adsorbed on the surface of the achiral support S, c_{D_s} . The experimental data, obtained according to eq (1.46) at the concentration of the quinine selector $c_{QN} = 146 \mu\text{mol/g}$, are given in **Table 6.1**. The lowest value of the ratio (1.46), corresponding to the highest nonenantioselective adsorption, was found for the compound **26** analyzed in normal mode, i.e.

$$\frac{c_{QN,2}}{c_{2s}} = 4 \text{ (determined for the first eluted enantiomer).}$$

The largest value of the ratio (1.46), showing the lowest nonenantioselective adsorption, was observed for the racemate **27** analyzed in polar organic mode, i.e. $\frac{c_{QN,3}}{c_{3s}} = 26$. The number 26 means that on each molecule of **27** adsorbed on the achiral mercaptopropyl silica surface there are 26 molecules of **27** associated with molecules of the quinine-selector.

As one can see from **Table 6.1**, the nonenantioselective adsorption is significantly increased when turning from the polar organic mode to the reversed and normal modes. For example, the value of K° for compound **26** obtained in reversed mode is more than 40 times higher than that obtained in polar organic mode. On the other hand, the strength of the enantioselective interactions is also increased, e.g. the association constant of the first eluted enantiomer, K_1^{assoc} , of compound **26** is increased from 8.2 measured in polar organic mode to approximately 270 obtained in reversed mode. This indicates that, upon turning from organic polar to reversed mode, the hydrophobic interactions are increased with both the mercaptopropyl silica surface and with the hydrophobic parts of the quinine-selector. It is worth noting that, despite the strong increase of the strengths of the selector-selectand interactions when turning from the polar organic to the reversed mode, the true enantioseparation factor, α_{true} , of compound **26** is reduced from 2.0 to 1.7. Since the true enantioseparation factor is considered, this reduction is solely the result of the decreased enantioselectivity of the chiral selector toward compound **26**. However, because of the presence of the nonenantioselective interactions, the enantioselectivity of the CSP is further reduced. Thus, the apparent enantioseparation factor, α_{app} , found to be 1.6 in the reversed mode with the concentration of the quinine selector, $c_{QN} = 146 \mu\text{mol/g}$.

Thus, this method allows one to analyze how one or another change in the chromatographic conditions or modification of silica or some other changes in the system influence the nonenantioselective vs. enantioselective interactions. In turn, this knowledge can

help to optimize the enantioseparation by varying the conditions of the separation or by modifying the CSP.

As predicted [207,33], the values of the apparent enantioseparation factors, α_{app} , are found to be lower than that of the true enantioseparation factors, α_{true} (**Table 6.1**). It is interesting to note that due to the very strong enantioselective interactions the apparent enantioseparation factors, α_{app} , are only slightly reduced upon decreasing the concentration of the quinine-selector from 146 to 48 $\mu\text{mol/g}$ (**Figure 6.5**). This behavior is in agreement with the predicted variation of the apparent enantioseparation factors, α_{app} , in the presence of strong enantioselective interactions (see Chapter 2) [127].

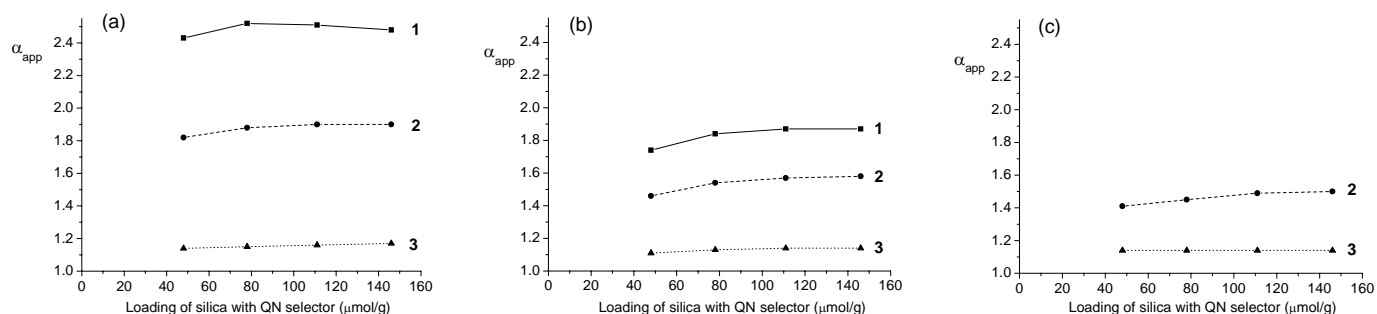


Figure 6.5 Plots of the apparent enantioseparation factors, α_{app} , of compounds **25** (1), **26** (2) and **27** (3) as functions of the concentration of the quinine-selector on the silica surface, c_{QN} ($\text{g}/\mu\text{mol}$). (a) Organic mode, (b) reversed mode, (c) normal mode

Chapter 7

7. Differentiation between racemic compounds and conglomerates by enantioselective GC

7.1 Introduction

Resolution of racemates into pure enantiomers by means of preferential crystallization in the spirit of Pasteur's work on tartaric acid is still the easiest and cheapest method available for generation of enantiomerically pure compounds [114,115,117]. However, only chiral compounds forming conglomerates, i.e. homochiral crystalline modifications where each single crystal is composed of only one enantiomer, are capable of the resolution through the preferential crystallization. The percentage of known conglomerate-forming substances, however, in the pool of chiral organic solids [114] is still limited and, therefore, the search for new conglomerates among the important synthons or their synthesized precursors is important. Since, the conglomerates and racemic compounds (heterochiral crystalline modifications of chiral compounds in which each single crystal is composed of both enantiomers) have different crystal structures, they can be differentiated by different solid-state techniques. Apart from X-ray diffraction techniques the well-known methods for detection and visualization of the differences between homo- and heterochiral crystal structures include solid state IR [210-213], Raman [210-215], solid state NMR [214,216] and solid state UV-VIS spectroscopies [214]. Solid state ESR spectra of radicals provide valuable information about their crystal structures, magnetic properties, local environment and spatial distribution in the lattice [217,218]. It has been shown that ESR spectroscopy is also capable of differentiating between homo- and heterochiral crystal structures [219]. Conglomerate formation may be confirmed if the solid state spectrum of the crystalline racemic form is identical to that of the enantiomerically pure substance.

Since single crystals of a conglomerate and a racemic compound have enantiomeric and racemic compositions, respectively, they can be differentiated by the analysis of separate single crystals (or their solutions) of the two forms by chiroptical methods like circular dichroism or optical rotation. Probably, the most convenient and effective method for the distinguishing between the racemic compound and a conglomerate, however, is enantioselective chromatography. The advantages of this method consist in high sensitivity and straightforwardness in comparison with the solid state methods, which require comparison of the spectra of the racemic sample with the enantiomerically pure one. In the following Section, two examples of using the enantioselective gas chromatography as a method for detecting the formation of a conglomerate are presented.

7.2 Results and discussion

2,3:6,7-dibenzobicyclo[3.3.1]nona-2,6-diene-4,8-dione (**28**) represents a rare example of a chiral substance that possesses diastereomorphism [114,220], i.e. it is capable of forming both a racemic compound (below 100°C) and a conglomerate (above 100°C) (**Figure 7.1**) [221, 222].

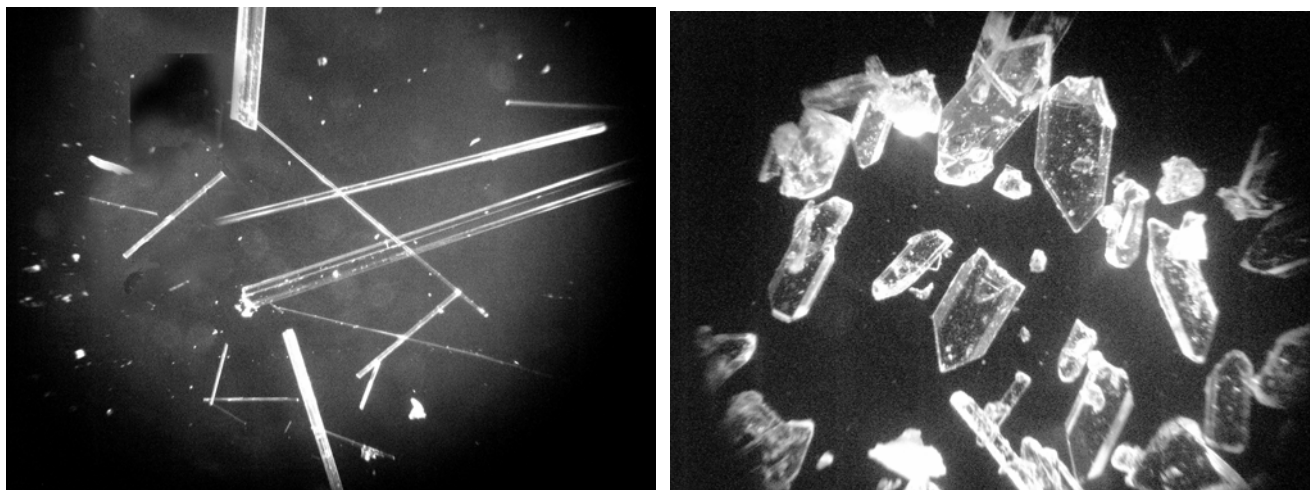


Figure 7.1 Single crystals of the racemic compound **28** (left); single crystals of the conglomerate **28** (right).

Therefore, **28** is especially appropriate for demonstrating the merit of enantioselective chromatography as a tool for distinguishing between the racemic compounds and the conglomerates. Compound **28** was synthesized according to a known procedure [223-225] and crystallized at two different temperatures: at 20°C (from acetone or *n*-octane) and at 100°C (from toluene or *n*-octane). The produced single crystals were dissolved in diethylether and analyzed by enantioselective GC using a 2 m fused-silica column (0.25 mm i.d. x 0.25 μm film thickness) coated with the Chirasil-Dex CSP. **Figure 7.2** represents chromatograms of the enantioseparation of the solutions of single crystals obtained by low-temperature crystallization and that obtained by high-temperature crystallization. As one can see, the single crystal obtained at 20°C contains the two enantiomers in the ratio of 1:1, while that obtained at 100°C contained essentially only one enantiomer. This unambiguously proves conglomerate formation by **28** upon crystallization above 100°C and racemic compound at 20°C. This result was later confirmed by X-ray structural analysis (conglomerate of **28**, space group $P2_12_12_1$; racemic compound of **28**, space group $P\bar{1}$) [221].

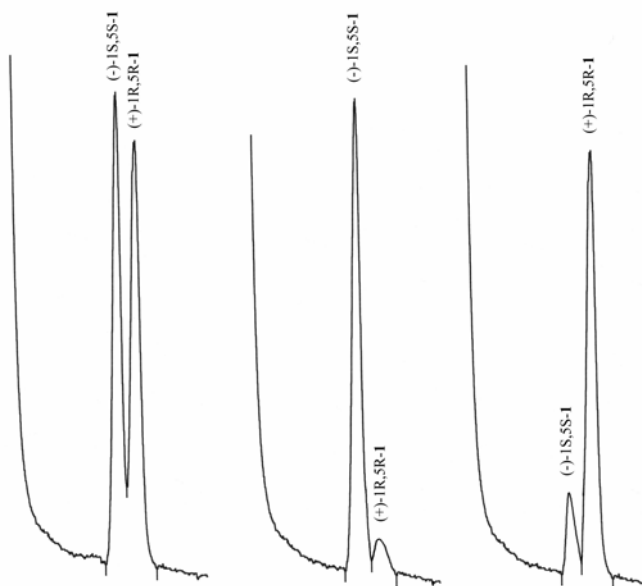


Figure 7.2 (a) Gas chromatogram of a solution of a single crystal of **28** obtained by low-temperature crystallization (left); (b) gas chromatograms of solutions of single crystals of **28** obtained by high-temperature crystallization (middle and right). CSP: Chirasil-Dex; carrier gas: dihydrogen; 50kPa, 130°C. Fused silica column: 2 m x 0.25 mm i.d. x 0.25 μm polymer film thickness.

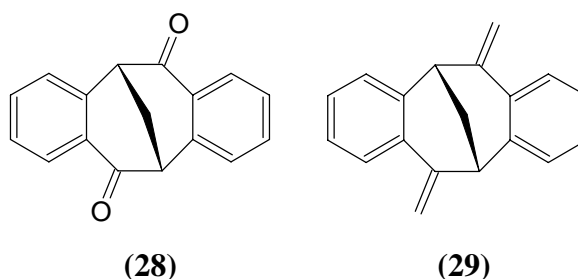


Figure 7.3 2,3:6,7-dibenzobicyclo[3.3.1]nona-2,6-diene-4,8-dione (**28**); 4,8-bis(methylene)-2,3:6,7-dibenzobicyclo[3.3.1]nona-2,6-diene (**29**)

4,8-bis(methylene)-2,3:6,7-dibenzobicyclo[3.3.1]nona-2,6-diene (**29**) represents another example of the conglomerate formation as identified by enantioselective GC. An attention was paid to the fact that the melting point of the pure enantiomers of **29** is much higher than that of the racemate ($\Delta T_{(T_{\text{enantiomer}} - T_{\text{racemate}})} = 43^\circ$), which is already an indication of the possible formation of a conglomerate [114]. Furthermore, all substituted dibenzodiketones studied by X-ray diffraction crystallized in achiral space groups [226]. In order to examine the nature of the crystals of **29**, the synthesis of this compound was performed. It was found that the racemate of **29** can be separated into enantiomers by enantioselective GC on Chirasil-Dex

CSP (**Figure 7.4**). However, single crystals grown from the racemic solution of **29** at 20°C and -10°C gave only one peak under the same chromatographic conditions (**Figure 7.4b,c**). Thus, it can be concluded that crystallization of **29** leads to a conglomerate of enantiomerically pure single crystals. The conglomerate formation of compound **29** was unambiguously confirmed by X-ray diffraction (space group $P2_12_12$) and polarimetry. Thus, the limited number of well-known hydrocarbon conglomerates (3,4-benzophenanthrene, 1,1'-binaphthyl, [5]-[9]-helicenes, *o*-hexaphenylene [114] and [4]-triangulan [227]) has been supplemented with a new example using enantioselective GC as a tool for the detection of the conglomerate formation.

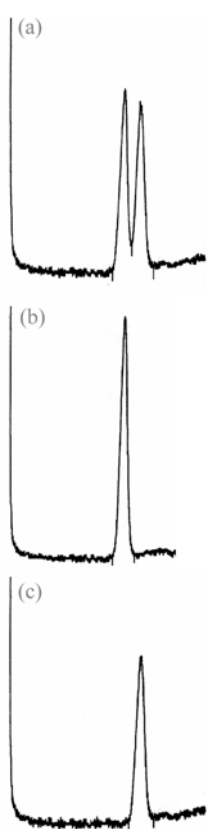


Figure 7.4 (a) Gas chromatogram of a solution of racemic **29**, (b and c) chromatograms of solutions of single crystals of **29**. CSP: Chirasil-Dex; carrier gas: dihydrogen; 50kPa, 115°C. Retention time for the first peak: 5.93 min; and for the second peak: 6.76 min. Fused silica column: 2 m x 0.25 i.d. x 0.25 μm film thickness.

Experimental part

8. Experimental part

8.1 Materials and methods

^1H and ^{13}C NMR spectra were recorded on a Bruker Avance 400 spectrometer operating at 400 MHz for protons and 100 MHz for carbon nuclei at 20°C. ^1H and ^{13}C NMR spectra of **28** and **29** were recorded on a Bruker DRX-500 spectrometer operating at 500 MHz for protons and 125 MHz for carbon nuclei at 20°C. NMR measurements of heptakis(6-*O*-(*N*-acetyl-*L*-valine-*tert*-butylamide)-2,3-di-*O*-methyl)- β -cyclodextrin (ValDex) were performed at the University of Pisa by S. Nazzi and Prof. G. Uccello-Barretta using a Varian Inova 600 spectrometer operating at 600 and 150 MHz for protons and carbons, respectively. The temperature was controlled to ± 0.1 °C. Chemical shifts were expressed in parts per million downfield from TMS. High-resolution ESI-MS (FT-ICR) was carried out on a Bruker Daltonic APEX 2 spectrometer. Ultrasonication was performed using an ultrasonic bath Elma Transsonic Digital-S (Singen, Germany). Optical rotations were measured using Jasco P-1020 Polarimeter. The melting points were recorded with a Büchi B-540. The course of the reactions was monitored by TLC: silica gel plates on plastic support, Polygram® SIL G/UV₂₅₄ Macherey-Nagel, Düren, Germany. Treatment with a mixture of *p*-anisaldehyde : conc. sulfuric acid : acetic acid (1 : 2 : 97) followed by heating up to 150°C was used for the visualization. Column chromatography was performed using silica gel 40-60 μm .

Capillary gas chromatography was performed on a Trace GLC (Thermo Finnigan, Milan, Italy) gas chromatograph equipped with an FID, dihydrogen as a carrier gas (50 kPa if not otherwise stated), autosampler (Thermo Finnigan AS2000) and software Chrom-Card 32-bit (2.0). Fused silica capillaries (0.25 mm I.D.) were purchased from Ziemer, Mannheim, Germany. The capillaries were heated at 250°C with a slow stream of dinitrogen overnight followed by coating with a selected CSP using the static method to yield a film thickness of 0.25 μm . The columns coated with CSPs were conditioned by gradual heating up to 190-200°C followed by keeping at this temperature for 5-10 h. The maximum gas-chromatographic working temperature was 190-200°C. The apparent enantioseparation factor, α_{app} , was determined as $\alpha = (t_2 - t_d) / (t_1 - t_d)$, where t_2 , t_1 are the retention times of the first and second eluted enantiomer, respectively, and t_d is the hold-up time approximated by co-injection of methane. The resolution factor was determined using the following expression: $R_s = 1.177 * (t_2 - t_1) / (w_{h1} + w_{h2})$, where w_{h1} and w_{h2} are the width of the peaks at the half height of the first and the second eluted enantiomer, respectively; k_1 is the

Experimental part

retention factor obtained as $(t_1 - t_d) / t_d$. The elution order was determined by using non-racemic standards of known configuration.

HPLC measurements were performed on a semi-preparative HPLC D-7000 HSM system equipped with a pump L-7150, autosampler L-7250 and DAD detector. Detection was performed at 254 nm. The rate of the mobile phase was 1 ml/min. The temperature was kept at $20^\circ\text{C} \pm 0.1^\circ\text{C}$. The HPLC columns (15cm x 4mm i.d.) were packed by a slurry method. All the solvents and reagents for the mobile phases were ordered from Fluka. Solvents were of "HPLC-grade". Organic polar mode: 20 mL of glacial acetic acid were placed in a 1L volumetric flask followed by addition of methanol up to 1L. After equilibration, 5g of ammonium acetate were added. Normal mode: 100 mL of ethanol were placed in a 1L volumetric flask followed by addition of *n*-heptane up to 1L. After equilibration 10 mL of glacial acetic acid were added. Reversed phase mode: 20 mL of glacial acetic acid and 400 mL of bi-distilled water were placed in a 1L volumetric flask followed by addition of methanol up to 1L. After equilibration, 5g of ammonium acetate were added.

Solvents were purified by using standard procedures. Methyloxirane, trifluoroacetic acid, trifluoroacetic acid anhydride, di-*tert*-butyldicarbonate, *N,N'*-dicyclohexylcarbodiimide, *tert*-butylamine, bromoacetyl chloride, undec-10-enoyl chloride, hexachloroplatinic acid, resorcinol, 10-undecenal, *tert*-butyldimethylsilyl chloride, methyl iodide, diiodomethane, benzyl cyanide were purchased from Fluka (Buchs, Switzerland) or Sigma-Aldrich (Steinheim, Germany). β -Cyclodextrin was purchased from Carl Roth GmbH (Karlsruhe, Germany).

Hydromethyl(7.4%)dimethylpolysiloxane was synthesized in-house according to a known procedure [47]. Derivatives of quinine and quinidine selectors and silica (5 μm) modified with the selectors (Chapter 5 and 6) were kindly provided by Dr. N. M. Maier and Prof. W. Lindner (University of Vienna). Derivatives of α -amino acids and 2-(2,4-dichlorophenoxy)propanoic acid used for the liquid chromatographic investigation (Chapter 5 and 6) were kindly provided by Dr. N. M. Maier. Amino acid derivatives **7-17** were prepared following the procedure reported by Pirkle et al. [228,229] or according the procedure reported in Section 8.2.

8.2 Synthetic procedures

***N*-Trifluoroacetyl amino acid ethyl esters.** Dry racemic amino acid (3 mg) was dissolved in 0.5 ml of ethanol solution of hydrochloric acid (15%) and was heated at 110°C

in a closed vial for 30 min. After cooling, the vial was opened and the solvent was removed in a stream of dry dinitrogen at 110°C. Dichloromethane (110 μ L) and trifluoroacetic anhydride (10 drops) were added to the residue. After mixing, the reaction mixture was heated up to 110°C in a closed vial for 10 min followed by cooling and evaporation of the solvents at room temperature in a stream of dry dinitrogen. The residue was dissolved in dichloromethane or diethyl ether and used for the gas chromatographic or NMR investigations without further purification. *N*-Trifluoroacetyl and *N*-pentafluoropropionyl amino acid *iso*-propyl esters were prepared according to the same procedure as in the case of ethyl esters except for the higher concentration of hydrochloric acid in 2-propanol (20%) and longer heating at the esterification step (1 h). To prepare a 15% solution of hydrochloric acid in ethanol, 6 ml of acetyl chloride was slowly added to a cooled 40 ml of dry ethanol upon stirring.

***N*-alkoxycarbonyl alkyl amide derivatives.** *N*-ethoxycarbonyl propyl amides of the amino acids were prepared according to Abe et al. [188,191].

***N*-Boc-*L*- or *D*-valine (1).** Triethylamine (92 ml, 0.658 mol) was added to a solution of *L*-valine (70.0 g, 0.598 mol) in water (500 ml) followed by a dropwise addition of a solution of di-*tert*-butyldicarbonate (Boc₂O) (157g, 0.722 mol) in dioxane (400 ml). The reaction mixture was stirred at room temperature overnight. The solution was concentrated to about half of the volume *in vacuo* and adjusted to pH 2 with HCl 3*M*. The mixture was extracted with ethyl acetate (4 x 200 ml). The combined organic phase was washed with brine and dried over anhydrous Na₂SO₄. The filtered solution was concentrated *in vacuo* to give **1** as a colorless oil (122.4 g, yield 94%). ¹H NMR (400 MHz, CDCl₃) δ (ppm): 0.93 (d, 3H, -CH(CH₃)₂, ³J=6.82Hz), 1.00 (d, 3H, -CH(CH₃)₂, ³J=6.82Hz), 1.46 (s, 9H, -C(CH₃)₃), 2.21 (m, 1H, CH-CH(CH₃)₂), 4.05 (br m, CH-CH(CH₃)₂), 4.26 (dd, CH-CH(CH₃)₂, ³J_{CH-CH}=4.55Hz, ³J_{CH-NH}=8.84Hz), 5.08 (d, NH, ³J_{NH-CH}=8.84Hz), 6.23 (d, NH), 10.04 (s, 1H, OH). ¹³C NMR (100MHz, CDCl₃) δ (ppm): 17.1 (-CH(CH₃)₂), 18.7 (-CH(CH₃)₂), 28.2 (-C(CH₃)₃), 30.7 (CH(CH₃)₂), 58.2 (NH-CH-C=O), 79.9 (-C(CH₃)₃), 155.6 (C=O), 176.9 (C=O).

***N*-Boc-*L*- or *D*-valine-*tert*-butylamide (2).** A solution of *N,N'*-dicyclohexylcarbodiimide (DCC) (116 g, 0.56 mol) in dichloromethane (100 ml) was added slowly to the solution of *N*-Boc-*L*-valine **1** (122 g, 0.56 mol) in dry dichloromethane (250 ml). The solution was cooled to 5°C and *tert*-butylamine (68 ml, 0.56 mol) was added

Experimental part

dropwise. After mechanical stirring (a solid bulk precipitate is formed(!)) at room temperature for 5 h the solution was diluted with dichloromethane and the urea produced was filtered off. The product was dissolved in ethyl acetate (200 ml) and heated up to 60°C. The non-dissolved urea was filtered off. This procedure was repeated two times followed by addition of *n*-hexane to the residue and cooling to 5°C overnight. The crystalline precipitate was filtered out and washed several times with *n*-hexane followed by drying *in vacuo* to give **2** as colorless solid (71.7 g, yield 47%). ¹H NMR (400 MHz, CDCl₃) δ (ppm): 0.84 (d, 3H, -CH(CH₃)₂, ³J= 6.82 Hz), 0.88 (d, 3H, -CH(CH₃)₂, J= 6.56 Hz), 1.28 (s, 9H, -NH-C(CH₃)₃), 1.37 (s, 9H, -O-C(CH₃)₃), 1.98 (m, 1H, -CH(CH₃)₂), 3.66 (dd, 1H, -NH-CH-CO, ³J= 7.58 and 7.83Hz), 5.07 (d, 1H, NH-CH, ³J=7.58Hz), 5.72 (br s, 1H, NH-C(CH₃)₃). ¹³C NMR (100 MHz, CDCl₃) δ (ppm): 18.6 (-CH(CH₃)₂), 19.8 (-CH(CH₃)₂), 28.9 (-C(CH₃)₃), 29.3 (-C(CH₃)₃), 31.6 (-CH(CH₃)₂), 51.9 (-NH-C(CH₃)₃), 61.0 (NH-CH-C=O), 80.2 (OC(CH₃)₃), 156.5 (C=O), 171.3 (C=O).

L- or D- Valine-*tert*-butylamide (3). Trifluoroacetic acid (TFA) (112 ml, 1.45 mol) was added at 0°C to a solution of *N*-Boc-*L*- or *D*-valine-*tert*-butylamide (**2**) (63.8 g, 0.234 mol) in dichloromethane (100 ml). The reaction mixture was stirred at room temperature for 2.5 h. The solvent and the unreacted acid were removed from the solution *in vacuo* followed by dissolution of the residue in water and washing with diethyl ether. The water fractions were collected and neutralized with NaHCO₃ (or aqueous ammonia) followed by extraction with dichloromethane. The collected dichloromethane fractions were dried with Na₂SO₄. The solvent was evaporated *in vacuo* to give a colorless oil which subsequently crystallized into a transparent crystalline mass of **3** (22.3 g, yield 67%). ¹H NMR (400 MHz, CDCl₃) δ (ppm): 0.76 (d, 3H, -CH(CH₃)₂, ³J=7.08Hz), 0.91 (d, 3H, -CH(CH₃)₂, ³J=6.82Hz), 1.29 (s, 9H, -C(CH₃)₃), 1.74 (s, 1H, NH), 2.21 (m, 1H, CH-CH(CH₃)₂), 3.07 (d, 1H, CH-C=O, ³J=3.29Hz). ¹³C NMR (100MHz, CDCl₃) δ (ppm): 18.6 (-CH(CH₃)₂), 22.2 (-CH(CH₃)₂), 31.3 (C(CH₃)₃), 33.3 (-CH(CH₃)₂), 53.0 (C(CH₃)₃), 62.9 (H₂N-CH), 175.7 (C=O).

***N*-(Undec-10-enoyl)-*L*-valine-*tert*-butylamide (4).** *L*-Valine-*tert*-butylamide (1.11 g, 6.43 mmol) was dissolved in anhydrous tetrahydrofuran (THF) (5 ml) in a two-necked 100 ml flask. Methyloxirane (1.35 ml, 19.29 mmol) (CAUTION! Suspected carcinogen) was added to the solution [228]. After cooling the reaction mixture to 0°C, a solution of undec-10-enoyl chloride (1.45 ml, 6.75 mmol) in anhydrous THF (5 ml) was added dropwise to the reaction mixture followed by heating up to room temperature. After stirring the reaction

mixture for one hour the solvent was removed under reduced pressure. The resulting oil was dissolved in ethyl acetate and was washed with water five times followed by drying with sodium sulphate and concentration under vacuum. The crude **4** selector was purified by column chromatography (ethyl acetate : *n*-hexane (1:3), $R_f = 0.34$ (ethyl acetate : *n*-hexane (1:2)) followed by dissolving the product in ethyl acetate and washing it successively with aqueous ammonia, brine (2x), hydrochloric acid (1M) and brine (2x). The ethyl acetate fraction was dried with sodium sulphate and the solvent was removed under reduced pressure to give 2.1 g of the pure product. ^1H NMR (400 MHz, CDCl_3) δ (ppm): 0.86 (t, $(\text{CHCH}_3)_2$), 1.21 (br. s, CH_2), 1.27 (s, $\text{C}(\text{CH}_3)_3$), 1.55 (m, $\text{CH}_2\text{CH}_2\text{CO}$), 1.96 (m, $\text{CH}(\text{CH}_3)_2 + \text{CHCH}_2$), 2.14 (t, $^3J = 7.6$ Hz, CH_2CO), 4.04 (dd, $^3J_{\text{NH-CH}} = 8.8$ Hz, $^3J_{\text{CH-CH}} = 7.58$ Hz, NHCH), 4.9 (m, $\text{CH}_2=\text{CH}$), 5.7 (m, $\text{CH}_2=\text{CH}$), 5.8 (s, NHC), 6.2 (d, $^3J_{\text{NH-CH}} = 8.8$ Hz, NH-CH). ^{13}C NMR (100MHz, CDCl_3) δ (ppm): 18.8 ($\text{CH}(\text{CH}_3)_2$), 19.5 ($\text{CH}(\text{CH}_3)_2$), 26.2 (CH_2), 29.1 ($\text{C}(\text{CH}_3)_3$), 29.3 (CH_2), 29.4(CH_2), 29.6(CH_2), 29.66(CH_2), 29.7(CH_2), 31.8 ($\text{CH}(\text{CH}_3)_2$), 34.2 (CHCH_2), 37.2 (CH_2CO), 51.9 ($\text{C}(\text{CH}_3)_3$), 59.3 (NHCH), 114.5 ($\text{CH}_2=\text{CH}$), 139.6 ($\text{CH}_2=\text{CH}$), 170.95 ($\text{C}=\text{O}$), 173.6 ($\text{C}=\text{O}$). HR-ESI-MS (positive mode, m/z) for **4**: $[\text{M}+\text{H}]^+_{\text{exp}} = 339.30062$, $\Delta m_{\text{theor-exp}} = 0.06$ ppm; $[\text{M}+\text{Na}]^+_{\text{exp}} = 361.28240$, $\Delta m_{\text{theor-exp}} = 0.42$ ppm.

***N*-Bromoacetyl-*L*-valine-*tert*-butylamide (5).** Under a dinitrogen atmosphere, methyloxirane (CAUTION! Suspected carcinogen) (6.15 ml, 87.9 mmol) was added to a solution of dry *L*-valine-*tert*-butylamide **3** (5.0 g, 29.0 mmol) in dry tetrahydrofuran (THF) (30 ml) and the reaction mixture was cooled to 0°C. A solution of bromoacetyl chloride (3.3 ml, 37.6 mmol) in 15 ml of dry tetrahydrofuran was added slowly to the reaction mixture upon stirring. After the addition, the reaction mixture was allowed to heat up to room temperature and it was stirred for one hour. The residue obtained after concentration of the reaction mixture was recrystallized from *n*-hexane/ethyl acetate (or acetonitrile). The precipitated white-yellowish crystalline substance was collected to afford 8.3 g of **5** (yield 94%). TLC (ethyl acetate – *n*-hexane, 1:1 v/v): R_f 0.66. ^1H NMR (400 MHz, CDCl_3) δ (ppm): 0.88 (d, 3H, $-\text{CH}(\text{CH}_3)_2$, $^3J = 3.28\text{Hz}$), 0.90 (d, 3H, $-\text{CH}(\text{CH}_3)_2$, $^3J = 3.03\text{Hz}$), 1.29 (s, 9H, $-\text{C}(\text{CH}_3)_3$), 2.0 (m, 1H, $-\text{CH}(\text{CH}_3)_2$), 3.82 (s, 2H, CH_2Br), 3.99 (dd, 1H, NH-CH , $^3J = 6.82\text{Hz}$ and 8.59Hz), 5.47 (s, 1H, $-\text{NH-C}(\text{CH}_3)_3$), 6.96 (d, 1H, $-\text{NH-CH}$, $J = 8.6\text{Hz}$). ^{13}C NMR (100MHz, CDCl_3) δ (ppm): 18.6 ($-\text{CH}(\text{CH}_3)_2$), 19.4 ($-\text{CH}(\text{CH}_3)_2$), 29.1 ($\text{C}(\text{CH}_3)_3$), 29.3 (Br-CH_2), 32.0 ($-\text{CH}(\text{CH}_3)_2$), 52.2 ($\text{C}(\text{CH}_3)_3$), 59.8 (HN-CH), 165.9 ($\text{C}=\text{O}$), 169.7 ($\text{C}=\text{O}$).

C-dec-9-enylresorcinarene (6). The synthesis of **6** was carried out according to a modified procedure [230]. 12 N hydrochloric acid (32 ml) was added to a solution of resorcinol (22.0 g, 0.2 mol) and 10-undecenal (33.6 g, 0.2 mol) in ethanol (200 ml) at 0°C over 10 min. The mixture was stirred at 60°C for 16 h. The red oil was poured into well-stirred demineralised water (600 ml). The orange precipitate was filtered off and washed thoroughly with hot water (80°C, 6 l) followed by drying. The solid product was dissolved in acetonitrile at 40°C and left at room temperature for 3 h. The precipitated dark oil was removed by decanting the solution. The yellow solution was concentrated approximately by one third and cooled to 0°C. After precipitation of another part of the dark oil the solvent was decanted. The procedure was repeated until no more dark oil was formed. The solvent was removed under reduced pressure to afford 10 g (22%) of **6**. It should be mentioned that crystallization of the crude product from acetonitrile, cyclohexane or light petroleum was not helpful for removing by-products. ¹H NMR (400 MHz, CDCl₃): 1.3 and 1.22 (two s, 48H, -CH₂-), 1.94-2.00 (q, 8H, -CH₂-CH-Ar, ³J=8Hz), 2.13 (m, 8H, -CH₂-CH=CH₂), 4.21-4.25 (t, 4H, Ar-CH-, ³J=8Hz), 4.84-4.94 (dd, 8H, -CH=CH₂), 5.69-5.78 (m, 4H, -CH=CH₂), 6.04 (s, 4H, Ar-H), 7.12 (s, 4H, Ar-H), 9.2-9.5 (br s, 8H, Ar-OH). ¹³C NMR (100MHz, CDCl₃) δ (ppm): 150.6, 139.2, 124.8, 123.8, 114.1, 102.7, 33.8, 33.2, 33.0, 30.9, 29.7, 29.5, 29.1, 29.0, 28.0. HR-ESI-MS (negative mode, m/z): [M-H]⁻_{theor}=1039.70324, [M-H]⁻_{exp}=1039.70378, Δm/z=0.5 ppm.

Octakis-O-(N-acetyl-D-valine-tert-butylamide)-C-decenyl-resorcinarene (D').

The synthesis of the selector **D'** was carried out according to a known procedure [126] using *N*-bromoacetyl-*D*-valine-*tert*-butylamide (**5**) which was attached to *C*-dec-9-enylresorcinarene (**6**). As the product was not soluble in diethyl ether, it was dissolved in ethyl acetate at 60°C followed by filtration from the salts. The solvent was removed under reduced pressure and the residue was washed with diethyl ether three times followed by decantation of the diethyl ether and by drying the obtained crystalline mass. The produced yellowish crystalline solid was subjected to column chromatography (eluent: ethyl acetate, R_f 0.2) to give pure compound **D'** (yield 20-40%). TLC: eluent ethyl acetate, R_f 0.2. ¹H NMR (400 MHz, CDCl₃): 0.86 (m, CH(CH₃)₂), 1.23 (br s, C(CH₃)₃ and -CH₂- of the spacer), 1.77 and 1.93 (br m, CH(CH₃)₃, CH₂-CH=CH₂ and CH₂-CH-Ar), 4.00 (m, Br-CH₂), 4.22 (br s, CH-Ar) 4.51 (br t, NH-CH), 4.87 (m, -CH=CH₂), 5.7 (m, -CH=CH₂), 6.12 (br m, aromatic protons), 6.73 (br s, NH), 7.70 (br s, NH). HR-ESI-MS (positive mode, m/z) for **D'**: [M+2H]²⁺_{theor}= 1369.97399, [M+H+Na]²⁺_{theor}= 1380.96342, [M+2Na]²⁺_{theor}= 1391.95439,

$[M+H+NH_4]^{2+}_{\text{theor}} = 1378.48572$; $[M+2H]^{2+}_{\text{exp}} = 1369.97633$, $[M+H+Na]^{2+}_{\text{exp}} = 1380.96822$, $[M+2Na]^{2+}_{\text{exp}} = 1391.95891$; $\Delta_{\text{theor-exp}}[M+2H]^{2+} = 1.7$ ppm, $\Delta_{\text{theor-exp}}[M+H+Na]^{2+} = 3.5$ ppm, $\Delta_{\text{theor-exp}}[M+2Na]^{2+} = 3.2$ ppm.

Octakis-*O*-(*N*-acetyl-*L*-valine-*tert*-butylamide)-*C*-decenyl-resorcinarene (L'**).** The synthesis of **L'** was performed analogously to that of **D'** using *N*-bromoacetyl-*L*-valine-*tert*-butylamide. HR-ESI-MS (positive mode, *m/z*) for **L'**: $[M+2H]^{2+}_{\text{exp}} = 1369.97296$, $[M+H+NH_4]^{2+}_{\text{exp}} = 1378.48627$, $[M+H+Na]^{2+}_{\text{exp}} = 1380.96069$; $\Delta_{\text{theor-exp}}[M+2H]^{2+} = 0.75$ ppm, $\Delta_{\text{theor-exp}}[M+H+NH_4]^{2+} = 0.4$ ppm, $\Delta_{\text{theor-exp}}[M+H+Na]^{2+} = 2.0$ ppm.

Monokis-2-*O*-undec-10-enyl-permethyl- β -cyclodextrin (CD**).** Preparation of monokis-2-*O*-(undec-10-enyl)- β -cyclodextrin and the subsequent permethylation leading to the selector **CD** (monokis-2-*O*-undec-10-enyl-permethyl- β -cyclodextrin) was carried out according to a described procedure[47,124,125] using 10-undecenylbromide instead of 7-octenylbromide. Selector **CD** was purified by column chromatography (ethanol : toluene, 1 : 16 v/v). *R_f* = 0.43 (ethanol : toluene, 1 : 8 v/v). Monokis-2-*O*-(undec-10-enyl)- β -cyclodextrin: $^1\text{H NMR}$ (400 MHz, DMSO-*d*₆): 1.26 (s, -CH₂- of the spacer), 1.36 (m, -CH₂- of the spacer), 1.50 (m, 2H, -CH₂-CH₂-O-), 2.00 (q, 2H, -CH₂-CH=CH₂, $^3\text{J}=7.08\text{Hz}$, $^3\text{J}=6.82\text{Hz}$), 3.2-3.7 (m), 4.45 (quin, 7H), 4.83 (s, 7H), 4.95 (s, 1H,), 4.9-5.0 (m, 2H, -CH=CH₂), 5.7-5.9 (m). HR-ESI-MS (positive mode, *m/z*) for monokis-2-*O*-(undec-10-enyl)- β -cyclodextrin: $[M+Na]^+_{\text{exp}} = 1309.51482$, $\Delta_{\text{theor-exp}} = 0.5$ ppm. **CD**: $^1\text{H NMR}$ (400 MHz, CDCl₃): 1.21 (s, -CH₂- of the spacer), 1.28 (m, -CH₂- of the spacer), 1.54 (m, 2H, -CH₂-CH₂-O-), 1.96 (q, 2H, -CH₂-CH=CH₂, $^3\text{J}=7.58\text{Hz}$, $^3\text{J}=6.82\text{Hz}$), 3.11-3.14 (dd, 6H, CH-2, $^3\text{J}=9.60\text{Hz}$, $^3\text{J}=2.7\text{Hz}$), 3.16-3.20 (dd, 1H, CH-2, $^3\text{J}=9.60\text{Hz}$, $^3\text{J}=3.28\text{Hz}$), 3.31 (br s, -OCH₃), 3.44 (m, -OCH₃), 3.58 (br s, -OCH₃), 3.4-3.9 (m), 4.85-4.94 (m, 2H, -CH=CH₂), 4.99 (d, 1H, CH-1, $^3\text{J}=3.53\text{Hz}$), 5.05 (d, 2H, CH-1, $^3\text{J}=3.28\text{Hz}$), 5.08 (d, 4H, CH-1, $^3\text{J}=2.6\text{Hz}$), 5.7-5.8 (m, 1H, -CH=CH₂). HR-ESI-MS (positive mode, *m/z*) for **CD** selector: $[M+Na]^+_{\text{exp}} = 1589.82987$, $\Delta_{\text{theor-exp}} = 0.9$ ppm.

Heptakis[6-*O*-(*tert*-butyldimethylsilyl)]- β -cyclodextrin. Dry (P₂O₅, 0.1 mbar, 24hrs) β -cyclodextrin (15.8 g, 13.92 mmol) was dissolved in pyridine (300ml) in a three neck flask of 1L, under dinitrogen atmosphere, under vigorous stirring (thick gel might be formed). A solution of *tert*-butyldimethylsilyl chloride (TBDMSCl) (25g, 165.65 mmol) in dry pyridine (180 mL) was added dropwise to the cooled (0°C) reaction flask over 4h. The reaction

Experimental part

mixture was stirred overnight at room temperature followed by the evaporation of the solvent under reduced pressure to give a white solid which was taken up with dichloromethane (300 ml). The dichloromethane solution was washed with a solution of KHSO₄ (250 ml, 1M), than with brine and dried over sodium sulphate. The dichloromethane layer was separated and evaporated to dryness. In order to remove residual pyridine the solid was dissolved in toluene and dried under reduced pressure several times. The residue was dried overnight to give white solid (22.3 g, yield 83%) which was used without further purification. TLC (*n*-hexane/ethanol, 3:1): R_f 0.63. The ¹H and ¹³C NMR data were in accordance with those previously reported [138,231].

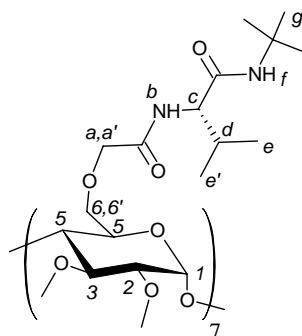
Heptakis(6-*O*-(*tert*-butyldimethylsilyl)-2,3-di-*O*-methyl)-β-cyclodextrin. NaH 60% (10.5g, 262.5 mmol) was weighed into the reaction vessel. Toluene (100 mL) was added and the mixture was stirred for some minutes before the suspension was allowed to settle and the toluene was decanted off. This procedure was repeated several times to obtain oil-free NaH. Under dinitrogen atmosphere per-6-(*tert*-butyldimethylsilyl)-β-cyclodextrin (15.2g, 7.86 mmol) was dissolved in dry THF (100 mL) and at -15°C it was added to the suspension of NaH. After 30 min the evolution of dihydrogen was ceased and methyl iodide (18 mL, 287 mmol) was added dropwise followed by stirring the reaction mixture overnight under protection from light. Cooling was maintained for the first hour of the reaction after which the suspension was allowed to warm up to room temperature. After 17 hours the reaction mixture was cooled with an ice bath and methanol was added dropwise in order to destroy the excess of NaH and methyl iodide followed by neutralization with diluted acetic acid. The solvent was removed under reduced pressure and the residue was suspended in dichloromethane. The mixture was washed with pure water and brine. The dichloromethane layer was filtered through silica gel (eluent: toluene/ethanol = 10:1). After filtration, the solvent was removed under reduced pressure. The residue was dried under vacuum overnight to give 15.6 g of the product (yield 93%). TLC (toluene/ethanol, 10:1): R_f 0.34. The ¹H and ¹³C NMR data were in accordance with those previously reported [138,231].

Heptakis(2,3-di-*O*-methyl)-β-cyclodextrin. Heptakis[6-*O*-(*tert*-butyldimethylsilyl)-2,3-di-*O*-methyl]-β-cyclodextrin (14.1 g, 6.62 mmol) was dissolved in a 250 ml flask in dry THF (190 ml). A solution of (tetrabutylammonium fluoride (TBAF) (22.3 g, 70.68 mmol) in dry THF (50 ml) was added to the reaction flask dropwise and the reaction mixture was heated and refluxed for 2.5 h. The solvent was removed under reduced pressure and the

residue was suspended in DCM. The solution was washed with brine and H₂O, dried with Na₂SO₄ and concentrated under reduced pressure overnight. The residue was purified by column chromatography on silica gel (8:1, 4:1, 1:1 DCM-MeOH, stepwise), to give 6.59 g of the product (yield 75%). TLC (DCM/EtOH, 1:1): R_f 0.63. The ¹H and ¹³C NMR data were in accordance with those previously reported [138,231].

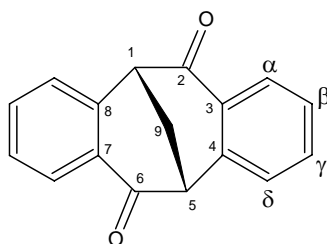
Octakis(3-*O*-butanoyl-2,6-di-*O*-*n*-pentyl)- γ -cyclodextrin (Lipodex E). For the synthesis of octakis(3-*O*-butanoyl-2,6-di-*O*-*n*-pentyl)- γ -cyclodextrin (Lipodex E) see references [88,131].

Heptakis(6-*O*-(*N*-acetyl-*L*-valine-*tert*-butylamide)-2,3-di-*O*-methyl)- β -cyclodextrin (ValDex). A solution of heptakis(2,3-di-*O*-methyl)- β -cyclodextrin (1.08 g, 0.811 mmol) in dry DMF (5 mL) was added to the NaH 60% (2.13 g, 88.92 mmol) under dinitrogen atmosphere at 0 °C and stirred until the evolution of dihydrogen was ceased. This mixture was added carefully to a solution of *N*-bromoacetyl-*L*-valine-*tert*-butylamide (**5**) (1.83 g, 6.25 mmol) at 0 °C in dry DMF (5 mL). The reaction mixture was stirred overnight at room temperature. An excess of methanol was added to the solution at 0 °C until the evolution of dihydrogen subsided. The solvent was removed under reduced pressure and the residue was dissolved in dichloromethane and washed several times with brine, water and dried with sodium sulphate. The solvent was removed under reduced pressure and the residue was purified by column chromatography on silica gel (ethyl acetate; 20:1 ethyl acetate-ethanol) to give ValDex (0.44 g, yield 20%) with ¹H NMR (600 MHz, CDCl₃, 25 °C) δ 0.90 (21H, H-e, d, J=7.4 Hz), 0.92 (21H, H-e', d, J=7.4 Hz), 1.32 (63H, H-g, s), 2.04 (7H, H-d, m), 3.18 (7H, H-2, dd, J₂₃=9.8 Hz, J₂₁=3.6 Hz), 3.49 (7H, H-3, dd, J₃₂=9.8 Hz, J₃₄=8.9 Hz), 3.50 (21H, OMe-2, s), 3.58 (7H, H-4, dd, J₄₅=9.5 Hz, J₄₃=8.9 Hz), 3.63 (21H, OMe-3, s), 3.73 (7H, H-6, br. d, J_{66'}=11.5 Hz), 3.81 (7H, H-5, br. dd, J₅₄=9.5 Hz, J_{56'}=4.0 Hz), 3.92 (7H, H-6', dd, J_{6'6}=11.5 Hz, J_{6'5}=4.0 Hz), 4.01 (7H, H-a, d, J_{aa'}=15.5 Hz), 4.08 (7H, H-a', d, J_{a'a}=15.5 Hz), 4.08 (7H, H-c, d, J_{cb}=8.8 Hz, J_{cd}=8.2 Hz), 5.15 (7H, H-1, d, J₁₂=3.6 Hz), 6.35 (7H, H-f, s), 7.56 (7H, H-b, d, J_{bc}=8.8 Hz); ¹³C NMR (150 MHz, CDCl₃, 25 °C) δ 18.9 (C-e), 19.3 (C-e'), 28.9 (C-g), 31.2 (C-d), 51.5 (CMe₃), 58.7 (OMe-2), 59.3 (C-c), 61.6 (OMe-3), 70.6 (CH₂-aa'), 70.9 (CH₂-66'), 71.2 (C-5), 80.9 (C-4), 81.8 (C-3), 82.3 (C-2), 99.6 (C-1), 170.2 (CONH-b), 170.3 (CONH-f).



Valdex

2,3:6,7-dibenzobicyclo[3.3.1]nona-2,6-diene-4,8-dione (28). Compound **28** was prepared by a modified procedure [223-225] as follows.



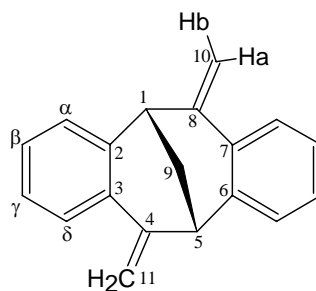
Benzyl cyanide (0.4 mol), diiodomethane (0.2 mol) and powdered sodium hydroxide (0.4 mol) were mixed and heated to 170°C under stirring for 30 min. To the cooled mixture of crude 1,3-diphenylglutarodinitrile (dark oil), dissolved in ethanol (250 ml), a solution of potassium hydroxide (105 g) in water (300 ml) was added and the resulting mixture was heated at 70°C for 20 h. The reaction mixture was diluted with water (500 ml) and washed with diethyl ether. The aqueous layer was acidified with concentrated hydrochloric acid and extracted with ethyl acetate. The extract was washed with brine, dried over sodium sulfate, and the solvent was removed under reduced pressure. The crude mixture of (±)- and meso-1,3-diphenylglutaric acids was obtained as a dark oil. The mixture of acids was dissolved in concentrated sulfuric acid and heated to 85°C with stirring for 1hr. The reaction mixture was poured onto ice and extracted with ethyl acetate. Undissolved solid residue was washed with water and recrystallized from methanol several times to give pure **28** as colorless needles. On vacuum-assisted evaporation of ethyl acetate from the extract a colorless solid was obtained which was recrystallized twice from methanol to yield the second portion of **28**. The two portions were combined to give 19.3 g of **28** (mp, 146-148°C).

The crystalline racemic compound of **28** (colorless needles, mp 146-148°C) was obtained by slow evaporation of its near-saturated solutions in various organic solvents at -6°C, 4°C, 23°C and from *n*-octane up to 90°C. The best single crystals of **28** (up to 43.4 mg) were obtained by slow evaporation of an acetone solution of **28** at room temperature.

The crystalline conglomerate of **28** (colorless plates, mp 160-190°C) was obtained by slow evaporation of its near-saturated *n*-octane solution at 100°C and higher.

^1H NMR 500MHz (CDCl_3) δ : 2.99(t., 2H, 9- CH_2 , $^3\text{J}=3.00$ Hz), 4.01(t., 2H, 1,5-CH, $^3\text{J}=3.00$ Hz), 7.36(m., 2H, 2 β -H, $^3\text{J}_{\alpha\beta}=7.80$ Hz, $^3\text{J}_{\beta\gamma}=7.39$, $^4\text{J}_{\beta\delta}=1.24$ Hz), 7.46(m., 2H, 2 δ -H, $^3\text{J}_{\gamma\delta}=7.74$, $^5\text{J}_{\alpha\delta}<0.4$ Hz), 7.50(m., 2H, 2 γ -H, $^4\text{J}_{\alpha\gamma}=1.51$ Hz), 7.96(m., 2H, 2 α -H); ^{13}C NMR 125MHz { ^1H } (CDCl_3) δ : 32.27 (9-C), 48.77(1,5-C), 128.23(α -C), 128.72(β -C), 128.76(δ -C), 128.80(3,7-C), 134.44(γ -C), 140.01(4,8-C), 194.37(2,6-C).

4,8-bis(methylene)-2,3:6,7-dibenzobicyclo[3.3.1]nona-2,6-diene (29). Compound **29** was obtained using a well-known procedure [224] *via* dimethyldiol without additional chromatography; the overall yield was 80%. The melting point was 124°C for a separate single crystal obtained by crystallization from methanol.



^1H NMR (500MHz, CDCl_3) δ : 2.36 (t., 2H, 9- CH_2 , ^3J 3.09 Hz) 3.90 (t., 2H, 1,5-CH, ^3J 3.09 Hz), 5.27 (br.s., 2H, 10,11-CHb), 5.46 (br.s., 2H, 10,11-CHa), 7.12 (t.d., 2H, 2 γ -CH, ^3J 7.6 Hz, ^4J 1.5 Hz), 7.18 (t.d., 2H, 2 β -CH, ^3J 7.6 Hz, ^4J 1.5 Hz), 7.30 (d.d., 2H, 2 α -CH, ^3J 7.6 Hz, ^4J 1.5 Hz), 7.56 (d.d., 2H, 2 δ -CH, ^3J 7.6 Hz, ^4J 1.5 Hz). ^{13}C {H} NMR (125MHz, CDCl_3) δ : 30.78 (9-C), 44.02 (1,5-C), 106.51 (10,11-C), 124.40 (δ -C), 126.83 (γ -C), 128.13 (β -C), 129.02 (α -C), 131.69 (3,7-C), 138.71 (2,6-C), 147.26 (4,8-C).

General procedure for the immobilization of chiral selectors to dimethylhydromethylpolysiloxane by platinum-catalyzed hydrosilylation. Platinum-catalyzed hydrosilylation was performed as follows. (a) In a dinitrogen atmosphere, 0.1 ml of a solution of hexachloroplatinic acid (1 mg) in anhydrous THF (1 ml) was added to a mixture of a chiral selector(s) and dimethylhydromethylpolysiloxane dissolved in anhydrous THF. The reaction mixture was ultrasonicated at 50°C for 24 h. (b) The reaction was carried out by refluxing the mixture of the dimethylhydromethylpolysiloxane and the chiral selector(s) in a mixture of anhydrous THF and toluene (1:1) for 24 or 48h. The completion of the reaction was monitored by the disappearing of the olefinic signals in the NMR spectra. The

percentage of a selector in the final polymer was monitored by NMR and by elemental analysis. Purification of the crude polymer and, in particular, removing the rest of the catalyst was performed by passing the polymer through a short column of activated charcoal followed by gel-filtration on Sephadex LH-20 (2x). It should be pointed out that avoiding the purification step leads to partial or complete depletion of derivatized Cys, Ser, Met and Tyr during GC experiments.

8.3 Preparation of the CSPs

Chirasil-Dex. 20% (w/w) of the permethyl- β -cyclodextrin selector in dimethylhydromethylpolysiloxane was used.

Chirasil-*L*(D)-Val-C₁₁. 30% (w/w) of the *N*-(undec-10-enoyl)-*L*-valine-*tert*-butylamide (**DA** selector) in dimethylhydromethylpolysiloxane was used.

Chirasil-DexVal. (a) 20% (w/w) of the **CD** and 15% (w/w) of the **DA** selector were used. (b) In the case of the binary CSP used for the improvement of the enantioseparation of Pro (Section 1.1), 8% (w/w) of the **CD** and 24% (w/w) of the **DA** selectors were used.

Chirasil-CalixDex. (a) 15% (w/w) of the **D'** (or **L'**) and 20% (w/w) of the **CD** selector were used.

Chirasil- γ -Dex. 20% of octakis(3-*O*-butanoyl-2,6-di-*O*-*n*-pentyl)- γ -cyclodextrin (Lipodex E) was dissolved in PS-255 polymer [88,131].

Chirasil-Val(γ -Dex). To prepare the binary-selector CSP Chirasil-Val(γ -Dex), 20 mg of a mixture of 8% of the neat selector Lipodex E (w/w) and 92% (w/w) of the Chirasil-*L*-Val-C₁₁ CSP was dissolved in 5 ml of dichloromethane/*n*-pentane (1:1 v/v). After shaking for 5 min the mixture was used for the coating of the column by the static method. Continuous use of the Chirasil-Val(γ -Dex) CSP with a temperature program (up to 170°C) for two months followed by heating of the column at 120°C for 1,5 months revealed no decrease in the enantioselectivity and efficiency of the CSP.

Reference stationary phase. The reference column was coated with dimethylhydromethyl(12%)polysiloxane. Coating solution: 4mg/ml of the polymer in dichloromethane or ether or a 1:1 mixture of dichloromethane with *n*-pentane.

Supplementary material 1: Retention data of the enantioseparation of Ala-ECPA and Val-ECPA on Chirasil-*L*-Val-C₁₁ chiral stationary phase. Column: 20m x 0.25mm i.d. x 0.25µm film thickness; carrier gas: dihydrogen; C16 – *n*-hexadecane, C18- *n*-octadecane.

<i>T</i> °C	P, kPa	Configuration of the first eluted enantiomer	<i>k</i> ₁	α_{app}	<i>r</i> ^o - relative retention on ref. column (standard C16)	<i>r</i> ^o - relative retention on ref. column (standard C18)	<i>r</i> ₁ - relative retention of the first eluted enantiomer (standard C16)	<i>r</i> ₂ - relative retention of the second eluted enantiomer (standard C16)	<i>r</i> ₁ - relative retention of the first eluted enantiomer (standard C18)	<i>r</i> ₂ - relative retention of the second eluted enantiomer (standard C18)	<i>R</i> ₁ - retention increment of the first eluted enantiomer (standard C16)	<i>R</i> ₂ - retention increment of the second eluted enantiomer (standard C16)	<i>R</i> ₁ - retention increment of the first eluted enantiomer (standard C18)	<i>R</i> ₂ - retention increment of the first eluted enantiomer (standard C18)	α_{assoc} (standard C16)	α_{assoc} (standard C18)
Ala-ECPA																
100	100	D	218.08	1.053	0.598	0.168	6.875	7.238	1.987	2.092	10.503	11.110	10.809	11.432	1.058	1.058
110	100	D	115.77	1.024	0.579	0.175	6.210	6.360	1.918	1.965	9.717	9.976	9.982	10.248	1.027	1.027
120	50	DL	60.56	1.000	0.593	0.190	5.706	5.706	1.863	1.863	8.621	8.621	8.810	8.810	1.000	1.000
130	50	L	34.56	1.016	0.588	0.200	5.182	5.264	1.785	1.813	7.813	7.952	7.920	8.060	1.018	1.018
140	50	L	20.63	1.026	0.605	0.218	4.767	4.893	1.725	1.771	6.883	7.091	6.928	7.138	1.030	1.030
150	50	L	12.72	1.038	0.618	0.235	4.397	4.564	1.668	1.731	6.110	6.379	6.106	6.375	1.044	1.044
160	50	L	8.12	1.044	0.624	0.249	4.079	4.260	1.619	1.691	5.534	5.823	5.511	5.800	1.052	1.052
170	50	L	5.87	1.046	0.634	0.265	3.670	3.841	1.563	1.636	4.787	5.056	4.909	5.184	1.056	1.056
180	50	L	3.98	1.050	0.628	0.275	3.404	3.575	1.506	1.582	4.416	4.688	4.482	4.758	1.062	1.061
190	50	L	2.74	1.049	0.647	0.296	3.185	3.342	1.470	1.543	3.923	4.165	3.971	4.215	1.062	1.062
200	50	L	1.94	1.046	0.665	0.316	2.934	3.069	1.433	1.499	3.416	3.618	3.538	3.746	1.059	1.059
Val-ECPA																
100	100	D	600.82	1.051	1.125	0.317	18.941	19.914	5.473	5.755	15.843	16.709	16.291	17.180	1.055	1.055
110	100	D	295.45	1.012	1.070	0.323	15.847	16.030	4.895	4.952	13.809	13.981	14.175	14.351	1.012	1.012
120	50	L	141.06	1.011	1.029	0.330	13.291	13.432	4.338	4.385	11.910	12.048	12.163	12.304	1.012	1.012
130	50	L	74.67	1.035	1.005	0.342	11.197	11.585	3.856	3.990	10.144	10.530	10.279	10.669	1.038	1.038
140	50	L	41.45	1.053	0.991	0.357	9.575	10.082	3.466	3.649	8.663	9.174	8.719	9.233	1.059	1.059
150	50	L	23.98	1.067	0.984	0.373	8.294	8.850	3.145	3.356	7.433	7.998	7.428	7.993	1.076	1.076
160	50	L	14.43	1.077	0.984	0.392	7.246	7.801	2.876	3.096	6.363	6.926	6.338	6.899	1.089	1.089
170	50	L	9.82	1.080	0.979	0.408	6.135	6.628	2.613	2.823	5.266	5.770	5.398	5.913	1.096	1.095
180	50	L	6.27	1.083	0.962	0.421	5.363	5.807	2.374	2.570	4.576	5.037	4.644	5.112	1.101	1.101
190	50	L	4.12	1.080	0.966	0.442	4.783	5.165	2.208	2.384	3.951	4.346	3.999	4.398	1.100	1.100
200	50	L	2.79	1.076	0.970	0.461	4.217	4.540	2.060	2.218	3.347	3.679	3.468	3.809	1.099	1.099

Supplementary material 2: Retention data of the enantioseparation of Leu-TFA-Et on Chirasil- β -Dex chiral stationary phase. Column: 10m or 50m x 0.25mm i.d. x 0.25 μ m film thickness; carrier gas: dihydrogen; C10 – *n*-decane, C12- *n*-dodecane.

$T^{\circ}\text{C}$	P(kPa)	Configuration of the first eluted enantiomer	k_1	α_{app}	r° - relative retention on ref. column (standard C10)	r° - relative retention on ref. column (standard C12)	r_1 - relative retention of the first eluted enantiomeron (standard C10)	r_2 - relative retention of the second eluted enantiomeron (standard C10)	r_1 - relative retention of the first eluted enantiomeron (standard C12)	r_2 - relative retention of the second eluted enantiomeron (standard C12)	R_1 - retention increment of the first eluted enantiomeron (standard C10)	R_2 - retention increment of the second eluted enantiomeron (standard C10)	R_1 - retention increment of the first eluted enantiomeron (standard C12)	R_2 - retention increment of the first eluted enantiomeron (standard C12)	α_{assoc} (standard C10)	α_{assoc} (standard C12)
10m-column																
25	50	D	905.88	1.138	16.079	2.193										
30	50	D	575.07	1.119	7.130	1.049	12.875	14.412	1.658	1.855	0.806	1.021	0.581	0.769	1.267	1.325
35	50	D	374.72	1.091	6.501	1.017	11.046	12.051	1.528	1.667	0.699	0.854	0.502	0.639	1.221	1.272
40	50	D	246.96	1.063	5.977	0.988	9.621	10.229	1.418	1.507	0.610	0.711	0.434	0.525	1.167	1.209
50	50	D	114.40	1.034	5.179	0.952	7.752	8.012	1.279	1.322	0.497	0.547	0.344	0.389	1.101	1.131
60	50	-	57.51	1.000	4.537	0.919	6.488	6.488	1.192	1.192	0.430	0.430	0.297	0.297	1.000	1.000
70	50	-	29.76	1.000	4.024	0.892	5.461	5.461	1.108	1.108	0.357	0.357	0.242	0.242	1.000	1.000
80	50	-	16.39	1.000	3.619	0.871	4.694	4.694	1.048	1.048	0.297	0.297	0.204	0.204	1.000	1.000
90	50	-	9.36	1.000	3.267	0.856	4.142	4.142	1.006	1.006	0.268	0.268	0.175	0.175	1.000	1.000
50m-column																
100	100	L	6.03	0.985	3.028	0.845	3.634	3.690	0.949	0.963	0.200	0.219	0.123	0.140	0.916	0.877
110	100	L	3.77	0.986	2.792	0.832	3.327	3.375	0.936	0.950	0.191	0.209	0.125	0.141	0.918	0.886
120	100	L	2.42	0.987	2.596	0.823	3.058	3.098	0.926	0.938	0.178	0.193	0.126	0.141	0.921	0.896
130	100	L	1.62	0.990	2.425	0.815	2.844	2.875	0.921	0.930	0.173	0.185	0.130	0.142	0.933	0.916
140	100	-	1.11	1.000	2.286	0.810	2.665	2.665	0.917	0.917	0.166	0.166	0.133	0.133	1.000	1.000
150	100	-	0.78	1.000	2.163	0.801	2.503	2.503	0.912	0.912	0.157	0.157	0.139	0.139	1.000	1.000
160	100	-	0.57	1.000	2.054	0.801	2.389	2.389	0.911	0.911	0.163	0.163	0.137	0.137	1.000	1.000
170	100	-	0.42	1.000	2.015	0.798	2.223	2.223	0.899	0.899	0.103	0.103	0.127	0.127	1.000	1.000
180	100	-	0.32	1.000	1.887	0.797	2.101	2.101	0.893	0.893	0.114	0.114	0.120	0.120	1.000	1.000

The phase ratios determined for CSPs (Chapter 5) QN100, QN99, QN95, QN87, QN74, QN48 and QD100 are 2.495, 2.528, 2.595, 2.401, 2.528, 2.528 and 2.463, respectively.

Conclusions

Combining the enantioselectivities of different selectors. Theoretical and experimental investigation aimed at the combination of two different chiral selectors in the same polymeric matrix in order to expand the enantioselective properties of the single-selector CSPs was performed. Several new binary-selector CSPs were synthesized. Thorough GC investigation of the binary- and the single-selector CSPs has been performed.

Thus, a modified convenient way for the synthesis of the valine-diamide CSP (Chirasil-Val-C₁₁) was developed. The diamide chiral selector used in Chirasil-Val-C₁₁ was chemically attached to a polysiloxane together with another versatile chiral selector, permethylated- β -cyclodextrin, to give a new binary-selector CSP, Chirasil-DexVal. This CSP possessed both the enantioselectivity of Chirasil-Val-C₁₁ towards α -amino acid derivatives and the enantioselectivity of the permethylated- β -cyclodextrin selector towards underivatized alcohols, ketones and hydrocarbons. Such unification of the enantioselectivity within the same CSP can be important for the search of homochirality in space in the programs Rosetta, Titan, ExoMars etc. [48,192,232-234] and for the routine analyses of different classes of racemates carried out in analytical laboratories. It was also shown that the presence of a small amount of the permethylated- β -cyclodextrin selector in Chirasil-Val-C₁₁ could significantly improve the enantioseparation of proline which represented a problematic amino acid on the diamide CSPs.

Similarly to the first approach, the valine-diamide moiety was chemically linked to a resorcin[4]arene to produce a macromolecular resorcinarene-based chiral selector possessing an aromatic cavity. This selector was synthesized in both enantiomerically pure forms which were combined with permethylated- β -cyclodextrin selector by simultaneous linking them to a polysiloxane by means of platinum-catalyzed hydrosilylation. A comprehensive gas-chromatographic investigation of the produced diastereomeric binary-selector CSPs Chirasil-*L*-CalixDex and Chirasil-*D*-CalixDex was performed. In order to analyse the influence of the presence of the diamide selector on the enantioselectivity of the cyclodextrin selector, a mixed ternary-selector CSP containing the same cyclodextrin selector and the *racemic* mixture of the resorcinarene-based valine-diamide chiral selectors has been prepared and investigated. An unfavourable effect of the racemic selector still possessing strong interactions with the selectands was observed.

Combination of the enantioselective properties of octakis(3-*O*-butanoyl-2,6-di-*O*-*n*-pentyl)- γ -cyclodextrin (Lipodex E) and Chirasil-Val-C₁₁ has been realized by doping the

Conclusions

Chirasil-Val-C₁₁ CSP with the non-polymeric selector Lipodex E. The resulting binary-selector CSP Chirasil-Val(γ -Dex) was found to have a greatly improved enantioselectivity toward proline and aspartic acid (as *N*-trifluoroacetyl ethyl or methyl esters) in comparison to that of the single-selector CSP Chirasil-Val-C₁₁. The presence of the cyclodextrin selector in Chirasil-Val(γ -Dex) extended the scope of gas-chromatographic enantioseparations achievable on Chirasil-Val-C₁₁ to underivatized alcohols, terpenes and other chiral compounds that are exclusively enantioseparated on Lipodex E.

As another approach, the *L*-valine-diamide moiety was chemically attached directly to heptakis[2,3-di-*O*-methyl]- β -cyclodextrin to produce a novel multi-functional macromolecular chiral selector heptakis[6-*O*-(*N*-acetylyl-*L*-valine-tert-butyl amide)-2,3-di-*O*-methyl]- β -cyclodextrin (ValDex). ValDex was utilized as a CSA in NMR spectroscopy. It was shown that the presence of the polar and hydrogen-bonding *L*-valine-diamide groups as well as the apolar cyclodextrin cavity in ValDex allowed the enantiodiscrimination of both polar α -amino acid derivatives and apolar trisubstituted allenes devoid of any functional groups, i.e. the enantioselective properties of the valine-diamide moiety and that of the cyclodextrin could be combined in one single molecule.

Theoretical treatment of the enantioseparation on binary-selector CSPs. The peculiarity of the binary-selector CSPs is the dependence of the apparent enantioseparation factor, α_{app} , on the ratio of the chiral selectors in the CSP. Thus, depending on the ratio of the selectors and the strength of their interactions with the selectand enantiomers, the apparent enantioseparation factor, α_{app} , can be greatly reduced in some cases even leading to coalescence of the peaks of the enantiomers (mismatched case). Besides, the elution order of the enantiomers can be inverted. Therefore, the rational control of the ratio between the chiral selectors present in a binary-selector CSP is important for achieving high enantioseparation factors. The theoretical treatment of the enantioseparation on binary-selector CSPs, including determination of apparent and true enantioseparation factors, α_{app} and α_{true} , respectively, and the analysis of the behavior of the apparent enantioseparation factor upon varying ratio between the chiral selectors and the strengths of the selector-selectand interactions was performed. An equation allowing the calculation of the apparent enantioseparation factor, α_{app} , on binary-selector CSPs has been derived and experimentally proven by enantioselective gas- and liquid chromatography.

Investigation of the inversion of the elution order of enantiomers caused by enthalpy-entropy compensation. The temperature-dependent inversion of the elution order of enantiomers was experimentally observed for different derivatives of α -amino acids on Chirasil-Val-C₁₁ and Chirasil-Dex CSPs. For the first time, a clear visual representation of the increase of the apparent enantioseparation factor, α_{app} , as the temperature raises was shown. The increase of α_{app} was accompanied by a concomitant reduction of the retention time. The comprehensive thermodynamic analysis of the enantioseparation of the derivatives of α -amino acids showed that the presence of NH-amide groups in the compounds analyzed significantly influenced the value of the isoenantioselective temperature, T_{iso} .

In the case of the enantioseparation of *N*-trifluoroacetyl, ethyl esters of α -amino acids on the cyclodextrin-based CSP, Chirasil-Dex, both inversion of the elution order of enantiomers at the isoenantioselective temperature, T_{iso} , and the nonlinearity of the plots $\ln(\alpha_{\text{app}})$ vs. $1/T$ was observed. The T_{iso} values were in the range from 20 to 170°C depending on the nature of the α -amino acid. Three α -amino acids showed coalescence of the peaks at two temperatures because of the nonlinear behavior of the Van't Hoff plots. Thus, it could be predicted that the inversion of the elution order of enantiomers could also be observed more than one time for a single racemate.

The following conclusions could be drawn from the thermodynamic investigation: (1) increase in the strength of the selector-selectand interactions does not necessarily result in an improved enantioselectivity of the system; (2) in order to optimize an enantiomeric separation of a single racemate isothermally or of mixtures of racemates in a temperature-programmed run using enantioselective GC it is necessary to conduct temperature-dependent studies; (3) it is shown that consideration of the elution order of enantiomers and the value of the apparent enantioseparation factor, α_{app} , alone, without performing temperature-dependent measurements, can easily lead to wrong conclusions regarding the enantiorecognition mechanism.

Study of the nature of non-linear plots $\ln(\alpha_{\text{app}})$ vs. $1/T$. Another interesting observation was made when analyzing *N*-ethoxycarbonyl propylamide derivatives of a number of α -amino acids on Chirasil-Val-C₁₁ CSP. Nonlinearity of the plots of the natural logarithm of the apparent enantioseparation factor as a function of the reciprocal temperature was observed. This phenomenon was investigated using the retention increment method. It was shown that the change of the association mechanism between the chiral selector and the

less interacting *D*-enantiomer of the α -amino acids was responsible for the observed nonlinear effect.

Determination of the activation parameters for the enantiomerization of 1,2-di-*tert*-butylpyrazolidine. Enantioselective chromatography has been widely used for the investigation of dynamic processes occurring during the separation, e.g. chemical reactions or interconversion of enantiomers. Enantioselective GC has been employed to study the interconversion of enantiomers of 1,2-di-*tert*-butylpyrazolidine in which stereogenic centers are located on the nitrogen atoms. The GC enantioseparation of the racemate of 1,2-di-*tert*-butylpyrazolidine on the Chirasil-Dex CSP above 100°C revealed the characteristic plateau formation between the peaks of the separated enantiomers which allowed to measure the activation parameters of the enantiomerization, ΔH^\ddagger and ΔS^\ddagger , using the “approximation function”. ΔH^\ddagger and ΔS^\ddagger were found to be $113.5 \pm 2.0 \text{ kJ}\cdot\text{mol}^{-1}$ and $-14.7 \pm 5.3 \text{ J}\cdot\text{mol}^{-1}\cdot\text{K}^{-1}$, respectively.

Investigation of the influence of an enantiomeric impurity of a chiral selector on the enantioselectivity. An important problem of enantioselective chromatography, namely, the use of enantiomerically impure chiral selectors, was treated as a separate project. Theoretical and experimental investigation of the influence of the enantiomeric impurity on the enantioseparation showed that, for highly enantioselective systems, even traces of the undesired enantiomer can dramatically reduce the apparent enantioseparation factor, α_{app} . This observation is especially important in the light of the increased enantioselectivity of the newly developed synthetic “receptor-like” chiral selectors.

Investigation of nonenantioselective versus enantioselective interactions in enantioselective liquid chromatography. Retention in enantioselective chromatography results from nonenantioselective and enantioselective interactions, only the latter being responsible for the enantioselectivity of the CSP. Therefore, for an efficient design of new enantioselective selectors and for the analysis and optimization of the behavior of the existent CSPs it is important to be able to study the enantioselective interactions without interference with the nonenantioselective ones. In the present work, the issue of the nonenantioselective interactions capable of reducing the apparent enantioseparation factor, α_{app} , was studied using anion-exchange liquid chromatography with a quinine-based brush-type CSP. A method for distinguishing between enantioselective and nonenantioselective interactions in liquid

chromatography on brush-type CSPs was developed. This method is based on the retention increment approach known for the calculation of the true enantioselectivity factor, α_{true} , in enantioselective GC. The equations derived account for two equilibrium processes: the nonenantioselective adsorption of the analyte on the achiral parts of the CSP and the enantioselective association of the analyte with the chiral selector present on the surface of the CSP. To verify the method, three compounds (*N*-fmoc-phenylalanine, *N*-[(3,5-dipropoxybenzyloxy)carbonyl]leucine and 2-(2,4-dichlorophenoxy)propanoic acid) were studied in three different mobile phase modes (organic polar, reversed and normal) on quinine-based CSPs with different loadings of the chiral selector. Generally, the nonenantioselective contribution to retention was found to be significantly lower than the enantioselective one in all the mobile phase modes studied. In the polar organic and reversed modes, the plots of the apparent adsorption equilibrium constant, K^{app} , as functions of the loading of the quinine-selector, c_{QN} , were found to be strictly linear converging in the same point and, therefore, confirming the validity of the method.

Application of enantioselective GC as a method for distinguishing between racemic compounds and conglomerates as two important crystalline modifications. An important application of the enantioselective GC, namely, distinguishing between the conglomerates (crystalline modification of a chiral substance where each single crystal is composed of only one enantiomer) and racemic compounds (crystalline modification of a chiral substance where each single crystal is composed of both enantiomers) was studied.

Conclusions

References

- 1 M. Laska, A. Liesen, P. Teubner, *Am. J. Physiol.* **1999**, R1098-R1103.
- 2 G. Ohloff, *Scent and Fragrances. The Fascination of Odors and Their Chemical Perspectives.*, Springer Verlag, Berlin, **1994**.
- 3 (a) H.J. Roth, C.E. Mueller, G. Folkers, *Stereochemie & Arzneistoffe*, Wiss. Verl.-Ges., Stuttgart, **1998**; (b) W. J. Wechter, *J. Clinical Pharm.* **1994**, *34*, 1036-1042.
- 4 S.C. Stinson, *Chem. & Eng. News* **1999**, *79*, 79-97.
- 5 S.G. Allenmark, *Chromatographic Enantioseparation - Methods and Applications*, Ellis Horwood, Chichester, **1988**.
- 6 N.M. Maier, P. Franco, W. Lindner, *J. Chromatogr. A* **2001**, *906*, 3-33.
- 7 V. Schurig, *J. Chromatogr. A* **2001**, *906*, 275-299.
- 8 V. Schurig, *Trends Anal. Chem.* **2002**, *21*, 647-661.
- 9 L. He, T.E. Beesley, *J. Liq. Chrom. Rel. Technol.* **2005**, *28*, 1075-1114.
- 10 B. Chankvetadze, G. Blaschke, *J. Chromatogr. A* **2001**, *906*, 309-363.
- 11 R. Kuhn, S. Hoffstetter-Kuhn, *Capillary Electrophoresis: Principles and Practice*, Springer Verlag, Heidelberg, **1993**.
- 12 B. Chankvetadze, *J. Sep. Sci.* **2001**, *24*, 691-705.
- 13 P. Macaudiere, M. Caude, R. Rosset, A. Tambute, *J. Chromatogr. Sci.* **1989**, *27*, 383.
- 14 M.L. Lee, K.E. Markides, *Analytical Supercritical Fluid Chromatography and Extraction*, Chrom. Confererences Inc., Provo, **1990**.
- 15 Z. Juvancz, K. Markides, *LC GC International* **1992**, *5*, 44.
- 16 M. Schleimer, V. Schurig in *Enantiomer Separation by Capillary Supercritical Fluid Chromatography: Analysis with Supercritical Fluids: Extraction and Chromatography* (Ed.: B. Wenclawiak), Springer Verlag, Berlin, **1992**.
- 17 T.J. Ward, *Anal. Chem.* **2000**, *72*, 4521-4528.
- 18 G. Terfloth, *J. Chromatogr. A* **2001**, *906*, 301-307.
- 19 V.A. Davankov, S.V. Rogozhin, A.V. Semechkin, T.P. Sachkova, *J. Chromatogr.* **1973**, *82*, 359.
- 20 G. Guebitz, W. Jellenz, W. Santi, *J. Chromatogr.* **1981**, *203*, 377-384.
- 21 V.A. Davankov, *Chromatographia* **1989**, *27*, 475-482.
- 22 V.A. Davankov, *J. Chromatogr. A* **1994**, *666*, 55-76.
- 23 E. Gil-Av, B. Feibush, R. Charles-Sigler, *Tetrahedron Lett.* **1966**, *7*, 1009-1015.
- 24 B. Feibush, E. Gil-Av, *Tetrahedron* **1970**, *26*, 1361-1368.

References

- 25 B. Feibush, *J. Chem. Soc. Chem. Commun.* **1971**, 11, 544-545.
- 26 E. Gil-Av, *J. Mol. Evol.* **1975**, 6, 131-144.
- 27 V. Schurig, *Angew. Chem. Int. Ed.* **1984**, 23, 747-765.
- 28 B. Feibush, *Chirality* **1998**, 10, 382-395.
- 29 H. Frank, G.J. Nicholson, E. Bayer, *J. Chromatogr. Sci.* **1977**, 15, 174-176.
- 30 (a) V. Schurig, R. Weber, *J. Chromatogr.* **1981**, 217, 51-70; (b) V. Schurig, W. Buerkle, *Angew. Chem.* **1978**, 90, 132-133.
- 31 V. Schurig, D. Schmalzing, M. Schleimer, *Angew. Chem. Int. Ed.* **1991**, 30, 987-989.
- 32 V. Schurig, F. Betschinger, *Chem. Rev.* **1992**, 92, 873-888.
- 33 V. Schurig, *J. Chromatogr. A* **2002**, 965, 315-356.
- 34 T. Koscielski, D. Sybilska, J. Jurczak, *J. Chromatogr.* **1983**, 261, 357.
- 35 T. Koscielski, D. Sybilska, J. Jurczak, *J. Chromatogr.* **1983**, 280, 131.
- 36 Z. Juvancz, G. Alexander, J. Szejtli, *J. High Res. Chromatogr.* **1987**, 10, 105.
- 37 Z. Juvancz, G. Alexander, J. Szejtli, *J. High Res. Chromatogr.* **1988**, 11, 110.
- 38 A. Venema, P.J.A. Tolsma, *J. High Res. Chromatogr.* **1989**, 12, 32-34.
- 39 V. Schurig, H.-P. Nowotny, *J. Chromatogr.* **1988**, 441, 155.
- 40 V. Schurig, M. Jung, D. Schmalzing, M. Schleimer, J. Duvekot, J.C. Buyten, J.A. Peene, P. Mussche, *J. High Res. Chromatogr.* **1990**, 13, 470-474.
- 41 W.A. König, S. Lutz, G. Wenz, *Angew. Chem.* **1988**, 100, 989-990.
- 42 W. A. Koenig, R. Krebber, P. Mischnick, *J. High Res. Chromatogr.* **1989**, 12, 732-738.
- 43 H. Frank, G.J. Nicholson, E. Bayer, *Angew. Chem. Int. Ed.* **1978**, 17, 363-365.
- 44 V. Schurig, M. Juza, M. Preschel, G. J. Nicholson, E. Bayer, *Enantiomer* **1999**, 4, 297-303.
- 45 V. Schurig, H.-P. Nowotny, *Angew. Chem. Int. Ed.* **1990**, 29, 939-957.
- 46 D. Schmalzing, M. Jung, S. Mayer, J. Rickert, V. Schurig, *J. High Res. Chromatogr.* **1992**, 15, 723-729.
- 47 H. Cousin, O. Trapp, V. Peulon-Agasse, X. Pannecoucke, L. Banspach, G. Trapp, Z. Jiang, J.C. Combret, V. Schurig, *Eur. J. Org. Chem.* **2003**, 17, 3273-3287.
- 48 U.J. Meierhenrich, M.J. Nguyen, B. Barbier, A. Brack, W.H-P. Thiemann, *Chirality* **2003**, 15, S13-S16.
- 49 C. Szopa, U.J. Meierhenrich, D. Coscia, L. Janin, F. Goesmann, R. Sternberg, J.-F. Brun, G. Israel, M. Cabane, R. Roll, F. Raulin, W. Thiemann, C. Vidal-Madjar, H. Rosenbauer, *J. Chromatogr. A* **2002**, 982, 303-312.
- 50 R.J. Laub, J.H. Purnell, *J. Chromatogr.* **1975**, 112, 71-79.

- 51 R.J. Laub, J.H. Purnell, *Anal. Chem.* **1976**, *48*, 1720-1725.
- 52 I.H. Hagestam, T.C. Pinkerton, *Anal. Chem.* **1985**, *57*, 1757.
- 53 C.P. Desilets, M.A. Rounds, F.E. Regnier, *J. Chromatogr.* **1991**, *544*, 25.
- 54 B. Feibush, C.T. Santasania, *J. Chromatogr.* **1991**, *544*, 41.
- 55 H.J. Issaq, D.W. Mellini, T.E. Beesley, *J. Liq. Chromatogr.* **1988**, *11*, 333-348.
- 56 L.A. Kennedy, W. Kopaciewicz, F.E. Regnier, *J. Chromatogr.* **1986**, *359*, 255.
- 57 H.J. Issaq, J. Gutierrez, *J. Liq. Chromatogr.* **1988**, *11*, 2851.
- 58 R. Bischoff, L. W. McLaughlin, *J. Chromatogr.* **1984**, *317*, 251-261.
- 59 J.B. Crowther, R.A. Hartwick, *Chromatographia* **1982**, *16*, 349-353.
- 60 Z. El Rassi, C. Horvath, *J. Chromatogr.* **1986**, *359*, 255-264.
- 61 Y.-F. Maa, F.D. Antia, Z.E. Rassi, C. Horvath, *J. Chromatogr.* **1988**, *452*, 331-345.
- 62 L.W. McLaughlin, *Chem. Rev.* **1989**, *89*, 309-319.
- 63 Klampfl, C. W.; Buchberger, W.; Haddad, P. R., *J. Chromatogr. A* **2001**, *911*, 277-283.
- 64 R. Nogueira, M. Laemmerhofer, W. Lindner, *J. Chromatogr. A* **2005**, *1089*, 158-169.
- 65 D.J. Pietrzyk, S.M. Senne, D.M. Brown, *J. Chromatogr.* **1991**, *546*, 101.
- 66 A.-F. Aubry, N. Markoglou, V. Descorps, I.W. Wainer, G. Felix, *J. Chromatogr. A* **1994**, *685*, 1-6.
- 67 T. Zhang, E. Francotte, *Chirality* **1995**, *7*, 425-433.
- 68 P.Murer, K. Lewandowski, F. Svec, J.M.J.Frechet, *Chem. Commun.* **1998**, 2559-2560.
- 69 L. Oliveros, C. Minguillon, B. Desmazieres, P.-L. Desbene, *J. Chromatogr.* **1991**, *543*, 277-286.
- 70 A. Tambute, L. Siret, M. Caude, A. Begos, R. Rosset, *Chirality* **1990**, *2*, 106-119.
- 71 M.H. Hyun, W.H. Pirkle, *J. Chromatogr.* **1987**, *393*, 357.
- 72 S. Allenmark, *Enantiomer* **1999**, *4*, 67-69.
- 73 W.H. Pirkle, C.J. Welch, *J. Chromatogr. A* **1996**, *731*, 322-326.
- 74 J. Magnusson, L.G. Blomberg, S. Claude, R. Tabacchi, A. Saxer, S. Schurch, *J. High Res. Chromatogr.* **2000**, *23*, 619-627.
- 75 X. Y. Shi, Y.Q. Zhang, R.N. Fu, *Anal. Chim. Acta* **2000**, *424*, 271-277.
- 76 M.Y. Nie, L.M. Zhou, Q.H. Wang, D.Q. Zhu, *Chromatographia* **2000**, *51*, 736-740.
- 77 S. Tamogami, K. Awano, M. Amaike, Y. Takagi, T. Kitahara, *Flavour Fragr. J.* **2001**, *16*, 349-352.
- 78 A. Ruderisch, J. Pfeiffer, V. Schurig, *J. Chromatogr. A* **2003**, *994*, 127-135.
- 79 M. Bayer, A. Mosandl, *Flavour Fragr. J.* **2004**, *19*, 515-517.

References

- 80 W. A. König, D. Icheln, T. Runge, B. Pfaffenberger, P. Ludwig, H. Huehnerfuss, *J. High Res. Chromatogr.* **1991**, *14*, 530-536.
- 81 B. Gallinella, F. La Torre, R. Cirilli, C. Villani, *J. Chromatogr.* **1993**, *639*, 193-196.
- 82 I. D'acquarica, F. Gasparrini, B. Giannoli, D. Misiti, C. Villani, G.P. Mapelli, *J. High Res. Chromatogr.* **1997**, *20*, 261-264.
- 83 A.X. Wang, J.T. Lee, T.E. Beesley, *LC GC International* **2000**, *18*, 626.
- 84 F. Gasparrini, D. Misiti, C. Villani, F. La Torre, *J. Chromatogr.* **1991**, *539*, 25-36.
- 85 W.H. Pirkle, R. Däppen, D.S. Reno, *J. Chromatogr.* **1987**, *407*, 211-216.
- 86 J. Pfeiffer, Dissertation, University of Tübingen, **1999**.
- 87 M. Karpf, Dissertation, University of Stuttgart, **1995**.
- 88 W. A. König, R. Krebber, P. Mischnick, *J. High Res. Chromatogr.* **1989**, *12*, 732-738.
- 89 W.A. König, R. Krebber, P. Evers, G. Bruhn, *J. High Res. Chromatogr.* **1990**, *13*, 328-332.
- 90 W.H. Pirkle, D.W. House, J.M. Finn, *J. Chromatogr.* **1980**, *192*, 143-158.
- 91 S. Allenmark, *Chirality* **1993**, *5*, 295-299.
- 92 T. Fornstedt, P. Sajonz, G. Guiochon, *Chirality* **1998**, *10*, 375-381.
- 93 G. Goetmar, T. Fornstedt, G. Guiochon, *Chirality* **2000**, *12*, 558-564.
- 94 L.D. Pettit, J.L.M. Swash, *J. Chem. Soc. Dalton Trans.* **1976**, 2416-2419.
- 95 A.A. Kurganov, L.Y. Zhuchkova, V.A. Davankov, *J. Inorg. Nucl. Chem.* **1978**, *40*, 1081-1083.
- 96 B. Koppenhöfer, E. Bayer, *Chromatographia* **1984**, *19*, 123.
- 97 V. Schurig, J. Ossig, R. Link, *Angew. Chem.* **1989**, *101*, 197-198.
- 98 K. Watabe, R. Charles, E. Gil-Av, *Angew. Chem.* **1989**, *101*, 194.
- 99 P.A. Levkin, A. Levkina, H. Czesla, V. Schurig, *Anal. Chem.* **2007**, *submitted*.
- 100 O. Trapp, V. Schurig, *J. Am. Chem. Soc.* **2000**, *122*, 1424-1430.
- 101 O. Trapp, V. Schurig, *Chirality* **2002**, *14*, 465-470.
- 102 V. Schurig, M. Jung, M. Schleimer, F.-G. Klaerner, *Chem. Ber.* **1992**, *125*, 1301.
- 103 R. G. Kostyanovsky, G.K. Kadorkina, V.R. Kostyanovsky, V. Schurig, O. Trapp, *Angew. Chem.* **2000**, *112*, 3066-3069.
- 104 G. Schoetz, O. Trapp, V. Schurig, *Anal. Chem.* **2000**, *72*, 2758.
- 105 O. Trapp, G. Schoetz, V. Schurig, *Chirality* **2001**, *13*, 403.
- 106 O. Trapp, V. Schurig, *Comput. Chem.* **2001**, *25*, 187-195.
- 107 O. Trapp, V. Schurig, *Chem. Eur. J.* **2001**, *7*, 1495.
- 108 O. Trapp, V. Schurig, *J. Chromatogr. A* **2001**, *911*, 167-175.

- 109 D.W. Armstrong, J.T. Lee, L.W. Chang, *Tetrahedron: Asymmetry* **1998**, *9*, 2043-2064.
- 110 D.W. Armstrong, L. He, T. Yu, J.T. Lee, Y.-S. Liu, *Tetrahedron: Asymmetry* **1999**, *10*, 37-60.
- 111 W.H. Pirkle, T.C. Pochapsky, *J. Chromatogr.* **1986**, *369*, 175-177.
- 112 M. Laemmerhofer, W. Lindner, *J. Chromatogr. A* **1996**, *741*, 33-48.
- 113 S. Rossi, G.M. Kyne, D.L. Turner, N.J. Wells, J.D. Kilburn, *Angew. Chem. Int. Ed.* **2002**, *41*, 4233-4236.
- 114 J. Jacques, A. Collet, S. H. Wilen, *Enantiomers, Racemates and Resolutions*, Krieger, Malabar, Florida, **1994**.
- 115 E.L. Eliel, S.H. Wilen, L.N. Mander, *Stereochemistry of Organic Compounds*, John Wiley and Sons, New York, **1994**.
- 116 A.N. Collins, G.N. Sheldrake, J. Crosby, *Chirality in Industry*, Wiley, Chichester, **1992**.
- 117 L. Perez-Garcia, D.B. Amabilino, *Chem. Soc. Rev.* **2002**, *31*, 342-356.
- 118 M. Walser, Dissertation, University of Tuebingen, **1987**.
- 119 H. Grosenick, V. Schurig, *J. Chromatogr. A* **1997**, *761*, 181-193.
- 120 M. Schleimer, V. Schurig, *J. Chromatogr.* **1993**, *638*, 85-96.
- 121 J. Pfeiffer, V. Schurig, *J. Chromatogr. A* **1999**, *840*, 145-150.
- 122 T. Hobo, S. Suzuki, K. Watabe, E. Gil-Av, *Anal. Chem.* **1985**, *57*, 362-364.
- 123 B. Koppenhöfer, U. Mühleck, K. Lohmiller, *Chromatographia* **1995**, *40*, 718-723.
- 124 M. Jung, V. Schurig, *J. Microcol. Sep* **1993**, *5*, 11-22.
- 125 A. Ghanem, C. Ginatta, Z.J. Jiang, V. Schurig, *Chromatographia* **2003**, *57*, 275-281.
- 126 A. Ruderisch, J. Pfeiffer, V. Schurig, *Tetrahedron: Asymmetry* **2001**, *12*, 2025-2030.
- 127 M. Jung, D. Schmalzing, V. Schurig, *J. Chromatogr.* **1991**, *552*, 43-57.
- 128 W.A. König, *J. High Res. Chromatogr.* **1993**, *16*, 569-586.
- 129 U. Ravid, E. Putievsky, I. Katzir, R. Ikan, V. Weinstein, *Flavour Fragr. J.* **1992**, *7*, 235-238.
- 130 U. Ravid, E. Putievsky, I. Katzir, *Flavour Fragr. J.* **1994**, *9*, 275-276.
- 131 V. Schurig, R. Schmidt, *J. Chromatogr. A* **2003**, *1000*, 311-324.
- 132 V. Schurig, H. Grosenick, M. Juza, *Recl. Trav. Chim. Pays-Bas* **1995**, *114*, 211-219.
- 133 G. Biressi, F. Quattrini, M. Juza, M. Mazzotti, V. Schurig, M. Morbidelli, *Chem. Eng. Sci.* **2000**, *55*, 4537-4547.
- 134 B. Kieser, C. Fietzek, R. Schmidt, G. Belge, U. Weimar, V. Schurig, G. Gauglitz, *Anal. Chem.* **2002**, *74*, 3005-3012.
- 135 I. Hardt, W. A. König, *J. Microcol. Sep* **1993**, *5*, 35-40.

References

- 136 P.A. Levkin, A. Levkina, V. Schurig, *Anal. Chem.* **2006**, *78*, 5143-5148.
- 137 P.A. Levkin, A. Ruderisch, V. Schurig, *Chirality* **2006**, *18*, 49-63.
- 138 K. Takeo, H. Mitoh, K. Uemura, *Carbohydr. Res.* **1989**, *187*, 203-221.
- 139 (a) G. R. Weisman in *Asymmetric synthesis, Vol. 1* (Ed.: J.D. Morrison), Academic Press, New York, **1983**, p. 153; (b) W.H. Pirkle, D.J. Hoover, *Topics in Stereochemistry* **1982**, *13*, 263-331; (c) D. Parker, *Chem. Rev.* **1991**, *91*, 1441-1457; (d) R. Rothchild, *Enantiomer* **2000**, *5*, 457-471; (e) T.J. Wenzel, J.D. Wilcox, *Chirality* **2003**, *15*, 256-270; (f) P. Lesot, M. Sarfati, J. Courtieu, *Chem. Eur. J.* **2003**, *9*, 1724-1745.
- 140 V. Schurig, *Methods of Organic Chemistry (Houben-Weyl), Stereoselective Synthesis, Volume E21a, Thieme (Stuttgart, New York), Determination of Enantiomeric Purity by Direct Methods, Chapter 3.1.4: NMR-Spectroscopy*, Thieme, Stuttgart, New York, **1995**, pp. 157-168.
- 141 H. Grosenick, M. Juza, J. Klein, V. Schurig, *Enantiomer* **1996**, *1*, 337-349.
- 142 (a) J.L. Atwood, J.E.D. Davies, D.D. Macnicol, F. Vögtle, *Comprehensive Supramolecular Chemistry, Vol. 3*, Pergamon Press, London, **1996**; (b) J. Szejtli, *Pure & Appl. Chem.* **2004**, *76*, 1825-1845; (c) M. Sollogoub, T. Lecourt, P. Sinay, *Recent Res. Devel. Chem.* **2003**, *1*, 31-39; (d) E. Engeldinger, D. Armspach, D. Matt, *Chem. Rev.* **2003**, *103*, 4147-4173; (e) V.T. D'Souza, *Supramol. Chem.* **2003**, *15*, 221-229.
- 143 G. Cravotto, G.M. Nano, G. Palmisano, *J. Carbohydr. Chem.* **2001**, *20*, 495-501.
- 144 E. Yashima, M. Yamada, C. Yamamoto, M. Nakashima, Y. Okamoto, *Enantiomer* **1997**, *2*, 225-240.
- 145 T. Kubota, C. Yamamoto, Y. Okamoto, *Chirality* **2002**, *14*, 372-376.
- 146 G. Uccello-Barretta, F. Balzano, G. Sicoli, A. Scarselli, P. Salvadori, *Eur. J. Org. Chem.* **2005**, *10*, 5349-5355.
- 147 G. Uccello-Barretta, F. Balzano, A.M. Caporusso, P. Salvadori, *J. Org. Chem.* **1994**, *59*, 836-839.
- 148 G. Uccello-Barretta, F. Balzano, A.M. Caporusso, A. Iodice, P. Salvadori, *J. Org. Chem.* **1995**, *60*, 2227-2231.
- 149 A. Dietrich, B. Maas, A. Mosandl, *J. High Res. Chromatogr.* **1995**, *18*, 152-156.
- 150 A. Dietrich, B. Maas, A. Mosandl, *J. Microcol. Sep* **1994**, *6*, 33-42.
- 151 V. Schurig, D. Schmalzing, U. Mühleck, M. Jung, M. Schleimer, P. Mussche, C. Duvekot, J. C. Buyten, *J. High Res. Chromatogr.* **1990**, *13*, 713-717.

- 152 W.A. König, *Gas Chromatographic Enantiomer Separation with Modified Cyclodextrins*, Huethig, Heidelberg, **1992**.
- 153 P.A. Levkin, A. Levkina, H. Czesla, S. Nazzi, V. Schurig, *J. Sep. Sci.* **2007**, *30*, in press.
- 154 E. Gil-Av, J. Herling, *J. Phys. Chem.* **1962**, *66*, 1208-1209.
- 155 M.A. Muhs, F.T. Weiss, *J. Am. Chem. Soc.* **1962**, *84*, 4697-4705.
- 156 V. Schurig, R.C. Chang, A. Zlatkis, B. Feibush, *J. Chromatogr.* **1974**, *99*, 147-171.
- 157 V. Schurig, *Inorg. Chem.* **1986**, *25*, 945-949.
- 158 A. Seidel-Morgenstern, G. Guiochon, *J. Chromatogr.* **1993**, *631*, 37-47.
- 159 P.A. Levkin, N.M. Maier, V. Schurig, W. Lindner, *in preparation*.
- 160 R.J. Laub, J.H. Purnell, D.M. Summers, P.S. Williams, *J. Chromatogr.* **1978**, *155*, 1-8.
- 161 R.J. Laub, J.H. Purnell, *Anal. Chem.* **1976**, *48*, 799-803.
- 162 R.J. Laub, J.H. Purnell, P.S. Williams, *Anal. Chim. Acta* **1977**, *95*, 135-143.
- 163 R.J. Laub, J.H. Purnell, *J. Am. Chem. Soc.* **1976**, *98*, 30-35.
- 164 R.J. Laub, J.H. Purnell, *J. Am. Chem. Soc.* **1976**, *98*, 35-39.
- 165 C.F. Chien, R.J. Laub, M.M. Kopecni, *Anal. Chem.* **1980**, *52*, 1402-1407.
- 166 M.W.P. Harbison, R.J. Laub, D.E. Martire, J.H. Purnell, P.S. Williams, *J. Phys. Chem.* **1979**, *83*, 1262.
- 167 S. Costiner, T. Kowalska, E. Gil-Av, *J. Phys. Chem.* **1996**, *100*, 17305-17309.
- 168 T. Kowalska, T. Hobo, K. Watabe, E. Gil-Av, *Chromatographia* **1995**, *41*, 221-226.
- 169 K. Watabe, E. Gil-Av, T. Hobo, S. Suzuki, *Anal. Chem.* **1989**, *61*, 126-132.
- 170 M. Junge, Dissertation, University of Hamburg, **2004**.
- 171 L.M. Yuan, R.N. Fu, S.H. Gui, X.T. Xie, R.J. Dai, X.X. Chen, Q.H. Xu, *Chromatographia* **1997**, *46*, 291-294.
- 172 L.M. Yuan, P. Ai, M. Zi, R.N. Fu, S.H. Gui, X.X. Chen, R.J. Dai, *J. Chromatogr. Sci.* **1999**, *37*, 395-399.
- 173 L.M. Yuan, R.N. Fu, X.X. Chen, S.H. Gui, R.J. Dai, *Chinese J. Chem* **1999**, *10*, 223-226.
- 174 D.Q. Xiao, Y. Ling, Y.X. Wen, R.N. Fu, J.L. Gu, R.J. Dai, A.Q. Luo, *Chromatographia* **1997**, *46*, 177-182.
- 175 X.D. Yu, L. Lin, C.Y. Wu, *Chromatographia* **1999**, *49*, 567-571.
- 176 W. H. Pirkle, *J. Chromatogr.* **1991**, *558*, 1-6.
- 177 V. Schurig, *Chirality* **2005**, *17*, S205-S226.
- 178 U. Beitler, B. Feibush, *J. Chromatogr.* **1976**, *123*, 149-166.
- 179 H. Hess, G. Burger, H. Musso, *Angew. Chem.* **1978**, *90*, 645.

References

- 180 W.A. König, D. Icheln, L. Hardt, *J. High Res. Chromatogr.* **1991**, *14*, 694-695.
- 181 B. Koppenhöfer, L. Bingcheng, V. Muschalek, U. Trettin, H. Willisch, E. Bayer, in *Proceedings of the 20th European Peptide Symposium, (Tuebingen 1988), E.Bayer, and G.Jung, eds. (Walter de Gruyter, Berlin 1989), 1989*, p. 109.
- 182 E. Benicka, J. Krupcik, I.Spanik, J. Hrouzek, P. Sandra, *J. Microcol. Sep* **1996**, *8*, 57-65.
- 183 T. Beck, J.-M. Liepe, J. Nadzik, S. Rohn, A. Mosandl, *J. High Res. Chromatogr.* **2000**, *23*, 569-575.
- 184 B. Maas, A. Dietrich, T. Beck, S. Boerner, A. Mosandl, *J. Microcol. Sep* **1995**, *7*, 65.
- 185 F. Kobor, G. Schomburg, *J. High Res. Chromatogr.* **1993**, *16*, 693-699.
- 186 K. Fulde, A.W. Frahm, *J. Chromatogr. A* **1999**, *858*, 33-43.
- 187 M. Schlauch, A.W. Frahm, *Anal. Chem.* **2001**, *73*, 262-266.
- 188 I. Abe, T. Nakahara, *J. High Res. Chromatogr.* **1996**, *19*, 511-514.
- 189 I. Abe, M. Kawazuma, N.Fujimoto, T. Nakahara, *Chem. Lett.* **1995**, 329-330.
- 190 I. Abe, T. Nishiyama, T. Nakahara, *Anal. Sci.* **1994**, *10*, 501.
- 191 I. Abe, N. Fujimoto, T. Nakahara, *Chem. Lett.* **1995**, 113.
- 192 V. Schurig, H. Czesla, *Enantiomer* **2001**, *6*, 107-128.
- 193 V.A. Davankov, *Chirality* **1997**, *9*, 99-102.
- 194 V. Schurig, W. Bürkle, K. Hintzer, R. Weber, *J. Chromatogr.* **1989**, *475*, 23-44.
- 196 V. Schurig, W. Bürkle, A. Zlatkis, C.F. Poole, *Naturwissenschaften* **1979**, *66*, 423.
- 197 W. Bürkle, H. Karfunkel, V. Schurig, *J. Chromatogr.* **1984**, *288*, 1.
- 198 K.P. Scharwaechter, D.H. Hochmuth, H. Dittmann, W.A. König, *Chirality* **2001**, *13*, 679.
- 199 O. Trapp, *Anal. Chem.* **2006**, *78*, 189-198.
- 200 M. Lämmerhofer, N.M. Maier, W. Lindner, *American Laboratory* **1998**, *30*, 71-78.
- 201 B. Chankvetadze, C. Yamamoto, Y. Okamoto, *Chem. Lett.* **2000**, 1176-1177.
- 202 G. Guiochon, *J. Chromatogr. A* **2002**, *965*, 129-161.
- 203 M. Schulte, J. Strube, *J. Chromatogr. A* **2001**, *906*, 399-416.
- 204 A.E. Rodrigues, L.S. Pais in *Modeling and simulation in SMB for chiral purification* (Ed.: G. Subramanian), 2 nd, Wiley-VCH, Weinheim, **2001**, pp. 219-251.
- 205 M.F. Kemmere, J.T.F. Keurentjes in *Membranes in chiral separations* (Ed.: G. Subramanian), 2 nd, Wiley-VCH, Weinheim, **2001**.
- 206 B.B. Lakshmi, C.R. Martin, *Nature* **1997**, *388*, 758-760.
- 207 P.A. Levkin, V. Schurig, *in preparation* **2007**.

- 208 V. Pino, A.W. Lantz, J.L. Anderson, A. Berthod, D.W. Armstrong, *Anal. Chem.* **2006**, 78, 113-119.
- 209 T. Fornstedt, P. Sajonz, G. Guiochon, *J. Am. Chem. Soc.* **1997**, 119, 1254-1264.
- 210 K.-K. Kunimoto, S.-I. Kitoh, M. Ichitani, N. Funaki, A. Kuwae, K. Hanai, *Heterocycles* **2002**, 57, 2011-2019.
- 211 S. Kitoh, H. Senda, K.-K. Kunimoto, S. Maeda, K. Hanai, *Cryst. Res. Technol.* **2004**, 39, 375-381.
- 212 S. Kitoh, K.-K. Kunimoto, N. Funaki, H. Senda, A. Kumae, K. Hanai, *J. Chem. Cryst.* **2002**, 32, 547-553.
- 213 H. D. Lutz, H. Haeuseler, *J. Mol. Struct.* **1999**, 511-512, 69-75.
- 214 G.W. Stockton, R. Godfrey, P. Hitchcock, R. Mendelsohn, P.C. Mowery, S. Rajan, A.F. Walker, *J. Chem. Soc. Perkin Trans. 2* **1998**, 2061-2071.
- 215 L.S. Taylor, *Am. Pharm. Rev.* **2001**, 4, 60-67.
- 216 M. Potrzebowski, *Eur. J. Org. Chem.* **2003**, 8, 1367-1376.
- 217 A. Carrington, A.D. McLachlan, *Introduction to Magnetic Resonance with Applications to Chemistry and Chemical Physics*, Harper & Row, New York, **1967**.
- 218 J.E. Wetrz, J.R. Bolton, *Electron Spin Resonance*, Mc Graw Hill, New York, **1972**.
- 219 P.A. Levkin, A.I. Kokorin, V. Schurig, R.G. Kostyanovsky, *Chirality* **2006**, 18, 232-238.
- 220 P.A. Levkin, V. Yu. Torbeev, D.A. Lenev, R.G. Kostyanovsky in *Topics in Stereochemistry* (Ed.: F. Toda), Wiley, **2006**.
- 221 P.A. Levkin, Y.A. Strelenko, K.A. Lyssenko, V. Schurig, R.G. Kostyanovsky, *Tetrahedron: Asymmetry* **2003**, 14, 2059-2066.
- 222 P.A. Levkin, E. Schweda, H.-J. Kolb, V. Schurig, R.G. Kostyanovsky, *Tetrahedron: Asymmetry* **2004**, 15, 1445-1450.
- 223 H. Stetter, A. Reischl, *Chem. Ber.* **1960**, 93, 791.
- 224 H. Tatemitsu, F. Ogura, Y. Nakagawa, M. Nakagawa, K. Naemura, M. Nakazaki, *Bull. Chem. Soc. Jpn.* **1975**, 48, 2473.
- 225 K. Naemura, R. Fukunaga, *Chem. Lett.* **1985**, 1651.
- 226 M.C. Kimber, A.C. Try, L. Painter, M.M. Harding, P. Turner, *J. Org. Chem.* **2000**, 65, 3042-3046.
- 227 R. Boese, T. Haumann, E.D. Jemmis, B. Kiran, S. Kozhushkov, A. de Meijere, *Liebigs Ann.* **1996**, 913.
- 228 W.H. Pirkle, T.C. Pochapsky, *J. Am. Chem. Soc.* **1987**, 109, 5975-5982.

References

- 229 W.H. Pirkle, M.H. Hyun, *J. Org. Chem.* **1984**, *49*, 3043-3046.
- 230 E. van Velzen, J. Engbersen, D. Reinhoudt, *Synthesis* **1995**, 989-997.
- 231 G. Uccello-Barretta, G. Sicoli, F. Balzano, P. Salvadori, *Carbohydr. Res.* **2005**, *340*, 271-281.
- 232 C.J. Welch, J.I. Lunine, *Enantiomer* **2001**, *6*, 67-68.
- 233 A.M. Skelley, J.R. Scherer, A.D. Aubrey, W.H. Grover, R.H.C. Ivester, P. Ehrenfreund, F.J. Grunthaner, J.L. Bada, R.A. Mathies, *Proc. Natl. Acad. Sci. USA* **2005**, *102*, 1041-1046.
- 234 F. Goesmann, M. Hilchenbach, *European Space Agency* **2004**, *543*, 102-109.

Meine akademischen Lehrer waren:

K. Albert, H. Bertagnolli, R.G. Kostyanovsky, V.A. Kutvitsky, E. Lindner, W. Lindner, M. Maier, H.A. Mayer, A.F. Mironov, U. Nagel, C. Ochsenfeld, N.I. Prokopov, W. Rosenstiel, G.A. Serebrennikova, V.G. Sevastianov, V. Schurig, A.D. Shutalev, E. Schweda, B. Speiser, E.K. Voloshin-Chelpan, V. Vyshnepolsky, L. Wesemann, K.-H. Wiesmüller, V.Y. Perelman, T. Ziegler, E.E. Zhukova

Curriculum Vitae

Pavel A. Levkin

Date of birth: July 17, 1980

Place of birth: Moscow, Russia

Married

2003(December) **PhD, University of Tübingen, Germany**
-2007(April) Title: "Practice and theory of gas chromatographic enantioseparation on single- and binary-selector chiral stationary phases"
Department of Organic Chemistry
Areas of study: practical and theoretical treatment of multi-selector systems in chromatography, enantio recognition mechanisms, cyclodextrin and amino acid-based chiral selectors, development of new chiral stationary phases for gas chromatography, conglomerate *versus* racemic compound formation
Supervisor: Prof. Dr. Volker Schurig

2001-2003 **M. Sc. (Chemistry and Chemical Technology)**
Received grade: **Excellent** (summa cum laude)
Department of Biotechnology and Organic Chemistry, M.V.
Lomonosov State Academy of Fine Chemical Technology, Moscow, Russia
Area of study: synthetic organic chemistry, stereochemistry and chemical thermodynamics
Supervisor: Prof. Dr. Remir Kostyanovsky

1997-2001 **B. Sc. (Chemistry and Chemical Technology)**
Received grade: **Excellent**
Department of Biotechnology and Organic Chemistry, M.V.
Lomonosov State Academy of Fine Chemical Technology, Moscow, Russia
Area of study: synthetic organic chemistry and stereochemistry
Supervisor: Prof. Dr. Remir Kostyanovsky

Academic Awards And Honours:

2006 the Ernst-Bayer-Prize from German Chemical Society (GDCh) "for an outstanding publication in the field of the separation science"

2004-2006 Fellowship at the Graduate College "Chemistry in interphases", Tübingen, Germany

2006 Participation Award. 18th Meeting of Nobel Prize Winners in Chemistry at Lindau, Germany

2005 Best poster award (first prize) 17th International Symposium on Chiral Discrimination held in Parma, Italy

2003 Top Master's thesis. Department of Biotechnology and Organic Chemistry Award at M.V. Lomonosov State Academy of Fine Chemical Technology, Moscow, Russia

2000 All-russian contest in engineering and computer technical drawing (first prize)
M.V. Lomonosov State Academy of Fine Chemical Technology, Moscow, Russia

2000 Municipal contest in engineering and computer technical drawing (first prize) M.V. Lomonosov State Academy of Fine Chemical Technology, Moscow, Russia

1999 All-russian contest in engineering (first prize) M.V. Lomonosov State Academy of Fine Chemical Technology, Moscow, Russia

1998 50th anniversary science-technical student conference, (first prize) M.V. Lomonosov State Academy of Fine Chemical Technology, Moscow, Russia

1998 All-russian contest in descriptive geometry, engineering and computer technical drawing (first prize) M.V. Lomonosov State Academy of Fine Chemical Technology, Moscow, Russia

1998 Municipal contest in descriptive geometry, engineering and computer technical drawing (first prize) M.V. Lomonosov State Academy of Fine Chemical Technology, Moscow, Russia

List of Publications:

“Temperature-induced reversal of elution order of enantiomers in gas chromatography: *N*-ethoxycarbonyl propyl amides and *N*-trifluoroacetyl ethyl esters of α -amino acids on Chirasil-Val and Chirasil- β -Dex CSP”

P.A. Levkin, A. Levkina, H. Czesla and V. Schurig
Analytical Chemistry, in press

“Quantitative analysis of non-enantioselective contribution to the retention in liquid chromatography on the quinine-type chiral stationary phase”

P.A. Levkin, N.M. Maier, V. Schurig, W. Lindner
in preparation

“Heptakis[6-*O*-(*n*-acetyl)-*L*-valine-*tert*-butylamide]-2,3-di-*O*-methyl]- β -cyclodextrin: a new multifunctional cyclodextrin with improved enantiodiscriminating efficiency towards polar and apolar substrates”

G. Uccello-Barretta, S. Nazzi, F. Balzano, P.A. Levkin, V. Schurig, P. Salvadori
European Journal of Organic Chemistry, submitted

“Apparent and association enantioselectivity of single- and multi-selector chiral stationary phases”

P.A. Levkin and V. Schurig
in preparation

“The large drop of the enantioseparation factor on a slightly enantiomerically impure chiral selector”

P.A. Levkin, N.M. Maier, V. Schurig, W. Lindner
in preparation

“Homo- and heterochirality in crystals“ *in Topics in stereochemistry*

P.A. Levkin, V.Yu. Torbeev, D.A. Lenev, R.G. Kostyanovsky
Ed.: F. Toda, John Wiley & Sons Ltd, 25 (2006), 81-134

“Expanding the enantioselectivity of the gas-chromatographic chiral stationary phase Chirasil-Val-C₁₁ by doping it with octakis(3-*O*-butanoyl-2,6-di-*O*-*n*-pentyl)- γ -cyclodextrin”

P.A. Levkin, A. Levkina, H. Czesla, S. Nazzi, V. Schurig
Journal of Separation Science, 2007, 30 (2007) 98-103.

„Combining the enantioselectivities of *L*-valine diamide and permethylated β -cyclodextrin in one gas chromatographic chiral stationary phase”

P.A. Levkin, A. Levkina, V. Schurig
Analytical Chemistry, 78 (2006), 5143-5148

"Combining the enantioselectivity of a cyclodextrin and a diamide selector in a mixed binary gas-chromatographic chiral stationary phase"

- P.A. Levkin, A. Ruderisch, V. Schurig
Chirality, 18 (2006), 49-63
"Absolute configuration of Träger bases: an X-ray diffraction and circular dichroism study"
- D.A. Lenev, K.A. Lyssenko, D.G. Golovanov, O.R. Malyshev, P.A. Levkin, R.G. Kostyanovsky
Tetrahedron Letters, 47 (2006), 319-321
"Solid-state ESR differentiation between racemate vs. enantiomer"
- P.A. Levkin, A. I. Kokorin, V. Schurig, R. G. Kostyanovsky
Chirality, 18 (2006) 232-238
"Solid-phase racemic compound-conglomerate transformation of 2,3:6,7-dibenzobicyclo[3.3.1]nona-2,6-diene-4,8-dione"
- P.A. Levkin, E. Schweda, H.-J. Kolb, V. Schurig, R.G. Kostyanovsky
Tetrahedr. Asymm., 15 (2004) 1445-1450
"Temperature-dependent racemic-compound-conglomerate crystallization of 2,3:6,7-dibenzobicyclo[3.3.1]nona-2,6-diene-4,8-dione"
- P. A. Levkin, Y. A. Strelenko, K. A. Lyssenko, V. Schurig, R. G. Kostyanovsky
Tetrahedr. Asymm., 14 (2003) 2059-2066
"A new conglomerate in a series of 2,3:6,7-dibenzobicyclo[3.3.1]nonanes"
- P. A. Levkin, K. A. Lyssenko, V. Schurig, R. G. Kostyanovsky
Mendeleev Commun., 13 (2003) 106-108
"Ångström-sized pore crystal"
- R. G. Kostyanovsky, P. A. Levkin, K. A. Lyssenko, Yu. A. Strelenko, D. G. Golovanov
Mendeleev Commun., 12 (2002) 220-222